Propositions

1. Either a low or high intake of vitamin B3 can lead to a worsening of metabolic health, but through distinct mechanisms.
   (this thesis)

2. White adipose tissue is very responsive to dietary vitamin B3 levels and is functionally involved in the whole body metabolic effects of vitamin B3 exposure.
   (this thesis)

3. Mechanistic studies employing animal models are essential to understand the outcomes of nutritional interventions.

4. Honest sharing of detailed experimental protocols across labs can improve the global efficiency of scientific research.

5. Understanding the mechanisms underlying tissue-specific effects of nervous regulation contributes to the establishment of a scientific foundation for Chinese acupuncture.

6. High-throughput ~omics data can provide novel findings, but do not train critical thinking.

7. Learning to compromise wisely is a life-long activity.

Propositions belonging to the thesis, entitled

"**Molecular physiological studies on health effects of dietary nicotinamide riboside, a vitamin B3**"

Wenbiao Shi

Wageningen, 16 April 2019.

Molecular physiological studies on health effects of dietary nicotinamide riboside, a vitamin B3

Wenbiao Shi

Thesis committee

Promotor
Prof. Dr J. Keijer
Professor of Human and Animal Physiology
Wageningen University & Research

Co-promotor
Dr V.C.J. Boer
Assistant professor, Human and Animal Physiology
Wageningen University & Research

Other members
Prof. Dr A.H. Kersten, Wageningen University & Research
Prof. Dr S. Klaus, German Institute of Human Nutrition, Potsdam, Germany
Prof. Dr A. Bast, Maastricht University, The Netherlands
Prof. Dr A. Verhoeven, University Medical Center Amsterdam/University of Amsterdam, The Netherlands.
This research was conducted under the auspices of the Graduate School VLAG (Advanced Studies in Food Technology, Agrobiotechnology, Nutrition and Health Sciences)

Molecular physiological studies on health effects of dietary nicotinamide riboside, a vitamin B3

Wenbiao Shi

Thesis

submitted in fulfilment of the requirements for the degree of doctor
at Wageningen University
by the authority of the Rector Magnificus
Prof. Dr A. P.J. Mol,
in the presence of the
Thesis Committee appointed by the Academic Board
to be defended in public
on Tuesday 16 April 2019
at 1.30 p.m. in the Aula.

Wenbiao Shi
Molecular physiological studies on health effects of dietary nicotinamide riboside, a vitamin B3,

152 pages.

PhD thesis, Wageningen University, Wageningen, the Netherlands (2019)
With references, with summary in English

ISBN: 978-94-6257-971-2
DOI: https://doi.org/10.18174/471911

Table of Contents

Chapter 1

General introduction

Natural sources of vitamin B3

Vitamin B3 is a soluble micronutrient that serves as the precursor of nicotinamide adenine dinucleotide (NAD^+). NAD^+ is a bioactive molecule consisting of a nicotinamide (Nam) and an adenosine diphosphate ribose moiety ($ADPR^+$) (Fig. 1). To date, there are four forms of vitamin B3 that naturally exist in dietary sources, including Nam, nicotinic acid (NA), nicotinamide mononucleotide (NMN) and nicotinamide riboside (NR) [1-3]. The structures of these vitamins B3 are given in Fig. 1. Nam and NA were the first-identified and are the most common dietary sources of vitamin B3 [4]. NMN and NR were subsequently discovered and more recently each has been proposed as a dietary supplement to boost cellular NAD^+ levels [5, 6]. All these forms of vitamin B3 are collectively referred to as *niacin*.

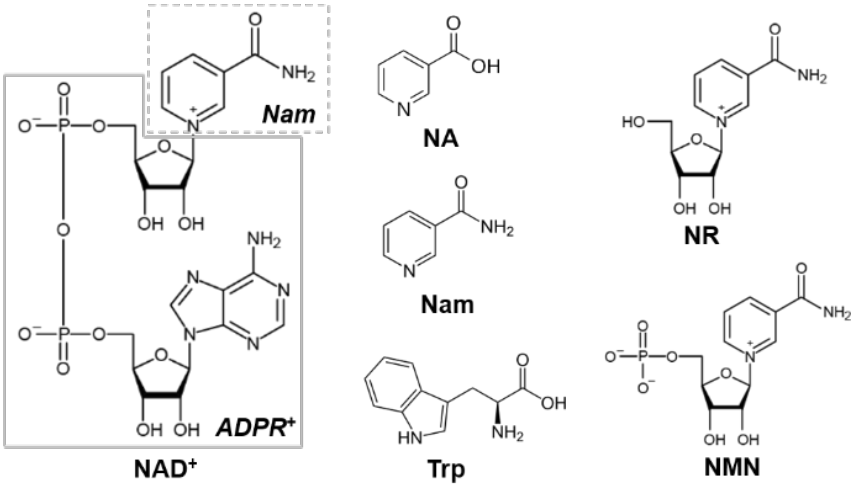

Figure 1. Structural formula of nicotinamide adenine dinucleotide (NAD^+), Tryptophan and four natural vitamins B3. NAD^+ consists of a Nicotinamide (the area indicated by grey dashed line) and an adenosine diphosphate ribose moiety ($ADPR^+$) (the area indicated by grey solid line).

The amounts of NA, Nam, NMN and NR varies widely among natural food sources. Free NA and Nam are hardly bioavailable in unprocessed natural food but this bioavailability increases by the course of food preparation or upon digestion in small intestine [1]. The main sources of NA and Nam are the cooked animal foods including liver, meat and fish as well as the mature cereal grains and peanuts [1, 7]. Roasted coffee provides relatively high amount of free NA [8]. Bovine milk [3] or roasted sweet corn [9] contain more free Nam. A higher content of NMN has been detected in vegetables and fruit, such as edamame and avocado, compared to raw meat or seafood [2], but the amounts are very small. Cow milk and yeast-containing foods are rich sources of NR [3, 4].

Tryptophan (Trp), an essential amino acid, is an alternative source of NAD^+. In terms of contribution to NAD^+ level, 60 mg of Trp is equivalent to 1 mg niacin [1]. Trp occurs in most protein-based foods and is particularly plentiful in foods rich in protein, e.g. meat, eggs, beans and dairy products [10]. Trp is lacking in gelatin, a partially hydrolyzed collagen obtained from animal skin, bones and connective tissues [11]. In addition, maize is a poor source of Trp.

Vitamin B3 and Trp breakdown in mammals

NA, Nam, NMN and NR follow distinct biochemical conversions to form NAD^+ (Fig. 2). NA is converted into NAD^+ via a three-step pathway called Preiss-Handler pathway, named after the two scientists who discovered this pathway [12]. Three

types of enzymes constitute the Preiss-Handler pathway, including nicotinic acid phosphoribosyltransferase (NAPRT), Nicotinamide mononucleotide adenylyltransferase isoforms (NMNAT1, NMNAT2 and NMNAT3) and NAD^+ synthase (NADS). The formation of NAD^+ from Nam is via a salvage pathway. Nam is converted into NMN by nicotinamide phosphoribosyltransferase (NAMPT). This enzyme is rate-limiting in NAD^+ synthesis [13]. NMN is subsequently converted into NAD^+ by NMNATs that are in common with those in the Preiss-Handler pathway. Alternatively, Nam can be methylated into N^1-methylnicotinamide (MeNam) by nicotinamide N-methyltransferase (NNMT). The phosphorylation of NR into NMN is the initial step of NR metabolism, which is rate-limiting and controlled by two nicotinamide riboside kinase isoforms (NRK1 and NRK2). This step is independent from the Preiss-Handler pathway and salvage pathway [12]. After this step, NR metabolism coincides with the salvage pathway. Extracellular NMN, from either diet or supplements, is converted into NR via the NRKs before absorption or entry into the cells [3, 14-16]. All these catalytic reactions are irreversible. In addition to NAD^+, vitamin B3 may be metabolized to their end products in the liver, i.e. MeNam, nicotinuric acid, N-methyl-2-pyridone-carboxamide (2-Py) and N-methyl-4-pyridone-carboxamide (4-Py), which are subsequently eliminated via urine.

NAD^+ can be synthesized from Trp via a *de novo* pathway that consists of a series of irreversible enzymatic reactions (Fig. 2). This pathway emphasizes the interaction between Trp and vitamin B3 in terms of metabolism. Indeed, niacin may not be required for normal growth in rodents if the diet contains sufficient Trp [17, 18]. On the other hand, a niacin-free diet slightly increased the Trp requirement in mice [19]. High dose of NA or Nam was shown to promote the *de novo* pathway [20, 21], while excessive Trp hardly affected vitamin B3 metabolism [22]. The *de novo* NAD^+ synthesis can be influenced by the other dietary components as well, such as unsaturated fatty acids, protein and some vitamins and minerals [23, 24]. In particular vitamin B2 and vitamin B6 provide cofactors for enzyme in the *de novo* pathway. Trp is also a key nutrient for protein synthesis and for serotonin biosynthesis (Fig. 2), thus cannot be removed from the diet for the evaluation of vitamin B3 requirements. In fact, sufficient Trp should be warranted during vitamin B3 deficiency as Trp is thought to be prioritized for protein synthesis when its level is low [25].

NAD^+ biosynthesis from vitamin B3 and Trp is tissue-specific. This may be attributed to the differential expression patterns and activities of the enzymes that are involved [4, 16, 26, 27]. The *de novo* pathway from Trp mainly takes place in the liver, and to a lesser extent in kidney, as these organs have all the required enzymes of this pathway [16, 23]. NAPRT is primarily expressed in liver and kidney, whereas the expression of NAMPT is ubiquitous and highest in adipose tissue, liver and skeletal muscle [28]. NRK1 is widely expressed, while NRK2 is specific in muscle and neural tissues like brain. Among NMNAT isoforms, NMNAT1 is most abundant and its mRNA has been detected in almost all tissues; NMNAT2 is neural cell-specific and relatively low transcriptional levels of NMNAT3 have been identified in lung, spleen and kidney [28].

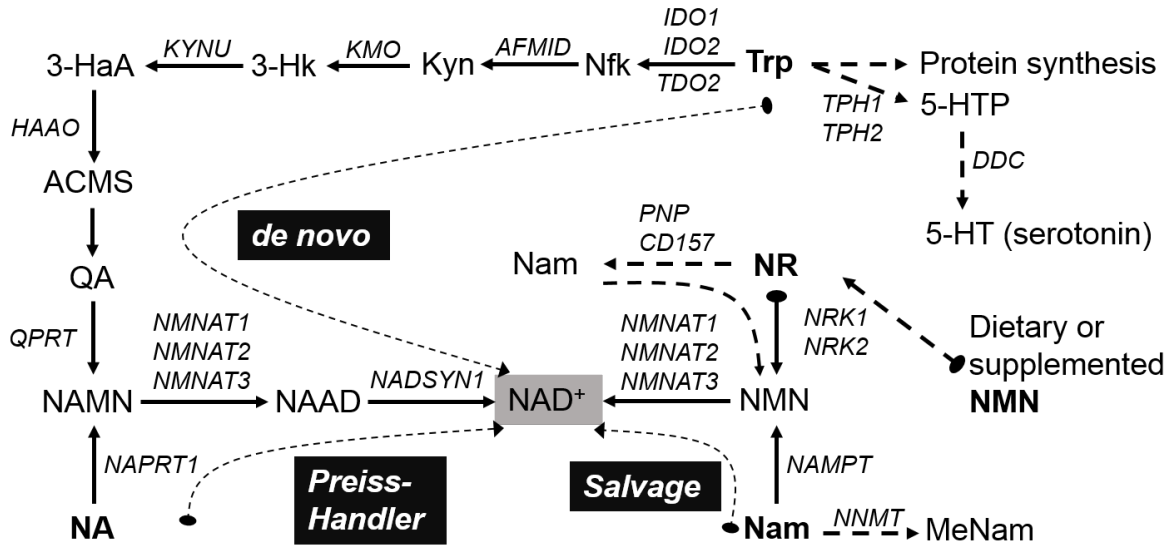

Figure 2. Schematic metabolism of Trp and four natural vitamins B3 in mammals (adapted from [4]). Pathways for NAD^+ biosynthesis are distinct; the *de novo* pathway from Trp, the Preiss-Handler pathway from NA, and the salvage pathway from Nam. These pathways are indicated by dashed lines, with the arrows showing their direction. NR metabolism to NMN is independent, controlled by NRKs. Exogenous NMN is converted into NR prior to intracellular metabolism. Natural sources for NAD^+ biosynthesis are in bold. Abbreviations metabolites: ACMS, α-amino-β-carboxymuconate-ε-semialdehyde; Kyn, kynurenine; MeNam, N1-methylnicotinamide; NAAD, nicotinic acid adenine dinucleotide; NAMN, nicotinic acid mononucleotide; Nfk, N-formylkynurenine; QA, quinolinic acid; 3-Hk, 3-hydroxykynurenine; 3-HaA, 3-hydroxyanthranilic acid; 5-HT (serotonin), 5-hydroxytryptamine; 5-HTP, 5-hydroxytryptophan. Abbreviations enzymes (*in Italic*): Arylformamidase, AFMID; DOPA decarboxylase, DDC; Indoleamine-pyrrole 2-3 dioxygenase isoform 1,2, IDO1, IDO2; Kynureninase, KYNU; 3-hydroxyanthranilate 3,4-dioxygenase, HAAO; NAD synthetase 1, NADSYN1; Nicotinamide phosphoribosyltransferase, NAMPT; Nicotinamide nucleotide adenylyltransferase isoforms 1-3, NMNAT1-3; Nicotinate phosphoribosyltransferase 1, nicotinamide N-methyltransferase, NNMT; Nicotinamide riboside kinase isoforms 1, 2, NRK1, NRK2; Quinolinate phosphoribosyltransferase, QPRT; Tryptophan 2,3-dioxygenase, TDO2; Kynurenine 3-monooxygenase, KMO; Tryptophan hydroxylase isoform 1, 2, TPH1, TPH2.

NAD^+ function in metabolism

NAD^+ is a versatile biomolecule that is very abundant in the body of mammals; for instance, the average amount of NAD^+ is approximately 3 grams in the body of humans [29]. NAD^+ is essential for energy metabolism. During nutrients breakdown in glycolysis and lipolysis, and the subsequent citric acid cycle, NAD^+ acts as a coenzyme, accepting a hydrogen ion (H^+) and two electrons to form NADH. The generated NADH delivers its electrons to mitochondrial complex I (NADH: ubiquinone oxidoreductase) and thus serves as an electron donor to the electron transport chain (ETC) [30]. The ETC, together with the ATP synthase (also called F_1F_O-ATPase or complex V), constitute oxidative phosphorylation (OXPHOS), the major process of sustainable cellular energy production.

The reversible conversion between NAD^+ and NADH plays a key role in many metabolisms. For instance, this interconversion is involved in various bioenzymatic reactions, including the metabolism of other B-vitamins such as vitamin B2 and folates (vitamin B11). In addition, NAD^+ can be phosphorylated by NAD^+ kinase to

nicotinamide adenine dinucleotide phosphate ($NADP^+$). $NADP^+$ is also a hydrogen and electron acceptor. NADPH performs an essential role in lipid biosynthesis [31]. The ratio of NAD^+/NADH and $NADP^+$/NADPH is crucial for the cellular redox state [31].

NAD^+ is also involved in several non-redox reactions that are mediated by a variety of NAD^+-consuming enzymes, including sirtuins, poly(ADP-ribose) polymerases (PARPs) and cADP-ribose synthases (e.g. CD38) [29]. These enzymes use NAD^+ for different purposes. Sirtuins are the family of the class III histone deacetylases that consists of seven members [32]. Sirtuin 1 (SIRT1) and Sirtuin 3 (SIRT3) are most studied among sirtuins and they use NAD^+ as a substrate for deacetylation. The targets of deacetylation by SIRT1 are key players in various metabolic pathways, including energy metabolism, inflammation and insulin signaling [29, 33]. One of the SIRT1 targets is peroxisome proliferator-activated receptor γ coactivator-1α (PGC-1α), a nodal regulator of mitochondrial biogenesis [34]. Boosting NAD^+ pool enhances SIRT1 activity, leading to PGC-1α deacetylation and a concomitant increase in activity, which further promotes mitochondrial biogenesis [5]. Notably, SIRT1 intrinsically deacetylates histone H3 at multiple lysine residues including Lys 9, Lys 14, Lys 56, as well as histone H4 at Lys 16 and histone H1 at Lys 26 [35]. Histone H3 de-acetylation at Lys 9 and Lys 14 is crucial for chromatin remodeling and circadian control [36]. SIRT3 is one of three primarily mitochondrial located sirtuins, the others being SIRT4 and SIRT5 [32]. SIRT3 also plays an important role in metabolism, with complex I and SOD2 among its established targets [5, 37]. The post-translational modifications by the other sirtuins, e.g. deacetylation, but also desuccinylation, demalonylation and ADP-ribosylation, are NAD^+-dependent as well [33]. PARPs catalyzes a unique post-translational modification called poly(ADP-ribosyl)ation, which requires NAD^+ as a $ADPR^+$ donor. This poly-ADP-ribosylation is best known for its important role in DNA repair and epigenetic modification. Recent studies have demonstrated a crucial role of (poly)ADP-ribosylation in inflammatory disorders and degenerative diseases [38]. Unlike sirtuins or PARPs, CD38 merely use NAD^+ to generate cyclic ADP-ribose (cADPR). cADPR has been implicated as a secondary messenger in Ca^{2+} signaling, cell cycle control and insulin signaling [39]. All these enzymes cause the cleavage of NAD^+ into Nam as a common product. Nam can be recycled to salvage NAD^+, but it may also exert an inhibitory effect on the activities of sirtuins and PARPs in a non-competitive manner [40, 41].

Vitamin B3 and health

Vitamin B3 is essential for health maintenance. A marked deficiency of vitamin B3 caused by inadequate dietary intake of vitamin B3 and/or Trp can lead to Pellagra. Pellagra is classically characterized by symptoms including diarrhea, dermatitis, dementia, and will eventually lead to death in humans [42]. Consumption of adequate levels of vitamin B3 and Trp prevents Pellagra in the normal population. Still, Pellagra can occur in undeveloped countries or when conditions, e.g. the use of alcohol or certain drugs, or diseases interfere with bioavailability of vitamin B3 [42-47]. An effective way to cure Pellagra is via vitamin B3 supplementation. In alcoholics, symptoms of vitamin B3 deficiency often become manifest and can be considerably ameliorated by treatment with NA or Nam [48-51].

Health effects of a high dose of vitamin B3 supplementation vary largely across human studies. Supplementing high dose vitamin B3 has been shown to improve compromised health conditions. NA is well-known for its pharmacological use to treat hyperlipidemia and hypercholesterolemia, leading to an improved lipid and cholesterol profile [52-55]. This improvement can lower the potential risk of atherosclerosis and cardiovascular events [52, 56]. Improved health effects have been identified in the Nam-treated type 1 diabetic patients [57, 58], but not in some large scale human studies [59-62]. NR and NMN are two newly dietary sources of vitamins B3 and have been used as a supplement in human trails. To date, five human studies of oral NR administration have been done, demonstrating that NR at doses up to 2000 mg/day (equivalent to approximately 300 mg/kg body weight/day) can be well-tolerated for a short-term (7-84 days) [59, 63-66]. The first human study for NMN clinical use is currently underway [67]. On the other hand, excessive intake of vitamin B3 may exert adverse effects on health. NA activates G protein-coupled receptor 109A (GPR109A) in dermal Langerhans cells. This activation elevates levels of arachidonic acid and prostaglandins in capillaries, leading to cutaneous vasodilatation [68]. NA may occasionally cause vasodilatory effects (flushing) at low dose, and the incidence of this effects rises with the consumption of NA in a dose-dependent manner [69]. Other side effects of NA use have been reported in humans, and include undesirable gastrointestinal effects, hepatotoxicity, glucose intolerance and others [69]. Unlike NA, clinical use of Nam does not cause flushing and the adverse effects have been suggested as mild and infrequent [69, 70]. However, concerns of Nam overload in type 2 diabetic patients and hypertensives have emerged recently [71-74].

The amount of vitamins B3 intake is also crucial for health in rodents. In rats, a pellagra-like phenotype, e.g. allopecia, anorexia, dermatitis, diarrhea and ataxia, has been reported [75, 76]. Vitamin B3 deficient mice exhibit growth retardation, but no overt pellagra-like signs, as appear in rats [77]. High doses of Nam are effective in treatment of neurodegenerative diseases [78-80], as well as obesity and type 2 diabetes [57, 58], in rat and mouse models. NA or NR administration in large doses has been shown to alleviate alcohol-induced fatty liver [3, 81]. NMN and NR have demonstrated a robust potency in counteracting the decline of metabolic health during aging and the development of obesity in rodents [2, 5, 6, 82, 83]. On the other hand, detrimental effects of health induced by a high dose of vitamin B3 have been demonstrated in rodent studies. Induction of insulin resistance has been identified in long-term high dose Nam-treated rats [84] and mice [85], as well as NA-treated mice [86]. NR use at high dose (300 mg/kg body weight/day) tended to compromise swimming performance of rats [87]. At very high doses of NR (1000 or 3000 mg/kg body weight/day) for 90 days, both male and female rats displayed negative physiological changes, more pronounced in females [88].

Vitamin B3 is required to maintain genomic stability and redox balance [89-92]. Genomic instability and increased oxidative stress are commonly seen in old and obese subjects [93-96]. Elderly and obese subjects also display a decline in NAD^+ in multiple tissues [6, 96-99], and may potentially be at risk of vitamin B3 deficiency. This is especially relevant since prevalence of obesity increases world-wide as does

the number of people over the age 65 [100, 101]. This population may need added vitamin B3 to preserve health.

Vitamin B3 intake in human and rodents

In view of the relevance of vitamin B3 for health, the population reference intake (PRI) and the tolerable upper intake level (UL) of niacin have been proposed. The PRI provides vitamin B3 requirement to minimize the potential risk of adverse health effects. The European Food Safety Authority (EFSA) suggests 6.6 mg NE/1000 kcal as PRI for niacin for adults and other populations, i.e. infants, children and pregnant women [1]. NE refers to niacin equivalent, which is defined as the following equation: NE (mg) = niacin (mg) + 1/60 of Trp (mg). The PRI of niacin includes the factor of energy intake, which can have a strong impact on the requirement for vitamin B3. The UL for NA is 10 mg/day, and for Nam is 900 mg/day in adults [1]. There are slight differences in the PRI and UL of niacin that are proposed among the regulatory organizations [1, 102].

The niacin requirement in rats is 15 mg per kg diet containing a minimum of 0.1 % (w/w) Trp, while no direct data of niacin requirement are available for mice [103-107]. The experimental rodent diet, e.g. AIN-93, contains 30 mg niacin/kg diet [108]. This concentration is considered adequate for growth maintenance of both rats and mice. Niacin appears to be well-tolerated up to around 1000 mg/kg body weight/day in rats [88]. To our knowledge, for mice the tolerance level of niacin has not been established.

NR and metabolic health

NR has gained attention from the scientific and public community as a health promoting compound. NR is capable of considerably increasing NAD^+ levels, *in vitro* and *in vivo* [5, 15, 63, 65, 83, 109, 110]. This capacity propelled NR as a novel NAD^+ booster to improve metabolic health. Indeed, the benefits from high dose NR supplementation (250-400 mg/kg body weight/day) have been demonstrated among a diversity of mouse models that are under certain stress or with defects. For instance, NR improves systemic insulin sensitivity, lipid profile and liver function in high-fat or high-fat-high-sucrose diet fed C57Bl6/J mice [5, 83, 111], preserves cognitive function in Alzheimer's mouse models [112], ameliorates mitochondrial myopathy in mitochondrial defects [82], and attenuates inflammation or prevents muscle stem cells senescence in the muscular dystrophy MDX mouse model [113, 114].

NR supplementation can bring additional benefits compared to the other forms of vitamin B3. Hepatic metabolic profile after NR administration is distinguishable from that of NA and Nam, with NR being most potent in improving NAD metabolome [63]. NR supplementation is more capable of enhancing NAD^+ pool in muscle compared to NMN [5]. Extracellular NR delays excitotoxin-induced axonal degeneration (AxD), while this AxD is not prevented by Nam [115]. However, the effects of NR as an exclusive source of vitamin B3 on metabolic health remains unknown. Linking to this, the underlying mechanisms should be investigated.

Assessment of health: challenging homeostasis

Deficient and excessive intakes of micronutrients may lead to physiological alterations and ultimately to pathological consequences. Early deficiency and toxicity biomarkers are important for the diagnosis before the onset of overt disease symptoms. Identifying such biomarkers has proven difficult under "normal" or "resting" conditions due to homeostasis, a robust state that acts to maintain levels of many functional biomarkers within a limited range [116]. Perturbing homeostatic systems has been proposed as a strategy to identify such biomarkers, because responses to a challenge may differ even if no differences exist in basal conditions, in other words, homeostatic perturbation can uncover early effects or predispositions that are masked under resting, non-perturbed conditions. Examples of well-established challenge tests are fasting-refeeding or the oral glucose tolerance test (OGTT).

In a fasting-refeeding challenge test, the response of fasted individuals to refeeding is examined. A fasting-refeeding challenge is usually assessed using indirect calorimetry (Fig. 3) [117, 118]. In indirect calorimetry, energy metabolism is assessed by measuring O_2 consumed and CO_2 produced. O_2 consumption and CO_2 production can also be used to calculate the respiratory exchange ratio (RER), which is normally in the range between 0.7 and 1 and is indicative for the substrate that is oxidized. An RER of 0.7 implies primarily fatty acid oxidation and RER of at 1.0 refers to predominantly glucose oxidation. The RER declines towards 0.7 with fasting, indicating a shift from glucose oxidation to fatty acid oxidation. When fully fasted subjects are provided a fixed amount of carbohydrate-containing diet, the RER increases by reaching a peak at between 0.85 and 1, depending on the amount and composition of the consumed diet. This increase reflects the switch from fatty acid oxidation to glucose oxidation. The ability to readily switch between glucose oxidation and fatty acid oxidation is defined as metabolic flexibility, a validated biomarker for metabolic health.

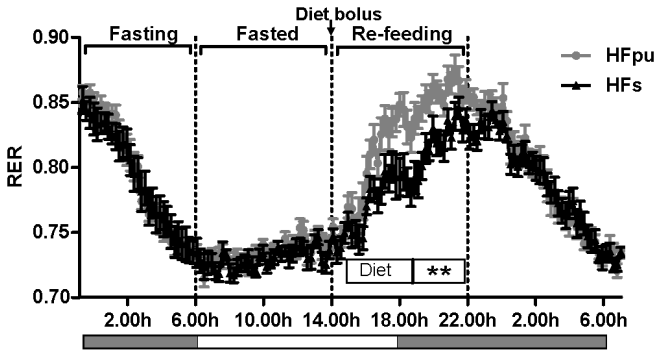

Figure 3. Fasting-refeeding challenge test (adapted from [117]). The fat components of HFpu diet differ from HFs diet. Mice were fasted and regained *ad libitum* access to their feed at 14.00h. Respiratory exchange ratio (RER) was measured in the meanwhile. The HFpu mice displayed higher RER in response to refeeding, suggesting greater metabolic flexibility compared with the HFs animals. Grey bars: dark phase; white bar: light phase.

For an OGTT, baseline blood glucose is measured in fasting subjects, after which the subjects are orally administrated with a dose of glucose. Blood glucose is measured at regular intervals thereafter (Fig. 4). An OGTT integrates glucose uptake and disposal. The response to an OGTT is used to as a measure for glucose tolerance. By parallel analysis of insulin during an OGTT, the amount of insulin released by the pancreas for glucose disposal in peripheral tissues, such as adipose tissue and muscle, can be determined. Combined with the glucose response, this

provides a measure for insulin sensitivity. Thus, challenge tests help to obtain information on the health status of an individual.

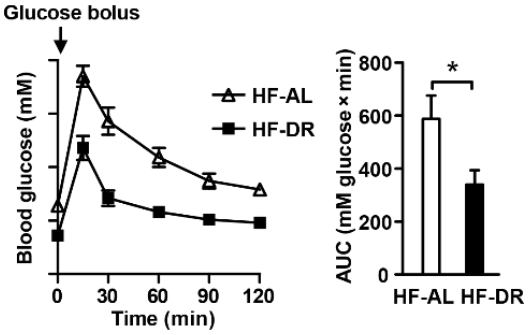

Figure 4. Oral glucose tolerance test (adapted from [119]). HF-AL, HF diet feeding *ad libitum*; HF-DR, the mice received 70% energy of the HF diet compared with the HF-AL animals. The HF-DR mice showed higher glucose disposal rate than the HF-AL animals.

Benefit-risk assessment

Benefit-risk assessment aims to establish the border levels of deficiency and toxicity based on the dietary intakes of micronutrients [120]. The amounts between these two border levels are defined as adequacy. Within the spectrum of adequacy, micronutrients can cause many physiological effects in a dose-dependent manner, wherein an optimal beneficial intake can occur (Fig. 5). Acquiring clear information on optimal intakes of micronutrients can contribute to their dietary strategies to keep maximal health over a lifespan. Understanding how our health is affected over a range of doses is a prerequisite to determine optimal beneficial intakes. Establishment of adequacy requires proper biomarkers that are specific, sensitive and reliable [116]. Such biomarkers are hard to be identified under "normal" or "resting" conditions, as mentioned in the beginning of this section. In those conditions, the effects of micronutrients can be very subtle, making the window of benefit hardly seen, thus making it even more difficult to determine the optimum. Indeed, for most of micronutrients this is not known. By using homeostasis challenges we can make the window of benefit become more visible (Fig. 5). This will help us obtain more robust and reliable information of how each subject responds to micronutrients and therefore contribute to determining the optimal intakes.

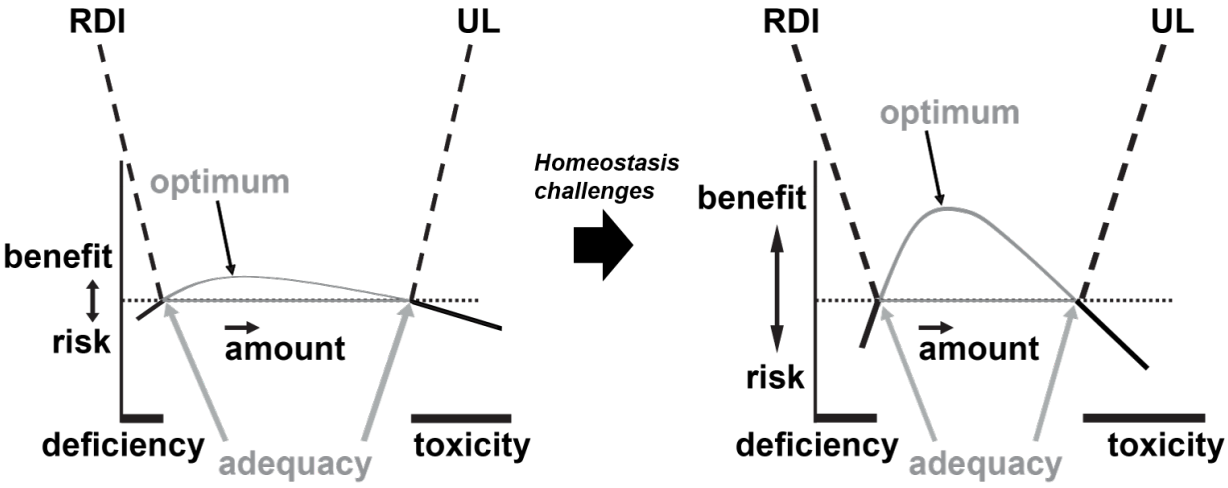

Figure 5. Homeostasis challenges visualize the window of benefit in a benefit-risk assessment (adapted from [121]). The borders where the deficiency changes into adequacy, are defined as the recommended daily intake (RDI), and where adequacy changes into toxicity, are defined as the upper limit (UL).

Aims and outline of this thesis

The aim of this thesis was to elucidate the effects of dietary NR on whole body metabolic health and to identify the associated molecular and physiological responses. To exclude the interference of other forms of vitamin B3, we employed a semi-purified rodent diet and used NR as an exclusive source of vitamin B3. To minimize the interaction effects of Trp on NR metabolism, we reduced dietary Trp by a low, but sufficient level. Since little is known about the dose-effects of NR as an exclusive vitamin B3 in rodents, we focus on four basic research questions (RQ) in this thesis:

- RQ1: what is the optimal dose of dietary NR for metabolic health in mice?
- RQ2: what are the molecular physiological consequences of high dose dietary NR in WAT?
- RQ3: what are the molecular physiological consequences of NR withdrawal in WAT?
- RQ4: what are the molecular responses to a wide range of dietary NR in hypothalamus?

To tackle RQ1, we designed a mildly obesogenic diet containing a wide range of concentrations of NR and reduced the Trp level to 0.14%. The fat content (40% energy derived from fat) of this diet is similar to the dietary fat intake in the Netherlands. To visualize the subtle physiological differences among the treatments, we employed a fasting-refeeding challenge during the indirect calorimetry measurement and analysed metabolic flexibility. We also examined the expression of the genes involving NAD^+ synthesis in various tissues, including liver, skeletal muscle (soleus and gastrocnemius), white adipose tissue (inguinal and epididymal WAT (eWAT)), and intestinal mucosa. Having established adipose tissue as the most responsive among these tissues, we further analysed morphology and the expression of additional genes in eWAT. This study is described in **Chapter 2**.

In **Chapter 2**, we found that the intervention with 900mg NR /kg diet reduced metabolic flexibility in mice compared to the optimal dose (30mg/kg). An even higher dose of NR supplementation (400mg/kg body weight/day) was shown to improve metabolic flexibility in another study (canto, 2012). We therefore examined an even higher dose of NR (9000mg NR /kg diet, equivalent to averagely 700mg/kg body weight/day) in the similar diet context as the first study and examined insulin sensitivity in more detail (RQ2). In addition to a fasting-refeeding challenge, we also employed an OGTT. We further focused on the focused on molecular regulation in eWAT and the results are elaborated in **Chapter 3**.

In **Chapter 4** I addressed RQ3. By applying vitamin B3 withdrawal (a diet without NR and just sufficient Trp), the finding of the first study that low vitamin B3 (NR) causes a decreased metabolic flexibility was confirmed. We then went on to identify molecular responses associated with vitamin B3 withdrawal. This was done using whole genome transcriptome analysis, which is an effective way to identify responsive biological processes. We focused the transcriptome analysis on eWAT and were able to identify several molecular markers for mild vitamin B3 insufficiency.

Based on the transcriptome analysis on eWAT in **Chapter 4**, we observed a signature of neurogenesis and therefore considered the brain as a target of interest in the dietary NR intervention. This is reminiscent us of a dose-response effect of dietary NR on grip strength and motor coordination that were measured during the animal experiment described in **Chapter 2**. We analysed the gene expression in hypothalamus (RQ4), a neuroendocrine organ that serves as a core regulator of motor function. The results are shown in **Chapter 5.**

Finally, **Chapter 6** is general discussion that consists of summary of the major outcomes and the approaches used in this thesis, as well as discussions on conflicting findings in vitamin B3 supplementation studies as well as recommendations for future studies.

References

[1] Food and Nutrition Board, Institute of Medicine. Niacin. In: *Dietary Reference Intakes for Thiamin, Riboflavin, Niacin, Vitamin B6, Folate, Vitamin B12, Panothenic Acid, Biotin, and Choline*, The National Academies Press, Washington DC 1998, pp. 123-145.
[2] Mills, K. F., Yoshida, S., Stein, L. R., Grozio, A., *et al.*, Long-term administration of nicotinamide mononucleotide mitigates age-associated physiological decline in mice. *Cell Metab.* 2016, *24*, 795-806.
[3] Trammell, S. A., *Novel nad+ metabolomic technologies and their applications to nicotinamide riboside interventions*, The University of Iowa, Iowa City 2016.
[4] Bogan, K. L., Brenner, C., Nicotinic acid, nicotinamide, and nicotinamide riboside: a molecular evaluation of NAD+ precursor vitamins in human nutrition. *Annu. Rev. Nutr.* 2008, *28*, 115-130.
[5] Canto, C., Houtkooper, R. H., Pirinen, E., Youn, D. Y., *et al.*, The NAD(+) precursor nicotinamide riboside enhances oxidative metabolism and protects against high-fat diet-induced obesity. *Cell Metab.* 2012, *15*, 838-847.
[6] Yoshino, J., Mills, K. F., Yoon, M. J., Imai, S., Nicotinamide mononucleotide, a key NAD(+) intermediate, treats the pathophysiology of diet- and age-induced diabetes in mice. *Cell Metab.* 2011, *14*, 528-536.
[7] EFSA Panel on Dietetic Products, Nutrition and Allergies (NDA), Scientific Opinion on Dietary Reference Values for niacin. *EFSA J.* 2014, *12*, 3759.
[8] Smith, R., Niacin content of coffee. *Nature* 1963, *197*, 1321.
[9] Kodicek, E., Ashby, D. R., Muller, M., Carpenter, K. J., The conversion of bound nicotinic acid to free nicotinamide on roasting sweet corn. *Proc. Nutr. Soc.* 1974, *33*, 105A-106A.
[10] USDA, A. R. S., *USDA National Nutrient Natabase for Standard Reference, Release 21*, 2008, Available database from: https://www.ars.usda.gov/northeast-area/beltsville-md-bhnrc/beltsville-human-nutrition-research-center/nutrient-data-laboratory/docs/sr21-home-page/.
[11] Dakin, H., Amino-acids of gelatin. *J. Biol. Chem.* 1920, *44*, 499-529.
[12] Bieganowski, P., Brenner, C., Discoveries of nicotinamide riboside as a nutrient and conserved NRK genes establish a Preiss-Handler independent route to NAD(+) in fungi and humans. *Cell* 2004, *117*, 495-502.
[13] Revollo, J. R., Grimm, A. A., Imai, S., The NAD biosynthesis pathway mediated by nicotinamide phosphoribosyltransferase regulates Sir2 activity in mammalian cells. *J. Biol. Chem.* 2004, *279*, 50754-50763.
[14] Gross, C. J., Henderson, L. M., Digestion and absorption of NAD by the small intestine of the rat. *J. Nutr.* 1983, *113*, 412-420.
[15] Ratajczak, J., Joffraud, M., Trammell, S. A., Ras, R., *et al.*, NRK1 controls nicotinamide mononucleotide and nicotinamide riboside metabolism in mammalian cells. *Nat. Commun.* 2016, *7*, 13103.
[16] Liu, L., Su, X., Quinn, W. J., 3rd, Hui, S., *et al.*, Quantitative analysis of NAD synthesis-breakdown fluxes. *Cell Metab.* 2018, *27*, 1067-1080 e1065.
[17] Terakata, M., Fukuwatari, T., Sano, M., Nakao, N., *et al.*, Establishment of true niacin deficiency in quinolinic acid phosphoribosyltransferase knockout mice. *J. Nutr.* 2012, *142*, 2148-2153.
[18] Terakata, M., Fukuwatari, T., Kadota, E., Sano, M., *et al.*, The niacin required for optimum growth can be synthesized from L-tryptophan in growing mice lacking tryptophan-2,3-dioxygenase. *J. Nutr.* 2013, *143*, 1046-1051.
[19] MacEwan, K., Carpenter, K., The nutritional value of supplementary D-tryptophan for growing mice. *Nutr. Rep. Int.* 1980, *21*, 279-283.
[20] Shibata, K., Fukuwatari, T., Suzuki, C., Pharmacological doses of nicotinic acid and nicotinamide are independently metabolized in rats. *J. Nutr. Sci. Vitaminol. (Tokyo)* 2014, *60*, 86-93.
[21] Mitchell, S. J., Bernier, M., Aon, M. A., Cortassa, S., *et al.*, Nicotinamide improves aspects of healthspan, but not lifespan, in mice. *Cell Metab.* 2018, *27*, 667-676. e664.
[22] Okuno, A., Fukuwatari, T., Shibata, K., Urinary excretory ratio of anthranilic acid/kynurenic acid as an index of the tolerable amount of tryptophan. *Biosci. Biotechnol. Biochem.* 2008, *72*, 1667-1672.

[23] Fukuwatari, T., Shibata, K., Nutritional aspect of tryptophan metabolism. *Int. J. Tryptophan Res.* 2013, *6*, 3-8.
[24] Shibata, K., *Tryptophan, Serotonin, and Melatonin*, Springer 1999, pp. 711-716.
[25] Kirkland, J. B., in: Zempleni, J., Suttie, J. W., Gregory III, J. F., Stover, P. J. (Eds.), *Handbook of vitamins*, CRC Press, Boca Raton 2013, p. 42.
[26] Houtkooper, R. H., Canto, C., Wanders, R. J., Auwerx, J., The secret life of NAD+: an old metabolite controlling new metabolic signaling pathways. *Endocr. Rev.* 2010, *31*, 194-223.
[27] Mori, V., Amici, A., Mazzola, F., Di Stefano, M., *et al.*, Metabolic profiling of alternative NAD biosynthetic routes in mouse tissues. *PLoS One* 2014, *9*, e113939.
[28] Christian Dölle*, R. H. S., Magali R. VanLinden and Mathias Ziegler, NAD biosynthesis in humans - enzymes, metabolites and therapeutic aspects. *Curr. Top. Med. Chem.* 2013, *13*, 11.
[29] Rajman, L., Chwalek, K., Sinclair, D. A., Therapeutic potential of NAD-boosting molecules: the in vivo evidence. *Cell Metab.* 2018, *27*, 529-547.
[30] Pollak, N., Dölle, C., Ziegler, M., The power to reduce: pyridine nucleotides–small molecules with a multitude of functions. *Biochem. J.* 2007, *402*, 205-218.
[31] Ying, W., NAD+/NADH and NADP+/NADPH in cellular functions and cell death: regulation and biological consequences. *Antioxid. Redox Signal.* 2008, *10*, 179-206.
[32] Michan, S., Sinclair, D., Sirtuins in mammals: insights into their biological function. *Biochem. J.* 2007, *404*, 1-13.
[33] Canto, C., Menzies, K. J., Auwerx, J., NAD(+) metabolism and the control of energy homeostasis: a balancing act between mitochondria and the nucleus. *Cell Metab.* 2015, *22*, 31-53.
[34] Fernandez-Marcos, P. J., Auwerx, J., Regulation of PGC-1α, a nodal regulator of mitochondrial biogenesis. *Am. J. Clin. Nutr.* 2011, *93*, 884S-890S.
[35] Seto, E., Yoshida, M., Erasers of histone acetylation: the histone deacetylase enzymes. *Cold Spring Harb. Perspect. Biol.* 2014, *6*, a018713.
[36] Nakahata, Y., Kaluzova, M., Grimaldi, B., Sahar, S., *et al.*, The NAD+-dependent deacetylase SIRT1 modulates CLOCK-mediated chromatin remodeling and circadian control. *Cell* 2008, *134*, 329-340.
[37] Giralt, A., Villarroya, F., SIRT3, a pivotal actor in mitochondrial functions: metabolism, cell death and aging. *Biochem. J.* 2012, *444*, 1-10.
[38] Schreiber, V., Dantzer, F., Ame, J. C., de Murcia, G., Poly(ADP-ribose): novel functions for an old molecule. *Nat. Rev. Mol. Cell Biol.* 2006, *7*, 517-528.
[39] Malavasi, F., Deaglio, S., Funaro, A., Ferrero, E., *et al.*, Evolution and function of the ADP ribosyl cyclase/CD38 gene family in physiology and pathology. *Physiol. Rev.* 2008, *88*, 841-886.
[40] Avalos, J. L., Bever, K. M., Wolberger, C., Mechanism of sirtuin inhibition by nicotinamide: altering the NAD(+) cosubstrate specificity of a Sir2 enzyme. *Mol. Cell* 2005, *17*, 855-868.
[41] Dominguez-Gomez, G., Diaz-Chavez, J., Chavez-Blanco, A., Gonzalez-Fierro, A., *et al.*, Nicotinamide sensitizes human breast cancer cells to the cytotoxic effects of radiation and cisplatin. *Oncol. Rep.* 2015, *33*, 721-728.
[42] Hegyi, J., Schwartz, R. A., Hegyi, V., Pellagra: dermatitis, dementia, and diarrhea. *Int. J. Dermatol.* 2004, *43*, 1-5.
[43] Seal, A. J., Creeke, P. I., Dibari, F., Cheung, E., *et al.*, Low and deficient niacin status and pellagra are endemic in postwar Angola. *Am. J. Clin. Nutr.* 2007, *85*, 218-224.
[44] Organization, W. H., *Pellagra and its prevention and control in major emergencies*, World Health Organization, Geneva, Switzerland 2002.
[45] Bapurao, S., Krishnaswamy, K., Vitamin-B6 nutritional-status of pellagrins and their leucine tolerance. *Am. J. Clin. Nutr.* 1978, *31*, 819-824.
[46] Baquet, S., Wuillaume, F., Van Egmond, K., Ibanez, F., Pellagra outbreak in Kuito, Angola. *Lancet* 2000, *355*, 1829-1830.
[47] Wan, P., Moat, S., Anstey, A., Pellagra: a review with emphasis on photosensitivity. *Br. J. Dermatol.* 2011, *164*, 1188-1200.
[48] Leevy, C. M., Moroianu, S. A., Nutritional aspects of alcoholic liver disease. *Clin. Liver Dis.* 2005, *9*, 67-81.

[49] Prakash, R., Gandotra, S., Singh, L. K., Das, B., Lakra, A., Rapid resolution of delusional parasitosis in pellagra with niacin augmentation therapy. *Gen. Hosp. Psychiatry* 2008, *30*, 581-584.
[50] Oldham, M. A., Ivkovic, A., Pellagrous encephalopathy presenting as alcohol withdrawal delirium: a case series and literature review. *Addict. Sci. Clin. Pract.* 2012, *7*, 12.
[51] Sharma, B., Sannegowda, R. B., Jain, R., Dubey, P., Prakash, S., A rare case of alcoholic pellagra encephalopathy with startle myoclonus and marked response to niacin therapy: time for a new dictum? *BMJ Case Rep.* 2013, *2013*, bcr2013008906.
[52] Lee, J. M., Robson, M. D., Yu, L. M., Shirodaria, C. C., *et al.*, Effects of high-dose modified-release nicotinic acid on atherosclerosis and vascular function: a randomized, placebo-controlled, magnetic resonance imaging study. *J. Am. Coll. Cardiol.* 2009, *54*, 1787-1794.
[53] Goldberg, A., Alagona, P., Jr., Capuzzi, D. M., Guyton, J., *et al.*, Multiple-dose efficacy and safety of an extended-release form of niacin in the management of hyperlipidemia. *Am. J. Cardiol.* 2000, *85*, 1100-1105.
[54] Gille, A., Bodor, E. T., Ahmed, K., Offermanns, S., Nicotinic acid: pharmacological effects and mechanisms of action. *Annu. Rev. Pharmacol. Toxicol.* 2008, *48*, 79-106.
[55] Vogt, A., Kassner, U., Hostalek, U., Steinhagen-Thiessen, E., Prolonged-release nicotinic acid for the management of dyslipidemia: an update including results from the NAUTILUS study. *Vasc. Health Risk Manag.* 2007, *3*, 467-479.
[56] Bruckert, E., Labreuche, J., Amarenco, P., Meta-analysis of the effect of nicotinic acid alone or in combination on cardiovascular events and atherosclerosis. *Atherosclerosis* 2010, *210*, 353-361.
[57] Yang, S. J., Choi, J. M., Kim, L., Park, S. E., *et al.*, Nicotinamide improves glucose metabolism and affects the hepatic NAD-sirtuin pathway in a rodent model of obesity and type 2 diabetes. *J. Nutr. Biochem.* 2014, *25*, 66-72.
[58] Kolb, H., Burkart, V., Nicotinamide in type 1 diabetes: Mechanism of action revisited. *Diabetes Care* 1999, *22 Suppl 2*, B16-20.
[59] Martens, C. R., Denman, B. A., Mazzo, M. R., Armstrong, M. L., *et al.*, Chronic nicotinamide riboside supplementation is well-tolerated and elevates NAD(+) in healthy middle-aged and older adults. *Nat. Commun.* 2018, *9*, 1286.
[60] Cabrera-Rode, E., Molina, G., Arranz, C., Vera, M., *et al.*, Effect of standard nicotinamide in the prevention of type 1 diabetes in first degree relatives of persons with type 1 diabetes. *Autoimmunity* 2006, *39*, 333-340.
[61] Libri, V., Yandim, C., Athanasopoulos, S., Loyse, N., *et al.*, Epigenetic and neurological effects and safety of high-dose nicotinamide in patients with Friedreich's ataxia: an exploratory, open-label, dose-escalation study. *Lancet* 2014, *384*, 504-513.
[62] Gale, E. A. M., Bingley, P. J., Knip, M., Emmett, C. L., *et al.*, European nicotinamide diabetes intervention trial (ENDIT): a randomised controlled trial of intervention before the onset of type 1 diabetes. *Lancet* 2004, *363*, 925-931.
[63] Trammell, S. A., Schmidt, M. S., Weidemann, B. J., Redpath, P., *et al.*, Nicotinamide riboside is uniquely and orally bioavailable in mice and humans. *Nat. Commun.* 2016, *7*, 12948.
[64] Airhart, S. E., Shireman, L. M., Risler, L. J., Anderson, G. D., *et al.*, An open-label, non-randomized study of the pharmacokinetics of the nutritional supplement nicotinamide riboside (NR) and its effects on blood NAD+ levels in healthy volunteers. *PLoS One* 2017, *12*, e0186459.
[65] Dellinger, R. W., Santos, S. R., Morris, M., Evans, M., *et al.*, Repeat dose NRPT (nicotinamide riboside and pterostilbene) increases NAD(+) levels in humans safely and sustainably: a randomized, double-blind, placebo-controlled study. *NPJ Aging Mech. Dis.* 2017, *3*, 17.
[66] Dollerup, O. L., Christensen, B., Svart, M., Schmidt, M. S., *et al.*, A randomized placebo-controlled clinical trial of nicotinamide riboside in obese men: safety, insulin-sensitivity, and lipid-mobilizing effects. *Am. J. Clin. Nutr.* 2018, *108*, 343-353.
[67] Tsubota, K., The first human clinical study for NMN has started in Japan. *NPJ Aging Mech. Dis.* 2016, *2*, 16021.
[68] Kamanna, V., Ganji, S., Kashyap, M., The mechanism and mitigation of niacin-induced flushing. *Int. J. Clin. Pract.* 2009, *63*, 1369-1377.

[69] Scientific Committee on Food (SCF), *Opinion of the scientific committee on food on the tolerable upper intake level of nicotinic acid and nicotinamide (niacin)*, Brussels, Belgium 2002.
[70] Knip, M., Douek, I. F., Moore, W. P., Gillmor, H. A., *et al.*, Safety of high-dose nicotinamide: a review. *Diabetologia* 2000, *43*, 1337-1345.
[71] Jeong, J. Y., Kim, J. Y., Kim, H. J., Choe, Y. R., Association between Niacin and Type 2 Diabetes Mellitus in Korean: Korean National Health and Nutrition Examination Survey 2012-2015. *Korean J. Fam. Med.* 2018, *8*, 136-141.
[72] Zhou, S. S., Li, D., Zhou, Y. M., Sun, W. P., *et al.*, Chronic nicotinamide overload and type 2 diabetes. *Sheng Li Xue Bao* 2010, *62*, 86-92.
[73] Sun, W. P., Li, D., Lun, Y. Z., Gong, X. J., *et al.*, Excess nicotinamide inhibits methylation-mediated degradation of catecholamines in normotensives and hypertensives. *Hypertens. Res.* 2012, *35*, 180-185.
[74] Zhou, S. S., Li, D., Sun, W. P., Guo, M., *et al.*, Nicotinamide overload may play a role in the development of type 2 diabetes. *World J. Gastroenterol.* 2009, *15*, 5674-5684.
[75] Rawling, J. M., Jackson, T. M., Driscoll, E. R., Kirkland, J. B., Dietary niacin deficiency lowers tissue poly(ADP-ribose) and NAD+ concentrations in Fischer-344 rats. *J. Nutr.* 1994, *124*, 1597-1603.
[76] Rawling, J. M., Jackson, T. M., Roebuck, B. D., Poirier, G. G., Kirkland, J. B., The effect of niacin deficiency on diethylnitrosamine-induced hepatic poly(ADP-ribose) levels and altered hepatic foci in the Fischer-344 rat. *Nutr. Cancer* 1995, *24*, 111-119.
[77] Terakata, M., Fukuwatari, T., Sano, M., Nakao, N., *et al.*, Establishment of true niacin deficiency in quinolinic acid phosphoribosyltransferase knockout mice. *J. Nutr.* 2012, *142*, 2148-2153.
[78] Mokudai, T., Ayoub, I. A., Sakakibara, Y., Lee, E.-J., *et al.*, Delayed treatment with nicotinamide (vitamin B3) improves neurological outcome and reduces infarct volume after transient focal cerebral ischemia in Wistar rats. *Stroke* 2000, *31*, 1679-1685.
[79] Hathorn, T., Snyder-Keller, A., Messer, A., Nicotinamide improves motor deficits and upregulates PGC-1α and BDNF gene expression in a mouse model of Huntington's disease. *Neurobiol. Dis.* 2011, *41*, 43-50.
[80] Green, K. N., Steffan, J. S., Martinez-Coria, H., Sun, X., *et al.*, Nicotinamide restores cognition in Alzheimer's disease transgenic mice via a mechanism involving sirtuin inhibition and selective reduction of Thr231-phosphotau. *J. Neurosci.* 2008, *28*, 11500-11510.
[81] Li, Q., Xie, G., Zhang, W., Zhong, W., *et al.*, Dietary nicotinic acid supplementation ameliorates chronic alcohol-induced fatty liver in rats. *Alcohol. Clin. Exp. Res.* 2014, *38*, 1982-1992.
[82] Khan, N. A., Auranen, M., Paetau, I., Pirinen, E., *et al.*, Effective treatment of mitochondrial myopathy by nicotinamide riboside, a vitamin B3. *EMBO Mol. Med.* 2014, *6*, 721-731.
[83] Trammell, S. A., Weidemann, B. J., Chadda, A., Yorek, M. S., *et al.*, Nicotinamide riboside opposes type 2 diabetes and neuropathy in mice. *Sci. Rep.* 2016, *6*, 26933.
[84] Li, D., Tian, Y. J., Guo, J., Sun, W. P., *et al.*, Nicotinamide supplementation induces detrimental metabolic and epigenetic changes in developing rats. *Br. J. Nutr.* 2013, *110*, 2156-2164.
[85] Qi, Z., Xia, J., Xue, X., He, Q., *et al.*, Long-term treatment with nicotinamide induces glucose intolerance and skeletal muscle lipotoxicity in normal chow-fed mice: compared to diet-induced obesity. *J. Nutr. Biochem.* 2016, *36*, 31-41.
[86] Heemskerk, M. M., van den Berg, S. A., Pronk, A. C., van Klinken, J.-B., *et al.*, Long-term niacin treatment induces insulin resistance and adrenergic responsiveness in adipocytes by adaptive downregulation of phosphodiesterase 3B. *Am. J. Physiol. Endocrinol. Metab.* 2014, *306*, E808-E813.
[87] Kourtzidis, I. A., Stoupas, A. T., Gioris, I. S., Veskoukis, A. S., *et al.*, The NAD(+) precursor nicotinamide riboside decreases exercise performance in rats. *J. Int. Soc. Sports Nutr.* 2016, *13*, 32.
[88] Conze, D. B., Crespo-Barreto, J., Kruger, C. L., Safety assessment of nicotinamide riboside, a form of vitamin B3. *Hum. Exp. Toxicol.* 2016, *35*, 1149-1160.

[89] Tang, K., Sham, H., Hui, E., Kirkland, J. B., Niacin deficiency causes oxidative stress in rat bone marrow cells but not through decreased NADPH or glutathione status. *J. Nutr. Biochem.* 2008, *19*, 746-753.
[90] Kirkland, J. B., Niacin requirements for genomic stability. *Mutat. Res.* 2012, *733*, 14-20.
[91] Benavente, C. A., Jacobson, E. L., Niacin restriction upregulates NADPH oxidase and reactive oxygen species (ROS) in human keratinocytes. *Free Radic. Biol. Med.* 2008, *44*, 527-537.
[92] Kirkland, J. B., Niacin status, NAD distribution and ADP-ribose metabolism. *Curr. Pharm. Des.* 2009, *15*, 3-11.
[93] Furukawa, S., Fujita, T., Shimabukuro, M., Iwaki, M.*, et al.*, Increased oxidative stress in obesity and its impact on metabolic syndrome. *J. Clin. Invest.* 2017, *114*, 1752-1761.
[94] Martins, I. J., Lim, W. L. F., Wilson, A. C., Laws, S. M., Martins, R., The acceleration of aging and Alzheimer's disease through the biological mechanisms behind obesity and type II diabetes. *Health (N. Y.)* 2013, *5*, 913-920.
[95] Burhans, W. C., Weinberger, M., DNA replication stress, genome instability and aging. *Nucleic Acids Res.* 2007, *35*, 7545-7556.
[96] Massudi, H., Grant, R., Braidy, N., Guest, J.*, et al.*, Age-associated changes in oxidative stress and NAD+ metabolism in human tissue. *PLoS One* 2012, *7*, e42357.
[97] Zhu, X. H., Lu, M., Lee, B. Y., Ugurbil, K., Chen, W., In vivo NAD assay reveals the intracellular NAD contents and redox state in healthy human brain and their age dependences. *Proc. Natl. Acad. Sci. U. S. A.* 2015, *112*, 2876-2881.
[98] Kim, H. J., Kim, J. H., Noh, S., Hur, H. J.*, et al.*, Metabolomic analysis of livers and serum from high-fat diet induced obese mice. *J. Proteome Res.* 2011, *10*, 722-731.
[99] Liu, S., Kim, T.-H., Franklin, D. A., Zhang, Y., Protection against high-fat-diet-induced obesity in MDM2C305F mice due to reduced p53 activity and enhanced energy expenditure. *Cell Rep.* 2017, *18*, 1005-1018.
[100] WHO, *The global strategy and action plan on ageing and health*, World Health Organization, Switzerland, Geneva 2016.
[101] WHO, *Child mortality and causes of death*, World Health Organization, Switzerland, Geneva 2016.
[102] Medicine, F. a. N. B. i. I. o., *Dietary reference intakes for thiamin, riboflavin, niacin, vitamin B6, folate, vitamin B12, pantothenic acid, biotin and choline*, National Academy Press, Washington, DC 1998, pp. 123-149.
[103] Krehl, W. A., P. S. Sarma, L. J. Teply, and C. A. Elvehjem, Factors affecting the dietary niacin and tryptophane requirement of the growing rat. *J. Nutr.* 1946, *31*, 22.
[104] Henderson, L. M., Deodhar, T., Krehl, W. A., Elvehjem, C. A., Factors affecting the growth of rats receiving niacin-tryptophan-deficient diets. *J. Biol. Chem.* 1947, *170*, 261-268.
[105] Hundley, J. M., Production of niacin deficiency in rats. *J. Nutr.* 1947, *34*, 10.
[106] Hundley, J. M., Influence of fructose and other carbohydrates on the niacin requirement of the rat. *J. Biol. Chem.* 1949, *181*, 1-9.
[107] National Research Council, *Nutrient Requirements of Laboratory Animals, Fourth Revised Edition*, National Academies Press, Washington DC 1995, pp. 92-95.
[108] Fox, J. G., Barthold, S., Davisson, M., Newcomer, C. E.*, et al.*, *The mouse in biomedical research: diseases*, Academic Press, Salt Lake City UT 2006.
[109] Belenky, P., Christensen, K. C., Gazzaniga, F., Pletnev, A. A., Brenner, C., Nicotinamide riboside and nicotinic acid riboside salvage in fungi and mammals. Quantitative basis for Urh1 and purine nucleoside phosphorylase function in NAD+ metabolism. *J. Biol. Chem.* 2009, *284*, 158-164.
[110] Belenky, P., Racette, F. G., Bogan, K. L., McClure, J. M.*, et al.*, Nicotinamide riboside promotes Sir2 silencing and extends lifespan via Nrk and Urh1/Pnp1/Meu1 pathways to NAD+. *Cell* 2007, *129*, 473-484.
[111] Gariani, K., Menzies, K. J., Ryu, D., Wegner, C. J.*, et al.*, Eliciting the mitochondrial unfolded protein response by nicotinamide adenine dinucleotide repletion reverses fatty liver disease in mice. *Hepatology* 2016, *63*, 1190-1204.
[112] Gong, B., Pan, Y., Vempati, P., Zhao, W.*, et al.*, Nicotinamide riboside restores cognition through an upregulation of proliferator-activated receptor-γ coactivator 1α regulated β-secretase 1 degradation and mitochondrial gene expression in Alzheimer's mouse models. *Neurobiol. Aging* 2013, *34*, 1581-1588.

[113] Zhang, H., Ryu, D., Wu, Y., Gariani, K., *et al.*, NAD(+) repletion improves mitochondrial and stem cell function and enhances life span in mice. *Science* 2016, *352*, 1436-1443.
[114] Ryu, D., Zhang, H., Ropelle, E. R., Sorrentino, V., *et al.*, NAD+ repletion improves muscle function in muscular dystrophy and counters global PARylation. *Sci. Transl. Med.* 2016, *8*, 361ra139.
[115] Vaur, P., Brugg, B., Mericskay, M., Li, Z., *et al.*, Nicotinamide riboside, a form of vitamin B3, protects against excitotoxicity-induced axonal degeneration. *FASEB J.* 2017, *31*, 5440-5452.
[116] van Ommen, B., Keijer, J., Heil, S. G., Kaput, J., Challenging homeostasis to define biomarkers for nutrition related health. *Mol. Nutr. Food Res.* 2009, *53*, 795-804.
[117] Duivenvoorde, L. P., van Schothorst, E. M., Swarts, H. M., Kuda, O., *et al.*, A difference in fatty acid composition of isocaloric high-fat diets alters metabolic flexibility in male C57BL/6JOlaHsd mice. *PLoS One* 2015, *10*, e0128515.
[118] Duivenvoorde, L. P., van Schothorst, E. M., Swarts, H. J., Keijer, J., Assessment of metabolic flexibility of old and adult mice using three noninvasive, indirect calorimetry-based treatments. *J. Gerontol. A Biol. Sci. Med. Sci.* 2015, *70*, 282-293.
[119] Duivenvoorde, L. P., van Schothorst, E. M., Bunschoten, A., Keijer, J., Dietary restriction of mice on a high-fat diet induces substrate efficiency and improves metabolic health. *J. Mol. Endocrinol.* 2011, *47*, 81-97.
[120] Palou, A., Pico, C., Keijer, J., From risk assessment to risk-benefit evaluation: the need for guidelines, concepts and mechanisms. *Crit. Rev. Food Sci. Nutr.* 2009, *49*, 11.
[121] Keijer, J., van Helden, Y. G., Bunschoten, A., van Schothorst, E. M., Transcriptome analysis in benefit–risk assessment of micronutrients and bioactive food components. *Mol. Nutr. Food Res.* 2010, *54*, 240-248.

Chapter 2

Effects of a wide range of dietary nicotinamide riboside concentrations on metabolic flexibility and white adipose tissue of mice fed a mildly obesogenic diet

Wenbiao Shi, Maria A. Hegeman, Dorien A.M. van Dartel, Jing Tang, Manuel Suarez, Hans Swarts, Bart van der Hee, Lluis Arola and Jaap Keijer

Published in: Molecular Nutrition & Food Research. 2017 Aug;61(8).

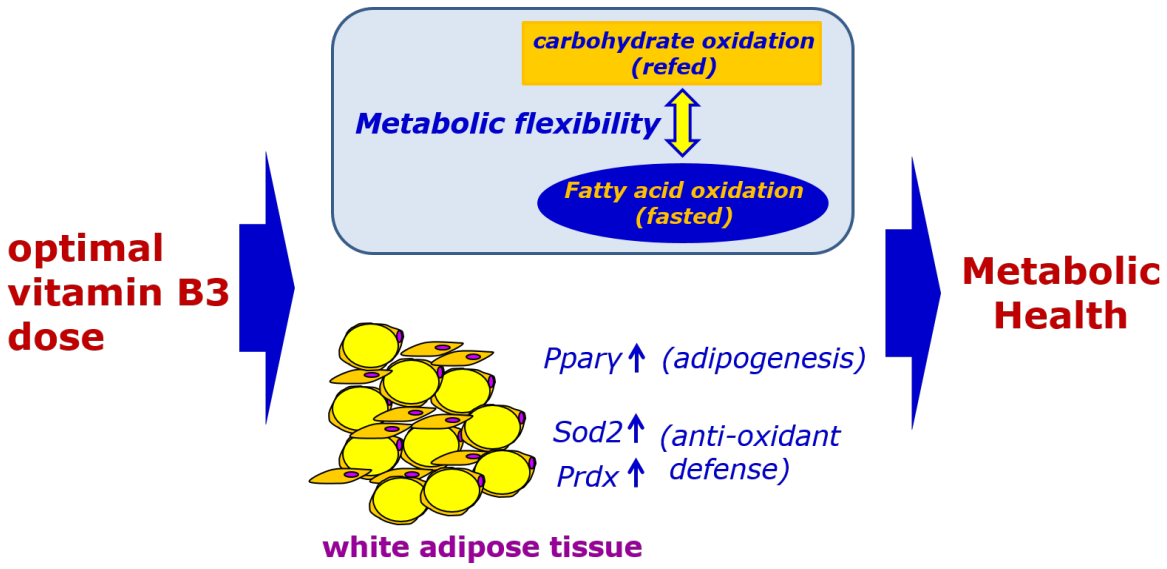

Abstract

Metabolic flexibility is the ability to switch metabolism between carbohydrate oxidation (CHO) and fatty acid oxidation (FAO) and is a biomarker for metabolic health. The effect on metabolic health of nicotinamide riboside (NR) as an exclusive source of vitamin B3 is unknown and is examined here for a wide range of NR. Thirteen-week-old male C57Bl/6JRccHsd mice received a semi-purified mildly obesogenic (40 en% fat) diet containing 0.14% L-tryptophan and either 5, 15, 30, 180 or 900 mg NR per kg diet for 15 weeks. Body composition and metabolic parameters were analysed. Metabolic flexibility was measured using indirect calorimetry. Gene expression in epididymal white adipose tissue (eWAT) was measured using qRT-PCR. Our results showed that the maximum delta respiratory exchange ratio when switching from CHO to FAO ($maxΔRER_{CHO1→FAO}$) and when switching from FAO to CHO ($maxΔRER_{FAO→CHO2}$) were largest in 30 mg NR per kg diet (30NR). In eWAT, the gene expression of *Pparγ*, a master regulator of adipogenesis, and of *Sod2* and *Prdx3*, two antioxidant genes, were significantly upregulated in 30NR compared to 5NR. In conclusion, 30NR is most beneficial for metabolic health, in terms of metabolic flexibility and eWAT gene expression, of mice on an obesogenic diet.

Introduction

Nicotinamide adenine dinucleotide (NAD^+) is essential to maintain cellular redox state and basal energy metabolism. Beyond its role as a reusable coenzyme, NAD^+ is also permanently degraded by various signalling enzymes, including sirtuins [1]. Although the degradation product, nicotinamide (Nam), can be recycled for NAD^+ generation, maintenance of NAD^+ levels is dependent on exogenous supplementation with vitamin B3, from which NAD^+ can be synthesized. Indeed plasma NAD^+ levels decrease when humans or rodents are exposed to a vitamin B3-deficient diet [2-4]. Severe vitamin B3 deficiency causes pellagra, a disease characterized by dermatitis, diarrhea, and dementia, ultimately resulting in death [5]. Even though pellagra has become rare in developed countries, it remains endemic in underdeveloped countries [6].

While severe vitamin B3 deficiency results in disease, hardly any information is available on physiological consequences of marginal vitamin B3 levels. This is particularly relevant because it was shown that obesogenic diets reduce NAD^+ levels in several tissues [7-10].Surprisingly, requirements for dietary vitamin B3 are still not well-established for rodents, especially mice [11, 12]. The National Research Council suggested the vitamin B3 requirement in rats to be 15 mg/kg diet, based on three scientific publications in the 1940s. However, these studies did not use purified diets and only used growth rate as a read-out parameter [13-15]. More importantly, requirements were based on studies with rats as no direct data were available for mice. Estimation of vitamin B3 requirements is not straightforward, since NAD^+ can also be synthesized *de novo* from the essential amino acid tryptophan (Trp) [16]. Dietary Trp may thus rescue vitamin B3 deficiency. Indeed, rodents can maintain optimal growth and tissue NAD^+ levels when supplied with a vitamin B3-free diet containing 0.23% L-Trp [17, 18]. It is, however, not possible to simply use Trp-deficient diets to establish vitamin B3 requirements, because Trp is essential for serotonin synthesis and protein synthesis [19]. The lack of data on vitamin B3 requirement thresholds precludes research into the molecular, metabolic and physiological consequences of marginal status of various forms of vitamin B3.

Nicotinic acid (NA) and Nam are the classic forms of vitamin B3, present in the diet. NA and Nam can be converted to NAD^+ via the Preiss-Handler and the salvage pathway, respectively [20]. Nicotinamide riboside (NR) is another source of vitamin B3 that naturally exists in cow's milk and yeast-containing food products. NR can be metabolized into NAD^+ directly via the Nrk pathway [21]. Recent studies have shown that supplementation of NR at pharmacological levels can provide physiological or metabolic benefits by boosting NAD^+ levels [8, 22-26]. No side effects of NR have been reported, in contrast to high dose treatment with NA, that may cause skin flushing, or Nam, that may lead to liver damage [27]. Therefore, NR has been proposed as the vitamin B3 of choice. Despite the benefits from pharmacological NR supplementation [8, 22, 24, 26], it would be necessary to re-evaluate the NR dose, as it appears strikingly high (400 mg NR/kg body weight

/day) compared to most commercially available supplements (60–500 mg/person/day) [28].

The metabolic health effects of NR as an exclusive source of vitamin B3 at nutritional relevant levels are unknown. Recently, the ability to rapidly switch metabolism between carbohydrate oxidation and fatty acid oxidation, so-called metabolic flexibility, has been recognized as a sensitive biomarker for metabolic health in nutritional interventions [29-32]. Metabolic flexibility can be assessed by analysing the respiratory exchange ratio (RER) during a fast-refeeding challenge in non-invasive indirect calorimetry. To examine the effects of nutritional relevant levels of NR on metabolic health, we performed a dose-response dietary intervention study using a wide range of NR, from 5 to 900 mg NR per kg of a defined semi-purified obesogenic diet, combined with a metabolic flexibility measurement. We used a mildly obesogenic diet (40 en% fat) to mimic a Western diet. To limit NAD^+ biosynthesis from Trp, we implemented a low level of Trp (0.14%). This Trp level is still sufficient for normal growth in mice [33]. Since white adipose tissue (WAT) may play a crucial role in metabolic flexibility at the whole body level [34-36], we focused on metabolic flexibility and WAT function.

Material and Methods

Dietary intervention

The animal experiment was approved by the Animal Welfare Committee of Wageningen University, Wageningen, The Netherlands (DEC2014029). Nine-week-old male C57Bl/6JRccHsd mice (Envigo, Horst, The Netherlands) were individually housed (12h light–dark cycle, 23±1°C, 55±15% humidity) with *ad libitum* access to feed and water. During a 4-week adaptation period, mice received a semi-synthetic diet (10% energy from fat), containing 0.14% L-tryptophan and 30 mg NR/kg diet (Research Diet Services, Wijk bij Duurstede, The Netherlands). At 13 weeks of age, mice were stratified into 5 experimental groups on mean body weight (n=12/group) and received a semi-synthetic obesogenic diet (40% energy from fat) containing 0.14% L-tryptophan and either 5, 15, 30, 180 or 900 mg NR per kg diet (referred to as 5NR, 15NR, 30NR, 180NR and 900NR, respectively) for 15 weeks (diet composition in Table 1). Feed intake and body weight as well as lean and fat mass (by NMR, EchoMRI, Houston, USA) were measured weekly. In the beginning of week 16 mice were sacrificed by decapitation after 2 hours of fasting. Blood was collected for immediate blood glucose measurement using a Freestyle blood glucose meter (Abbott Diabetes Care, Hoofddorp, the Netherlands). The remaining blood was centrifuged at 3,000*g* and 4°C for 10 minutes and serum was stored at –80°C. Tissues were rapidly dissected, snap frozen in liquid nitrogen and stored at -80°C (i.e. left epididymal white adipose tissue (eWAT), liver, soleus muscle, brain, mucosa scraped from small intestine). In addition, right eWAT was weighted, divided in half and fixed for 24 hours at 4°C in PBS with 4.0% formaldehyde (pH=7.40) as described [37].

Table 1. Composition of diets

Ingredients (g·kg-1 diet)	Run-in	5NR	15NR	30NR	180NR	900NR
Casein	120.0	120.0	120.0	120.0	120.0	120.0
Wheat starch	385.9	215.7	215.7	215.7	215.7	215.7
Gelatin (hydrolysed)	100.0	100.0	100.0	100.0	100.0	100.0
Maltodextrin	100.0	100.0	100.0	100.0	100.0	100.0
Sugar	100.0	100.0	100.0	100.0	100.0	100.0
Dextrose	50.0	50.0	50.0	50.0	50.0	50.0
Arbocel B800	50.0	50.0	50.0	50.0	50.0	50.0
Linseed oil	5.2	4.0	4.0	4.0	4.0	4.0
Palm oil	–	206.0	206.0	206.0	206.0	206.0
Coco oil	7.7	–	–	–	–	–
Sunflower oil	30.1	–	–	–	–	–
Mineral mixture AIN-93	35.0	35.0	35.0	35.0	35.0	35.0
Vitamin mixture AIN-93[1]	10.0	10.0	10.0	10.0	10.0	10.0
L-Cystine	3.3	3.3	3.3	3.3	3.3	3.3
L-Phenylalanine	0.4	3.5	3.5	3.5	3.5	3.5
Choline chloride 50%	2.5	2.5	2.5	2.5	2.5	2.5
Nicotinamide riboside (mg·kg-1 diet)	30.0	5.0	15.0	30.0	180.0	900.0
Calculated amount of L-Trp (%)	1.4	1.4	1.4	1.4	1.4	1.4
Calculated energy (kcal·kg-1)	3825	4660	4660	4660	4660	4660
Energy (% of total energy content)						
Carbohydrate	66	40	40	40	40	40
Fat	10	40	40	40	40	40
Protein	23	20	20	20	20	20

[1]without any form of vitamin B3

Indirect Calorimetry

Indirect calorimetry was performed in week 14, using a PhenoMaster System (TSE Systems, Bad Homburg, Germany) as described [31]. Briefly, mice were individually housed with a steady normal air flow, 12h light–dark cycle (07:00h lights on). Oxygen consumption, carbon dioxide production, activity (infrared beam breaks) and food and drink intake were automatically recorded. After 20 hours of adaptation, *ad libitum* fed mice were monitored for 24 hours starting from 07:00h. Next, the mice were exposed to a fast and refeeding challenge. For this, the mice were provided with 1.5 gram of fresh experimental diet at 16:00h. The mice fully consumed this, after which they changed to a fully fasted state. The next day at 16:00h they were provided with 1.8 gram of fresh experimental diet (refeeding), which was fully consumed. Respiratory exchange ratio (RER) and energy expenditure (EE) were calculated by TSE software (TSE systems). Metabolic flexibility was assessed as described [36], with the following modifications: the maximum delta RER was calculated when switching from CHO1 (mean of 5 highest values) to FAO (mean of 5 lowest values) during fasting ($maxΔRER_{CHO1→FAO}$), and when switching from FAO (mean of 5 lowest values) to CHO2 (mean of 5 highest values) during refeeding ($maxΔRER_{FAO→CHO2}$). How a specific RER value relates to percentage lipid or carbohydrate oxidation can be found in [38].

Serum parameters
Serum triglycerides (TG) and non-esterified fatty acids (NEFA) were measured as described [39]. Serum insulin, leptin and adiponectin were measured with a Bio-Plex Pro Mouse Diabetes Assay using a Bio-Plex 200 system according to manufacturer's instructions (Bio-Rad, Veenendaal, The Netherlands). Samples were diluted 1:12.5 with sample diluent for insulin and leptin measurement and 1:1600 with serum-based diluent for adiponectin measurement. To assess insulin resistance HOMA-IR was calculated as (glucose (mmol/l)×insulin(μU/ml)/22.5) [40].

NR metabolites in serum and liver
NR metabolites were extracted from serum as well as liver and subsequently identified and quantified using LC-ESI-MS/MS according to the procedure described in Supporting Methods.

Gene expression
Tissues were grinded in liquid nitrogen, after which RNA was isolated from liver, brain and mucosa with a RNeasy Mini kit (Qiagen, Venlo, The Netherlands) and from eWAT with Trizol, as described [41]. RNA purity and integrity was verified using Nanodrop (NanoDrop, Wilmington, USA) and Experion (Bio-Rad, CA, USA), respectively. cDNA synthesis, followed by regular qRT-PCR was performed as described [41]. Low expressed genes were pre-amplified for 12 cycles before qRT-PCR using SsoAdvanced PreAmp Supermix (Bio-Rad, CA, U.S.A.). The expression of each gene was normalized by the stably expressed reference genes using CFX Manager software (Bio-Rad, CA, U.S.A.). Primer sequences and PCR annealing temperatures for each gene are in Supporting Table 1. References genes were selected based on stable expression in the selected tissues.

Mitochondrial density
eWAT mitochondrial DNA (mtDNA) and nuclear DNA (nDNA) were analysed by qRT-PCR as described [31]. mtDNA/nDNA was used to assess mitochondrial density.

eWAT morphology
Adipocyte cell size determination as well as macrophage staining and counting were performed as described previously [37]. Detailed description of these methods can be found in the Supporting methods.

Statistics
Data are expressed as mean ± SEM for n=10-12 mice, but n=6 for IHC. Statistical analyses were performed using GraphPad Prism v5.04 (Graphpad, San Diego, CA, USA). Data were verified for normality using the D'Agostino and Pearson omnibus normality test and log transformed if needed. Body weight, cumulative feed intake, lean mass, fat mass and mean RER were analysed using two-way repeated measures ANOVA (factor 1=NR, factor 2=WEEK) followed by Bonferroni post-hoc analysis. All other data were analysed using one-way ANOVA following by Dunnett's multiple comparison test, with 30NR as control (unless otherwise stated). Pearson correlation analysis was performed on serum NR and NAD^+, liver NR and NAD^+ as well as leptin/adiponectin ratio and $\Delta RER_{FAO\text{-}CHO2}$. P-values < 0.05 were considered to be statistically significant.

Results

Body physiological parameters and metabolic flexibility

No differences were found in body weight, cumulative feed intake, lean mass or fat mass, when comparing mice with 5, 15, 30, 180 or 900 mg NR/kg diet, after the 15 week intervention (Fig. 1). Metabolic flexibility was assessed by calculating maxΔRER in response to a fast and refeeding in week 14 (Fig. 2A). Fasting metabolic flexibility, $\max\Delta RER_{CHO1\rightarrow FAO,}$ was significantly better in 30NR than in 5NR (Fig. 2B). Refeeding metabolic flexibility, $\max\Delta RER_{FAO\rightarrow CHO2}$, was significantly greater in 30NR than in 5NR, 15NR, or 900NR (Fig. 2C). No differences were found in energy expenditure or physical activity (Supporting Fig. 1). Under the non-challenged condition no significant differences in RER or feed intake were found among NR doses (Supporting Fig. 2).

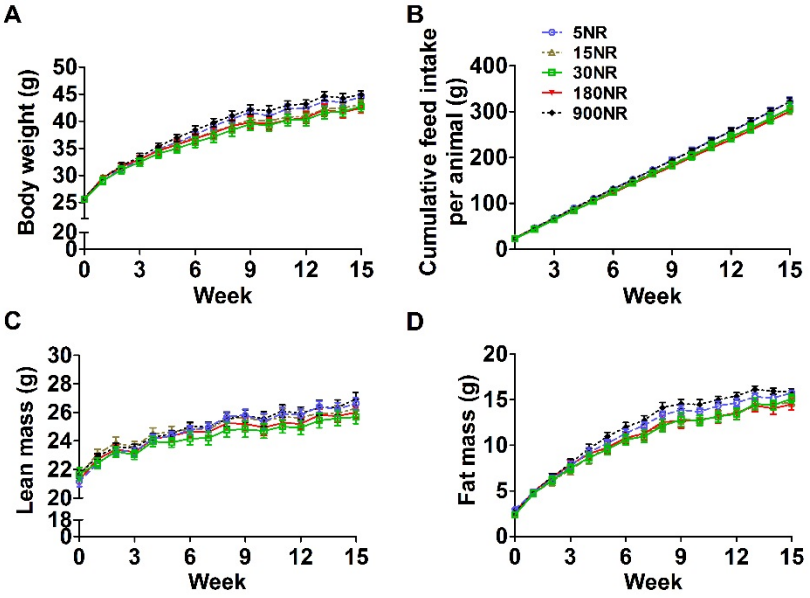

Figure 1. Effects of dietary NR on whole body physiological parameters. Mice were on obesogenic diets different levels of NR for 15 weeks. Body weight (A), cumulative feed intake (B), lean mass (C), fat mass (D). 5NR open circle, 15NR open upward triangle, 30NR open square, 180NR closed downward triangle, 900NR closed diamond. NR in mg/kg diet. Data are analysed using two-way ANOVA and presented as mean±SEM (n=11-12 mice per treatment).

Blood glucose and serum lipids and adipokines

No differences were seen in blood glucose, serum TG or NEFA among NR doses (Fig. 3A-C). Serum insulin, leptin, adiponectin, leptin/adiponectin ratio and HOMA-IR index exhibited a tendency towards a dose-response curve, without reaching statistical significance (Fig. 3D-H). In all cases, except adiponectin which shows opposite behaviour, the measured value decreased and then increased, with 30NR being the turning point. Of note, 30NR resulted in lower leptin/adiponectin ratio compared to 5NR using t-test (p=0.0499), supporting our observations in metabolic flexibility.

Serum and liver NR metabolites

No differences were found in levels of NR, nicotinic acid mononucleotide (NaMN), Trp or Nam (p=0.0546 when comparing 900NR with 15, 30 or 180NR groups) in serum (Fig. 4A-D) and NAD^+, NR, nicotinamide mononucleotide (NMN), Trp, Nam, NA, NaMN in liver (Fig 4E-K) between the different groups. NAD^+, NA, NMN could not be detected in serum, neither were the vitamin B3 status markers N-methylnicotinamide (MeNam) and 2-pyridone (2PY) detectable in serum.

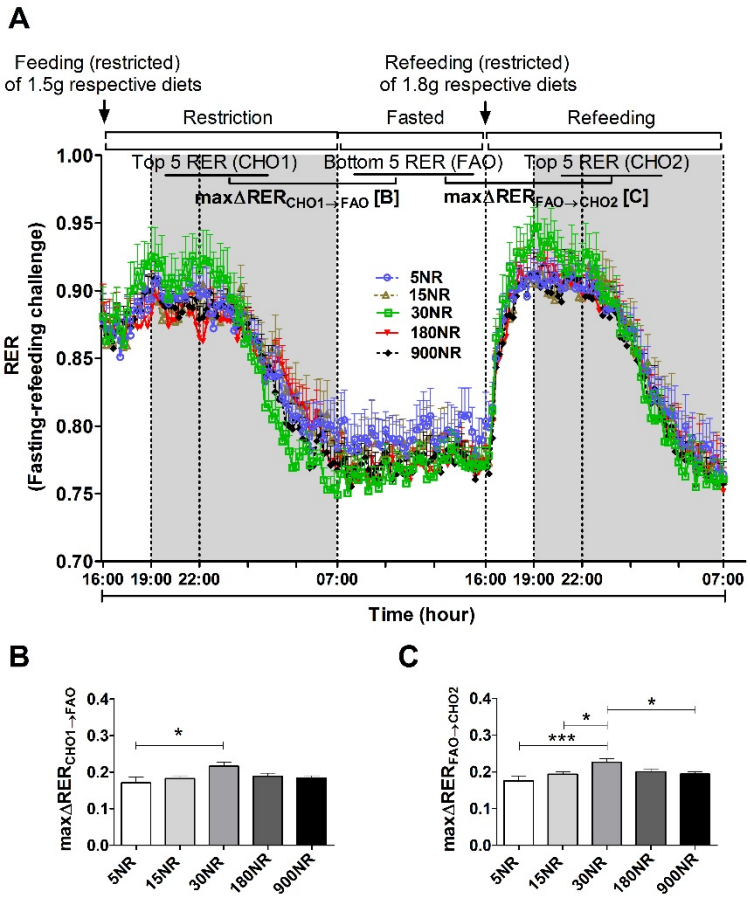

Figure 2. Effects of dietary NR on ΔRER during fast-refeeding challenge at week 14. Fast-refeeding (A): restriction (from 16:00h to 07:00h), fasted (from 07:00h to 16:00h), refeeding (from 16:00h to 07:00h) periods. Shaded areas indicate the dark, active phases. Max$\Delta RER_{CHO1 \rightarrow FAO}$ (B) is difference between mean of 5 highest RER values in restriction period and mean of 5 lowest RER values in fasted period. $\Delta RER_{FAO \rightarrow CHO2}$ (C) is difference between mean of 5 lowest RER values in fasted period and 5 highest RER values in refeeding period. The ΔRER values represent metabolic flexibility. Data are analysed using either two-way ANOVA (A) or one-way ANOVA followed by Dunnett's multiple comparison test, with 30NR as control (B and C), and presented as mean±SEM (n=11-12). * p<0.05, *** p<0.005.

eWAT morphology and gene expression

We focused the remainder of the analyses on the 5NR, 30NR and 900NR interventions, the three most dose-representative treatments which also showed differences in max$\Delta RER_{FAO \rightarrow CHO2}$.

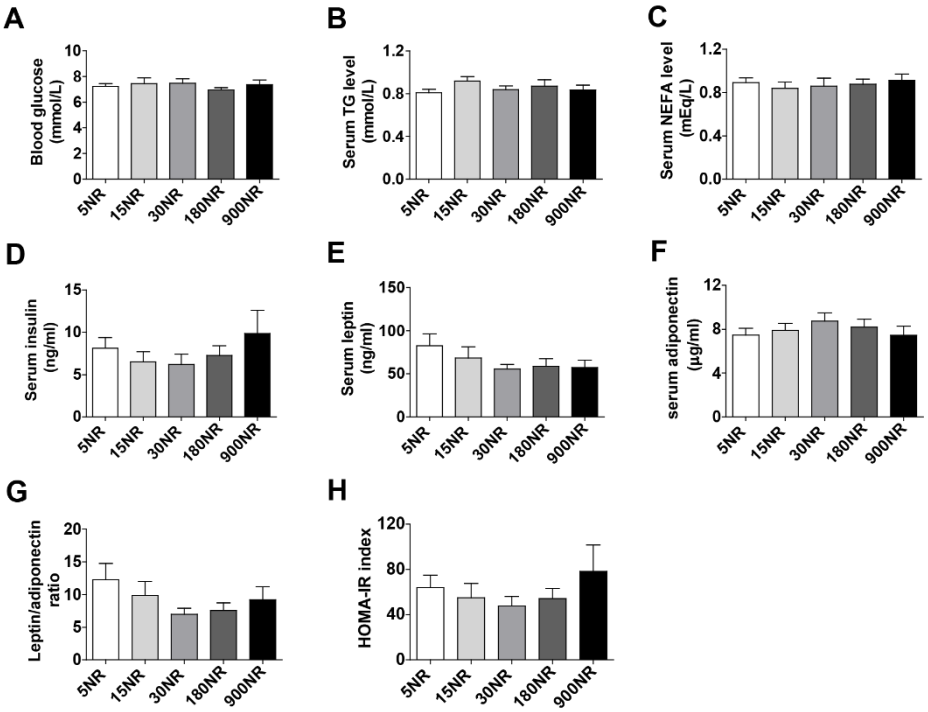

Figure 3. Effects of dietary NR on circulating parameters. Blood glucose (A), serum TG (B), serum NEFA (C), and serum insulin, leptin and adiponectin (D-F). Leptin/adiponectin ratio (G, p = 0.0499 between 5NR and 30NR via Student's t-test) and HOMA-IR index (H). Correlation between leptin /adiponectin ratio and metabolic flexibility (I). Data are analysed using one-way ANOVA and mean±SEM (n=11-12).

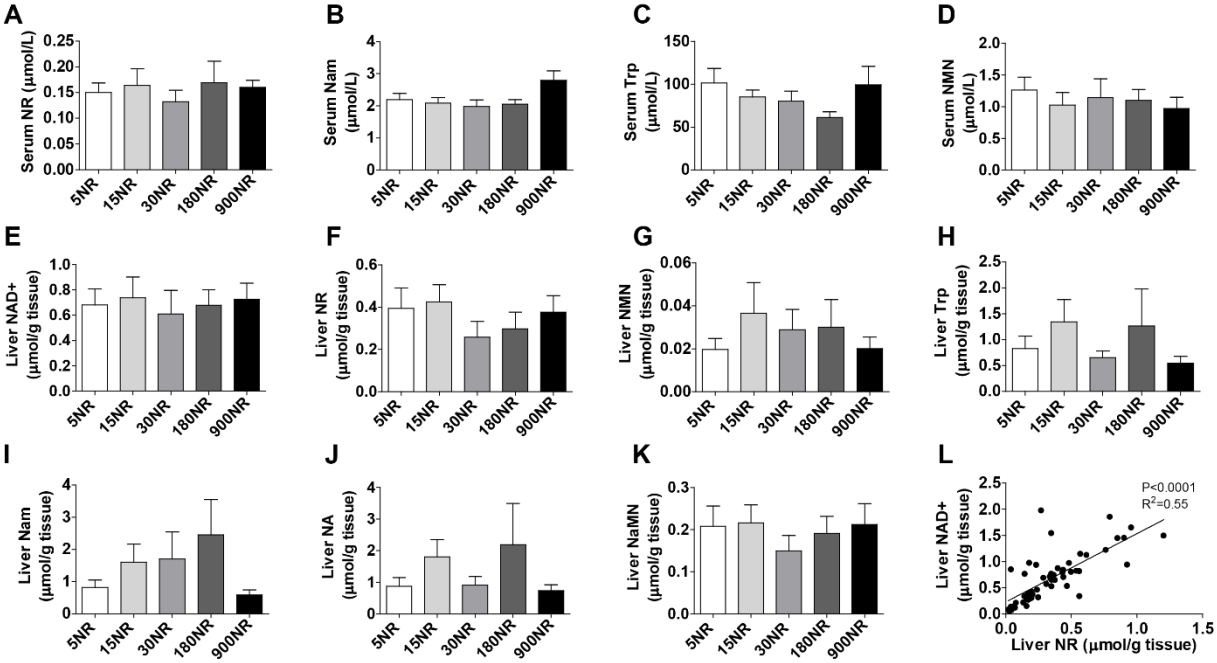

Figure 4. Effects of dietary NR on NR metabolites. Serum (A-D), liver (E-K). The correlation between NAD^+ and NR concentration in liver (L). Data are analysed using one-way ANOVA and presented as mean±SEM (n=10-12, serum NaMN n=5-10).

mRNA levels of rate limiting enzymes involved in the NR pathway, *Ido1, Ido2, Tdo2, Qprt* (*de novo* pathway), *Nrk1,Nrk2* (Nrk pathway) and *Nampt, Nmnat1, Nmnat3* (salvage pathway), were determined. No differences were found in the expression of these genes in either liver (Supporting Fig. 3A), small intestinal mucosa (Supporting Fig. 3B) , skeletal muscle (Supporting Fig. 3C), or eWAT (Supporting Fig. 3D).

eWAT morphology was assessed by adipocyte size and CLS number. 900NR showed a smaller average adipocyte cell surface area (4015±224.3µm^2) than 5NR (5032±363.8µm^2) or 30NR (5015±873.5µm^2) (Fig. 5A-D). Compared to the two other treatments, 30NR showed the largest number of small adipocytes (100-1500 µm^2) as well as the smallest number of medium size adipocytes (>1500-6000 µm^2), while 900NR showed the smallest number of large adipocytes (>6000µm^2) (Fig. 5E-H). 900NR showed the lowest number of CLS, compared to 5NR and 30NR (Fig. 5I-L). The expression of genes related to mitochondrial function, adipogenesis, antioxidant response, lipid metabolism, glucose metabolism as well as the adipokines leptin and adiponectin were analysed. *Cs* was not affected by the treatments (Fig. 6A). The expression of *Pparγ*, *Sod2* and *Prdx3* was highest in 30NR, a difference that was significant compared to 5NR (Fig. 6A and B). The expression of *C/ebpa, C/ebpβ and Pgc1a*, three adipogenesis related genes involved in the regulation of *Pparγ*, showed a similar dose-response pattern as *Pparγ*, but differences did not reach statistical significance (Fig. 6A). The expression of the anti-oxidant genes *Cat, Gpx3, Sod1*, *Trp53* showed a dose-response pattern similar to *Sod2* and *Prdx3*, but without reaching significance (Fig. 6B). Although we did not find differences in the expression of lipid metabolism, glucose metabolism or adipokine genes, 30NR tended to show higher levels of *Acox1, Fasn, Ppara, Glut4* and *Adipoq* (Fig. 6C and D). *Lept* was not different, in agreement with no difference in adiposity.

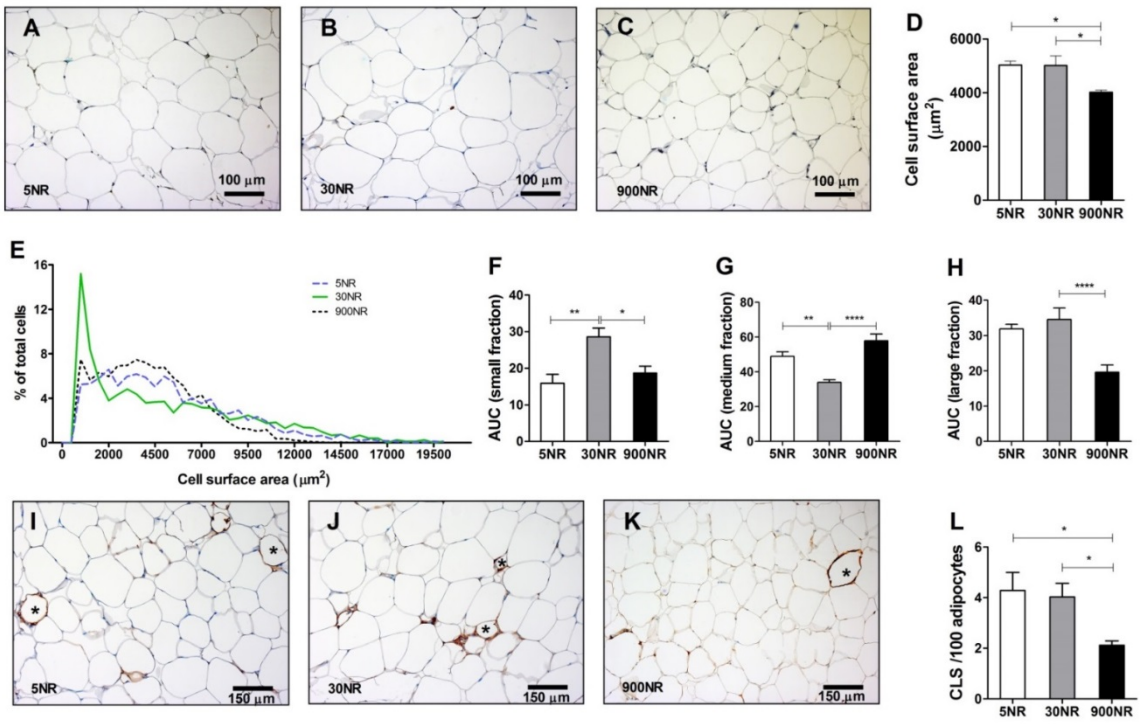

Figure 5. Effects of dietary NR on eWAT morphology. Representative images for 5NR (A), 30NR (B), 900NR (C); NR in mg/kg diet. Bar represents 100µm and A-C are same magnification (20×). Cell surface area (D). Frequency distribution (E) and area under the curve (AUC) of small (100-1500µm2, F), medium (<1500-6000µm2, G and large (>6000µm2, H) fractions. Representative images of crown-like structures (CLS, indicated by stars) for 5NR (I), 30NR (J), 900NR (K). Bar represents 150µm and I-K are same magnification (20×). Total CLS number per 100 adipocytes (L). striped 5NR, continuous 30NR, dotted 900NR. Data are analysed using one-way ANOVA followed by Dunnett's multiple comparison test, with 30NR as control (F-H), or Bonferroni post-hoc test (D and L) and presented as mean±SEM (n=6). * $p<0.05$, ** $p<0.01$, *** $p<0.005$, **** $p<0.001$.

Discussion

To assess beneficial and adverse effects of metabolic health, it is important that metabolic health is compromised, but not deteriorated. The mice in our study were metabolically compromised as they displayed a higher weight gain and worsened metabolic parameters compared to the same substrain of mice on a LFD in another study and comparable or slightly worse than the mice on the HFD in that study [42]. On the other hand, these parameters were not fully deteriorated as, for example, in Ob/Ob mice [43]. Metabolic flexibility is a biomarker for metabolic health that can be assessed non-invasively using indirect calorimetry [31, 32]. Using a fast-refeeding challenge, we here found a dose-response effect, showing that mice fed 30 mg NR/kg diet (30NR) were more metabolically flexible than the wide range of other NR concentrations.

By challenging homeostatic systems subtle metabolic effects, difficult to detect using static biomarkers, may be identified [44, 45]. Indeed, despite an absence of changes in whole body physiological parameters and RER under the non-challenged conditions, we did find differences in metabolic flexibility measured during a fast-refeeding challenge. NR influenced metabolic flexibility in a dose-response manner,

with 30NR being most metabolically flexible. This was not caused by differences in activity or energy expenditure as these parameters were not influenced by NR. The dose-dependent changes of dietary NR in metabolic flexibility might be associated with the activity of sirtuins, enzymes that are regulated by intracellular NAD+ levels and are linked to longevity and other health benefits such as improved insulin sensitivity [46, 47]. The HOMA-IR index [48] and the leptin/adiponectin ratio [49] are markers for insulin resistance. Because insulin resistance interacts with glucose and glucose disposal [29, 50], a causal relation exists. Indeed, insulin resistance and metabolic flexibility were negatively correlated in another study [51]. The HOMA-IR index and the leptin/adiponectin ratio show a dose-response pattern opposite to the metabolic flexibility dose-response pattern therefore enforces our observation.

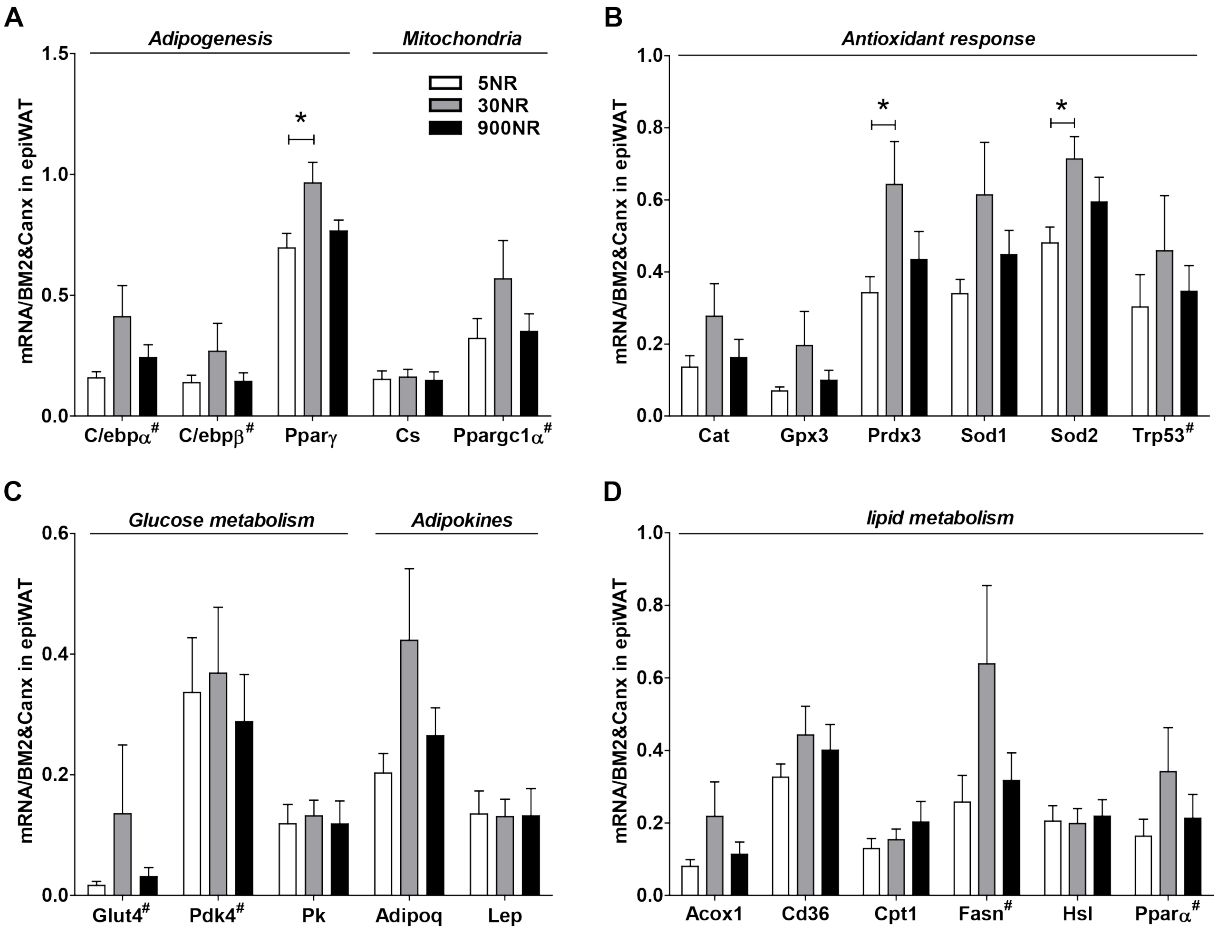

Figure 6. Effects of dietary NR on eWAT gene expression. mRNA levels (normalized to mean of indicated reference mRNAs) of adipogenesis and mitochondria (*C/ebpa*, *C/ebpβ*, *Pparγ*, *Cs*, *Ppargc1a*; A), antioxidant response (*Cat*, *Gpx3*, *Sod*, *Sod2*, *Trp53*; B), glucose metabolism and adipokine (*Glut4*, *Pdk4*, *Pk*, *Adipoq*, *Lep*; C) genes, lipid metabolism (*Acox1*, *Cd36*, *Cpt1*, *Fasn*, *Hsl*, *Ppara*; D) . White 5NR, grey 30NR, black 900NR. # indicates qRT-PCR determination was after 12-cycle pre-amplification. Full gene names are in supporting Table 2. Data are analysed using one-way ANOVA followed by Dunnett's multiple comparison test, with 30NR as control and presented as mean±SEM (n=10-11). * $p<0.05$.

In this study we used a semi-synthetic obesogenic diet with moderate levels of fat (40 en%) resembling the average fat intake in the Netherlands and identified 30NR as the most optimal dose of NR in terms of metabolic health. Metabolic flexibility was not improved at 900NR (equivalent to 102 mg NR /kg BW/day at the start of the experiment to 65 mg NR/kg BW/day in the end); if anything it was decreased. This contrasts with Canto *et al.* who found that metabolic flexibility, assessed by the difference of RER between dark phase and light phase, was increased by supplementation with 400 mg NR/kg BW/day of a high fat diet that already contained 30 mg/kg diet of vitamin B3 (Nam) [8]. This improvement in metabolic flexibility, on the other hand, was not observed in mice fed a high-fat-high-sucrose (HFHS) diet [22], nor in mice fed a chow diet [24], even though the same high dose of NR was used. This suggests a modifying effect of the diet on improvement of metabolic flexibility at high NR concentrations. Alternatively, differences may be due to the absence and presence of the nicotinamide nucleotide transhydrogenase (*Nnt)* gene. The C57Bl/6JRccHsd mice used in our study have, similar to humans, an intact *Nnt* gene, which is absent in the strain used by Canto *et al.* [8]. NNT has a key role in redox and peroxide metabolism [52, 53] and is responsible for maintenance of mitochondrial NAD^+ levels [54]. Its absence impairs regulation of insulin secretion and thus affects glucose homeostasis [55]. Absence or presence of *Nnt* thus affects disease development as well as NAD^+ levels which may explain the observed differences in protective effects of high dose NR supplementation, which needs to be tested experimentally.

WAT plays an important role in metabolic flexibility, in addition to skeletal muscle and liver [34]. Although several studies have shown a decrease in fat mass or WAT weight upon high dose NR supplementation, no WAT morphological parameters were investigated [8, 22, 56]. Since adipocyte morphology and especially adipocyte size mirrors overall WAT biological function [57], we newly investigated this. 900NR decreased the average adipocyte size compared to 5NR or 30NR. However, the calculated total adipocyte number (according to Skurk T et al., 2007) [57], tended to be higher in the 900NR group as there were no differences found in eWAT weight (data not shown). 30NR showed less medium-size adipocytes, compared to 5NR and 900NR, but had higher numbers of small (compared to 5NR and 900NR) as well as large (compared to 900NR) adipocytes. The functional differences between small and large adipocytes have been described in several studies. Smaller adipocytes tend to be more sensitive to insulin stimulation, showing a two times larger translocation of GLUT4 to the plasma membrane and increased adiponectin release [58, 59]. Large adipocytes, on the other hand, have a higher ability to buffer fatty acid flux and promote lipid mobilization [60]. We sacrificed the mice in the fasted state and it may have been necessary to sacrifice them at the peak of RER (3h after refeeding) to detect clear differences in the serum parameters related to adipose tissue function. Nevertheless, the adipocyte size frequency distribution in 30NR agrees with the dose-response profile of HOMA-IR index and serum adipokines, supporting the best metabolic flexibility at 30NR.

We examined the inflammatory state of the adipocytes by Mac-2 staining and measuring CLS in eWAT. CLS per 100 adipocytes were lowest in 900NR compared

to 5 NR and 30NR, although also there the numbers of CLS remained low. This supports the association of CLS with (clearance of) large adipocytes. Our data may also indicate that 900NR affects WAT inflammation beneficially. In agreement, treatment with 200 mg NA/kg body weight/day for 5 weeks was shown to attenuate WAT inflammation by reducing the expression of gene MCP-1, IL-1b and the pro-inflammatory M1 macrophage marker CD11c in HFD-fed mice [61]. However, when taking the total adipocyte number into account, there is no statistical difference in total number of CLS in eWAT (data not shown). To definitely conclude on the effect of NR on inflammation in our study, more inflammatory markers, such as Tumor Necrosis Factor α, should be measured.

PPARγ is the master regulator of adipogenesis [62]. *Pparγ* mRNA levels were significantly higher at 30NR compared to 5NR, the same trend, although not significant, was seen for *Acox1* and *Glut4,* key genes involved in fatty acid oxidation and glucose disposal. PPARγ activation in adipocytes has been shown to promote glucose metabolism by facilitating glucose uptake and enhancing glucose oxidation, as well as to increase lipid metabolism by stimulating fat uptake and mobilization and enhancing free fatty acid oxidation [63, 64]. Thus, PPARγ may contribute to the increased metabolic flexibility of 30NR compared to 5NR. *Pparγ* was not further increased at 900NR. A similar pattern is seen for antioxidant defence. SOD2 and PRDX3 were significantly elevated at the transcriptional level at 30NR compared to 5NR, suggesting a higher mitochondrial antioxidant defence activity. This was not due to a change in mitochondrial density (Supporting figure 3), confirmed by no change in expression of *Cs*. Since selective downregulation of *Sod2* and *Prdx3* in eWAT upon high fat diet feeding resulted in oxidative stress [65], their upregulation suggests increased protection against damage by reactive oxygen species (ROS). As for *Pparγ*, 900NR did not increase the expression of *Sod2* and *Prdx3 any* further. Our data suggest that adipogenesis and antioxidant response in eWAT are sensitive to low dietary NR, but not to supplemental NR.

Vitamin B3 deficiency leads to low tissue or blood NAD^+ level and growth retardation in rodents [3, 4, 66]. In our study, no decrease in body weight or body mass were observed in 5NR, neither were any vitamin B3 deficiency symptoms, such as rough skin, diarrhoea seen (data are not shown). Most importantly, there were no differences between the treatments in the expression of the genes involving in NAD^+ biosynthesis in many tissues, e.g. liver, skeletal muscle, WAT and mucosa. In line with this, NAD^+ levels and the other NR metabolites in liver and serum did not show differ between treatments. It should be noted that the Trp content used in this study can maintain normal vitamin B3 status in mice fed a vitamin B3-free diet [17, 18]. Furthermore, NR has been shown be converted to Nam before being absorbed or reaching tissues [67, 68], where it is rapidly metabolized [69]. Considering that fasted plasma Nam levels are very low [70], blood and tissue collection at the fasted status may provide another explanation for the small alteration in NR metabolites. Regretfully, we did not collect whole blood at section for the whole blood NAD measurement, which has been shown as a good biomarker for vitamin B3 status [71]. Nevertheless, metabolic flexibility and gene expression in eWAT suggest that the 5NR mice were are less metabolically healthy. 5 mg NR per kg diet, with low but sufficient

Trp, may therefore constitute a potential cut-off for marginal vitamin B3 sufficiency, with metabolic flexibility as a sensitive marker. However, before this can be definitively concluded, dose-response studies with lower vitamin B3 concentrations and other forms of vitamin B3 are needed.

In conclusion, we investigated the effects of a wide range of dietary NR on metabolic health, focusing on metabolic flexibility and WAT function. To the best of our knowledge, this is the first time that NR is used as an exclusive source of vitamin B3, applied in a range between marginal sufficiency and supplemental amounts in the context of an mildly obesogenic diet in a rodent study. Based on metabolic flexibility, the data linked to WAT function and no effect on growth, we conclude that 30 mg NR/kg diet constitutes the optimal concentration to support metabolic health.

Acknowledgements

We thank ChromaDex for the generous and kind supply of nicotinamide riboside. We thank our colleagues at Human and Animal Physiology and the animal facility for their help. We thank Isabella Schuijf and Wessel Theeuwes for practical contributions. Financial support by the Chinese Scholarship Council (grant# 201303250054 for WS and 201403250064 for JT) is gratefully acknowledged.

References

[1] Nikiforov, A., Kulikova, V., Ziegler, M., The human NAD metabolome: functions, metabolism and compartmentalization. *Crit. Rev. Biochem. Mol. Biol.* 2015, *50*, 284-297.
[2] Jacobson, E. L., Jacobson, M. K., Tissue NAD as a biochemical measure of niacin status in humans. *Methods enzymol.* 1997, *280*, 221-230.
[3] Rawling, J. M., Jackson, T. M., Driscoll, E. R., Kirkland, J. B., Dietary niacin deficiency lowers tissue poly (ADP-ribose) and NAD+ concentrations in Fischer-344 rats. *J. Nutr.* 1994, *124*, 1597-1597.
[4] Terakata, M., Fukuwatari, T., Sano, M., Nakao, N., *et al.*, Establishment of true niacin deficiency in quinolinic acid phosphoribosyltransferase knockout mice. *J. Nutr.* 2012, *142*, 2148-2153.
[5] Sydenstricker, V. P., The history of pellagra, its recognition as a disorder of nutrition and its conquest. *Am. J. Clin. Nutr.* 1958, *6*, 409-414.
[6] Seal, A. J., Creeke, P. I., Dibari, F., Cheung, E., *et al.*, Low and deficient niacin status and pellagra are endemic in postwar Angola. *Am. J. Clin. Nutr.* 2007, *85*, 218-224.
[7] Bai, P., Cantó, C., Oudart, H., Brunyánszki, A., *et al.*, PARP-1 inhibition increases mitochondrial metabolism through SIRT1 activation. *Cell Metab.* 2011, *13*, 461-468.
[8] Canto, C., Houtkooper, R. H., Pirinen, E., Youn, D. Y., *et al.*, The NAD(+) precursor nicotinamide riboside enhances oxidative metabolism and protects against high-fat diet-induced obesity. *Cell Metab.* 2012, *15*, 838-847.
[9] Kraus, D., Yang, Q., Kong, D., Banks, A. S., *et al.*, Nicotinamide N-methyltransferase knockdown protects against diet-induced obesity. *Nature* 2014, *508*, 258-262.
[10] Yoshino, J., Mills, K. F., Yoon, M. J., Imai, S., Nicotinamide mononucleotide, a key NAD(+) intermediate, treats the pathophysiology of diet- and age-induced diabetes in mice. *Cell Metab.* 2011, *14*, 528-536.
[11] Lewis, S. M., Ullrey, D. E., Barnard, D. E., Knapka, J. J., in: Suckow, M. A., Weisbroth, S. H., Franklin, C. L., *The laboratory rat*, Academic Press 2005, pp. 219-301.
[12] Tobin, G., Stevens, K. A., Russell, R. J., in: Fox, J. G., Barthold, S., Davisson, M., Newcomer, C. E., *et al.*, *The Mouse in biomedical research*, Academic Press 2006, pp. 323-337.
[13] Henderson, L., Deodhar, T., Krehl, W., Elvehjem, C., Factors affecting the growth of rats receiving niacin-tryptophandeficient diets. *J. Biol. Chem.* 1947, *170*, 261-268.
[14] Krehl, W., Sarma, P., Teply, L., Elvehjem, C., Factors affecting the dietary niacin and tryptophane requirement of the growing rat. *J. Nutr.* 1946, *31*, 85-106.
[15] Hundley, J. M., Influence of fructose and other carbohydrates on the niacin requirement of the rat. *J. Biol. Chem.* 1949, *181*, 1-9.
[16] Fukuwatari, T., Shibata, K., Nutritional aspect of tryptophan metabolism. *Int. J. Tryptophan. Res.* 2013, *6*, 3-8.
[17] Fukuwatari, T., Wada, H., Shibata, K., Age-related alterations of B-group vitamin contents in urine, blood and liver from rats. *J. Nutr. Sci. Vitaminol.* 2008, *54*, 357-362.
[18] Terakata, M., Fukuwatari, T., Kadota, E., Sano, M., *et al.*, The niacin required for optimum growth can be synthesized from L-tryptophan in growing mice lacking tryptophan-2, 3-dioxygenase. *J. Nutr.* 2013, *143*, 1046-1051.
[19] Kantak, K. M., Hegstrand, L. R., Whitman, J., Eichelman, B., Effects of dietary supplements and a tryptophan-free diet on aggressive behavior in rats. *Pharmacol. Biochem. Behav.* 1980, *12*, 173-179.
[20] Erdman Jr, J. W., MacDonald, I. A., Zeisel, S. H., *Present knowledge in nutrition*, John Wiley & Sons 2012.
[21] Bieganowski, P., Brenner, C., Discoveries of nicotinamide riboside as a nutrient and conserved NRK genes establish a Preiss-Handler independent route to NAD+ in fungi and humans. *Cell* 2004, *117*, 495-502.
[22] Gariani, K., Menzies, K. J., Ryu, D., Wegner, C. J., *et al.*, Eliciting the mitochondrial unfolded protein response by nicotinamide adenine dinucleotide repletion reverses fatty liver disease in mice. *Hepatology* 2016, *63*, 1190-1204.
[23] Gong, B., Pan, Y., Vempati, P., Zhao, W., *et al.*, Nicotinamide riboside restores cognition through an upregulation of proliferator-activated receptor-γ coactivator 1α regulated β-secretase 1 degradation and mitochondrial gene expression in Alzheimer's mouse models. *Neurobiol. Aging* 2013, *34*, 1581-1588.

[24] Khan, N. A., Auranen, M., Paetau, I., Pirinen, E., *et al.*, Effective treatment of mitochondrial myopathy by nicotinamide riboside, a vitamin B3. *EMBO Mol. Med.* 2014, *6*, 721-731.
[25] Nikiforov, A., Dolle, C., Niere, M., Ziegler, M., Pathways and subcellular compartmentation of NAD biosynthesis in human cells: from entry of extracellular precursors to mitochondrial NAD generation. *J. Biol. Chem.* 2011, *286*, 21767-21778.
[26] Zhang, H., Ryu, D., Wu, Y., Gariani, K., *et al.*, NAD+ repletion improves mitochondrial and stem cell function and enhances life span in mice. *Science* 2016, aaf2693.
[27] Bogan, K. L., Brenner, C., Nicotinic acid, nicotinamide, and nicotinamide riboside: a molecular evaluation of NAD+ precursor vitamins in human nutrition. *Annu. Rev. Nutr.* 2008, *28*, 115-130.
[28] Lightowlers, R. N., Chrzanowska-Lightowlers, Z. M., Salvaging hope: Is increasing NAD+ a key to treating mitochondrial myopathy? *EMBO Mol. Med.* 2014, e201404179.
[29] Galgani, J. E., Moro, C., Ravussin, E., Metabolic flexibility and insulin resistance. *Am. J. Physiol. Endocrinol. Metab.* 2008, *295*, E1009-1017.
[30] Horakova, O., Medrikova, D., van Schothorst, E. M., Bunschoten, A., *et al.*, Preservation of metabolic flexibility in skeletal muscle by a combined use of n-3 PUFA and rosiglitazone in dietary obese mice. *PloS ONE* 2012, *7*, e43764.
[31] Duivenvoorde, L. P., van Schothorst, E. M., Swarts, H. J., Keijer, J., Assessment of metabolic flexibility of old and adult mice using three noninvasive, indirect calorimetry-based treatments. *J. Gerontol. A Biol. Sci. Med. Sci.* 2015, *70*, 282-293.
[32] Duivenvoorde, L. P., van Schothorst, E. M., Swarts, H. M., Kuda, O., *et al.*, A difference in fatty acid composition of isocaloric high-fat diets alters metabolic flexibility in male C57Bl/6JOlaHsd mice. *PloS ONE* 2015, *10*, e0128515.
[33] Maeta, A., Fukuwatari, T., Funakoshi, H., Nakamura, T., Shibata, K., Tryptophan-restriction diets help to maintain L-tryptophan homeostasis in tryptophan 2,3-dioxygenase knockout mice. *Int. J. Tryptophan. Res.* 2013, *6*, 55-65.
[34] Storlien, L., Oakes, N., Kelley, D., Adipose tissue-liver-muscle interactions leading to insulin resistance. *Proc. Nutr. Soc* 2004, *63*, 363-368.
[35] Sparks, L. M., Ukropcova, B., Smith, J., Pasarica, M., *et al.*, Relation of adipose tissue to metabolic flexibility. *Diabetes Res. Clin. Pract.* 2009, *83*, 32-43.
[36] Asterholm, I. W., Scherer, P. E., Enhanced metabolic flexibility associated with elevated adiponectin levels. *Am. J. Pathol.* 2010, *176*, 1364-1376.
[37] Hoek-van den Hil, E. F., van Schothorst, E. M., van der Stelt, I., Swarts, H. J., *et al.*, Direct comparison of metabolic health effects of the flavonoids quercetin, hesperetin, epicatechin, apigenin and anthocyanins in high-fat-diet-fed mice. *Genes Nutr.* 2015, *10*, 469.
[38] Péronnet, F., Massicotte, D., Table of nonprotein respiratory quotient: an update. *Can. J. Sport Sci.* 1991, *16*, 23-29.
[39] Hoek-van den Hil, E. F., Keijer, J., Bunschoten, A., Vervoort, J. J., *et al.*, Quercetin induces hepatic lipid omega-oxidation and lowers serum lipid levels in mice. *PloS ONE* 2013, *8*, e51588.
[40] Lee, S., Muniyappa, R., Yan, X., Chen, H., *et al.*, Comparison between surrogate indexes of insulin sensitivity and resistance and hyperinsulinemic euglycemic clamp estimates in mice. *Am. J. Physiol. Endocrinol. Metab.* 2008, *294*, E261-E270.
[41] Hoevenaars, F. P., Bekkenkamp-Grovenstein, M., Janssen, R. J., Heil, S. G., *et al.*, Thermoneutrality results in prominent diet-induced body weight differences in C57Bl/6J mice, not paralleled by diet-induced metabolic differences. *Mol. Nutr. Food Res.* 2014, *58*, 799-807.
[42] Voigt, A., Agnew, K., Schothorst, E. M., Keijer, J., Klaus, S., Short-term, high fat feeding-induced changes in white adipose tissue gene expression are highly predictive for long-term changes. *Mol. Nutr. Food Res.* 2013, *57*, 1423-1434.
[43] Kennedy, A. J., Ellacott, K. L., King, V. L., Hasty, A. H., Mouse models of the metabolic syndrome. *Dis. Model. Mech.* 2010, *3*, 156-166.
[44] van Ommen, B., Keijer, J., Heil, S. G., Kaput, J., Challenging homeostasis to define biomarkers for nutrition related health. *Mol. Nutr. Food Res.* 2009, *53*, 795-804.
[45] Puiggròs, F., Canela, N., Arola, L., Metabolome responses to physiological and nutritional challenges. *Current Opinion in Food Science* 2015, *4*, 111-115.
[46] Liang, F., Kume, S., Koya, D., SIRT1 and insulin resistance. *Nat. Rev. Endocrinol.* 2009, *5*, 367-373.

[47] Mouchiroud, L., Houtkooper, R. H., Moullan, N., Katsyuba, E.*, et al.*, The NAD+/sirtuin pathway modulates longevity through activation of mitochondrial UPR and FOXO signaling. *Cell* 2013, *154*, 430-441.
[48] Singh, B., Saxena, A., Surrogate markers of insulin resistance: A review. *World J. Diabetes* 2010, *1*, 36-47.
[49] Zaletel, J., Barlovic, D. P., Prezelj, J., Adiponectin-leptin ratio: a useful estimate of insulin resistance in patients with Type 2 diabetes. *J. Endocrinol. Invest.* 2010, *33*, 514-518.
[50] Corpeleijn, E., Mensink, M., Kooi, M. E., Roekaerts, P. M.*, et al.*, Impaired skeletal muscle substrate oxidation in glucose-intolerant men improves after weight loss. *Obesity* 2008, *16*, 1025-1032.
[51] Chu, L., Riddell, M. C., Schneiderman, J. E., McCrindle, B. W., Hamilton, J. K., The effect of puberty on fat oxidation rates during exercise in overweight and normal-weight girls. *J. Appl. Physiol.* 2014, *116*, 76-82.
[52] Ronchi, J. A., Figueira, T. R., Ravagnani, F. G., Oliveira, H. C.*, et al.*, A spontaneous mutation in the nicotinamide nucleotide transhydrogenase gene of C57Bl/6J mice results in mitochondrial redox abnormalities. *Free Radic. Biol. Med.* 2013, *63*, 446-456.
[53] Ronchi, J. A., Francisco, A., Passos, L. A., Figueira, T. R., Castilho, R. F., The contribution of nicotinamide nucleotide transhydrogenase to peroxide detoxification is dependent on the respiratory state and counterbalanced by other sources of NADPH in liver mitochondria. *J. Biol. Chem.* 2016, 291, 20173-20187.
[54] Son, M. J., Kwon, Y., Son, T., Cho, Y. S., Restoration of mitochondrial NAD+ levels delays stem cell senescence and facilitates reprogramming of aged somatic cells. *Stem Cells* 2016, 34, :2840-2851
[55] Freeman, H. C., Hugill, A., Dear, N. T., Ashcroft, F. M., Cox, R. D., Deletion of nicotinamide nucleotide transhydrogenase. *Diabetes* 2006, *55*, 2153-2156.
[56] Lee, H. J., Hong, Y. S., Jun, W., Yang, S. J., Nicotinamide riboside ameliorates hepatic metaflammation by modulating NLRP3 inflammasome in a rodent model of type 2 diabetes. *J. Med. Food.* 2015, *18*, 1207-1213.
[57] Skurk, T., Alberti-Huber, C., Herder, C., Hauner, H., Relationship between adipocyte size and adipokine expression and secretion. *J. Clin. Endocrinol. Metab.* 2007, *92*, 1023-1033.
[58] Franck, N., Stenkula, K. G., Öst, A., Lindström, T.*, et al.*, Insulin-induced GLUT4 translocation to the plasma membrane is blunted in large compared with small primary fat cells isolated from the same individual. *Diabetologia* 2007, *50*, 1716-1722.
[59] Hammarstedt, A., Graham, T. E., Kahn, B. B., Adipose tissue dysregulation and reduced insulin sensitivity in non-obese individuals with enlarged abdominal adipose cells. *Diabetol. Metab. Syndr.* 2012, *4*, 42.
[60] Frayn, K., Adipose tissue as a buffer for daily lipid flux. *Diabetologia* 2002, *45*, 1201-1210.
[61] Wanders, D., Graff, E. C., White, B. D., Judd, R. L., Niacin increases adiponectin and decreases adipose tissue inflammation in high fat diet-fed mice. *PloS ONE* 2013, *8*, e71285.
[62] Siersbæk, R., Nielsen, R., Mandrup, S., PPARγ in adipocyte differentiation and metabolism–Novel insights from genome-wide studies. *FEBS lett.* 2010, *584*, 3242-3249.
[63] Jay, M. A., Ren, J., Peroxisome proliferator-activated receptor (PPAR) in metabolic syndrome and type 2 diabetes mellitus. *Curr. Diabetes Rev.* 2007, *3*, 33-39.
[64] Ahmadian, M., Suh, J. M., Hah, N., Liddle, C.*, et al.*, PPAR [gamma] signaling and metabolism: the good, the bad and the future. *Nat. Med.* 2013, *99*, 557-566.
[65] Long, E. K., Olson, D. M., Bernlohr, D. A., High-fat diet induces changes in adipose tissue trans-4-oxo-2-nonenal and trans-4-hydroxy-2-nonenal levels in a depot-specific manner. *Free Radic. Biol. Med.* 2013, *63*, 390-398.
[66] Boyonoski, A. C., Spronck, J. C., Gallacher, L. M., Jacobs, R. M.*, et al.*, Niacin deficiency decreases bone marrow poly (ADP-ribose) and the latency of ethylnitrosourea-induced carcinogenesis in rats. *J. Nutr.* 2002, *132*, 108-114.
[67] Gross, C. J., Henderson, L. M., Digestion and absorption of NAD by the small intestine of the rat. *J. Nutr.* 1983, *113*, 412-420.
[68] Frederick, D. W., Loro, E., Liu, L., Davila, A.*, et al.*, Loss of NAD Homeostasis Leads to Progressive and Reversible Degeneration of Skeletal Muscle. *Cell Metab.* 2016, *24*, 269-282.

[69] Cantó, C., Menzies, K. J., Auwerx, J., NAD+ metabolism and the control of energy homeostasis: A balancing act between mitochondria and the nucleus. *Cell Metab.* 2015, *22*, 31-53.
[70] Hara, N., Yamada, K., Shibata, T., Osago, H., Tsuchiya, M., Nicotinamide phosphoribosyltransferase/visfatin does not catalyze nicotinamide mononucleotide formation in blood plasma. *PloS ONE* 2011, *6*, e22781.
[71] Shibata, K., Blood NAD as an index of niacin nutrition. *Nutr. Int.* 1986, *2*, 177-181.

Supporting methods

NR metabolites in serum and liver

Metabolite extraction from serum was performed as described before [1]. Briefly, 100 µL serum was vortexed with 200 µL acetonitrile (ACN) for 90 seconds, kept for 20 minutes at 4°C and centrifuged for 10 minutes at 16,600*g*, 4°C. 150 µL supernatant was evaporated under nitrogen flow until samples were dry.
Liver extraction was done as described previously [2] with the following modifications: 30 mg lyophilized tissue was vortexed in 0.5mL physiological saline for 30 seconds, followed by 30 seconds sonication (Vibra Cell, Sonics, Newton, USA). 0.5 mL acetone was added, vortexed and centrifuged for 15 minutes at 10,000*g*, 4°C. This procedure was repeated three time, after which all 3 upper phases were combined, and evaporated under nitrogen flow. Dried serum or liver samples were dissolved in 200 µL ACN:milliQ water (50:50, v/v) filtered through 0.45 µm, respectively. 10 µL. BP3 at 25 ppm for serum or 20 µL for liver samples was added prior to extraction as internal standard.

NR metabolites were identified and quantified using an LC-ESI-MS/MS system consisting of an Agilent HPLC 1200 Series coupled to a triple quadrupole mass spectrometer 6410 (both Agilent Technologies, CA, U.S.A.). Chromatographic separation was done at 30°C with a flow rate at 0.6 mL/minute using a XBridge Amide 3.5 µm; 100 mm x 2.1 mm i.d. column (Waters, Hertfordshire, U.K.). Solvent A was 10 mM ammonium formiate 0.1% formic acid and solvent B was acetonitrile. Separation was done using the following gradient: initially phase B was set at 90% and it was reduced gradually up to 50% B in 15 minutes. Then it was maintained isocratically for 5 minutes and finally it was returned to initial conditions for 2 minutes. A post-run of 6 minutes was set between samples to re-equilibrate the column. Analyses were performed in the positive mode in electrospray ionization (ESI), with a drying gas temperature of 325°C and flow rate of 9 L/minute. Nebulizer gas pressure was 30 psi and the capillary voltage was set at 4000V. The selected reaction monitoring transitions (SRM) and individual fragmentor voltage and collision energy for each compound were evaluated using commercial standards to obtain the best instrumental conditions. Two transitions were acquired for each compound, one for quantification and a second for confirmation purposes. The selected SRM transitions were 255<123 and 255<255 for NR, 124<53 and 124<80 for NA, 123<53 and 123<80 for Nam, 205<146 and 205<188 for Trp, 335<123 and 335<97 for nicotinamide mononucleotide (NMN), 664<427 and 664<523 for NAD and 336<124 and 336<97 for nicotinic acid mononucleotide (NaMN), 96<78 and 96<51 for 2-pyridone (2PY) and 137<108 and 137<80 for N-methylnicotinamide (MeNam). Data acquisition and treatment was carried out using Masshunter software.

eWAT morphology

Adipocyte size as well as macrophage staining and counting were by immunohistochemistry (IHC) as described [3]. Briefly, tissue was fixed, washed in PBS, embedded in paraffin and sectioned at 5 µm using an automated microtome (Microm GmbH, Heidelberg, Germany). Sections after 20 sequential cuts were used to ensure no repetitive adipocytes were present. Tissue sections were deparaffinised, rehydrated and then stained with Mayer's haematoxylin for 30 seconds (Vector, CA, U.S.A.). Representative pictures were photographed and adipocyte size was measured using Axiovision (Zeiss, Munich, Germany) and expressed in surface area (µm^2) per adipocyte. The frequency distribution of adipocyte size was calculated as described [4], with some modifications. Briefly, adipocyte surface area was distributed in 100 µm^2 clusters in Excel and subsequently clustered as defined fractions of small (100-1500 µm^2), medium (>1500-6000 µm^2), and large (>6000 µm^2). Values less than 100 µm^2 were excluded. Crown-like structures (CLS) from 1000 adipocytes per animal were counted, and expressed as CLS/100 adipocytes.

Supporting references

[1] Szafarz, M., Lomnicka, M., Sternak, M., Chlopicki, S., Szymura-Oleksiak, J., Simultaneous determination of nicotinic acid and its four metabolites in rat plasma using high performance liquid chromatography with tandem mass spectrometric detection (LC/MS/MS). *J. Chromatogr. B* 2010, *878*, 895-902.
[2] Aragones, G., Suarez, M., Ardid-Ruiz, A., Vinaixa, M., *et al.*, Dietary proanthocyanidins boost hepatic NAD(+) metabolism and SIRT1 expression and activity in a dose-dependent manner in healthy rats. *Sci. Rep.* 2016, *6*, 24977.
[3] Hoek-van den Hil, E. F., van Schothorst, E. M., van der Stelt, I., Swarts, H. J., *et al.*, Direct comparison of metabolic health effects of the flavonoids quercetin, hesperetin, epicatechin, apigenin and anthocyanins in high-fat-diet-fed mice. *Genes Nutr.* 2015, *10*, 469.
[4] Parlee, S. D., Lentz, S. I., Mori, H., MacDougald, O. A., Quantifying size and number of adipocytes in adipose tissue. *Methods Enzymol.* 2014, *537*, 93-122.

Supporting figures

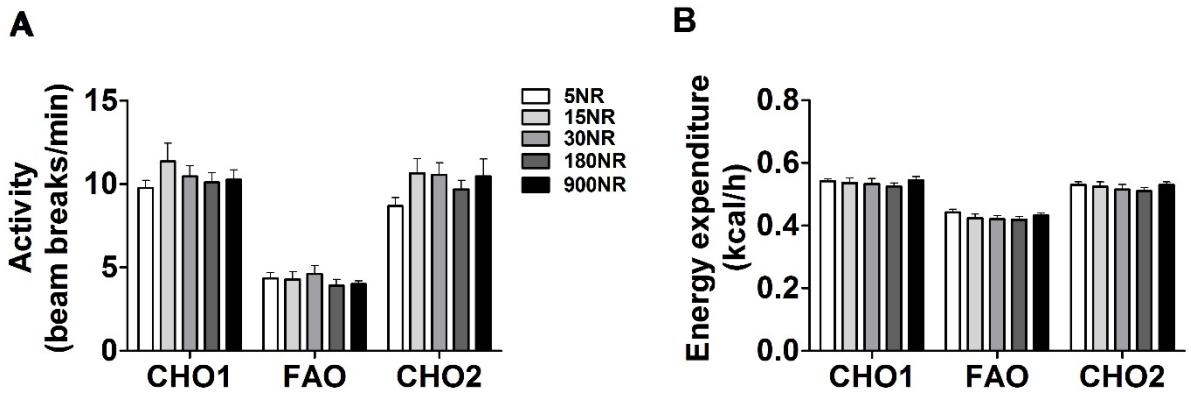

Supporting Figure S1. Effects of dietary NR on energy expenditure and activity. *A*ctivity (A) and energy expenditure (B) during the fast and refeeding challenge were measured in indirect calorimetry in week 14. 5NR white, 15NR light grey, 30NR grey, 180NR dark grey, 900NR black. NR in mg/kg diet. Data are analysed using one-way ANOVA and shown as mean±SEM (n=11-12 mice per treatment).

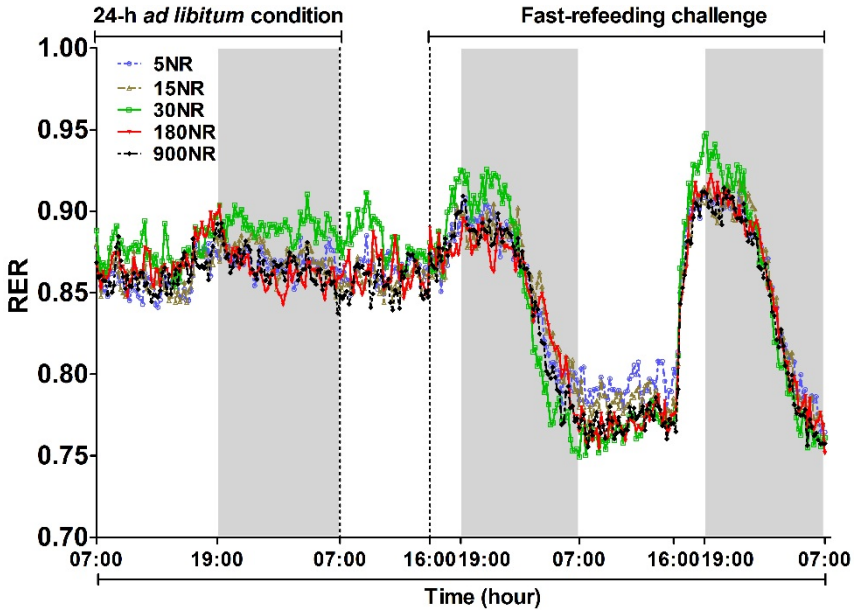

Supporting Figure S2. Effects of dietary NR on RER during Indirect Calorimetry. RER under *ad libitum* conditions was measured for 24hrs prior to the fast-refeeding challenge in indirect calorimetry in week 14. 5NR open circle, 15NR open upward triangle, 30NR open square, 180NR closed downward triangle, 900NR closed diamond. Shaded areas indicated dark, active periods. Data are analysed using two-way ANOVA and mean±SEM (n=11-12).

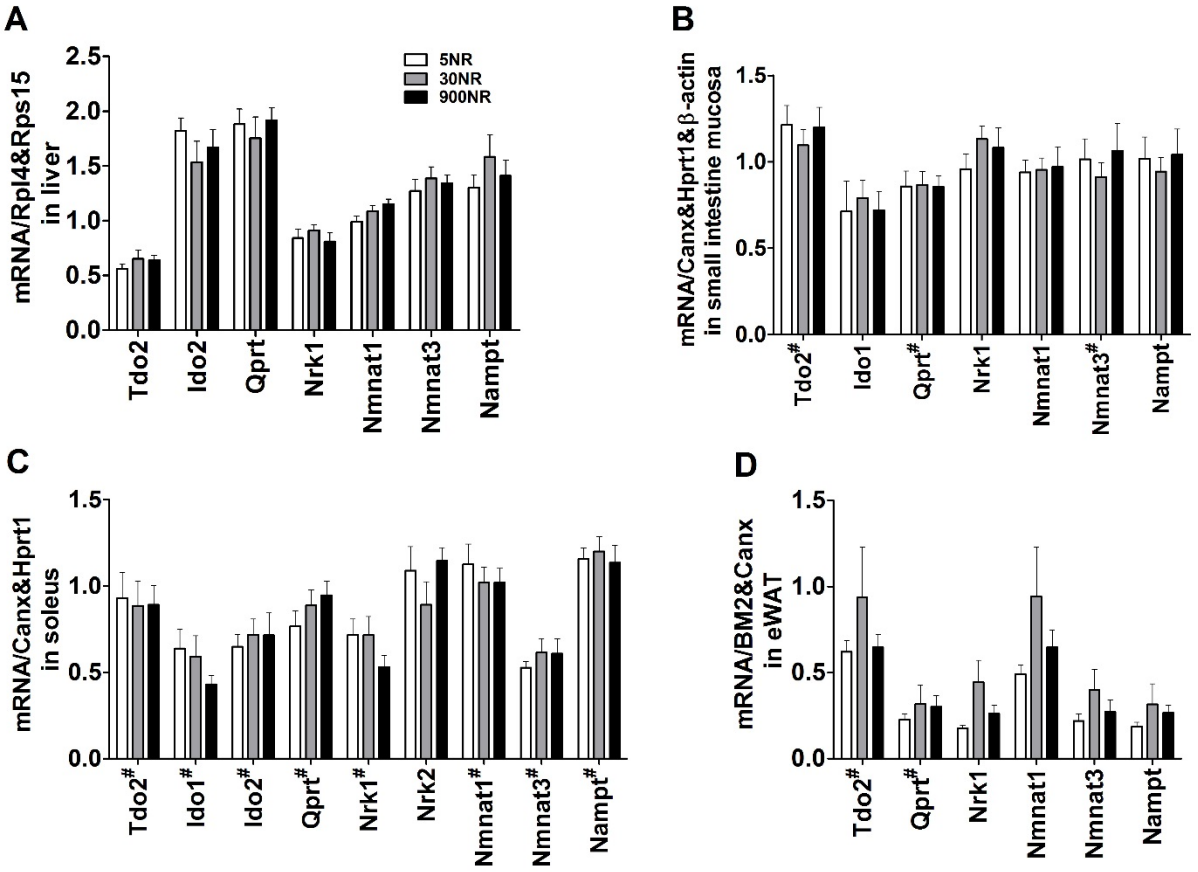

Supporting Figure S3. Effects of dietary NR on expression of NR metabolism genes. mRNA levels (normalized to mean of indicated reference mRNAs) of de *novo* pathway (*Tdo2, Ido1, Ido2, Qprt*), Nrk pathway (*Nrk1, Nrk2*), salvage pathway (*Nampt, Nmnat1, Nmnat3*) in liver (A), small intestinal mucosa (B), *soleus* muscle (C), eWAT (D). White 5NR, grey 30NR, black 900NR. # indicates qRT-PCR determination was after 12-cycle pre-amplification. Full gene names are in Supporting Table 2. Data are analysed using one-way ANOVA and shown as mean±SEM (n=11-12).

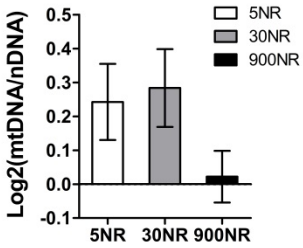

Supporting Figure S4. Mitochondrial density in epiWAT. Ratio of mitochondrial over nuclear DNA. White 5NR, grey 30NR, black 900 NR. Data are analysed using one-way ANOVA and shown as mean±SEM (n=11-12).

Supporting Table 1. Sequences of primers for qRT-PCR

Gene	primer forward 5'-3'	primer reverse 5'-3'	AT °C
Acox1	TGCGGTGGGCACGGCTATTC	CGCTGGCTCGGCAGGTCATT	60
Actb (ß-actin)#	GGGATGTTTGCTCCAACCAA	GCGCTTTTGACTCAAGGATTTAA	60
Adipoq	CCCATGAGTACCAGACTAATGAGACC	TGACTGGGCAGGATTAAGAGGAAC	60
B2m#	CCCCACTGAGACTGATACATACGC	AGAAACTGGATTTGTAATTAAGCAGGTTC	60
Canx#	GCAGCGACCTATGATTGACAACC	GCTCCAAACCAATAGCACTGAAAGG	60
Cat	CTCGCAGAGACCTGATGTCC	TGTGGAGAATCGAACGGCAA	60
Cd36	GACGCAGCCTCCTTTCC	GGCATTGGCTGGAAGAAC	60
Cebpa (C/Ebpa)	GCCAAACTGAGACTCTTCACTAACG	CACTACTACATACACCCTTGGACAAC	60
Cebpb(C/EBPß)	GAGCGACGAGTACAAGATGCG	GCTGCTCCACCTTCTTCTGC	60
Cpt1	CTGAGACAGACTCACACCGC	GTGGAGCCTACGGTTGTTCT	58
Cs	ACAGTGAAAGCAACTTCGCC	GTCAATGGCTCCGATACTGC	58
Fasn	GTGCAGAGCTGTGCTCCTGA	GTGCAGAGCTGTGCTCCTGA	55
Gpx3	CCATTCGGCCTGGTCATTCT	GGAGGGCAGGAGTTCTTCAG	60
Hprt1#	TGACACTGGTAAAACAATGCAAACTTTG	GAGGTCCTTTTCACCAGCAAGCT	60
Hsl	TCAGGGACAGAGGCAGAGGAC	TCCACTTAGTTCCAGGAAGGAGTTG	58
Ido1	TCTGCTGTATGAGGGGGTCT	GGAGATTCTTTGCCAGCCTC	60
Ido2	ATTGCCCTCAGACTTCCTCAC	TCTTGGCAGCACCTTTTGGG	60
Lep	GGCTTTGGTCCTATCTGTCTTATGTTC	CCCTCTGCTTGGCGGATACC	60
Nuclear DNA	CTTAGAGGGACAAGTGGCGTTC	CGCTGAGCCAGTCAGTGTAG	58
Mito DNA	CCGCAAGGGAAAGATGAAAGAC	TCGTTTGGTTTCGGGGTTTC	60
Nampt	GATTGAGACTATTCTTGTTCAGT	GTAACTTGTATTCCAGACCATC	60
Nmnat1	CCAAACCAACAGGTGTGCC	CCACGATTTGCGTGATGTCC	60
Nmnat3	TAGCCCCACGGTCACTTTTC	GCAGTGGCCACCCTGTTTTA	60
Nmrk1	CTTGAAGCTTGCTCTGCGAC	CTCCGTTTGTCACACCACCA	60
Nmrk2	CGGGGTGGAAGTGGTCTATTT	GGACCATACAGGACGCCAG	60
Pdk4	TCAGTGACTCAAAGACGGGAAACC	TGTGGTGAAGGTGTGAAGGAACG	60
Pk	CAAGTCTGGCAGGAGTGC	TTCAGCACGGCATCCTTA	60
Ppara (Ppara)	AAGAACCGGAACAAATGCCAGTAC	TCTTCAGGTAGGCTTCGTGGATTC	59
Pparg (Pparγ)	GAAGTTCAATGCACTGGAATTAGATGAC	TTGTCTTGGATGTCCTCGATGGG	60
Ppargc1a (Pgc1a)	CCCTGCCATTGTTAAGACC	TGCTGCTGTTCCTGTTTTC	60
Prdx3	GTGGTTTGGGCCACATGAAC	AGAGACCTCTGAGCGCAATG	60

Qprt	AGACAACCATGTAGTGGCGG	TGCAGCTCCTCAGGCTTAAA	60
Rpl4#	ACAACAGACAGCCCTATGCC	CCCCCACGACACATATTTCCA	58
Rps15#	CGGAGATGGTGGGTAGCATGG	ACGGGTTTGTAGGTGATGGAGAAC	60
Slc2a4 (Glut4)	CCATTCCCTGGTTCATTGTG	GTTTTGCCCCTCAGTCATTC	60
Sod1	TCGGCTTCTCGTCTTGCTCTC	GTTCACCGCTTGCCTTCTGC	60
Sod2	TTCTGGACAAACCTGAGCCCTAAG	GCAGCAATCTGTAAGCGACCTTG	60
Tdo2	ACTGTGAGCGACAGGTACAA	CTGTCACTGTACTCGGCTGT	60
Trp53	AGTATTTCACCCTCAAGATCCGC	AGCAGTTTGGGCTTTCCTCC	60

AT=annealing temperature

= reference genes

Acox1, Acyl-coenzyme A oxidase 1; *Actb*, Actin beta; Adipoq, Adiponectin; *B2m,* Beta-2-Microglobulin; *Canx*, Calnexin; *Cat*, Catalase; *Cd36*, Cluster of differentiation 36; *C/ebpa*, CCAAT/enhancer binding protein alpha; *C/ebpβ*, CCAAT/enhancer binding protein beta; *Cpt1*, Carnitine palmitoyltransferase-1; *Cs*, Citrate synthase; *Fasn*, Fatty acid synthase; *Gpx3*, Glutathione peroxidase 3; *Hprt1*, Hypoxanthine Phosphoribosyltransferase 1; *Hsl*, Hormone-sensitive lipase; *Ido1*, Indoleamine 2,3-dioxygenase 1; *Ido2*, Indoleamine 2,3-dioxygenase 2; *Lep*, Leptin; *Nuclear DNA; Mito DNA*, Mitochondrial DNA; *Nampt*, Nicotinamide phosphoribosyltransferase; *Nmnat1*, Nicotinamide mononucleotide adenylyltransferase 1; *Nmnat3*, Nicotinamide mononucleotide adenylyltransferase 3; *Nrk1*, Nicotinamide riboside kinase 1; *Nrk2*, Nicotinamide riboside kinase 2; *Pdk4*, Pyruvate dehydrogenase kinase 4; *Pk*, Pyruvate kinase; *Ppara*, Peroxisome proliferator-activated receptor alpha; *Pparγ*, Peroxisome proliferator-activated receptor gamma; *Ppargc1a*,Peroxisome proliferator-activated receptor gamma coactivator 1-alpha; *Prdx3*, Peroxiredoxin 3; *Qprt*, Quinolinate phosphoribosyltransferase; *Rpl4*, Ribosomal Protein L4; *Rps15*, Ribosomal Protein S15; *Slc2a4*, Facilitated glucose transporter 4; *Sod1*, Superoxide dismutase 1; *Sod2*, Superoxide dismutase 2; *Tdo2*, Tryptophan 2,3-dioxygenase; *Trp53*, Transformation related protein 53.

Chapter 3

High dose of dietary nicotinamide riboside induces glucose intolerance and white adipose tissue dysfunction of mice fed a mildly obesogenic diet

Wenbiao Shi, Maria A. Hegeman, Atanaska Doncheva, Melissa Bekkenkamp-Grovenstein, Vincent C. J. de Boer, Jaap Keijer

Submitted to: The FASEB Journal (2019)

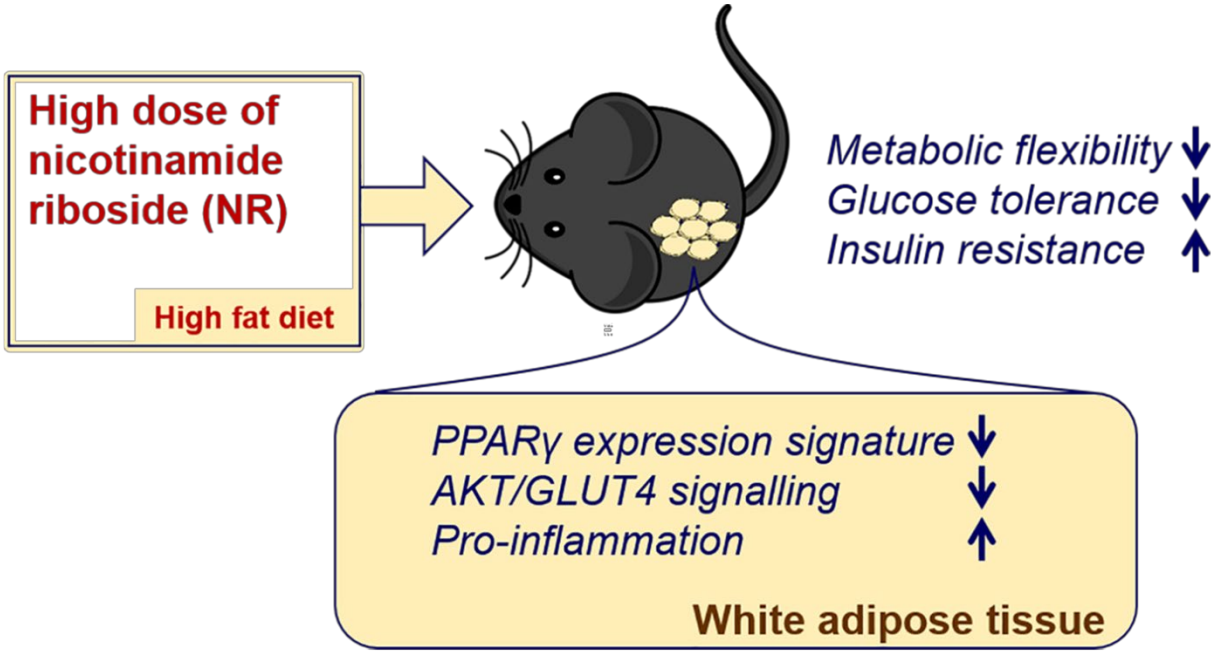

Abstract

Nicotinamide riboside (NR) is a nicotinamide adenine dinucleotide (NAD^+) booster. However, high dose NR has also been reported to have adverse effects on metabolic health, but the underlying mechanisms were not extensively studied. Here, we aimed to identify the molecular and physiological responses to high dose NR in the context of a mildly obesogenic diet. An 18-week dietary intervention was conducted in male C57Bl/6JRccHsd mice, in which a diet with 9000 mg NR per kg diet (High NR) was compared to a diet with NR at the recommended vitamin B3 level (Ctrl NR). Both diets were mildly obesogenic (40 en% fat). Metabolic flexibility and glucose tolerance were analyzed and immunoblotting, qRT-PCR and histology of epididymal white adipose tissue (eWAT) were performed. Mice fed with High NR showed a reduced metabolic flexibility, a lower glucose clearance rate and aggravated systemic insulin resistance. This was consistent with molecular and morphological changes in eWAT, including a lowered PPARγ expression signature, a downregulated AKT/GLUT4 signaling, an increased number of crown-like structures and macrophages, and an upregulation of pro-inflammatory gene markers. In conclusion, high dose NR induces the onset of a WAT dysfunction, which may be, in part, associated with deterioration of metabolic health.

Introduction

Nicotinamide adenine dinucleotide (NAD^+) is an essential metabolic co-factor that supports proper cell functioning. In humans, long-term inadequate intake of the NAD^+ precursors, vitamin B3 and tryptophan (Trp), can cause NAD^+ decline in multiple organs and ultimately lead to pellagra, a disease of vitamin B3 deficiency [1, 2]. Apart from vitamin B3 deficiency, NAD^+ levels can also be influenced by other nutritional conditions. In mice, long-term high fat (HF) diet feeding reduced tissue NAD^+ levels, leading to compromised metabolic performance, such as blunted metabolic flexibility and insulin sensitivity [3-7]. In obese individuals, reduced gene expression of the NAD^+ synthesis pathway enzymes as well as NAD^+-dependent enzymes was observed, which was associated with impaired metabolic health, e.g. insulin resistance and dyslipidemia [8]. A central role of NAD^+ in the link between obesity and its associated metabolic dysfunctions is not surprising, because NAD^+ mainly serves as a coenzyme in nutrient breakdown and energy production [9]. Besides, NAD^+ also acts as an essential substrate for several enzymatic reactions. One of the key players of these reactions are the sirtuin family of NAD^+-dependent deacetylases, with important roles in the regulation of metabolic disease [10].

Multiple strategies that aimed to boost NAD^+ levels have been shown to enhance sirtuin activity, including NAD^+ precursor supplementation, activation of NAD^+ biosynthetic enzymes and inhibition of NAD^+ consumers [10, 11]. Supplementation with NAD^+ precursors has been studied the most and seems to be the most promising strategy to boost NAD^+ levels. NAD^+ can be synthesized *in vivo* from several precursors via distinct pathways, including Trp and various forms of vitamin B3 [10]. These precursors have different properties with respect to their contribution to the NAD^+ pool and the functional consequences. Trp contributes much less efficiently to the NAD^+ pool than vitamin B3. Sixty times as much miligrams of Trp is needed to generate NAD^+, than is generated from vitamin B3 (as has been reported for niacin-equivalents) [12]. Therefore, it is not likely that Trp is a suitable source for enriching NAD^+ pool, also because an overload of Trp can cause toxicity especially in the central nervous system [13]. The vitamin B3 forms nicotinic acid (NA) and nicotinamide (Nam) are commonly used, but high dose supplementation can induce negative side effects, including skin flushing by NA and inhibition of sirtuins by Nam [14].

Nicotinamide mononucleotide (NMN) and nicotinamide riboside (NR) have been described as potent NAD^+ boosters, that can activate especially sirtuin 1 (SIRT1) activity [4, 5, 15-17]. Supplementation with NMN and with NR in mice were shown to induce beneficial metabolic adaptation, which counteracted metabolic dysfunctions induced by nutrient overload [4-7]. However, NMN, an intermediate in NAD^+ biosynthesis and final precursor to NAD^+, was shown to be metabolized into either NR or Nam extracellularly [18, 19]. This potentially compromises the potency to boost cellular NAD^+ levels. NR appears to be superior to the other NAD^+ precursors, because of its higher potency to raise NAD^+ levels in multiple cell lines and tissues [5, 19-21]. These promising results subsequently led to the set-up of multiple human supplementation studies and clinical trials using NR as supplementation product [21-24].

White adipose tissue (WAT) is a lipid storage organ, protecting the body against lipotoxicity and providing nutrients in time of need. WAT actively communicates with other organs and secretes peptide hormones, e.g. cytokines and chemokines that modulate insulin-stimulated glucose metabolisms in other organs such as liver, muscle and brain, thus playing a crucial role in the whole body glucose homeostasis [25]. WAT dysfunction induced by nutrient overload was associated with impaired transcriptional regulation of the NAD^+/sirtuin pathway and decreased NAD^+ level [4, 8, 26, 27], and ameliorated upon vitamin B3 supplementation or calorie restriction in both mice and humans [28-30]. Therefore, WAT health is likely sensitive to changes in NAD^+ flux and responsive to exogenous NAD^+ boosters. In agreement, our previous NR dose-response study in mice showed that morphological and molecular alterations occurred in WAT upon NR supplementation [31].

Despite demonstration of beneficial effects of NR supplementation, a limited number of studies have also indicated adverse effects of high dose NR in rodents on either excise performance [32, 33] or metabolic flexibility [31]. Although the underlying mechanisms were not extensively investigated, these contrasting results highlight the relevance of studying the metabolic consequences in detail on a molecular as well as physiological level. We now investigated the effects of high dose of NR, in the context of a mildly obesogenic diet, on whole body metabolic homeostasis, as well as, on its molecular and physiological effects in WAT.

Material and methods

Animals and diets

The animal experiment was approved by the Animal Welfare Committee of Wageningen University, Wageningen, The Netherlands (DEC2016033.b). This experiment was designed as an independent experiment, but performed as part of a larger experiment to reduce the number of (control) animals. Eight or nine-week-old C57BI/6JHsdRcc male mice (Envigo, Horst, The Netherlands) were individually housed (12h light–dark cycle, 23±1°C, 55±15% humidity), with *ad libitum* access to feed and water throughout the whole experiment, unless indicated otherwise. A semi-synthetic diet (Research Diet Services, Wijk bij Duurstede, The Netherlands), containing 40% energy from fat was used, to resemble the average human consumption of fat in the Netherlands [34, 35]. The diet contained 0.115% L-tryptophan and either 30 or 9000 mg NR as an exclusive source of vitamin B3 (referred to as Ctrl NR and High NR, respectively) and dietary composition is shown in Supplemental Table S1. Mice were acclimatized on the Ctrl NR diet for two weeks. Next, mice were stratified on body weight into 2 experimental groups (n=12/group) and received the Ctrl NR or High NR diet for 18 weeks. Body weight and feed intake as well as lean and fat mass (by NMR, EchoMRI, Houston, USA) were measured weekly.

Metabolic flexibility

Metabolic flexibility was assessed by the change of respiratory exchange ratio (RER) upon a fasting-refeeding challenge that was measured by indirect calorimetry using

a PhenoMaster System (TSE Systems, Bad Homburg, Germany), as published [31] and described in the Supplemental Methods.

Oral glucose tolerance test

Oral glucose tolerance test (OGTT) was conducted in week 17 as described [36], with some modifications. Briefly, feed was removed in the morning and mice were weighed. After exactly 6 hours of fasting, a tail cut was conducted and blood glucose was measured using a Freestyle blood glucose meter (Abbott Diabetes Care, Hoofddorp, The Netherlands) as t=0 timepoint. Then 2 gram glucose/kg body weight was administrated via oral gavage. Blood glucose was measured at the timepoints of 15, 30, 60, 90 and 120 minutes after oral gavage. At t=0, 15 and 30, 20 µl of blood was collected using Microvette CB 300 tubes (Sarstedt, Etten-Leur, The Netherlands). Plasma was obtained after centrifuging at 2000*g*, 4°C for 20 minutes, for insulin measurement.

Sample collection at sacrifice

At the end of the study, mice were provided with a limited amount of diet (0.8 gram of fresh experimental diet) at the start of the dark phase so they were fasted at the end of the dark phase; they were subsequently refed with 1.8 gram of diet at the start of the light phase for 4 hours and then sacrificed by decapitation. The purpose of this refeeding regime is to achieve the maximal discrepancy of RER between two groups, which was seen in the metabolic flexibility assessment. Any remaining feed before dissection was recorded to calculate feed intake. Blood was collected to obtain serum and to measure immediate blood glucose concentrations using a Freestyle blood glucose meter (Abbott Diabetes Care). For serum collection blood was centrifuged at 3,000*g*, 4°C for 10 minutes, which was immediately stored at -80°C. Right epididymal white adipose tissue (eWAT) was rapidly dissected, snap frozen in liquid nitrogen and stored at -80°C. Left eWAT was weighted, divided in half and fixed for 24 hours at 4°C in PBS with 4.0% paraformaldehyde (pH=7.40), as described [31]. Fresh liver was dissected, weighed, snap frozen in liquid nitrogen and stored at -80°C.

Plasma or serum parameters

Plasma insulin was measured using mouse insulin ELISA kit according to the manufacturer's instructions (Crystal Chem, Downers Grove, USA). Serum total cholesterol (TC), high density lipoprotein (HDL) cholesterol, triglycerides (TG) and non-esterified fatty acids (NEFA) were measured using liquicolor enzymatic colorimetric tests (Instruchemie, Delfzijl, The Netherlands), as described before [37]. Serum low density lipoprotein (LDL) cholesterol concentrations were calculated using the modified Friedewald formula (LDL cholesterol = total cholesterol - HDL cholesterol - triglycerides×0.16, for rodents) [38]. Serum leptin was measured with a Bio-Plex Pro Mouse Diabetes Assay using a Bio-Plex 200 system (Bio-Rad, Veenendaal, The Netherlands), as published [31]. Serum adiponectin was diluted in 1:10000 assay buffer and then measured using mouse adiponectin ELISA kit according to the manufacturer's instructions (Crystal Chem, Downers Grove, USA). To assess insulin resistance, HOMA-IR was calculated as: (fasting glucose (mmol/L)× fasting insulin (mU/L)/14.1) [39].

Liver TG

Liver TG content was measured using Triglycerides Liquicolor Kit (Human, Wiesbaden, Germany) as described [36] with some modifications. In brief, liver tissue was homogenized in ice-cold extraction buffer using an automated pellet mixer (VWR, Boxmeer, The Netherlands), equalizing to 20 mg tissue per ml extraction buffer, followed by sonication 18× (amplitude 40, duty cycle 40, output control 1) (Branson Ultrasonics, Danbury, CT, USA). After brief vortex, tissue extraction was employed for TG determination in triplicates.

Gene expression

RNA was isolated from eWAT using Trizol combined with a RNeasy Mini kit (Qiagen, Venlo, The Netherlands), as described [31]. RNA purity and integrity was verified using Nanodrop (NanoDrop, Wilmington, USA) and TapeStation (Agilent, Santa Clara, CA, USA), respectively. cDNA synthesis, followed by regular qRT-PCR was performed as described [40]. Low expressed genes were pre-amplified for 12 cycles before qRT-PCR using SsoAdvanced PreAmp Supermix (Bio-Rad). References genes were selected based on stable expression. The expression of each gene was normalized by the reference genes using CFX Manager software (Bio-Rad). Primer sequences and PCR annealing temperatures are shown in Supplemental Table S2.

Antibodies

Anti-GLUT4, anti-phospho-AKT (Thr308) and anti-ACTB antibodies were purchased from Abcam (Cambridge, MA, USA); anti-phospho-AKT (Ser473) and anti-AKT antibodies were from Cell signaling (Beverly, MA, USA); anti-MAC2 antibody was from Cedarlane (Ontario, Canada); Rabbit IgG antibody was from Vector Laboratories (Burlingame, CA, USA). Goat anti-rabbit Alexa Fluor 488 secondary antibody was from Life technologies (Carlsbad, CA, USA); Goat anti-mouse for ACTB or otherwise donkey anti-rabbit secondary antibodies were from LI-COR (Lincoln, NE, USA).

Western blot

eWAT protein extraction and immunoblotting were performed as published [41], with the following modifications. Frozen tissue was homogenized using an automated pellet mixer (VWR) in ice-cold lysis buffer [42], containing complete protease inhibitor cocktail (Roche, Mannheim, Germany), phosphatase inhibitor-Mix I (Serva, Heidelberg, Germany), 2 µM trichostatin A, and 10 mM Nam (Sigma-Aldrich), followed by sonication 18× (amplitude 40, duty cycle 40, output control 1). The lysate was centrifuged at 18,620*g*, 4°C for 15 minutes, supernatant retrieved, centrifuged again with the same procedure. The obtained clear lysate was employed to measure protein concentration using DC protein assay (Bio-Rad), mixed with LDS loading buffer and dithiothreitol, heated at 70°C for 10 minutes, briefly centrifuged and run on a 4-12% Bis-Tris gel (Invitrogen, Carlsbad, CA, USA) at 110V for 40 minutes, then 150V for 50 minutes. The protein was transferred to an Immobilon PVDF membrane (Merck Millipore, Amsterdam, the Netherlands) at 300 mA for 1 hour, after which the membrane was blocked with 5% BSA in TBS containing 0.1% tween (TBSt) at RT for 1 hour and then incubated with primary antibody at 4°C overnight. After 6 times washes using TBSt, the membrane was

incubated with secondary antibody at RT for 1 hour. The membrane was washed using TBS and scanned on an Odyssey scanner (LI-COR). Bands were analyzed using Odyssey software V3.0 (LI-COR).

Immunohistochemistry

Adipocyte cell size determination, number calculation as well as macrophage staining and counting were performed as described previously [31], with some modifications which can be found in the Supplemental Methods. Fluorescence microscopy of glucose transporter type 4 (GLUT4 or SLC2A4) was conducted as follows. Sections were de-paraffinized, rehydrated and heat-induced epitope retrieved in 10mM sodium citrate buffer (pH=6) for 10 minutes. Sections were subsequently blocked using 5% normal goat serum in PBS-BSAc (S-1000, Vector Laboratories, CA, USA) at RT for 1 hour, and then incubated with GLUT4 antibody (1:500) or rabbit IgG antibody at 4°C overnight. After 6 times washes using PBS, sections were incubated with Alexa Fluor 488 antibody (1:200) at RT for 1 hour, followed by DAPI staining (Sigma-Aldrich, Steinheim, Germany) for 5 minutes. Sections were then mounted and kept at 4°C in the dark. Representative pictures (n=15 per animal plus a negative control) were made at 20× magnification using a Leica DM6B microscope (Leica microsystems, Wetzlar, Germany), and done at 100× magnification using a Zeiss Axioscope 2 microscope (Zeiss, Munich, Germany), with 350 nm (DAPI) and 475 nm (FITC) channels. Staining and microscopy were performed at the same time for Ctrl NR and High NR, with identical settings.

Quantification of GLUT4 fluorescence intensity at 20× magnification was done using ImageJ software as follows. GLUT4 fluorescence of the whole area of each image (n=15 images per animal) was quantified, corrected by the background of each image and the negative control. The nuclei of each image was counted based on binary images of DAPI. GLUT4 intensity was expressed as corrected integrated density by the number of the nuclei.

Statistics

Statistical analysis was performed using GraphPad Prism v5.04 (San Diego, CA, USA) and indicated in the figure legends. Data were verified for normality using the D'Agostino and Pearson omnibus normality test and log transformed if needed. *P*-values < 0.05 were considered to be statistically significant.

Results

High dose NR reduces metabolic flexibility in HF diet fed male C57BI/6JRccHsd mice

Since dietary NR was shown in multiple animal studies to improve metabolic health [5, 7, 15, 17], but also was shown to either have no effect [43] or have detrimental effects depending on the dose and animal model used [31-33, 44], we analyzed long-term (18 weeks) metabolic health effects of dietary high dose of NR in HF-diet fed male C57BI/6JRccHsd mice. The diet contained 9000 mg NR/kg diet, which approximately equals 700 mg NR/kg BW/day and is in a similar range as doses that have been used in previously published NR animal studies [5, 6, 15, 17, 43].

We compared High NR to Ctrl NR, unless indicated otherwise. We monitored body weight, feed intake, fat mass, and lean mass weekly.

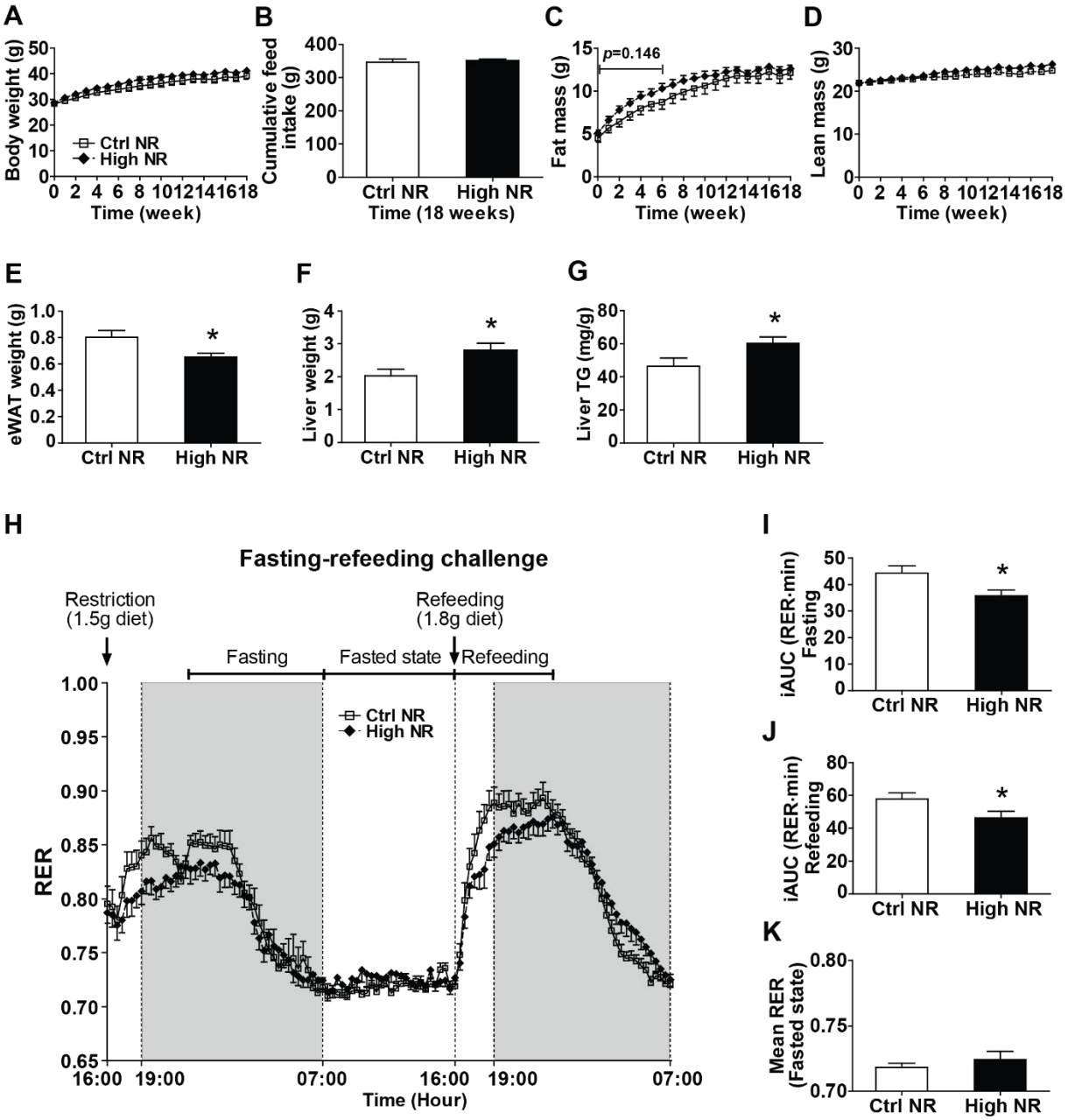

Figure 1. A high dose of NR reduces metabolic flexibility and eWAT weight. Mice were on obesogenic diets containing either 30 mg vitamin B3 (nicotinamide riboside, NR) per kg diet (Ctrl NR) or 9000 mg per kg diet (High NR) for 18 weeks. Body weight (A), fat mass (B), lean mass (C), cumulative feed intake (D). Fresh tissue weight of eWAT (E) and liver (F). Liver TG content was determined and expressed per gram of tissue (G). Fasting-refeeding challenge (H): restriction with 1.5 gram of diet at 16:00h, fasting (from 22:00h to 07:00h), fasted (from 07:00h to 16:00h), refeeding with 1.8 gram of diet at next 16:00h, refeeding (from 16:00h to 23:00h) periods. Shaded areas indicate the dark, active periods. iAUC of RER during fasting (I) and during refeeding (J) were analyzed to represent metabolic flexibility. Mean RER of the fasted state (K). Ctrl NR open square with solid line or white bar, High NR closed diamond with black dashed line or black bar. Data are analyzed using either two-way repeated measures ANOVA followed by Bonferroni post-hoc analysis (A-C, and H) or Student's t test (D-G, I-K), and presented as mean ± SEM (n=11-12 mice per treatment). * $p<0.05$.

We did not observe significant differences in body weight and feed intake over the whole 18-week period (Fig. 1A and D). Whole body fat mass tended to be higher in the first 6 weeks during NR treatment (p=0.146), but was normalized after 18 weeks (Fig. 1B), while lean mass did not differ (Fig. 1C). We sacrificed the animals after a refeeding to be able to analyze plasma and tissue metabolic parameters in a postprandial state. No difference was seen in refeeding feed intake (Supplemental Fig. S1). We observed a decrease in eWAT weight in the High NR group (Fig. 1E), concomitant with an increase in both liver weight (Fig. 1F) and liver TG (Fig. 1G). Furthermore, we also found a significant elevation of serum TC and a tendency to elevated LDL cholesterol (p = 0.053) in the High NR treated mice, whereas other circulating markers of lipid metabolism (TG, NEFA, HDL cholesterol, adiponectin and leptin) and blood glucose were not different (Supplemental Table S3).

To further study the metabolic impact of high dose of dietary NR, we analyzed whole body metabolic flexibility using indirect calorimetry. Previously, we showed by using a fasting-refeeding challenge that a dose of 900 mg NR/kg diet compromised metabolic flexibility [31]. Performing the same fasting-refeeding challenge now on a 9000 mg NR/kg diet, again demonstrated a decrease in metabolic flexibility by dietary high dose of NR (Fig. 1H). High NR significantly reduced the change of RER during the transition from food withdrawal to a physiologically fasted state (when RER reaches 0.7) (Fig. 1I) as well as during refeeding (Fig. 1J). High NR did not alter RER in the fasted period, where RER for both groups was near 0.7 (Fig. 1K). No differences were observed in energy expenditure or physical activity (Supplemental Fig. S2).

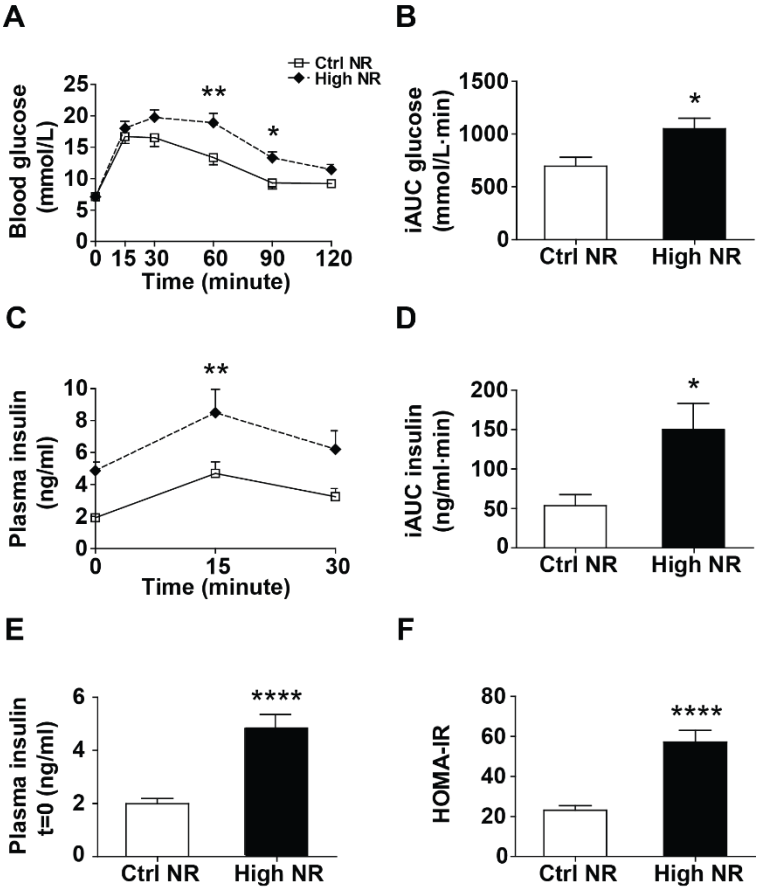

Figure 2. High NR induces lower glucose tolerance and higher circulating insulin levels during OGTT. Blood glucose was measured at indicated timepoints before and after an oral glucose administration (A) and iAUC was calculated to assess glucose tolerance (B). Plasma insulin was measured at indicated timepoints during OGTT (C) and iAUC (Baseline = 1.994) was analyzed (D). Plasma insulin at t=0 represents fasted circulating insulin (E) and the corresponding HOMA-IR was calculated to assess insulin resistance (F). Data are analyzed using either two-way repeated measures ANOVA followed by Bonferroni post-hoc analysis (A, C) or Student's t test (B, D-F), and presented as mean±SEM (n=11-12 mice per treatment). * p<0.05, ** p<0.01, **** p<0.001.

High NR fed mice have lower glucose tolerance

The observed decrease in metabolic flexibility in mice fed High NR was most prominent in the first few hours during the refeeding transition from fat oxidation to carbohydrate oxidation (Fig. 1G), indicating that postprandial carbohydrate metabolism might be hampered by High NR. To analyze this in more detail we analyzed how High NR-treated mice responded to an oral glucose bolus via an OGTT. We observed a decreased glucose clearance rate (Fig. 2A and B), which was accompanied by an impaired insulin response (Fig. 2C and D) in the High NR-treated mice during OGTT. Compared to the control group, the fasting plasma insulin level was elevated almost 2.5-fold in mice fed High NR (Fig. 2E), leading to a much higher HOMA-IR index (Fig. 2F). Combined, these results show that treating HF-diet fed mice with a high dose of NR lowers glucose tolerance and aggravates systemic insulin resistance.

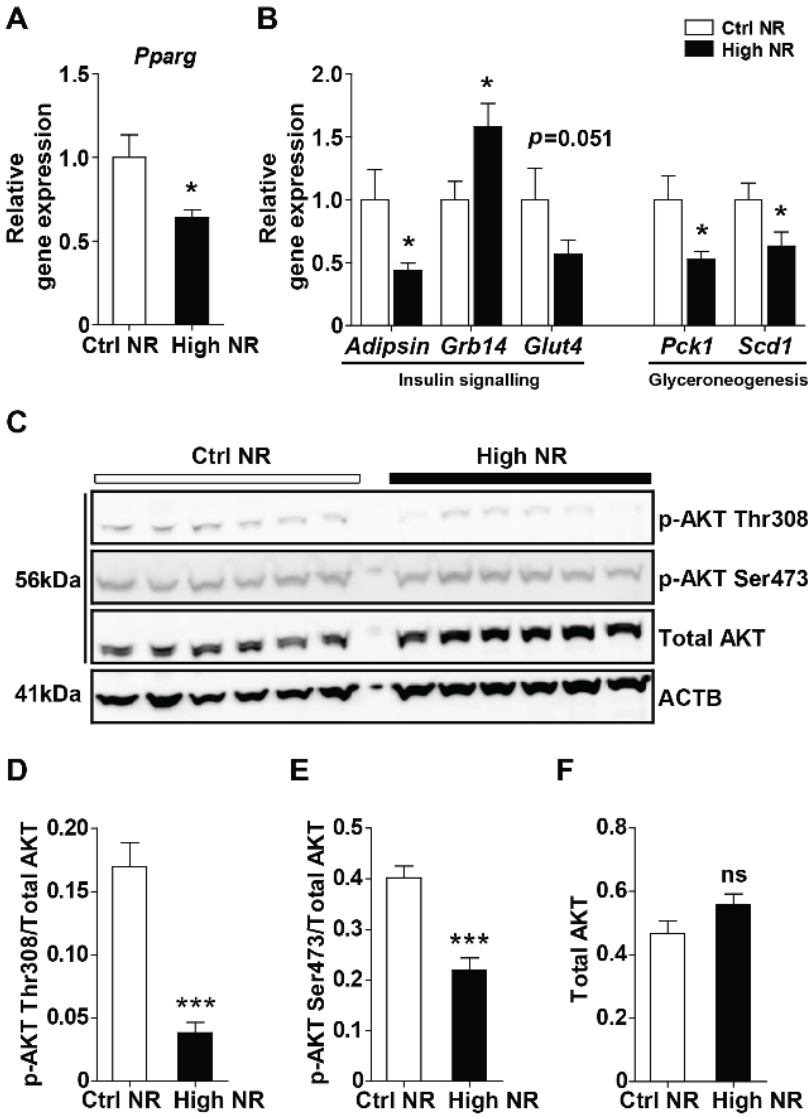

Figure 3. High NR feeding results in a lowered PPARγ expression signature. Relative gene expression of PPARγ (A) and its targeted genes (B) (normalized to the reference genes, n=10-12 per treatment). Phosphorylation and total AKT in eWAT were measured by immunoblotting, using ACTB as a loading control (C). Densitometry analysis on the ratio of p-AKT Thr308/AKT (D), p-AKT Ser473/AKT (E) and total AKT/ACTB (F) (n=6 mice per treatment). Data are analyzed using Student's t test and presented as mean±SEM. * $p<0.05$, *** $p<0.005$.

High NR feeding results in a lowered peroxisome proliferator-activated receptor γ (PPARγ) expression signature in WAT

Since High NR-fed mice were insulin resistant, and also showed decreased weight of eWAT depots, we aimed to analyze whether WAT from the High NR-treated mice was

metabolically dysfunctional. PPARγ is widely known as a master regulator of WAT functions, including insulin sensitivity, adipogenesis and inflammation [45, 46]. Therefore, we analyzed gene expression of PPARγ and its target genes in the eWAT. *Pparg* gene expression was significantly reduced upon High NR feeding (Fig. 3A). Concomitantly, PPARγ-target genes in insulin signaling (*Adipsin*, *Grb14*, *Glut4*) [47-49] and glyceroneogenesis (*Pck1*, *Scd1*) [50, 51] were regulated. All PPARγ-positively regulated genes were downregulated (*Adipsin*, *Scd1*, *Pck1* and *Glut4*), whereas the negative regulator of the insulin receptor, *Grb14*, which is physiologically downregulated upon PPARγ activation, was upregulated (Fig. 3B). This is in line with a downregulation of a PPARγ expression signature in WAT upon High NR feeding.

PPARγ regulation of insulin resistance in WAT is accompanied by alterations of several components of the insulin signaling and is often co-regulated. Although we did not find differences in the gene expression of *Insr*, *Irs1* or *Irs2* (Supplemental Fig. S3), phosphorylation of AKT at both the Thr308 and Ser473 sites was decreased upon High NR feeding in the eWAT (Fig. 3C-E), whereas total AKT levels were not different. Phosphorylation of AKT serves as a core modulator in regulation of insulin signaling resulting in downstream GLUT4 translocation [52, 53].

GLUT4 expression in WAT is crucial for whole-body glucose disposal and has been shown to be increased upon PPARγ activation or decreased due to PPARγ repression [49, 54-57]. Since *Glut4* gene expression was decreased upon high dose NR, but did not reach statistical significance (p=0.051), we analyzed expression of GLUT4 protein levels. GLUT4 expression was observed in the adipocytes (Fig. 4A). The intensity of GLUT4 staining was significantly reduced in the eWAT from mice treated with High NR (Fig. 4B and C). Combined, the lowered PPARγ expression signature, decreased AKT phosphorylation and lower GLUT4 expression in eWAT demonstrate on the molecular level that eWAT of high dose NR treated HF-diet mice is less insulin responsive.

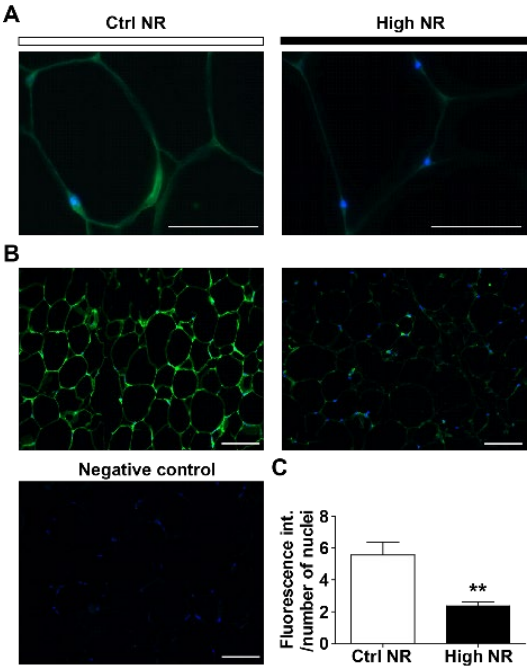

Figure 4. High NR results in lower GLUT4 expression in eWAT. Representative pictures of GLUT4 expression at 100× magnification (A): Ctrl NR left, High NR right. Representative pictures of GLUT4 expression at 20× magnification (B): Ctrl NR left, High NR right; Negative control from Ctrl NR animal, left bottom. Green staining represents GLUT4, blue dots are nuclei. Quantification of GLUT4 fluorescence intensity, normalized by the number of the nuclei (C, n=15 pictures at 20× magnification per animal, 6 animals per treatment). Scale bar represents 50 µm. Data are analyzed using Mann-Whitney test and presented as mean±SEM. ** p<0.01.

High dose NR leads to more severe WAT inflammation

Despite reduced eWAT weight in the High NR group (Fig. 1E), we did not observe any differences in mean adipocyte size (Fig. 5A and B) or frequency distribution of adipocyte sizes (Supplemental Fig. S4). Insulin resistance is often associated with higher WAT inflammation, characterized by higher expression of pro-inflammatory markers and macrophage infiltration or aggregation (presented as crown like structures (CLSs)) [58]. First, using specific staining for macrophages in WAT sections, we were able to analyze macrophage infiltration and aggravation (Fig. 5C). An increased number of single macrophages was observed in sections of WAT from High NR fed mice (Fig. 5C, D). Furthermore, the number of CLSs was also increased upon High NR feeding (Fig. 5C, E). Second, using qRT-PCR we found a marked upregulation of pro-inflammatory genes, including the M1 macrophage markers (*Cd11c* and *Cd11d*) as well as those in acute-phase response (*C3*, *S1008a*, *Saa1* and *Saa3*) and in apoptosis (*Casp1*), in WAT of High NR fed mice (Fig. 5F). Collectively, these results demonstrate that High NR feeding induced pro-inflammatory gene expression and macrophage infiltration in WAT.

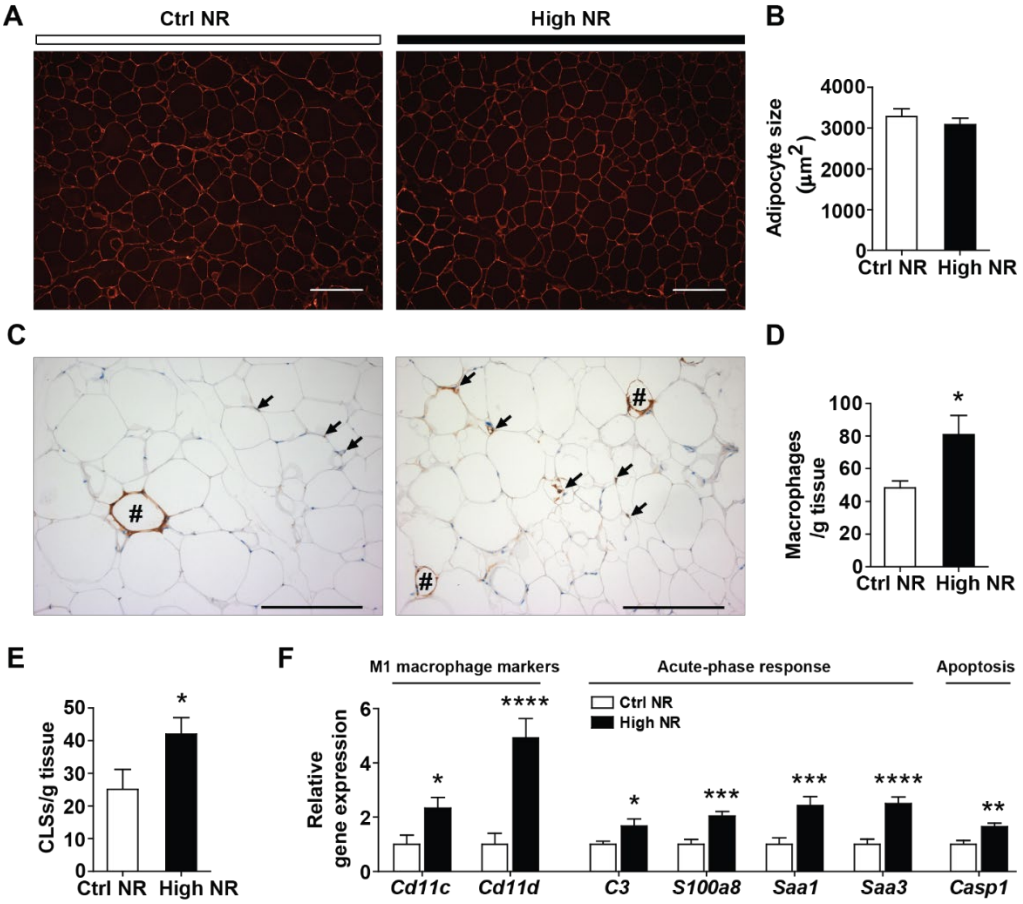

Figure 5. High NR impairs visceral WAT function characterized as more severe inflammation. Representative images of cell size (A) and mean adipocyte size (B). Representative images of CLSs (indicated by hashes) as well as single macrophages (indicated by arrows). Scale bar represents 200 µm. Single macrophages and CLSs were counted (n=8 animals per treatment) and expressed as macrophages or CLSs per gram eWAT weight (D and E). Relative gene expression (normalized to the reference genes) of pro-inflammatory genes (F). n=11-12 per treatment. Data are analyzed using Student's t test and presented as mean±SEM. * p<0.05, ** p<0.01, *** p<0.005, **** p<0.001.

Discussion

Metabolic health of C57BI/6JRccHsd mice fed a high dose NR diet (9000 mg NR/kg diet) was deteriorated in our study, since metabolic flexibility was reduced, glucose clearance rate was lower and insulin resistance on the whole body level was aggravated. eWAT depot weights were decreased by High NR feeding, whereas liver weight and liver TG were increased. We found a lowered PPARγ expression signature, a downregulation of AKT/GLUT4 signaling and aggravated pro-inflammatory responses in the eWAT of mice on the High NR diet. Altogether, these alterations in mice treated with high dose NR suggest the onset of a WAT dysfunction, which may be, in part, associated with deterioration of metabolic health.

Metabolic flexibility on the whole body level is defined as the ability to readily switch between carbohydrate oxidation and fatty acid oxidation in response to a physiological or nutritional intervention [59]. We observed a decreased metabolic flexibility by high dose of NR treatment, in agreement with our previous finding that mice fed a mildly obesogenic diet containing a moderately high dose of NR (900 mg NR/kg diet) were less metabolically flexible compared to those with NR at the recommended vitamin B3 level [31]. In contrast, Canto *et al.* found that metabolic flexibility, assessed by the subtraction of mean RER of dark phase from those from light phase, was increased by supplementation with 400 mg NR/kg BW/day in mice fed a HF diet [5]. This increase in metabolic flexibility, however, was not seen in mice fed a high-fat-high-sucrose (HFHS) diet [6], nor in mice fed a low fat diet [60], even though a similar high dose of NR was used. This suggests a modifying effect of the obesogenic diet on improvement of metabolic flexibility at high NR doses. A change in metabolic flexibility implicates altered metabolic homeostasis [61]. Our data imply that whole body lipid homeostasis may remain unchanged in response to high dose NR, since the whole body fat mass, the fasted RER as well as the postprandial circulating TG and NEFA levels were similar between groups (Fig. 1C, 1H and Supplemental Table S3). On the other hand, our observations during an OGTT suggest that glucose homeostasis was impaired by high dose NR (Fig. 2). This is consistent with another study showing that 3000 mg NR/kg standard chow diet feeding led to glucose intolerance [7]. Altogether, these data suggest that a worsening of glucose homeostasis is likely a main feature of high dose NR-induced deterioration of metabolic health in our study.

WAT plays a critical role in whole body glucose disposal [62, 63]. A defect of insulin signaling in WAT can have a significant impact on glucose homeostasis [64, 65]. The observed downregulation of AKT/GLUT4 signaling in eWAT induced by High NR treatment (Fig. 3 and Fig. 4), implicates that WAT of the high dose NR-treated mice is likely less capable of maintaining glucose homeostasis. Phosphorylation of AKT in adipocytes is regulated by distinct players in insulin signaling pathways, for example, phosphoinositide-dependent protein kinase 1 (PDPK1) induces Thr308 phosphorylation [53, 66], and mechanistic target of rapamycin complex 2 (mTORC2) mediates Ser473 phosphorylation [53, 67]. Possibly, the concurrent regulation of Thr308 and Ser473 phosphorylation of AKT in WAT response to high dose NR, implicates PDPK1 and mTORC2 in regulation of insulin signaling. GLUT4 is thought

to be the major glucose transporter in WAT, serving as a downstream effector of insulin signaling cascade mediating glucose uptake [65]. AKT activation ultimately leads to GLUT4 translocation and the maximal activity of AKT for this event requires phosphorylation of both Thr308 and Ser473 [68-70]. It is conceivable that the downregulation of Thr308 and Ser473 phosphorylation at both sites by High NR treatment may lead to depressed GLUT4 translocation. Furthermore, High NR treatment resulted in almost 2-fold downregulation of GLUT4 expression on the transcriptional and protein levels in eWAT, indicating an impairment of WAT glucose handling. Adipocyte-specific GLUT4 knockout mice also displayed glucose intolerance and systemic insulin resistance [71], indicating that adipose GLUT4 could be a driver of the glucose intolerance identified in our high dose NR-treated mice.

A lowered PPARγ expression signature in eWAT induced by high dose NR treatment may also contribute to worsening glucose homeostasis and insulin resistance. This signature was composed of the downregulation of *Pparg*, *Adipsin*, *Glut4*, *Scd1* and *Pck1* and the upregulation of *Grb14* (Fig. 3A and B). The observed reduced transcription levels of PPARγ in visceral fat depots of obese and insulin resistant dogs [72], implicates PPARγ gene expression in WAT in the development of insulin resistance. Adipsin (Complement factor D, CFD) is a crucial adipokine that can improve insulin secretion and glucose homeostasis [73]. *Adipsin* gene expression in WAT and circulating adipsin levels were found dramatically decreased in *ob/ob* and *db/db* mice, probably associated with the diabetic phenotypes in those models [74]. GRB14 binds to the activated insulin receptor and inhibits its catalytic activity, thus blocking insulin signal transduction [75, 76]. *Grb14* is upregulated in WAT of insulin resistant mice and type 2 diabetic patients [48]. *Pck1* encodes the gluconeogenic enzyme PCK1, but in WAT this enzyme is more glyceroneogenic [77]. SCD1 catalytically de-saturates fatty acyl-CoA substrates and also plays a role in glyceroneogenesis [78, 79]. Targeted deletion of *Scd1* in adipocytes impaired glyceroneogenesis in WAT, concomitant with the reduced other glyceroneogenesis markers, including downregulation of *Pck1* [79]. Dysregulation of glyceroneogenesis in WAT induced by *Pck1* mutation resulted in elevated TG levels in liver [50, 80], impaired WAT glucose uptake and global glucose intolerance [80], a similar metabolic phenotype as seen in high dose NR-treated mice in our study.

High dose of NR aggravated pro-inflammatory responses in eWAT both on the morphological level and the gene level (Fig. 5C-F), implicating WAT pro-inflammation in whole body insulin resistance [81]. The typical M1 macrophage markers, *Cd11c* and *Cd11d*, were transcriptionally increased, indicating that more M1 macrophages were present. WAT M1 macrophages generate pro-inflammatory cytokines, such as tumor necrosis factor α (TNFA-α), and interleukin 6 (IL6), thus contributing to the induction of insulin resistance [82]. *C3, Saa1* and *Saa3*, which is regulated by *S100a8* [83], express secretory proteins that can excrete from adipocytes into local environment, leading to the enhanced inflammation in WAT and insulin resistance [84-86]. Interestingly, these four genes have been reported to be down regulated in response to PPARγ-agonist treatment, in agreement with the amelioration of inflammation [84, 85, 87, 88]. The upregulation of *C3, Saa1*, *Saa3*,

and *S100a8* aligns with the observed lowered PPARγ expression signature. *Casp1* expresses Caspase 1 that governs the production of pro-inflammatory cytokines IL1β and IL18. Caspase 1 controls PPARγ protein degradation, thus playing a role in inflammasome-mediated adipogenesis and insulin sensitivity [89, 90].

WAT serves as a dynamic storage organ for the excessive lipid load that can lead to WAT expansion, characterized by the adipocytes increase in both number (hyperplasia) and size (hypertrophy). The characteristics of adipocyte size are comparable (Fig. 5A, 5B and Supplemental Fig. S3), suggesting that high dose NR did not affect WAT expansion towards hypertrophy. However, considering that tissue weight was lower (Fig. 1E), a total number of adipocytes of the whole tissue might be also lower, indicating that obesogenic diet-induced WAT expansion towards hyperplasia was, to some extent, inhibited by high dose of NR. Furthermore, the increased number of CLSs in WAT of the high dose NR-treated mice suggests enhanced apoptosis of adipocytes. Taking together, it is plausible that less functional adipocytes were available for lipid or cholesterol storage, which could potentially lead to increased ectopic deposition of lipids in other metabolic organs [91, 92]. In line, we observed that serum TC (Supplemental Table S3) and liver TG levels (Fig. 1G) were increased by high dose of NR.

Three studies have shown that supplementation with a high dose of NR improves glucose homeostasis in C57Bl/6J mice fed either a HF diet or a HFHS diet [5-7]. In our C57Bl/6JRccHsd mouse strain we observed impaired glucose homeostasis upon treatment with a similar high dose of NR and a mildly obesogenic diet. In addition to a possible modifying effect of the obesogenic diet, the genetic differences in mice models may also play a role. The C57Bl/6JRccHsd mouse strain in our study contains a functional nicotinamide nucleotide transhydrogenase (*Nnt*) gene, whereas the C57Bl/6J model that was used in the studies showing beneficial effects of high dose NR supplementation harbors a spontaneous mutation in *Nnt,* which has been described to be responsible for an impaired glucose tolerance and decreased insulin secretion in this model [93, 94]. More importantly, NNT is a mitochondrial inner membrane located protein that catalyzes the reversible transfer of hydrogen between NAD^+ and $NADP^+$, thus contributing to NAD^+ homeostasis. It has been shown that loss of NNT decreases the NAD^+/NADH ratio whereas NNT overexpression increased this ratio [95, 96]. Other models with a functional *Nnt* gene did not show a beneficial effect of high dose NR supplementation. For example, NR supplementation impaired redox homeostasis in skeletal muscle of young rats, a model containing functional *Nnt* gene, leading to decreased exercise performance [32, 33].

To conclude, high dose of NR induced deterioration of metabolic health that was characterized by impaired glucose homeostasis and insulin resistance in C57Bl/6JRccHsd mice. The underlying mechanisms may be associated with molecular and morphological changes related to WAT dysfunction, including a decreased AKT/GLUT4 signaling, a lowered PPARγ expression signature and aggravated pro-inflammation. We propose a role of genetic difference *Nnt* in high dose of NR induced metabolic effects, which may possibly explain for the beneficial effects reported in other studies. Considering the fact that NNT is generally expressed and functional in humans [97] and the increasing concerns on the validation of C57Bl/6J

model for human diabetes research [93, 94, 98], further investigation using the proper models is warranted to fully understand biological functions of NR before more human trials are being performed.

Acknowledgements

We thank ChromaDex (ChromaDex Corporation, Irvine, CA, USA) for the generous and kind supply of NR. Financial support by the Chinese Scholarship Council (grant# 201303250054) is gratefully acknowledged. The authors declare no conflicts of interest. We thank our colleagues at Human and Animal Physiology (HAP, Wageningen University, Wageningen, The Netherlands) and the animal facility (Wageningen University, Wageningen, The Netherlands) for their help. We thank Ruth Van Heerbeek (HAP) for practical contributions.

References

[1] Hegyi, J., Schwartz, R. A., Hegyi, V., Pellagra: dermatitis, dementia, and diarrhea. *Int. J. Dermatol.* 2004, *43*, 1-5.
[2] Wan, P., Moat, S., Anstey, A., Pellagra: a review with emphasis on photosensitivity. *Br. J. Dermatol.* 2011, *164*, 1188-1200.
[3] Kim, H. J., Kim, J. H., Noh, S., Hur, H. J., *et al.*, Metabolomic analysis of livers and serum from high-fat diet induced obese mice. *J. Proteome Res.* 2011, *10*, 722-731.
[4] Yoshino, J., Mills, K. F., Yoon, M. J., Imai, S., Nicotinamide mononucleotide, a key NAD(+) intermediate, treats the pathophysiology of diet- and age-induced diabetes in mice. *Cell Metab.* 2011, *14*, 528-536.
[5] Canto, C., Houtkooper, R. H., Pirinen, E., Youn, D. Y., *et al.*, The NAD(+) precursor nicotinamide riboside enhances oxidative metabolism and protects against high-fat diet-induced obesity. *Cell Metab.* 2012, *15*, 838-847.
[6] Gariani, K., Menzies, K. J., Ryu, D., Wegner, C. J., *et al.*, Eliciting the mitochondrial unfolded protein response by nicotinamide adenine dinucleotide repletion reverses fatty liver disease in mice. *Hepatology* 2016, *63*, 1190-1204.
[7] Trammell, S. A., Weidemann, B. J., Chadda, A., Yorek, M. S., *et al.*, Nicotinamide riboside opposes type 2 diabetes and neuropathy in mice. *Sci. Rep.* 2016, *6*, 26933.
[8] Jukarainen, S., Heinonen, S., Ramo, J. T., Rinnankoski-Tuikka, R., *et al.*, Obesity is associated with low NAD(+)/SIRT pathway expression in adipose tissue of BMI-discordant monozygotic twins. *J. Clin. Endocrinol. Metab.* 2016, *101*, 275-283.
[9] Canto, C., Menzies, K. J., Auwerx, J., NAD(+) metabolism and the control of energy homeostasis: a balancing act between mitochondria and the nucleus. *Cell Metab.* 2015, *22*, 31-53.
[10] Elhassan, Y. S., Philp, A. A., Lavery, G. G., Targeting NAD+ in metabolic disease: new insights into an old molecule. *J Endocr Soc* 2017, *1*, 816-835.
[11] Rajman, L., Chwalek, K., Sinclair, D. A., Therapeutic potential of NAD-boosting molecules: the in vivo evidence. *Cell Metab.* 2018, *27*, 529-547.
[12] Horwitt, M. K., Harper, A. E., Henderson, L. M., Niacin-tryptophan relationships for evaluating niacin equivalents. *Am. J. Clin. Nutr.* 1981, *34*, 423-427.
[13] Fukuwatari, T., Shibata, K., Nutritional aspect of tryptophan metabolism. *Int. J. Tryptophan Res.* 2013, *6*, 3-8.
[14] Bogan, K. L., Brenner, C., Nicotinic acid, nicotinamide, and nicotinamide riboside: a molecular evaluation of NAD+ precursor vitamins in human nutrition. *Annu. Rev. Nutr.* 2008, *28*, 115-130.
[15] Khan, N. A., Auranen, M., Paetau, I., Pirinen, E., *et al.*, Effective treatment of mitochondrial myopathy by nicotinamide riboside, a vitamin B3. *EMBO Mol. Med.* 2014, *6*, 721-731.
[16] de Picciotto, N. E., Gano, L. B., Johnson, L. C., Martens, C. R., *et al.*, Nicotinamide mononucleotide supplementation reverses vascular dysfunction and oxidative stress with aging in mice. *Aging Cell* 2016, *15*, 522-530.
[17] Ryu, D., Zhang, H., Ropelle, E. R., Sorrentino, V., *et al.*, NAD+ repletion improves muscle function in muscular dystrophy and counters global PARylation. *Sci. Transl. Med.* 2016, *8*, 361ra139.
[18] Ratajczak, J., Joffraud, M., Trammell, S. A., Ras, R., *et al.*, NRK1 controls nicotinamide mononucleotide and nicotinamide riboside metabolism in mammalian cells. *Nat. Commun.* 2016, *7*, 13103.
[19] Liu, L., Su, X., Quinn, W. J., 3rd, Hui, S., *et al.*, Quantitative analysis of NAD synthesis-breakdown fluxes. *Cell Metab.* 2018, *27*, 1067-1080 e1065.
[20] Yang, T., Chan, N. Y., Sauve, A. A., Syntheses of nicotinamide riboside and derivatives: effective agents for increasing nicotinamide adenine dinucleotide concentrations in mammalian cells. *J. Med. Chem.* 2007, *50*, 6458-6461.
[21] Trammell, S. A., Schmidt, M. S., Weidemann, B. J., Redpath, P., *et al.*, Nicotinamide riboside is uniquely and orally bioavailable in mice and humans. *Nat. Commun.* 2016, *7*, 12948.
[22] Dellinger, R. W., Santos, S. R., Morris, M., Evans, M., *et al.*, Repeat dose NRPT (nicotinamide riboside and pterostilbene) increases NAD(+) levels in humans safely and

sustainably: a randomized, double-blind, placebo-controlled study. *NPJ Aging Mech. Dis.* 2017, *3*, 17.
[23] Dollerup, O. L., Christensen, B., Svart, M., Schmidt, M. S., *et al.*, A randomized placebo-controlled clinical trial of nicotinamide riboside in obese men: safety, insulin-sensitivity, and lipid-mobilizing effects. *Am. J. Clin. Nutr.* 2018, *108*, 343-353.
[24] Martens, C. R., Denman, B. A., Mazzo, M. R., Armstrong, M. L., *et al.*, Chronic nicotinamide riboside supplementation is well-tolerated and elevates NAD(+) in healthy middle-aged and older adults. *Nat. Commun.* 2018, *9*, 1286.
[25] Wang, P., Mariman, E., Renes, J., Keijer, J., The secretory function of adipocytes in the physiology of white adipose tissue. *J. Cell. Physiol.* 2008, *216*, 3-13.
[26] Caton, P. W., Kieswich, J., Yaqoob, M. M., Holness, M. J., Sugden, M. C., Metformin opposes impaired AMPK and SIRT1 function and deleterious changes in core clock protein expression in white adipose tissue of genetically-obese db/db mice. *Diabetes Obes. Metab.* 2011, *13*, 1097-1104.
[27] Chalkiadaki, A., Guarente, L., High-fat diet triggers inflammation-induced cleavage of SIRT1 in adipose tissue to promote metabolic dysfunction. *Cell Metab.* 2012, *16*, 180-188.
[28] Yang, S. J., Choi, J. M., Kim, L., Park, S. E., *et al.*, Nicotinamide improves glucose metabolism and affects the hepatic NAD-sirtuin pathway in a rodent model of obesity and type 2 diabetes. *J. Nutr. Biochem.* 2014, *25*, 66-72.
[29] Rappou, E., Jukarainen, S., Rinnankoski-Tuikka, R., Kaye, S., *et al.*, Weight loss is associated with increased NAD(+)/SIRT1 expression but reduced PARP activity in white adipose tissue. *J. Clin. Endocrinol. Metab.* 2016, *101*, 1263-1273.
[30] Stromsdorfer, K. L., Yamaguchi, S., Yoon, M. J., Moseley, A. C., *et al.*, NAMPT-mediated NAD(+) biosynthesis in adipocytes regulates adipose tissue function and multi-organ insulin sensitivity in mice. *Cell Rep.* 2016, *16*, 1851-1860.
[31] Shi, W., Hegeman, M. A., van Dartel, D. A. M., Tang, J., *et al.*, Effects of a wide range of dietary nicotinamide riboside (NR) concentrations on metabolic flexibility and white adipose tissue (WAT) of mice fed a mildly obesogenic diet. *Mol. Nutr. Food Res.* 2017, *61*, 1600878.
[32] Kourtzidis, I. A., Stoupas, A. T., Gioris, I. S., Veskoukis, A. S., *et al.*, The NAD(+) precursor nicotinamide riboside decreases exercise performance in rats. *J. Int. Soc. Sports Nutr.* 2016, *13*, 32.
[33] Kourtzidis, I. A., Dolopikou, C. F., Tsiftsis, A. N., Margaritelis, N. V., *et al.*, Nicotinamide riboside supplementation dysregulates redox and energy metabolism in rats: Implications for exercise performance. *Exp. Physiol.* 2018, *103*, 1357-1366.
[34] Lambert, J., Agostoni, C., Elmadfa, I., Hulshof, K., *et al.*, Dietary intake and nutritional status of children and adolescents in Europe. *Br. J. Nutr.* 2004, *92 Suppl 2*, S147-211.
[35] Van Rossum, C., Buurma-Rethans, E., Vennemann, F., Beukers, M., *et al.*, *The diet of the Dutch: Results of the first two years of the Dutch National Food Consumption Survey 2012-2016*, RIVM, Bilthoven, The Netherlands 2016.
[36] Duivenvoorde, L. P., van Schothorst, E. M., Swarts, H. M., Kuda, O., *et al.*, A difference in fatty acid composition of isocaloric high-fat diets alters metabolic flexibility in male C57BL/6JOlaHsd mice. *PLoS One* 2015, *10*, e0128515.
[37] Hoek-van den Hil, E. F., Keijer, J., Bunschoten, A., Vervoort, J. J., *et al.*, Quercetin induces hepatic lipid omega-oxidation and lowers serum lipid levels in mice. *PLoS One* 2013, *8*, e51588.
[38] Friedewald, W. T., Levy, R. I., Fredrickson, D. S., Estimation of the concentration of low-density lipoprotein cholesterol in plasma, without use of the preparative ultracentrifuge. *Clin. Chem,* 1972, *18*, 499-502.
[39] Van Dijk, T., Laskewitz, A., Grefhorst, A., Boer, T. S., *et al.*, A novel approach to monitor glucose metabolism using stable isotopically labelled glucose in longitudinal studies in mice. *Lab. Anim.* 2013, *47*, 79-88.
[40] Hoevenaars, F. P., Bekkenkamp-Grovenstein, M., Janssen, R. J., Heil, S. G., *et al.*, Thermoneutrality results in prominent diet-induced body weight differences in C57BL/6J mice, not paralleled by diet-induced metabolic differences. *Mol. Nutr. Food Res.* 2014, *58*, 799-807.
[41] Duivenvoorde, L. P., van Schothorst, E. M., Swarts, H. J., Keijer, J., Assessment of metabolic flexibility of old and adult mice using three noninvasive, indirect calorimetry-based treatments. *J. Gerontol. A Biol. Sci. Med. Sci.* 2015, *70*, 282-293.

[42] Li, Y., Silva, J. C., Skinner, M. E., Lombard, D. B., Mass spectrometry-based detection of protein acetylation. *Methods Mol. Biol.* 2013, 81-104.
[43] Purhonen, J., Rajendran, J., Tegelberg, S., Smolander, O.-P., *et al.*, NAD+ repletion produces no therapeutic effect in mice with respiratory chain complex III deficiency and chronic energy deprivation. *FASEB J.* 2018, fj. 201800090R.
[44] Conze, D. B., Crespo-Barreto, J., Kruger, C. L., Safety assessment of nicotinamide riboside, a form of vitamin B3. *Hum. Exp. Toxicol.* 2016, *35*, 1149-1160.
[45] Sharma, A. M., Staels, B., Peroxisome proliferator-activated receptor γ and adipose tissue—understanding obesity-related changes in regulation of lipid and glucose metabolism. *J. Clin. Endocrinol. Metab.* 2006, *92*, 386-395.
[46] Ahmadian, M., Suh, J. M., Hah, N., Liddle, C., *et al.*, PPARγ signaling and metabolism: the good, the bad and the future. *Nat. Med.* 2013, *19*, 557.
[47] Sugii, S., Olson, P., Sears, D. D., Saberi, M., *et al.*, PPARγ activation in adipocytes is sufficient for systemic insulin sensitization. *Proc. Natl. Acad. Sci. U. S. A.* 2009, pnas. 0912487106.
[48] Cariou, B., Capitaine, N., Le Marcis, V., Vega, N., *et al.*, Increased adipose tissue expression of Grb14 in several models of insulin resistance. *FASEB J.* 2004, *18*, 965-967.
[49] Armoni, M., Harel, C., Karnieli, E., Transcriptional regulation of the GLUT4 gene: from PPAR-gamma and FOXO1 to FFA and inflammation. *Trends Endocrinol. Metab.* 2007, *18*, 100-107.
[50] Olswang, Y., Cohen, H., Papo, O., Cassuto, H., *et al.*, A mutation in the peroxisome proliferator-activated receptor gamma-binding site in the gene for the cytosolic form of phosphoenolpyruvate carboxykinase reduces adipose tissue size and fat content in mice. *Proc. Natl. Acad. Sci. U. S. A.* 2002, *99*, 625-630.
[51] Yao-Borengasser, A., Rassouli, N., Varma, V., Bodles, A. M., *et al.*, Stearoyl-coenzyme A desaturase 1 gene expression increases after pioglitazone treatment and is associated with peroxisomal proliferator-activated receptor-γ responsiveness. *J. Clin. Endocrinol. Metab.* 2008, *93*, 4431-4439.
[52] Van Dam, E. M., Govers, R., James, D. E., Akt activation is required at a late stage of insulin-induced GLUT4 translocation to the plasma membrane. *Mol. Endocrinol.* 2005, *19*, 1067-1077.
[53] Beg, M., Abdullah, N., Thowfeik, F. S., Altorki, N. K., McGraw, T. E., Distinct Akt phosphorylation states are required for insulin regulated Glut4 and Glut1-mediated glucose uptake. *Elife* 2017, *6*, e26896.
[54] Wu, Z., Xie, Y., Morrison, R. F., Bucher, N. L., Farmer, S. R., PPARgamma induces the insulin-dependent glucose transporter GLUT4 in the absence of C/EBPalpha during the conversion of 3T3 fibroblasts into adipocytes. *J. Clin. Invest.* 1998, *101*, 22-32.
[55] Yonemitsu, S., Nishimura, H., Shintani, M., Inoue, R., *et al.*, Troglitazone induces GLUT4 translocation in L6 myotubes. *Diabetes* 2001, *50*, 1093-1101.
[56] Schreiber, I., Dörpholz, G., Ott, C.-E., Kragesteen, B., *et al.*, BMPs as new insulin sensitizers: enhanced glucose uptake in mature 3T3-L1 adipocytes via PPARγ and GLUT4 upregulation. *Sci. Rep.* 2017, *7*, 17192.
[57] Fang, J., Ianni, A., Smolka, C., Vakhrusheva, O., *et al.*, Sirt7 promotes adipogenesis in the mouse by inhibiting autocatalytic activation of Sirt1. *Proc. Natl. Acad. Sci. U. S. A.* 2017, *114*, E8352-E8361.
[58] Cinti, S., Mitchell, G., Barbatelli, G., Murano, I., *et al.*, Adipocyte death defines macrophage localization and function in adipose tissue of obese mice and humans. *J. Lipid Res.* 2005, *46*, 2347-2355.
[59] Galgani, J. E., Moro, C., Ravussin, E., Metabolic flexibility and insulin resistance. *Am. J. Physiol. Endocrinol. Metab.* 2008, *295*, E1009-1017.
[60] Khan, N. A., Auranen, M., Paetau, I., Pirinen, E., *et al.*, Effective treatment of mitochondrial myopathy by nicotinamide riboside, a vitamin B3. *EMBO Mol Med* 2014, *6*, 721-731.
[61] van Ommen, B., Keijer, J., Heil, S. G., Kaput, J., Challenging homeostasis to define biomarkers for nutrition related health. *Mol. Nutr. Food Res.* 2009, *53*, 795-804.
[62] Ciaraldi, T. P., Kong, A. P., Chu, N. V., Kim, D. D., *et al.*, Regulation of glucose transport and insulin signaling by troglitazone or metformin in adipose tissue of type 2 diabetic subjects. *Diabetes* 2002, *51*, 30-36.

[63] Scherer, P. E., Adipose tissue: from lipid storage compartment to endocrine organ. *Diabetes* 2006, *55*, 1537-1545.
[64] Jiang, Z. Y., Zhou, Q. L., Coleman, K. A., Chouinard, M., *et al.*, Insulin signaling through Akt/protein kinase B analyzed by small interfering RNA-mediated gene silencing. *Proc. Natl. Acad. Sci. U. S. A.* 2003, *100*, 7569-7574.
[65] Huang, S., Czech, M. P., The GLUT4 glucose transporter. *Cell Metab.* 2007, *5*, 237-252.
[66] Frech, M., Andjelkovic, M., Ingley, E., Reddy, K. K., *et al.*, High affinity binding of inositol phosphates and phosphoinositides to the pleckstrin homology domain of RAC/protein kinase B and their influence on kinase activity. *J. Biol. Chem.* 1997, *272*, 8474-8481.
[67] Olsen, J. M., Sato, M., Dallner, O. S., Sandström, A. L., *et al.*, Glucose uptake in brown fat cells is dependent on mTOR complex 2–promoted GLUT1 translocation. *J. Cell Biol.* 2014, *207*, 365-374.
[68] Czech, M. P., Corvera, S., Signaling mechanisms that regulate glucose transport. *J. Biol. Chem.* 1999, *274*, 1865-1868.
[69] Hemmings, B. A., Restuccia, D. F., PI3K-PKB/Akt pathway. *Cold Spring Harb. Perspect. Biol.* 2012, *4*, a011189.
[70] Tsuchiya, A., Kanno, T., Nishizaki, T., PI3 kinase directly phosphorylates Akt1/2 at Ser473/474 in the insulin signal transduction pathway. *J. Endocrinol.* 2013, *220*, 49-59.
[71] Abel, E. D., Peroni, O., Kim, J. K., Kim, Y.-B., *et al.*, Adipose-selective targeting of the GLUT4 gene impairs insulin action in muscle and liver. *Nature* 2001, *409*, 729.
[72] Gayet, C., Leray, V., Saito, M., Siliart, B., Nguyen, P., The effects of obesity-associated insulin resistance on mRNA expression of peroxisome proliferator-activated receptor-γ target genes, in dogs. *Br. J. Nutr.* 2007, *98*, 497-503.
[73] Lo, J. C., Ljubicic, S., Leibiger, B., Kern, M., *et al.*, Adipsin is an adipokine that improves beta cell function in diabetes. *Cell* 2014, *158*, 41-53.
[74] Flier, J. S., Cook, K. S., Usher, P., Spiegelman, B. M., Severely impaired adipsin expression in genetic and acquired obesity. *Science* 1987, *237*, 405-408.
[75] Kasus-Jacobi, A., Perdereau, D., Auzan, C., Clauser, E., *et al.*, Identification of the rat adapter Grb14 as an inhibitor of insulin actions. *J. Biol. Chem.* 1998, *273*, 26026-26035.
[76] Béréziat, V., Kasus-Jacobi, A., Perdereau, D., Cariou, B., *et al.*, Inhibition of insulin receptor catalytic activity by the molecular adapter Grb14. *J. Biol. Chem.* 2002, *277*, 4845-4852.
[77] Beale, E. G., Hammer, R. E., Antoine, B., Forest, C., Disregulated glyceroneogenesis: PCK1 as a candidate diabetes and obesity gene. *Trends Endocrinol. Metab.* 2004, *15*, 129-135.
[78] ALjohani, A. M., Syed, D. N., Ntambi, J. M., Insights into stearoyl-coA desaturase-1 regulation of systemic metabolism. *Trends Endocrinol. Metab.* 2017, *28*, 831-842.
[79] Dragos, S. M., Bergeron, K. F., Desmarais, F., Suitor, K., *et al.*, Reduced SCD1 activity alters markers of fatty acid reesterification, glyceroneogenesis, and lipolysis in murine white adipose tissue and 3T3-L1 adipocytes. *Am. J. Physiol. Cell Physiol.* 2017, *313*, C295-C304.
[80] Millward, C. A., Desantis, D., Hsieh, C. W., Heaney, J. D., *et al.*, Phosphoenolpyruvate carboxykinase (Pck1) helps regulate the triglyceride/fatty acid cycle and development of insulin resistance in mice. *J. Lipid Res.* 2010, *51*, 1452-1463.
[81] McArdle, M. A., Finucane, O. M., Connaughton, R. M., McMorrow, A. M., Roche, H. M., Mechanisms of obesity-induced inflammation and insulin resistance: insights into the emerging role of nutritional strategies. *Front. Endocrinol.* 2013, *4*, 52.
[82] Gordon, S., Alternative activation of macrophages. *Nat. Rev. Immunol.* 2003, *3*, 23.
[83] Sekimoto, R., Kishida, K., Nakatsuji, H., Nakagawa, T., *et al.*, High circulating levels of S100A8/A9 complex (calprotectin) in male Japanese with abdominal adiposity and dysregulated expression of S100A8 and S100A9 in adipose tissues of obese mice. *Biochem. Biophys. Res. Commun.* 2012, *419*, 782-789.
[84] Yang, R. Z., Lee, M. J., Hu, H., Pollin, T. I., *et al.*, Acute-phase serum amyloid A: An inflammatory adipokine and potential link between obesity and its metabolic complications. *PLoS Med.* 2006, *3*, 884-894.
[85] Han, C. Y., Subramanian, S., Chan, C. K., Omer, M., *et al.*, Adipocyte-derived serum amyloid A3 and hyaluronan play a role in monocyte recruitment and adhesion. *Diabetes* 2007, *56*, 2260-2273.

[86] Munkonda, M. N., Lapointe, M., Miegueu, P., Roy, C., *et al.*, Recombinant acylation stimulating protein administration to C3−/− mice increases insulin resistance via adipocyte inflammatory mechanisms. *PLoS One* 2012, *7*, e46883.
[87] Wang, P., Renes, J., Bouwman, F., Bunschoten, A., *et al.*, Absence of an adipogenic effect of rosiglitazone on mature 3T3-L1 adipocytes: increase of lipid catabolism and reduction of adipokine expression. *Diabetologia* 2007, *50*, 654-665.
[88] Hiuge-Shimizu, A., Maeda, N., Hirata, A., Nakatsuji, H., *et al.*, Dynamic changes of adiponectin and S100A8 levels by the selective peroxisome proliferator–activated receptor-γ agonist rivoglitazone. *Arterioscler. Thromb. Vasc. Biol.* 2011, *31*, 792-799.
[89] He, F., Doucet, J. A., Stephens, J. M., Caspase-mediated degradation of PPARγ proteins in adipocytes. *Obesity* 2008, *16*, 1735-1741.
[90] Stienstra, R., Joosten, L. A., Koenen, T., van Tits, B., *et al.*, The inflammasome-mediated caspase-1 activation controls adipocyte differentiation and insulin sensitivity. *Cell Metab.* 2010, *12*, 593-605.
[91] Angel, A., Farkas, J., Regulation of cholesterol storage in adipose tissue. *J. Lipid Res.* 1974, *15*, 491-499.
[92] Parlee, S. D., Lentz, S. I., Mori, H., MacDougald, O. A., *Methods in enzymology*, Elsevier 2014, pp. 93-122.
[93] Toye, A. A., Lippiat, J. D., Proks, P., Shimomura, K., *et al.*, A genetic and physiological study of impaired glucose homeostasis control in C57BL/6J mice. *Diabetologia* 2005, *48*, 675-686.
[94] Freeman, H. C., Hugill, A., Dear, N. T., Ashcroft, F. M., Cox, R. D., Deletion of nicotinamide nucleotide transhydrogenase: a new quantitive trait locus accounting for glucose intolerance in C57BL/6J mice. *Diabetes* 2006, *55*, 2153-2156.
[95] Son, M. J., Kwon, Y., Son, T., Cho, Y. S., Restoration of mitochondrial NAD(+) levels delays stem cell senescence and facilitates reprogramming of aged somatic cells. *Stem Cells* 2016, *34*, 2840-2851.
[96] Ho, H. Y., Lin, Y. T., Lin, G., Wu, P. R., Cheng, M. L., Nicotinamide nucleotide transhydrogenase (NNT) deficiency dysregulates mitochondrial retrograde signaling and impedes proliferation. *Redox Biol.* 2017, *12*, 916-928.
[97] Meimaridou, E., Kowalczyk, J., Guasti, L., Hughes, C. R., *et al.*, Mutations in NNT encoding nicotinamide nucleotide transhydrogenase cause familial glucocorticoid deficiency. *Nat. Genet.* 2012, *44*, 740-742.
[98] Santos, L. R. B., Muller, C., de Souza, A. H., Takahashi, H. K., *et al.*, NNT reverse mode of operation mediates glucose control of mitochondrial NADPH and glutathione redox state in mouse pancreatic beta-cells. *Mol. Metab.* 2017, *6*, 535-547.

Supplemental Methods

Metabolic flexibility

Indirect calorimetry was performed in week 14, using a PhenoMaster System (TSE Systems, Bad Homburg, Germany) as described [1]. Briefly, mice were individually housed with a steady normal air flow, 12h light–dark cycle (07:00h lights on). Oxygen consumption, carbon dioxide production, activity (infrared beam breaks) and food and drink intake were automatically recorded. After 20 hours of adaptation, *ad libitum* fed mice were monitored for 24 hours starting from 07:00h. Next, the mice were exposed to a fasting-refeeding challenge. For this, the mice were provided with 1.5 gram of fresh experimental diet at 16:00h. The mice fully consumed this, after which they changed to a fully fasted state. The next day at 16:00h they were provided with 1.8 gram of fresh experimental diet (refeeding), which was fully consumed. Respiratory exchange ratio (RER) and energy expenditure were calculated by TSE software (TSE systems). Metabolic flexibility was assessed as described [2], with the following modifications: incremental area under the RER curve (iAUC) between 22:00h to 07:00h during fasting and between 16:00h to 23:00h during refeeding were individually analysed using GraphPad

software. The iAUC of RER represents metabolic flexibility. Mean RER of the fasted period was calculated to indicate fatty acid oxidation. How a specific RER value relates to percentage lipid or carbohydrate oxidation can be found in [3].

eWAT morphology

Adipocyte size as well as macrophage staining and counting were measured by immunohistochemistry (IHC) as described [4]. Briefly, tissue was fixed, washed in PBS, embedded in paraffin and sectioned at 5 µm using an automated microtome (Microm GmbH, Heidelberg, Germany). Sections after 20 sequential cuts were used to ensure no repetitive adipocytes were present. Tissue sections were deparaffinised, rehydrated and then stained with Mayer's haematoxylin for 75 seconds (Klinipath BV, Duiven, The Netherlands) and with 0.1% eosin for 15 seconds (Brunswig, Southborough, MA, USA). Subsequently, sections were dehydrated, mounted and then dried overnight at 37˚C. Representative pictures were made using a Leica DM6B microscope (Leica Microsystems, Wetzlar, Germany). Adipocyte size was measured using CellProfiler software v2.1.1 (The Carpenter Lab, Massachusetts, USA) and expressed in surface area (μm^2) per adipocyte. The frequency distribution of adipocyte size was calculated as described [5], with some modifications. Briefly, adipocyte surface area was distributed in 100 μm^2 clusters in Excel and subsequently clustered as defined fractions of small (100-1500 μm^2), medium (>1500-6000 μm^2), and large (>6000 μm^2). Values less than 100 μm^2 were excluded. Macrophages were stained using anti-MAC2 antibody from Cedarlane (Ontario, Canada). Single macrophages and crown-like structures (CLSs) from 1000 adipocytes per animal were counted, and expressed as macrophages or CLSs per gram eWAT weight.

Supplemental references

[1] Duivenvoorde, L. P., van Schothorst, E. M., Swarts, H. J., and Keijer, J., Assessment of metabolic flexibility of old and adult mice using three noninvasive, indirect calorimetry-based treatments. *J. Gerontol. A Biol. Sci. Med. Sci.* 2015, 70, 282-293.

[2] Asterholm, I. W., Scherer, P. E., Enhanced metabolic flexibility associated with elevated adiponectin levels. *The American journal of pathology* 2010, *176*, 1364-1376.

[3] Péronnet, F., Massicotte, D., Table of nonprotein respiratory quotient: an update. *Can J Sport Sci* 1991, *16*, 23-29.

[4] Hoek-van den Hil, E. F., van Schothorst, E. M., van der Stelt, I., Swarts, H. J., *et al.*, Direct comparison of metabolic health effects of the flavonoids quercetin, hesperetin, epicatechin, apigenin and anthocyanins in high-fat-diet-fed mice. *Genes Nutr.* 2015, *10*, 469.

[5] Parlee, S. D., Lentz, S. I., Mori, H., MacDougald, O. A., Quantifying size and number of adipocytes in adipose tissue. *Methods Enzymol* 2014, *537*, 93-122.

Supplemental figures

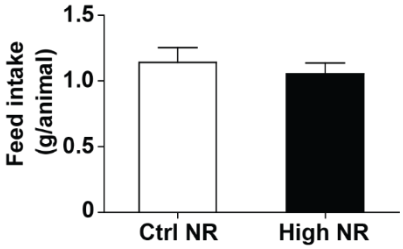

Supplemental Figure S1. No difference in feed intake before dissection. Individual feed intake before the dissection was measured in week 18. Ctrl NR white bar, High NR black bar. Data are analyzed using Student's t test and shown as mean±SEM (n=11-12 mice per treatment).

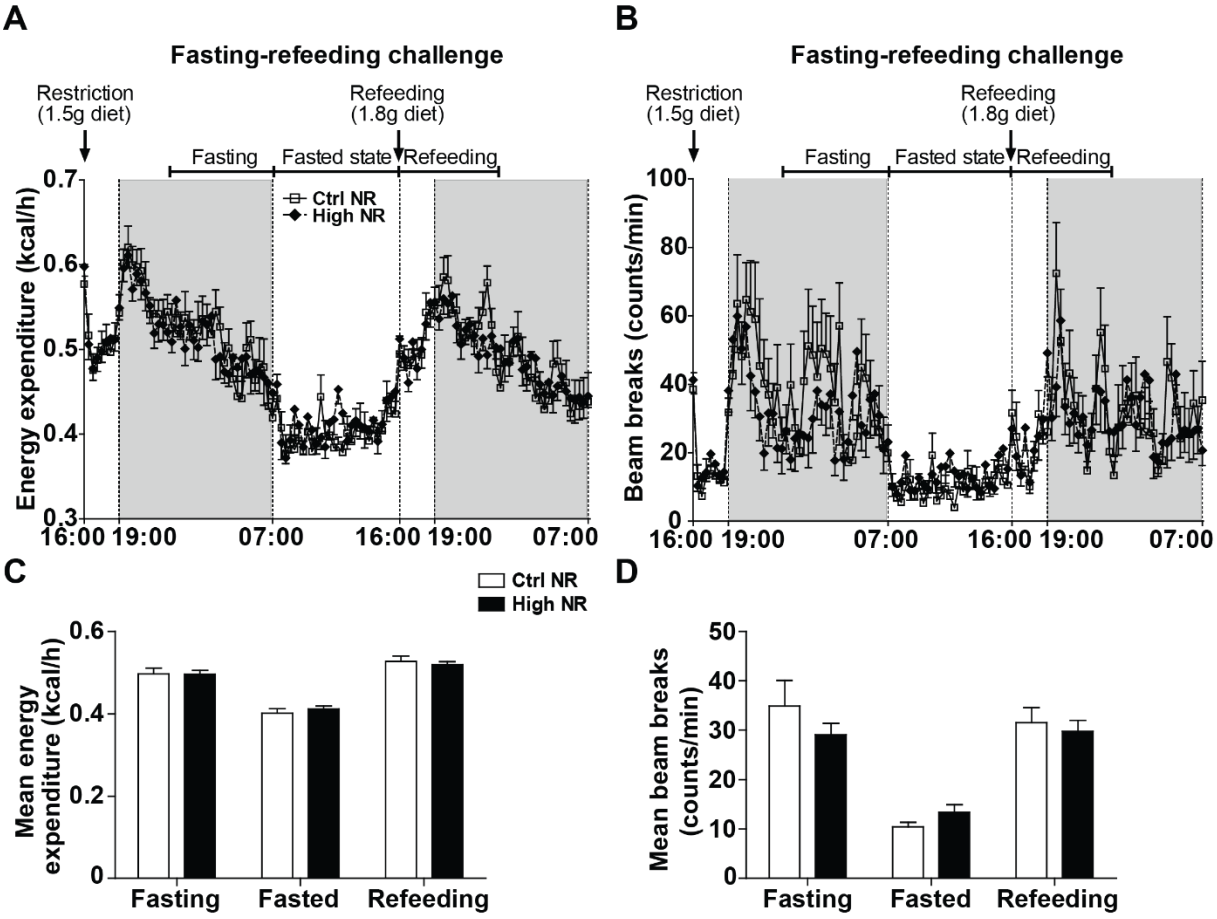

Supplemental Figure S2. Energy expenditure and physical activity do not differ between Ctrl NR and High NR. Energy expenditure (A) and real-time physical activity (indicated as beam breaks per min, B) during the fast-refeeding challenge were measured using indirect calorimetry in week 14: restriction with 1.5 gram of diet at 16:00h, fasting (from 22:00h to 07:00h), fasted (from 07:00h to 16:00h), refeeding with 1.8 gram of diet at the next 16:00h, refeeding (from 16:00h to 23:00h) periods. Shaded areas indicate the dark, active periods. Mean energy expenditure (C) and beam breaks (D) were analyzed for each period. Ctrl NR (30NR) open square with solid line or white bar, High NR (9000NR) closed diamond with black dashed line or black bar. NR in mg/kg diet. Data are analysed using two-way repeated measures ANOVA followed by Bonferroni post-hoc analysis and shown as mean±SEM (n=11-12 mice per treatment).

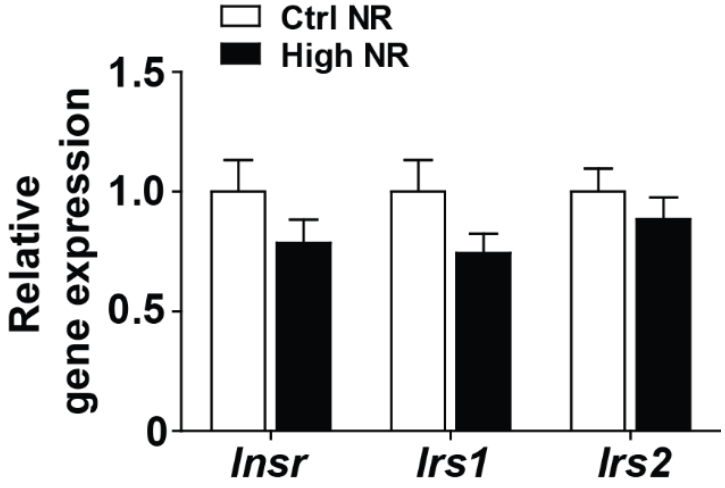

Supplemental Figure S3. High NR does not alter insulin receptor genes in eWAT. Relative gene expression (normalized to the reference genes) of insulin receptor genes. Data are analyzed using Student's t test and shown as mean±SEM (n=11 mice per treatment).

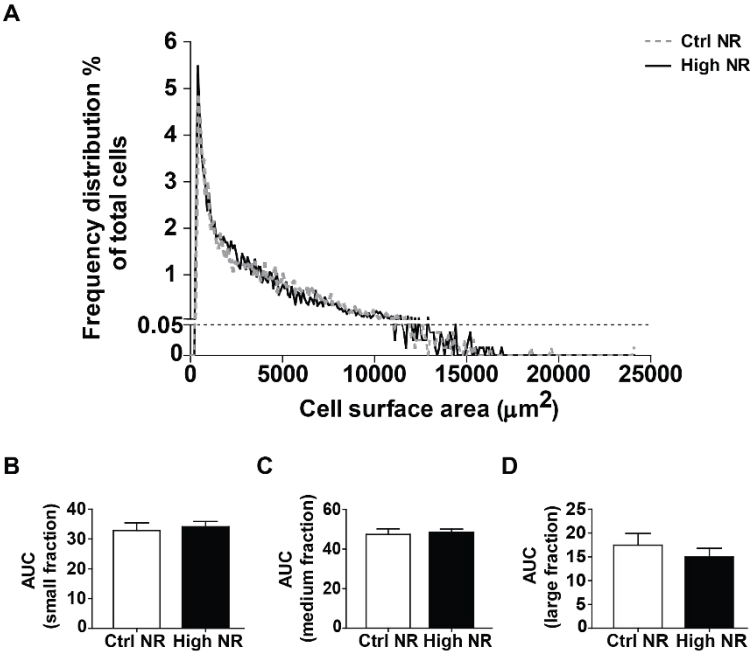

Supplemental Figure S4. Adipocyte size frequency distribution is comparable between Ctrl NR and High NR. Frequency distribution (A) and area under the curve (AUC) of small (100-1500µm^2, B), medium (<1500-6000µm^2, C) and large (>6000µm^2, D) adipocyte fractions. Ctrl NR grey solid line or white bar, High NR black dashed line or black bar. Data are analyzed using Student's t test and shown as mean±SEM (n=8 mice per treatment).

Supplemental Table S1. Composition of diets

Ingredients (g·kg-1 diet)	Adaptation	Ctrl NR	High NR
Casein	100.0	100.0	100.0
Wheat starch	233.1	233.1	233.1
Gelatin (hydrolysed)	100.0	100.0	100.0
Maltodextrin	100.0	100.0	100.0
Sugar	100.0	100.0	100.0
Dextrose	50.0	50.0	50.0
Arbocel B800	50.0	50.0	50.0
Linseed oil	4.0	4.0	4.0
Palm oil	206.0	206.0	206.0
Mineral mixture AIN-93	35.0	35.0	35.0
Vitamin mixture AIN-93 [a]	10.0	10.0	10.0
L-Cystine	3.25	3.25	3.25
L-Phenylalanine	4.32	4.32	4.32
Choline chloride 50%	1.55	1.55	1.55
Nicotinamide riboside (mg·kg-1 diet)	30.0	30.0	9000.0
Calculated amount of L-tryptophan (%)	1.15	1.15	1.15
Calculated energy (kcal·kg-1)	4653	4653	4653
Carbohydrate (% of total energy)	41	41	41
Fat (% of total energy)	40	40	40
Protein (% of total energy)	19	19	19

[a] Vitamin B3 withdrawn

Supplemental Table S2. Sequences of primers for qRT-PCR [a]

Gene symbol	Primer forward 5'-3'	Primer reverse 5'-3'
B2m [b]	CCCCACTGAGACTGATACATACGC	AGAAACTGGATTTGTAATTAAGCAGGTTC
C3	AAAGATTTCACACACCGAAGAAGACTG	GAGCATCCCATCGTCCTTCTCTG
Casp1	CCATGGCTGACAAGATCCTGAG	CATAGGTCCCGTGCCTTGTC
Cfd (*Adipsin*)	TCACCATTAACATGATGTGTGCAGAG	GGATGACACTCGGGTATAGACGC
Grb14	CGGTCCCAGCCATGGTTTCAC	GTTACTCTGACTATCCCGTACC
Insr	CATCATGTGGTCCGCCTTCT	CCGGTGCACAAACTTCTTGG
Irs1	TTAGGCAGCAATGAGGGCAA	TCTTCATTCTGCTGTGATGTCCA
Irs2	GCACCTATGCAAGCATCGAC	GCGCTTCACTCTTTCACGAC
Itgad (Cd11d)	TTAGGCAGCAATGAGGGCAA	TCTTCATTCTGCTGTGATGTCCA
Itgax (Cd11c)	GTTTGAGTGTCAGGAGCAGGT	GAGGTCACCTAGTTGGGTCTTG
Pck1	GTTTGTAGGAGCAGCCATGAGATC	CCAGAGGAACTTGCCATCTTTGTC
Pparg (Pparγ)	GAAGTTCAATGCACTGGAATTAGATGAC	TTGTCTTGGATGTCCTCGATGGG
Rps15 [b]	CGGAGATGGTGGGTAGCATGG	ACGGGTTTGTAGGTGATGGAGAAC
S100a8	ACTTCGAGGAGTTCCTTGCG	TGCTACTCCTTGTGGCTGTC
Saa1	AGACACCAGGATGAAGCTACT	AAGGCCTCTCTTCCATCACT
Saa3	AAAGAAGCTGGTCAAGGGTC	TGTCCCGTGAACTTCTGAAC
Scd1	TCATGGTCCTGCTGCACTTGG	CTGTGGCTCCAGAGGCGATG
Slc2a4 (Glut4)	CCATTCCCTGGTTCATTGTG	GTTTTGCCCCTCAGTCATTC

a All the primers were used with the optimal annealing temperature at 60°C.
b Reference genes.

Supplemental Table S3. Effects of High NR on circulating indicators for WAT function [a]

Indicators	Ctrl NR [b]		High NR		p value [c]
	mean	SEM	mean	SEM	
Blood glucose (mmol/L)	5.9	0.2	5.5	0.2	0.173
TG (mg/dL)	131.6	7.0	131.3	4.0	0.976
NEFA (mmol/L)	1.1	0.1	0.9	0.1	0.342
Total cholesterol (mg/dL)	134.8	9.9	165.2	9.1	**0.035**
HDL cholesterol (mg/dL)	75.4	8.7	77.4	5.1	0.841
LDL cholesterol (mg/dL)	43.9	6.2	66.8	9.1	0.055
Leptin (mg/mL)	1.3	0.2	1.7	0.2	0.102
Adiponectin (mg/mL)	1.1	0.3	0.8	0.1	0.356

a Samples were collected from animals which were in a postprandial state.
b Ctrl NR, 30NR; High NR, 9000NR. NR in mg/kg diet.
c Data are analyzed using Student's t test (n=10-12 mice per treatment).

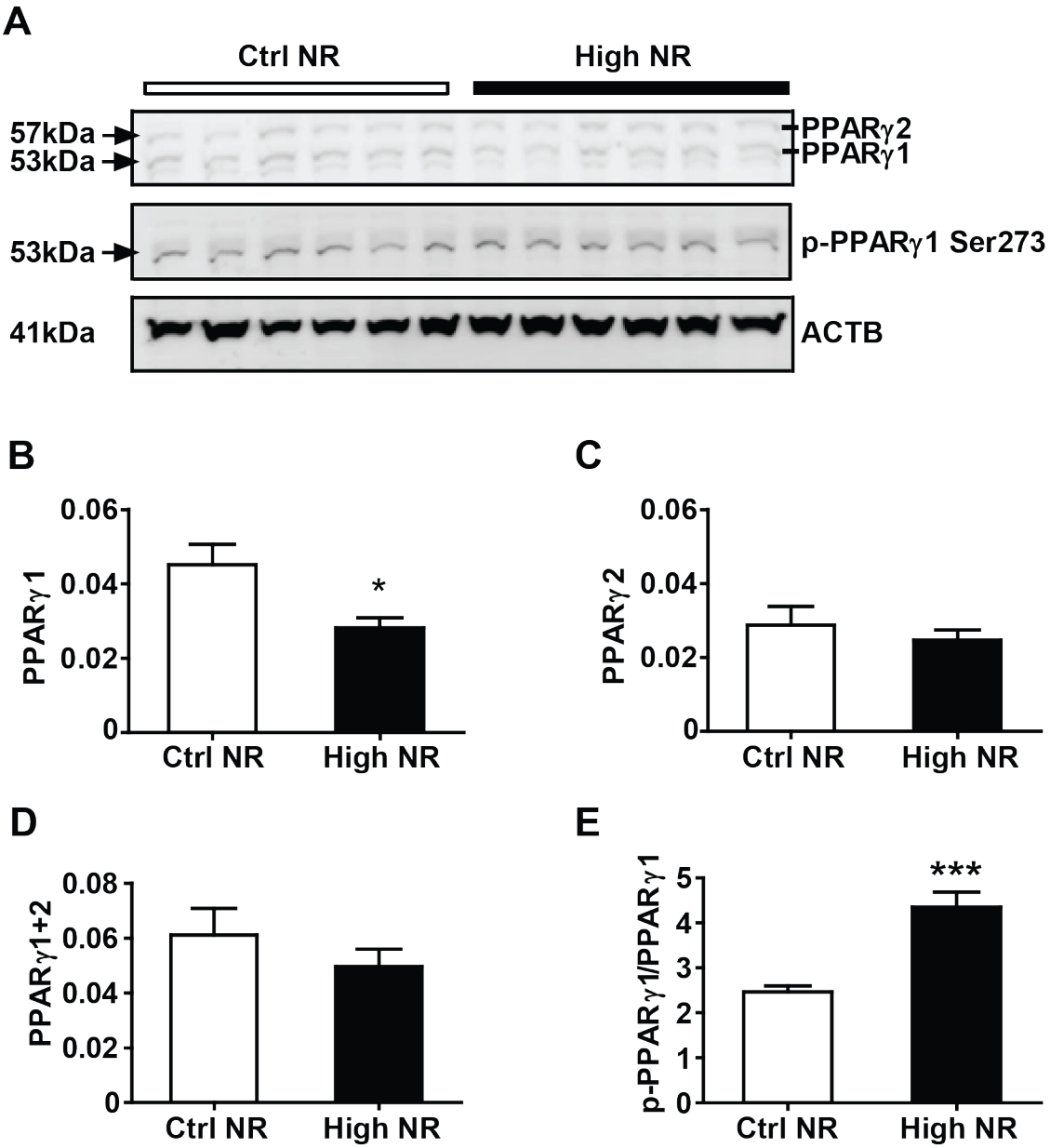

Supplemental Figure S5. PPARγ expression and phosphorylation of PPARγ isoform 1. Protein expression of PPARγ1 and PPARγ2 as well as Ser 237 phosphorylation of PPARγ1 in eWAT were measured by immunoblotting, using ACTB as a loading control (A). Densitometry analysis on the ratio of PPARγ1/ACTB (B), PPARγ2/ACTB (C), PPARγ1+ PPARγ 2/ACTB (D), and p-PPARγ1 Ser273/ PPARγ1 (E) (n=6 mice per treatment). Data are analyzed using Student's t test and presented as mean±SEM. * $p<0.05$, *** $p<0.005$.

Chapter 4

Transcriptional response of white adipose tissue to withdrawal of vitamin B3

Wenbiao Shi, Maria A. Hegeman, Atanaska Doncheva, Inge van der Stelt, Melissa Bekkenkamp-Grovenstein, Evert M. van Schothorst, Vincent C.J. de Boer and Jaap Keijer

Submitted to: Molecular Nutrition & Food Research (2019).

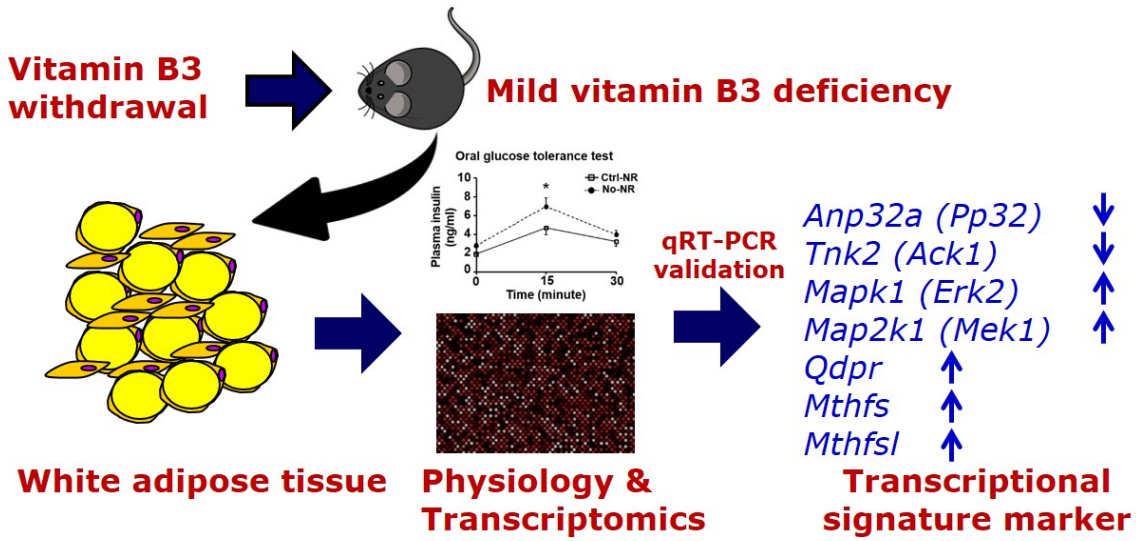

Abstract

Distinct markers for mild vitamin B3 deficiency are lacking. To identify these, we examined the molecular responses of white adipose tissue (WAT) to vitamin B3 withdrawal. A dietary intervention was performed in male C57Bl/6JRccHsd mice, in which a diet without nicotinamide riboside (NR) was compared to a diet with NR at the recommended vitamin B3 level. Both diets contained low but adequate level of tryptophan. Metabolic flexibility and systemic glucose tolerance were analysed and global transcriptomics, qRT-PCR and histology of epididymal WAT (eWAT) were performed. We observed a decreased insulin sensitivity and a shift from carbohydrate to fatty acid oxidation in response to vitamin B3 withdrawal. This was consistent with molecular changes in eWAT, including an activated MEK/ERK signalling, a lowering of glucose utilization markers and an increase in makers of fatty acid catabolism, possibly related to the consistent lower expression of mitochondrial electron transport complexes. The synthesis pathway of tetrahydropteridine (BH4), an essential cofactor for neurotransmitter synthesis, was transcriptionally activated. Genes marking these processes were technically validated. We propose the downregulation of *Anp32a,Tnk2* and the upregulation of *Mapk1*, *Map2k1*, *Qdpr*, *Mthfs*, and *Mthfsl* as a WAT transcriptional signature marker for mild vitamin B3 deficiency.

Introduction

Vitamin B3 represents nicotinic acid, nicotinamide, nicotinamide mononucleotide and nicotinamide riboside (NR), which are precursors of nicotinamide adenine dinucleotide (NAD^+) [1]. NAD^+ supports multiple essential cellular functions and is principally involved in redox reactions, as electron acceptor (NAD^+) or donor (NADH) [2].

In mammals, NAD^+ can also be synthesized from the essential amino acid tryptophan (Trp) [3]. Long term inadequate intake of vitamin B3 and Trp can lead to the development of Pellagra in humans. Pellagra has a number of unspecific symptoms, including lesions of the skin, soreness of tongue and mouth, diarrhoea, and dementia. Weakness and fatigue are early symptoms of this disease. Pellagra can ultimately result in death due to multi-organ failure, when not treated [4]. Rats fed a vitamin B3-free and Trp-limited diet can show a pellagra-like phenotype [5, 6].

In terms of contribution to NAD^+ level, dietary Trp is equivalent to vitamin B3 in a ratio of approximately 1/60 in humans [7], while this ratio is slightly higher in mice [8]. The conversion of Trp to NAD^+ is dependent on Trp intake, since lower Trp intake prioritizes tryptophan for protein synthesis [9]. Trp is also required for biosynthesis of the neurotransmitter serotonin. In mice, 0.1% tryptophan in the diet is considered to be an adequate level of intake for normal growth [10, 11]. A higher intake of Trp may negate the consequences of vitamin B3 deficiency. Indeed, mice fed a chow diet without vitamin B3, but with 0.23% Trp, were shown to maintain normal growth and a normal blood NAD(H) level [12, 13].

In mice or *in vitro*, NAD^+ deficiency has been successfully established through genetic manipulation or pharmaceutical intervention that aim to either disrupt NAD^+ synthesis or regeneration [13-15], or to enhance NAD^+ consumption [16, 17]. These strategies generally cause severe NAD^+ depletion and consequential physiological deterioration and provide important mechanistic insights, but are less human relevant since severe vitamin B3 deficiency is rare nowadays [4].

The prevalence of mild vitamin B3 deficiency is, however, not well established, because clinical symptoms and physiological signs of vitamin B3 deficiency are relative unspecific [8]. Possibly, molecular responses to vitamin B3 withdrawal in mice could be used to provide more specific markers for mild vitamin B3 deficiency, a condition that is likely more common in human than severe deficiency [4]. Therefore, we aimed here to identify molecular responses to vitamin B3 withdrawal using global transcriptome analysis. We used NR as exclusive source of vitamin B3, as the optimal dietary level of this B3 vitamin has been established in mice and can be used as control [18]. We focused on white adipose tissue (WAT), since we previously established WAT as an organ that is sensitive to especially low levels of NR [19]. Furthermore, diet induced obesity induces a NAD^+ decline in WAT [20, 21]. We performed a dietary intervention in male C57Bl/6JRccHsd mice using a diet without NR and with NR at the recommended vitamin B3 level. To identify effects, a large influx of NAD^+ from tryptophan had to be prevented and we therefore used a diet with a low, but adequate level of Trp (0.115%).

Material and Methods

Animal study and diet

The animal experiment was ethically approved (DEC2016033b) and performed in full accordance with national and EU-regulations. This independent experiment was performed as part of a larger experiment to reduce the number of (control) animals. C57Bl/6JRccHsd male mice (Envigo, Horst, The Netherlands) were individually housed (12h light–dark cycle, 23±1°C, 55±15% humidity), with *ad libitum* access to feed and water, unless indicated otherwise. A semi-synthetic diet (Supporting information Table S1) was employed, containing 40% energy from fat, a low but sufficient amount of tryptophan (calculated 0.115% L-tryptophan) and either 0 or 30 mg NR per kg diet as vitamin B3 source (referred to as No-NR and Ctrl-NR, respectively). Nine week old mice were accustomed to the Ctrl-NR diet for two weeks. Subsequently, mice were stratified based on their body weight into 2 experimental groups (n=12/group) and received the No-NR or Ctrl-NR diet for 18 weeks. Body parameters measurements, sample collection and processing are in Supporting information methods.

Metabolic flexibility and energy expenditure

Indirect calorimetry was conducted in week 14 using a PhenoMaster System (TSE Systems, Bad Homburg, Germany), as described [19]. Respiratory exchange ratio (RER) and energy expenditure (EE) were recorded using TSE software. Metabolic flexibility was assessed based on the change of RER in response to a fasting-refeeding challenge as the incremental area under the RER curve (iAUC) between 16:00h and 23:00h, with the RER of each group at 16:00h as baseline. The mean of EE of the fasted and the refeeding period were calculated. RER and EE were measured under the non-challenged conditions before the fasting-refeeding challenge.

Oral glucose tolerance test

An oral glucose tolerance test (OGTT) was performed in week 17, as described [22] and detailed in Supporting information methods.

Circulating parameters

Determination of circulating parameters and related calculations are in Supporting information methods.

RNA isolation

Total RNA was isolated from eWAT using Trizol combined with a RNeasy Mini kit (Qiagen, Venlo, The Netherlands), as described [23]. RNA purity and yield were measured using Nanodrop (NanoDrop, Wilmington, USA) and RNA integrity was verified using TapeStation (Agilent, Santa Clara, CA, USA).

Genome wide gene expression

200ng RNA of each sample (n=12 per group) was assayed using mouse whole genome 8×60K microarrays (Agilent Technologies Inc., Santa Clara, CA, USA), as published [24]. Signals were extracted (Feature extraction 10.7.3.1., Agilent), quality controlled and normalized as described [24]. All microarray data are MIAME

compliant and were stored in GEO (GSE116483). 26384 probes (44.0% of total) were considered expressed (average expression >2x background). 4795 probes were differentially expressed with a Benjamini-Hochberg false discovery rate adjusted Student's *t*-test *p* value of less than 0.5 (FDR<0.5) and 368 probes were with FDR<0.2. Fold change is the ratio of mean expression of No-NR over Ctrl-NR. Probes with FDR<0.2 were used for the analysis of pathway maps and GO processes using MetaCore (Thomson Reuters, New York, NY, USA). Genes enriched in the top 10 pathway maps were gathered and presented as a heatmap using GeneMaths XT (Applied Maths, Sint-Martens-Latem, Belgium). The top 30 down- and upregulated annotated genes with FDR<0.2 were annotated using public databases (MGI (www.informatics.jax.org), Nextprot (www.nexprot.org) and Pubmed (www.ncbi.nlm.nih.gov/pubmed)). From these, genes related to insulin sensitivity were selected and their net effect on insulin sensitivity was indicated, based on scientific literature (PubMed). Similarly, from the FDR<0.2 dataset, genes related to tetrahydrobiopterin (BH4) synthesis were selected, supplemented with relevant FDR<0.5 genes and their net effect on BH4 synthesis was indicated. Mitochondrial gene expression was separately interrogated. Nuclear encoded mitochondrial genes extracted from the mouse MitoCarta2.0 database (https://www.broadinstitute.org/files/shared/metabolism/mitocarta/mouse.mitocarta.2.0.html), and distribution of down- and up- regulated probes was analysed for FDR<0.5 and for FDR<0.2. Pathway analysis using MetaCore was performed based on subset of "mitochondrial genes", in which we used FDR<0.5 to ensure a sufficient number of genes. The distribution of down&up regulated probes for the top 1 pathway map was analysed.

qRT-PCR validation

cDNA synthesis and regular qRT-PCR were performed as described [19]. Gene expression was presented as fold change of expression value normalized by reference genes with mean value of Ctrl-NR at 1. Primer sequences are in Supporting information Table S2.

Immunohistochemistry

Fluorescence microscopy of glucose transporter type 4 (GLUT4/SLC2A4) was performed as described in Supporting information methods. Adipocyte cell size as well as macrophages were measured as described [19], with minor modifications and details are in Supporting information methods.

Western blot

Levels of mitochondrial oxidative phosphorylation (OXPHOS) complex proteins in eWAT were assessed by western blot using an OXPHOS antibody cocktail (Abcam, Cambridge, MA, USA) with β-actin (Abcam) as control. Details are in Supporting information methods.

Statistics

Statistical analysis was performed using GraphPad Prism v5.04 (San Diego, CA, USA). Data were verified for normality using the D'Agostino and Pearson omnibus normality test and log transformed if needed. Statistical differences were analysed using two-way repeated measures ANOVA followed by Bonferroni post-hoc analysis or students' *t*-test. *P* values<0.05 were considered statistically significant.

Results

Body parameters and metabolic flexibility

Since vitamin B3 deficiency can affect health, we monitored progression of body weight and composition as well as metabolic parameters. We compared No-NR to Ctrl-NR, unless indicated otherwise. No significant differences were observed over the 18 week period in body weight, lean mass, fat mass and feed intake (Fig. 1A-D). In line with this, no significant differences were seen in RER or EE under non-challenged conditions (Supporting information Fig. S1). Under fasting-refeeding challenge conditions, the Ctrl-NR animals tended to have a higher iAUC of RER (p=0.061) (Fig. 1E, 1G), suggesting that these animals were better able to switch from fatty acid oxidation (FAO) to carbohydrate oxidation (CHO) during the refeeding transition. No significant differences were seen in EE during the challenge test (Fig. 1F, 1H). In the refed condition, glucose, triglycerides (TG), non-esterified fatty acids (NEFA), total cholesterol, HDL cholesterol, LDL cholesterol, leptin and adiponectin, exhibited comparable circulating levels between groups (Table 1). The serum serotonin level, which is associated with tryptophan metabolism, was not changed in No-NR (Table 1).

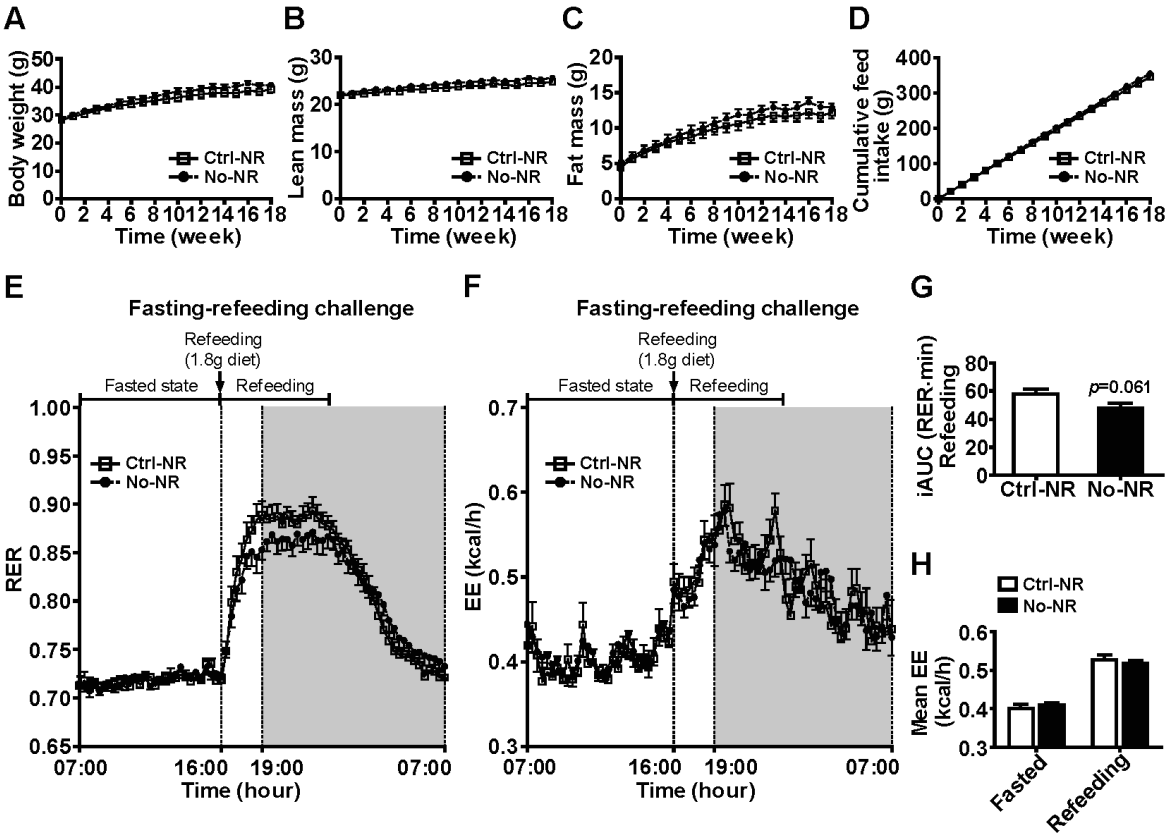

Figure 1. **Whole body parameters and metabolic flexibility.** Body weight (A), lean mass (B), fat mass (C), cumulative feed intake (D). Metabolic flexibility (E) and EE (F) in week 14. The challenge (1.8 gr diet at 16.00h) was given when the animals were fully fasted (on fatty acid oxidation) resulting in a switch to carbohydrate oxidation. The shaded area indicates the dark, active period. Metabolic flexibility was analysed as incremental area under the RER curve (iAUC; baseline = mean of RER at 16:00h) during the refeeding transition (G). Mean of EE for each period (H). Ctrl-NR: open square with solid line or white bar. No-NR: closed circle with black dashed line or black bar. Data as mean±SEM. n=11-12. Analysis with two-way ANOVA for A-F, H and Student's t test for G.

Systemic glucose tolerance

An OGTT was performed to assess insulin-stimulated glucose clearance. The blood glucose levels and glucose iAUC did not differ between the No-NR and the Ctrl-NR animals during the OGTT (Fig. 2A, 2B). The No-NR animals required higher levels of insulin, with a significantly elevated peak insulin level (t=15 min) and a tendency towards a larger iAUC (p=0.083; Fig. 2C, 2D). These animals also exhibited significantly higher fasting circulating insulin levels (Fig. 2E). HOMA-IR, an indicator of insulin resistance, was higher in No-NR (Fig. 2F). These data implicate that mice on No-NR were less insulin sensitive.

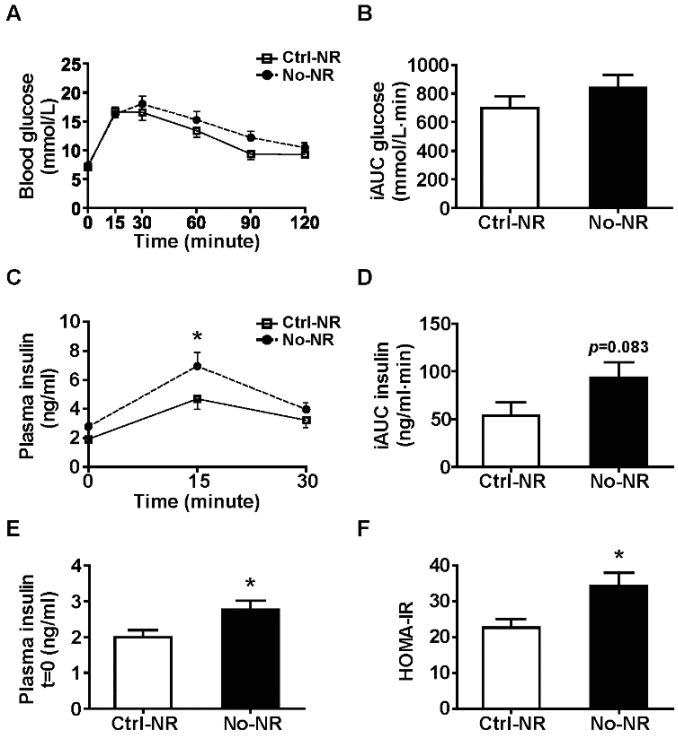

Figure 2. Oral glucose tolerance test. Blood glucose levels at the indicated time points before and after an oral glucose administration in week 17 (A). iAUC (B). Plasma insulin at indicated timepoints during OGTT (C) and plasma insulin iAUC (baseline is mean of t=0 insulin in Ctrl-NR, D). Plasma insulin at t=0 (E). HOMA-IR(F). Data as mean±SEM. n=11-12. Analysis with two-way ANOVA (A, C) or Student's t test (B, D, E, F). * p<0.05.

eWAT transcriptome enrichment analysis

WAT plays an important role in the regulation of metabolic flexibility and systemic insulin sensitivity [25, 26]. Therefore, we focused on the molecular responses of WAT and performed a whole-genome transcriptome analysis of eWAT. The most affected pathways and GO-processes were bioinformatically established. In the top10 pathways, developmental processes and white adipocyte differentiation stand out (Fig. 3A). Eight of the top 10 GO processes were related to cellular localization (G5, G7, G8, G9) and intracellular transportation, including endosomal and cytoplasmic transport and regulation of Golgi (G1, G2, G3, G4) (Fig. 3C). While the pathways and GO processes seemed to differ, the underlying genes were not. The pathways were represented by a set of 10 differentially expressed genes, with 3 genes appearing in all pathways: *Mapk1* (also known as *Erk2*), *Map2k1* (also known as *Mek1*) and *Map2k2* (also known as *Mek2*) (Fig. 3C). *Mapk1* also appeared in all top 10 GO processes, while *Map2k1* and *Map2k2* were present in 9 out of 10 GO processes (Fig. 3C). *Dnm2, Rdx* and *Arghf1* were present in several pathway maps, while *Jak3, Ftna, Raptor* and *Stim1* appeared in one pathway map. *Dmn2*, *Rdx, Jak3*, *Fnta* and *Raptor* also appeared in the top 10 GO processes. Of these genes, *Mapk1*, *Map2k1* and *Fnta* were upregulated, while the remainder were downregulated.

Since pathway analysis suggested WAT differentiation, we examined eWAT morphological parameters (Supporting information Fig. S2). In line with similar adiposity and eWAT weight (Supporting information Fig. S3A-B), no significant differences were found in mean adipocyte size and its frequency distribution (Supporting information Fig. S3C-F). In agreement with the data-analysis output that did not indicate inflammation, no differences in the number of crown-like structures (CLSs) or single macrophages were observed (Supporting information Fig. S3G, S3H).

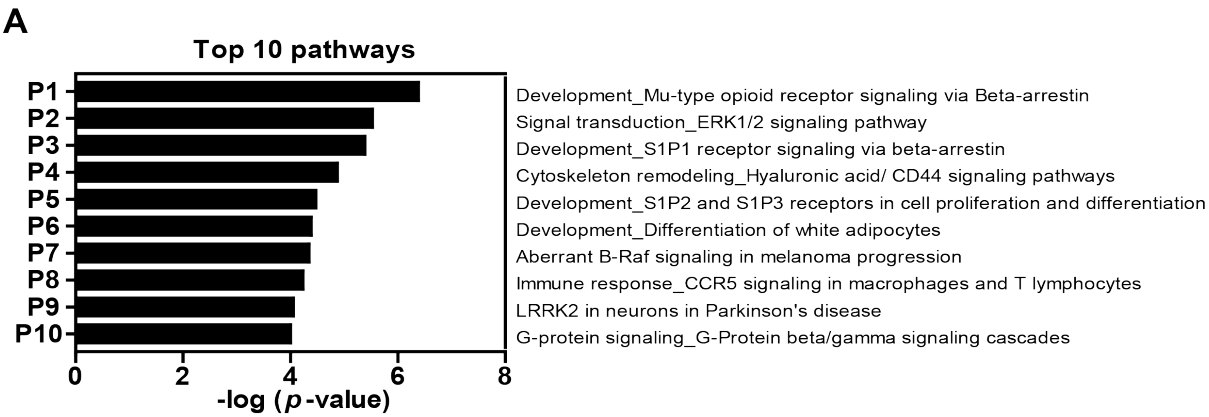

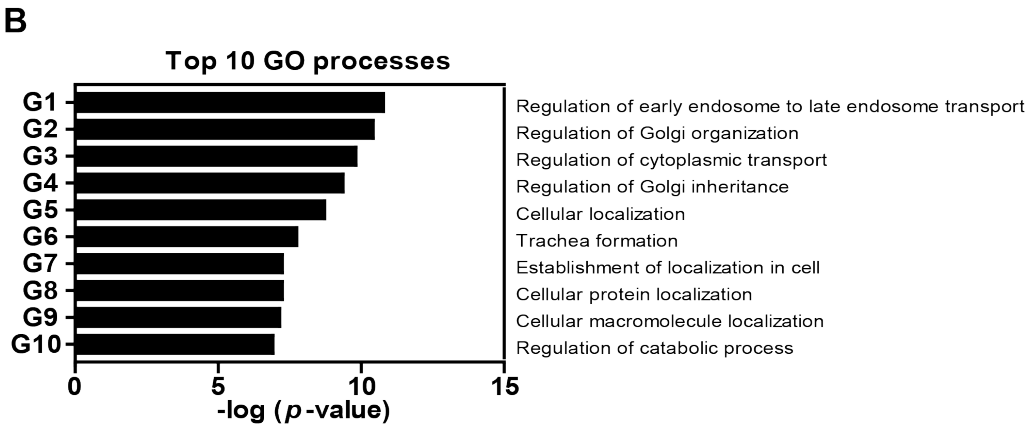

C

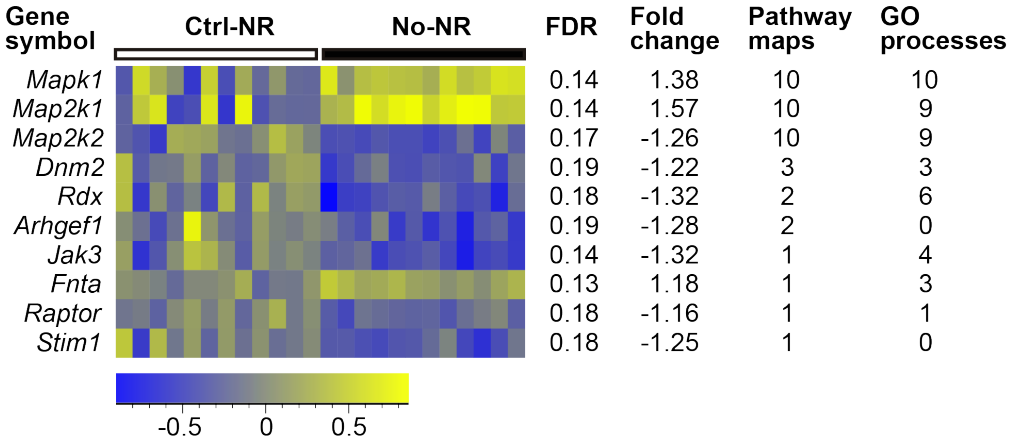

Gene symbol	FDR	Fold change	Pathway maps	GO processes
Mapk1	0.14	1.38	10	10
Map2k1	0.14	1.57	10	9
Map2k2	0.17	-1.26	10	9
Dnm2	0.19	-1.22	3	3
Rdx	0.18	-1.32	2	6
Arhgef1	0.19	-1.28	2	0
Jak3	0.14	-1.32	1	4
Fnta	0.13	1.18	1	3
Raptor	0.18	-1.16	1	1
Stim1	0.18	-1.25	1	0

Figure 3. Transcriptome analysis of eWAT. The top 10 pathway maps (A). The top 10 GO processes (B). Significant genes in the top 10 pathway maps, their expression as heat map (n=12), FDR, fold change (No-NR over Ctrl-NR) and number of times appearing in a top 10 pathway maps and GO processes (C). The expression is presented as absolute expression in a sample minus the mean of the respective gene.

Table 1. Circulating parameters [a]

Indicators	Ctrl-NR		No-NR		*p* value [b]
	mean	SEM	Mean	SEM	
Blood glucose (mmol/L)	5.9	0.2	5.7	0.2	0.290
TG (mg/dL)	131.6	7.0	127.3	7.9	0.692
NEFA (mmol/L)	1.1	0.1	1.1	0.1	0.906
Total cholesterol (mg/dL)	134.8	9.9	137.9	7.7	0.808
HDL cholesterol (mg/dL)	75.4	8.7	65.3	7.2	0.242
LDL cholesterol (mg/dL)	43.9	6.2	52.2	7.1	0.399
Leptin (mg/mL)	1.3	0.2	1.4	0.1	0.496
Adiponectin (mg/mL)	1.1	0.3	0.7	0.1	0.228
Serotonin (µg/mL)	12.0	1.7	12.0	1.1	0.972

a At necropsy (refed)
b Student's t test (n=10-12).

Table 2. Top 30 down- and up- regulated unique genes (FDR<0.2, No-NR over Ctrl-NR)

Gene symbol	Fold change	Gene symbol	Fold change
Anp32a	-1.95	**Mthfsl**	1.70
Isoc2a	-1.86	Rnu3b1	1.66
Fmr1nb	-1.76	Gm10115	1.64
DefB36	-1.72	**Map2k1**	1.57
Pakap	-1.59	5330406M23Rik	1.54
Ino80d	-1.52	**Tmem123**	1.52
Esr1	-1.47	**Dcc**	1.47
Cmtm4	-1.46	Gmpr2	1.46
Cd151	-1.45	**Mthfs**	1.45
Nr3c1	-1.45	**Qdpr**	1.42
Dtx1	-1.44	**Gcm1**	1.42
Rnd1	-1.44	Rhox8	1.42
Chtf8	-1.43	LOC553096	1.41
Akap11	-1.41	**Ermn**	1.41
4833439L19Rik	-1.38	**Sumo2**	1.40
Kdsr	-1.36	Pnma2	1.40
Ehd2	-1.35	Gm33195	1.40
Tnk2	-1.35	Dynlt3	1.40
Arl4d	-1.34	Trpm1	1.39
Abca2	-1.34	B020031M17Rik	1.39
Pbrm1	-1.34	GaB3	1.39
Rita1	-1.34	**Eif2a**	1.39
Arl6ip5	-1.33	**Meg3**	1.38
Chpf2	-1.33	1700097N02Rik	1.38
Rdx	-1.32	**Mapk1**	1.38
Mta1	-1.32	4932431P20Rik	1.38
Cxx1a	-1.32	Slfn9	1.38
Cldnd1	-1.32	5033418A18Rik	1.37
Jak3	-1.32	D030002E05Rik	1.37
Hk1	-1.32	Zdhhc6	1.36

Gene in bold are discussed. Gene annotation, systematic names and gene function are in Supporting information Table S3.

eWAT insulin signalling

To obtain a more detailed insight in eWAT gene regulation in response to No-NR, the top 30 (fold change, FC) down- and up- regulated genes FDR<0.2 genes were further studied (Table 2, Supporting information Table S3). Among the 60 genes, several are directly related to insulin signalling, including the lower expressed genes *Anp32a,*

Esr1, Ehd2, Tnk2 (also known as *Ack1*), *Pbrm1, Jak3* and *Hk1*, and the higher expressed genes *Map2k1*, *Meg3* and *Mapk1* (Fig. 4A and in bold in Table 2). Functional interpretation based on their direction of expression is consistently linked to a decreased activity of AKT [27-36], implicating a downregulation of insulin signalling (Fig. 4A). For technical validation, *Anp32a, Ehd2, Tnk2*, *Map2k1 and Mapk1* plus *Glut4* were selected and examined using qRT-PCR. All these genes, except *Ehd2*, were significantly or tended to be regulated, confirming the microarray data (Fig. 4B). The gene expression of *Mapk1* and *Map2k1* was considerably higher in No-NR. The expression of *Tnk2* and *Anp32a* was more than 2 fold lower in No-NR.

GLUT4 plays a key role in the downstream regulation of insulin signalling in WAT [37]. Since *Glut4* gene expression tended to be lower in No-NR (p=0.07), we analysed GLUT4 protein expression. Using fluorescence microscopy, we observed GLUT4 expression on the adipocytes. The intensity of the GLUT4 staining was markedly reduced in No-NR (Fig. 4C), suggesting lower GLUT4 protein levels.

A

Assignment of genes from Table 2 to net effect on insulin sensitivity

Gene symbol	Fold change	Function	Net effect on insulin sensitivity	Ref-erence
Anp32a	-1.95	Positively regulates AKT phosphorylation	Down	[27]
Esr1	-1.47	Positively regulates AKT phosphorylation and IRS1 activity	Down	[28]
Ehd2	-1.35	Plays a role in insulin-induced GLUT4 recruitment	Down	[29]
Tnk2	-1.35	Activates AKT phosphorylation at tyrosine 176 site	Down	[30]
Pbrm1	-1.34	Activates AKT phosphorylation and glucose uptake	Down	[31]
Jak3	-1.32	Activates AKT phosphorylation	Down	[32]
Hk1	-1.32	Promotes glycolysis and associated with AKT activation	Down	[33]
Mapk1	1.38	Inhibits AKT phosphorylation	Down	[34]
Meg3	1.38	Inhibits phosphorylation of PI3K and AKT	Down	[35]
Map2k1	1.57	Inhibits AKT phosphorylation	Down	[36]

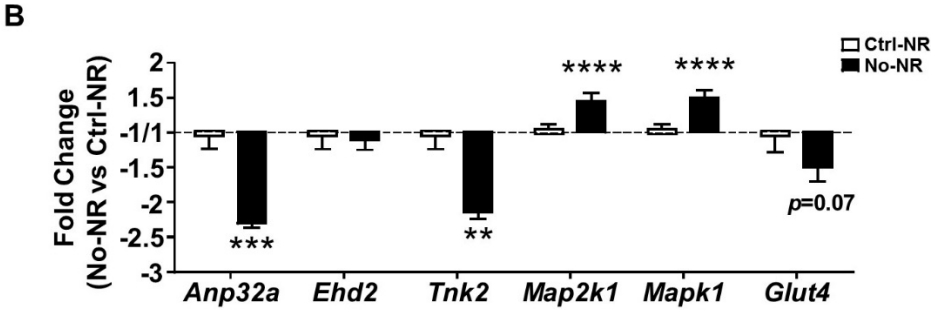

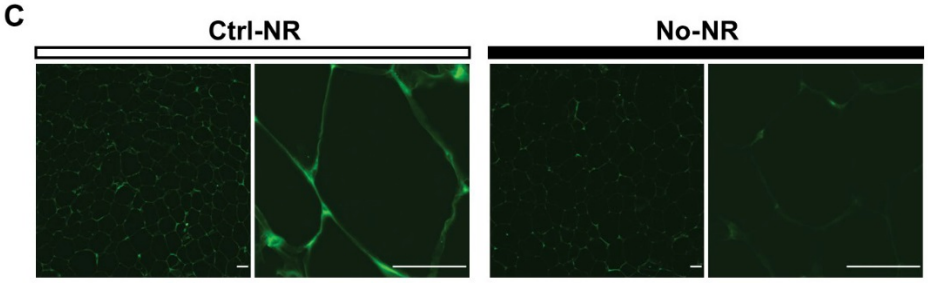

Figure 4. Insulin sensitivity. The net effect on insulin sensitivity of eWAT genes related to insulin signalling (from top regulated genes, Table 2) (A). Validation of insulin signalling related genes using qRT-PCR (B). Gene expression as No-NR over Ctrl-NR (n=11-12). Data as mean±SEM. Analysis with Student's ttest. **p<0.01, ***p<0.005, ****p<0.001. Representative pictures for expression of GLUT4 (C): Ctrl-NR left (10× magnification), right (63×); No-NR left (10× magnification), right (63×). n=6. Scale bar 50µm.

eWAT Mitochondria

Three mitochondrial genes *Mthfs (FC 1.7), Mthfsl (FC 1.45)* and *Qdpr* (FC 1.42) are among the most upregulated genes (Table 2). This was not due to a general upregulation of mitochondrial genes. Examining the 1661 mitochondrial probes in our dataset, derived from mouse MitoCarta 2.0, we found that 74.5% of the probes with FDR<0.5 were downregulated (5.0% for all expressed probes with FDR<0.5). This predominant downregulation was slightly more overt for FDR <0.2 (78,3%, while this was 4.9% for all expressed probes) (Fig. 5A). In the samples selected to represent the average gene expression in the group (Supporting information Fig. S4), OXPHOS proteins were decreased in No-NR, especially proteins representing complex II, III and V (Fig. 5B), confirming the mitochondrial gene expression data.

An enrichment analysis of the FDR<0.5 mitochondrial genes showed that the ubiquinone metabolism pathway was most affected (Fig. 6A). Without exception this pathway consisted of genes encoding for NADH:ubiquinone oxidoreductase subunits that compose mitochondrial OXPHOS Complex I, with the majority of these genes being downregulated (22/24, 91.7%; Fig. 6B). Among the limited number of upregulated mitochondrial genes (FDR<0.5) were 4 key fatty acid oxidation genes *Acsf2, Cpt1a, Etfa* and *Slc25a20* (Fig. 6C). This might indicate an increased fatty acid oxidation, supported by the lower RER of the No-NR group at all time-points over a 24hr-period (Supporting information Fig. S1A).

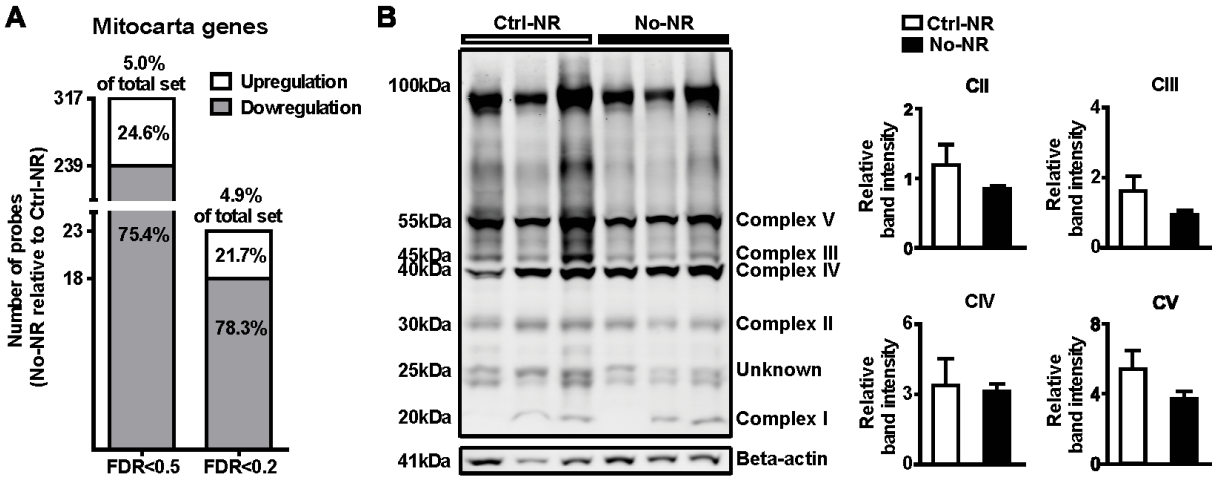

Figure 5. Mitochondrial gene analysis and OXPHOS protein expression. Distribution of down- and up- regulated (No-NR over Ctrl-NR) eWAT mitochondrial genes (n=12) according to Mouse MitoCarta2.0, up/down distribution in FDR<0.5 set and FDR<0.2 set (A). OXPHOS proteins and relative intensity (n=3, mean±SEM) (B).

Implications in tetrahydrobiopterin synthesis in eWAT

The upregulation of the mitochondrial genes *Qdpr*, *Mthfs*, and *Mthfsl* was fully confirmed by qRT-PCR (Fig. 7A). Since the function of QDPR is uniquely in salvaging of tetrahydrobiopteridin (BH4) [38], and *Mthfs* and *Mthfsl* are implicated in the *de novo* BH4 synthesis, the more extensive FDR<0.5 gene list was examined for additional genes directly related to these processes. One gene associated with BH4 salvage, *Mthfd1*, and two genes related to the *de novo* BH4 synthesis, *Sumo2* and *Gchfr*, were identified (Fig. 7B). The direction of expression of these 6 genes is consistent with upregulation of BH4 synthesis [38-43] (Fig. 7B).

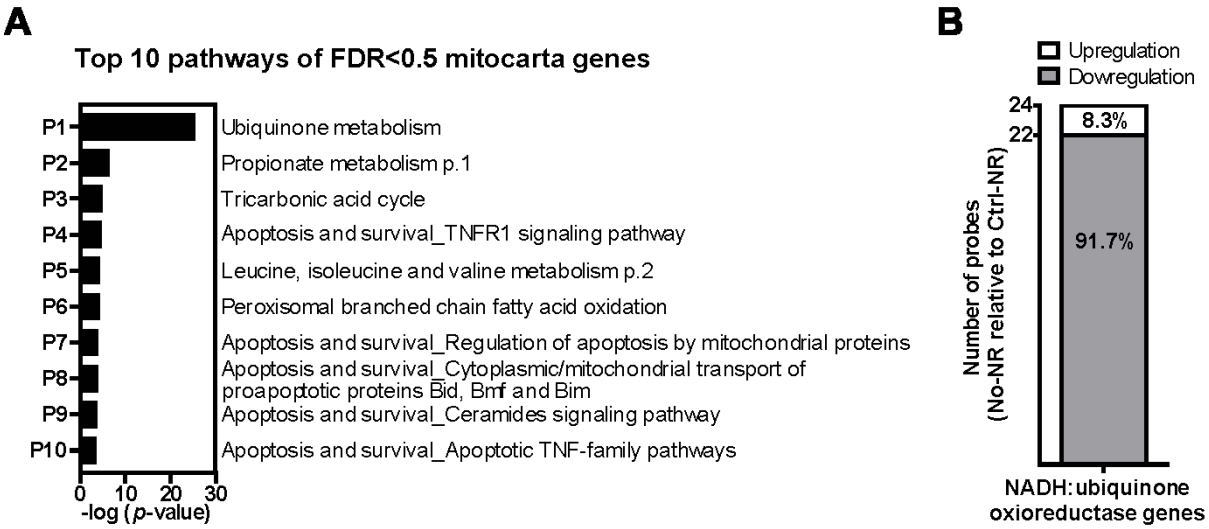

C

Fatty acid oxidation genes (FDR<0.5, No-NR relative to Ctrl-NR)

Gene symbol	FDR	Fold change	Function
Etfa	0.35	1.28	Transfers the electrons to the main mitochondrial respiratory chain for fatty acid oxidation
Acsf2	0.19	1.21	Catalyzes the initial reaction in fatty acid metabolism
Cpt1a	0.43	1.20	Mediates mitochondrial uptake of long-chain fatty acids and their subsequent beta-oxidation
Slc25a20	0.47	1.17	Transports acylcarnitines into mitochondrial matrix for fatty acid oxidation

Figure 6. Enrichment analysis of mitochondrial genes. Pathway maps analysis of FDR<0.5 mitochondrial genes (A). Distribution of up/down regulated genes in the top 1 pathway ubiquinone metabolism (B). Fatty acid oxidation genes (C). n=12. Gene names and systemic names are in Supporting information Table S4.

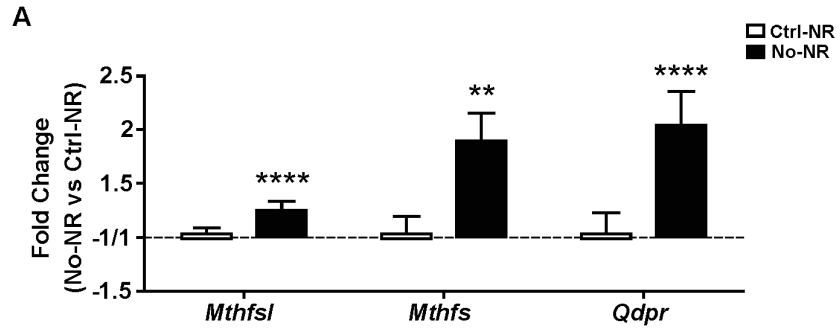

B

Assignment of genes from FDR<0.5 to net effect on BH4 synthesis (No-NR relative to Ctrl-NR)

Gene symbol	Fold change	FDR	Function	Net effect on BH4 synthesis	Reference
Mthfsl	1.70	0.14	Similarity with MTHFS function is indicated	Up	n. a.
Mthfs	1.45	0.17	Involves folinic acid-induced BH4 salvage synthesis via 5-MTHF; or enhances yield of GTP, a *de novo* precursor of BH4, via promoting *de novo* purine synthesis	Up	[40,43]
Qdpr	1.42	0.14	Mediates BH4 salvage synthesis	Up	[38,40]
Sumo2	1.40	0.13	MTHFS-induced *de novo* purine synthesis requires SUMO	Up	[39]
Mthfd1	1.16	0.34	Together with MTHFS, involving folinic acid-induced BH4 salvage synthesis	Up	[40]
Gchfr	-1.38	0.40	Negatively regulates *de novo* BH4 synthesis from GTP by inhibiting GCH1 activity	Up	[41,42]

Figure 7. Tetrahydropteridin (BH4) biosynthesis. Validation of expression of selected genes in eWAT using qRT-PCR (A). Relevant genes were assigned according to their net effect on BH4 synthesis (B). Gene expression as fold change of No-NR over Ctrl-NR. Data as mean±SEM. Analysis with Student's t test. ** p<0.01, **** p<0.001. n=11-12.

Discussion

Here, we observed a decreased insulin sensitivity in mice fed a vitamin B3 withdrawal diet. Since WAT was shown to be sensitive to vitamin B3 status [19, 20], we identified the molecular responses to vitamin B3 withdrawal in eWAT. The transcriptome data indicated a differential regulation of a set of genes involved in insulin signalling and lowering of markers of glucose utilization. Furthermore, biosynthesis of BH4, an essential cofactor for neurotransmitter synthesis, was found to be transcriptionally activated. A set of significant and strongly regulated genes related to these processes were technically validated and could serve as a WAT transcriptional signature marker for mild vitamin B3 deficiency. This signature is composed of downregulation of *Anp32a,Tnk2* and the upregulation of *Mapk1*, *Map2k1*, *Qdpr*, *Mthfs*, and *Mthfsl*.

To impose a vitamin B3 insufficiency stress, we provided male C57Bl/6JRccHsd mice with a diet without vitamin B3 and a low, but sufficient, amount of Trp to limit the rate of *de novo* NAD^+ synthesis. The latter is essential to be able to observe effects of vitamin B3 withdrawal [12, 13]. Due to cellular use of NAD^+, which has a high turnover rate [3], and urinary secretion of NAD^+ breakdown metabolites, this diet should gradually lead to vitamin B3 insufficiency. After the 18 week intervention, no differences were seen between the No-NR group and the Ctrl-NR group in body weight, lean mass, fat mass, EE, WAT weight, adipocyte size, WAT inflammation, or a range of circulating markers, including circulating serotonin levels, supporting the notion that the animals only have no or only a marginal vitamin B3 deficiency. Nevertheless, applying whole-genome transcriptome analysis, qRT-PCR and physiological analyses to eWAT, we were able to establish differential regulation of insulin signalling. A lowering in markers of glucose utilization and an increase in makers of fatty acid catabolism, implicate a shift from glucose to lipids for energy supply, which may be related to the consistent reduction of the expression of the mitochondrial electron transport complexes. Finally, we observed transcriptional activation of the synthesis pathway of BH4, an essential cofactor for neurotransmitter synthesis.

The mild vitamin B3 deficiency resulted in a decreased insulin sensitivity. The underlying mechanisms were molecularly traceable in WAT. The top 10 GO processes center on the regulation of intracellular transport and localization (Fig. 3B), which play an important role in insulin signal transduction and especially in downstream glucose transporter trafficking [44]. The downregulation of most of the genes involved in these GO processes potentially implicate a down regulation of insulin signalling in the No-NR group (Fig. 3C). This is supported by decrease in the activation state of AKT, a key node in growth factor/insulin mediated glucose uptake [45] (Fig. 4A). GLUT4, the major glucose transporter in adipocytes, was lower expressed in No-NR (Fig. 4C). GLUT4 is responsible for insulin-stimulated glucose uptake, and lower expression of GLUT4 is associated with local as well as systemic insulin sensitivity [46]. The transcriptional activation of MEK/ERK may be implicated in a down regulation of insulin signalling as well. MEK/ERK activation was shown to decrease insulin-stimulated glucose uptake, concomitant with the downregulation of *Glut4* and the reduced glucose oxidation in adipocytes [47, 48].

The upregulation of *Map2k1* (*Mek1*) and *Mapk1* (*Erk2*) indicate MEK/ERK activation. In agreement, *Eif2a* and *Gcm1*, targets of activated MEK/ERK [34, 49], were also upregulated (Table 2). *Map2k2* (*Mek2*) was transcriptionally decreased, which might be due to the feedback regulation of an activated MEK/ERK pathway [50]. We also technically validated the 2-fold downregulation of *Anp32a (Pp32)*, which is the most responsive gene in the dataset. Its downregulation is in line with MEK/ERK activation, since silencing of *Anp32a* has been shown to induce MEK/ERK activation [51]. Of note, all of the top 10 pathway maps and 9 of the top 10 GO processes contain *Mapk1* and *Map2k1*, validating these genes as the core of the transcriptional signature of vitamin B3 deficiency in eWAT.

Concomitant with decreased levels of GLUT4, the gene expression of hexokinase 1 (HK1), that controls the initial rate-limiting step of glycolysis, is downregulated, indicating that glucose utilization is inhibited in WAT of the No-NR animals. Meanwhile, key mitochondrial FAO genes were upregulated (Fig. 6C), contrasting with the downregulation of glycolysis and overall downregulation of mitochondrial genes (Fig. 5A). This suggests a shift from CHO to FAO in the No-NR animals, supported by a reduced ability to switch from FAO to CHO (from a fasted RER of 0.7 to a refed RER approaching 1.0; Fig. 1E), and the 24hr-RER being lower at all time-points in No-NR (Supporting information Fig. S1A), confirming previously published data [19]. This may be explained by the lower requirement for NAD^+ of FAO, compared to aerobic CHO, to produce the same amount of ATP. Supporting this explanation, the RER was distinctly decreased upon the transition to a high fat diet in WAT-specific *Nampt* knockout mice displaying WAT NAD^+ deficiency [14], suggesting a clear preference of FAO compared to control. In WAT of No-NR animals, we also observed a preferred downregulation of the mitochondrial Complex I genes (Fig. 6B) and reduced expression of most of OXPHOS proteins (Fig. 5B), coinciding with the putatively inhibited glucose utilization. OXPHOS Complex I accepts electrons from NADH, possibly implicating that the downregulation serves to liberate NAD^+ for other cellular functions. Indeed, NAD^+ biosynthesis or other consumer genes were absent from FDR<0.2 gene set (data not shown). This implication agrees with findings in kidney-derived cancer cells with an inherent Complex I defect, which show a 2-fold higher NAD^+ level compared to normal kidney tissue [52]. Furthermore, in bovine primary chondrocytes, the use of the complex I inhibitor rotenone leads to a more than 80% drop in intracellular NADH, concomitant with an approximate 60% increase in NAD^+ [53]. The lower levels of GLUT4, of *Hk1* expression and of mitochondrial Complex I gene expression, and the increased FAO genes molecularly support a bioenergetic shift to liberate NAD^+ for other processes, providing a possible mechanistic explanation for the reduced metabolic flexibility of the mice on the vitamin B3 withdrawal diet.

An intriguing finding of this study was the upregulation of *Qdpr*, *Mthfs*, and *Mthfsl* (Fig. 7A), which sharply contrasts with the downregulation that was observed for the majority of mitochondrial genes (Fig. 5A). *Mthfs* and *Qdpr* have an established role in pteridine metabolism. *Mthfs encodes* 5-formyltetrahydrofolate cyclo-ligase (MTHFS) that irreversibly catalyses the conversion of 5-formyltetrahydrofolate, also known as folinic acid, to 5,10-methenyltetrahydrofolate [39]. *Qdpr* encodes quinoid

dihydropteridine reductase (QDPR) with a unique function in the salvage synthesis of BH4 from dihydrobiopterin (BH2) [38]. The concurrent elevation of *Mthfs* and *Qdpr*, and possibly also structurally related *Mthfsl,* may indicate an enhanced interconnection between folate metabolism and BH4 salvage synthesis. In the brain, MTHFS, QDPR and MTHFD1 have been proposed to cooperate in support of the BH4 pool as a favourable pathway to bypass the "methyl trap" [40]. Downregulated *Gchfr* [41, 42] and upregulated *Mthfs* [43] and *Sumo2* [39] support an increased *de novo* BH4 biosynthesis (Fig. 7B). It has been shown that stimulation of this pathway by folinic acid or folic acid is effective as treatment of genetic defects of QDPR, that display abnormal low BH4 levels [38, 40]. The observed gene expression changes are in line with a published metabolomics analysis of *in vitro* NAMPT silencing that showed an enhanced folate metabolism and *de novo* purine synthesis [54], that may potentiate BH4 biosynthesis. NAD^+ and its reduced form NADH are essential cofactors of pteridine metabolic enzymes [40], but how exactly intracellular NAD^+ and NADH levels, and their ratios, regulate those enzymes is not known.

Neural signals have an important role in the regulation of the WAT metabolic function [55, 56]. In the current study, the No-NR mice displayed an upregulation of *Dcc*, *Gcm1*, *Ermn*, *Pnma2* and *Tmem123* (Table 2), genes with a proven role in neuronal cell survival and maturation [57-61], possibly indicating an effect on WAT innervation. BH4 serves as an essential cofactor for tryptophan hydroxylase (TPH), phenylalanine hydroxylase, tyrosine hydroxylase as well as nitric oxide synthases. BH4 thus plays a vital role in the generation of neurotransmitters, such as serotonin, dopamine and nitric oxide. It is tempting to speculate that the upregulation of BH4 synthesis serves to support the neuronal regulation of WAT metabolic function. To fully establish why increased BH4 synthesis occurs following vitamin B3 withdrawal and how this affects WAT metabolism awaits more detailed dedicated experimentation.

In conclusion, the current study showed an impaired insulin sensitivity in mice with mild vitamin B3 deficiency. Molecularly examined in WAT, the underlying metabolism is putatively associated with MEK/ERK activation and liberation of NAD^+ from oxidative glucose metabolism to other NAD^+ dependent cellular functions. Our data also implicate a possible increase in BH4 synthesis, which is an essential cofactor in neurotransmitter biosynthesis. We propose the expression of seven technically validated FDR<0.2 genes related to these processes, the downregulation of *Anp32a,Tnk2* and the upregulation of *Mapk1, Map2k1, Qdpr*, *Mthfs*, and *Mthfsl*, as a WAT transcriptional signature marker for mild vitamin B3 deficiency.

Acknowledgements

We thank ChromaDex for the generous and kind supply of nicotinamide riboside. We thank our colleagues at Human and Animal Physiology and the animal facility for their help. We thank Ruth Van Heerbeek for practical contributions. Financial support by the Chinese Scholarship Council (grant# 201303250054) is gratefully acknowledged.

References

[1] Rajman, L., Chwalek, K., Sinclair, D. A., Therapeutic potential of NAD-boosting molecules: the in vivo evidence. *Cell Metab.* 2018, *27*, 529-547.
[2] Ying, W., NAD+/NADH and NADP+/NADPH in cellular functions and cell death: regulation and biological consequences. *Antioxid. Redox Signal.* 2008, *10*, 179-206.
[3] Liu, L., Su, X., Quinn, W. J., 3rd, Hui, S., *et al.*, Quantitative analysis of NAD synthesis-breakdown fluxes. *Cell Metab.* 2018, *27*, 1067-1080 e1065.
[4] Wan, P., Moat, S., Anstey, A., Pellagra: a review with emphasis on photosensitivity. *Br. J. Dermatol.* 2011, *164*, 1188-1200.
[5] Rawling, J. M., Jackson, T. M., Driscoll, E. R., Kirkland, J. B., Dietary niacin deficiency lowers tissue poly(ADP-ribose) and NAD+ concentrations in Fischer-344 rats. *J. Nutr.* 1994, *124*, 1597-1603.
[6] Rawling, J. M., Jackson, T. M., Roebuck, B. D., Poirier, G. G., Kirkland, J. B., The effect of niacin deficiency on diethylnitrosamine-induced hepatic poly(ADP-ribose) levels and altered hepatic foci in the Fischer-344 rat. *Nutr. Cancer* 1995, *24*, 111-119.
[7] Horwitt, M. K., Harper, A. E., Henderson, L. M., Niacin-tryptophan relationships for evaluating niacin equivalents. *Am. J. Clin. Nutr.* 1981, *34*, 423-427.
[8] Kirkland, J. B., in: Zempleni, J., Suttie, J. W., Gregory III, J. F., Stover, P. J. (Eds.), *Handbook of vitamins*, CRC Press, Boca Raton 2013, p. 42.
[9] Bender, D. A., *Nutritional biochemistry of the vitamins*, Cambridge university press, London 2003.
[10] National Research Council (NRC), *Nutrient Requirements of Laboratory Animals, Fourth Revised Edition*, National Academies Press, Washington DC 1995.
[11] Fox, J. G., Barthold, S., Davisson, M., Newcomer, C. E., *et al.*, *The Mouse in biomedical research: diseases*, Academic Press, Salt Lake City UT 2006.
[12] Terakata, M., Fukuwatari, T., Kadota, E., Sano, M., *et al.*, The niacin required for optimum growth can be synthesized from L-tryptophan in growing mice lacking tryptophan-2,3-dioxygenase. *J. Nutr.* 2013, *143*, 1046-1051.
[13] Terakata, M., Fukuwatari, T., Sano, M., Nakao, N., *et al.*, Establishment of True Niacin Deficiency in Quinolinic Acid Phosphoribosyltransferase Knockout Mice–3. *J. Nutr.* 2012, *142*, 2148-2153.
[14] Nielsen, K. N., Peics, J., Ma, T., Karavaeva, I., *et al.*, NAMPT-mediated NAD(+) biosynthesis is indispensable for adipose tissue plasticity and development of obesity. *Mol. Metab.* 2018, *11*, 178-188.
[15] Frederick, D. W., Loro, E., Liu, L., Davila, A., Jr., *et al.*, Loss of NAD Homeostasis Leads to Progressive and Reversible Degeneration of Skeletal Muscle. *Cell Metab.* 2016, *24*, 269-282.
[16] Camacho-Pereira, J., Tarrago, M. G., Chini, C. C. S., Nin, V., *et al.*, CD38 Dictates Age-Related NAD Decline and Mitochondrial Dysfunction through an SIRT3-Dependent Mechanism. *Cell Metab.* 2016, *23*, 1127-1139.
[17] Yamamoto, H., Uchigata, Y., Okamoto, H., Streptozotocin and alloxan induce DNA strand breaks and poly (ADP–ribose) synthetase in pancreatic islets. *Nature* 1981, *294*, 284.
[18] Bieganowski, P., Brenner, C., Discoveries of nicotinamide riboside as a nutrient and conserved NRK genes establish a Preiss-Handler independent route to NAD(+) in fungi and humans. *Cell* 2004, *117*, 495-502.
[19] Shi, W., Hegeman, M. A., van Dartel, D. A. M., Tang, J., *et al.*, Effects of a wide range of dietary nicotinamide riboside (NR) concentrations on metabolic flexibility and white adipose tissue (WAT) of mice fed a mildly obesogenic diet. *Mol. Nutr. Food Res.* 2017, *61*, 1600878.
[20] Yoshino, J., Mills, K. F., Yoon, M. J., Imai, S., Nicotinamide mononucleotide, a key NAD(+) intermediate, treats the pathophysiology of diet- and age-induced diabetes in mice. *Cell Metab.* 2011, *14*, 528-536.
[21] Liu, S., Kim, T.-H., Franklin, D. A., Zhang, Y., Protection against High-Fat-Diet-Induced Obesity in MDM2C305F Mice Due to Reduced p53 Activity and Enhanced Energy Expenditure. *Cell Rep.* 2017, *18*, 1005-1018.
[22] Duivenvoorde, L. P., van Schothorst, E. M., Swarts, H. M., Kuda, O., *et al.*, A difference in fatty acid composition of isocaloric high-fat diets alters metabolic flexibility in male C57BL/6JOlaHsd mice. *PLoS One* 2015, *10*, e0128515.

[23] Hoevenaars, F. P., Bekkenkamp-Grovenstein, M., Janssen, R. J., Heil, S. G., *et al.*, Thermoneutrality results in prominent diet-induced body weight differences in C57BL/6J mice, not paralleled by diet-induced metabolic differences. *Mol. Nutr. Food Res.* 2014, *58*, 799-807.
[24] van Schothorst, E. M., Pagmantidis, V., de Boer, V. C. J., Hesketh, J., Keijer, J., Assessment of reducing RNA input for Agilent oligo microarrays. *Anal. Biochem.* 2007, *363*, 315-317.
[25] Storlien, L., Oakes, N., Kelley, D., Adipose tissue-liver-muscle interactions leading to insulin resistance. *Proc. Nutr. Soc* 2004, *63*, 363-368.
[26] Sparks, L. M., Ukropcova, B., Smith, J., Pasarica, M., *et al.*, Relation of adipose tissue to metabolic flexibility. *Diabetes research and clinical practice* 2009, *83*, 32-43.
[27] Yan, W., Bai, Z., Wang, J., Li, X., *et al.*, ANP32A modulates cell growth by regulating p38 and Akt activity in colorectal cancer. *Oncol. Rep.* 2017, *38*, 1605-1612.
[28] Ribas, V., Nguyen, M. A., Henstridge, D. C., Nguyen, A.-K., *et al.*, Impaired oxidative metabolism and inflammation are associated with insulin resistance in ERα-deficient mice. *Am. J. Physiol. Endocrinol. Metabol.* 2009, *298*, E304-E319.
[29] Park, S. Y., Ha, B. G., Choi, G. H., Ryu, J., *et al.*, EHD2 interacts with the insulin-responsive glucose transporter (GLUT4) in rat adipocytes and may participate in insulin-induced GLUT4 recruitment. *Biochemistry* 2004, *43*, 7552-7562.
[30] Mahajan, K., Coppola, D., Challa, S., Fang, B., *et al.*, Ack1 mediated AKT/PKB tyrosine 176 phosphorylation regulates its activation. *PLoS One* 2010, *5*, e9646.
[31] Chowdhury, B., Porter, E. G., Stewart, J. C., Ferreira, C. R., *et al.*, PBRM1 Regulates the Expression of Genes Involved in Metabolism and Cell Adhesion in Renal Clear Cell Carcinoma. *PLoS One* 2016, *11*, e0153718.
[32] Wang, H., Brown, J., Gao, S., Liang, S., *et al.*, The role of JAK-3 in regulating TLR-mediated inflammatory cytokine production in innate immune cells. *J. Immunol.* 2013, *191*, 1164-1174.
[33] Gottlob, K., Majewski, N., Kennedy, S., Kandel, E., *et al.*, Inhibition of early apoptotic events by Akt/PKB is dependent on the first committed step of glycolysis and mitochondrial hexokinase. *Genes Dev.* 2001, *15*, 1406-1418.
[34] Shin, S., Buel, G. R., Wolgamott, L., Plas, D. R., *et al.*, ERK2 Mediates Metabolic Stress Response to Regulate Cell Fate. *Mol. Cell* 2015, *59*, 382-398.
[35] Zhu, X., Wu, Y. B., Zhou, J., Kang, D. M., Upregulation of lncRNA MEG3 promotes hepatic insulin resistance via increasing FoxO1 expression. *Biochem. Biophys. Res. Commun.* 2016, *469*, 319-325.
[36] Fujishiro, M., Gotoh, Y., Katagiri, H., Sakoda, H., *et al.*, Three mitogen-activated protein kinases inhibit insulin signaling by different mechanisms in 3T3-L1 adipocytes. *Mol. Endocrinol.* 2003, *17*, 487-497.
[37] Scherer, P. E., Adipose tissue: from lipid storage compartment to endocrine organ. *Diabetes* 2006, *55*, 1537-1545.
[38] Ponzone, A., Spada, M., Ferraris, S., Dianzani, I., de Sanctis, L., Dihydropteridine reductase deficiency in man: from biology to treatment. *Med. Res. Rev.* 2004, *24*, 127-150.
[39] Field, M. S., Anderson, D. D., Stover, P. J., Mthfs is an essential gene in mice and a component of the purinosome. *Front Genet.* 2011, *2*, 36.
[40] Kaufman, S., Some metabolic relationships between biopterin and folate: implications for the "methyl trap hypothesis". *Neurochem. Res.* 1991, *16*, 1031-1036.
[41] Richardson, M. A., Read, L. L., Taylor Clelland, C. L., Reilly, M. A., *et al.*, Evidence for a tetrahydrobiopterin deficit in schizophrenia. *Neuropsychobiology* 2005, *52*, 190-201.
[42] Xie, L., Smith, J. A., Gross, S. S., GTP cyclohydrolase I inhibition by the prototypic inhibitor 2, 4-diamino-6-hydroxypyrimidine. Mechanisms and unanticipated role of GTP cyclohydrolase I feedback regulatory protein. *J. Biol. Chem.* 1998, *273*, 21091-21098.
[43] Field, M. S., Szebenyi, D. M., Stover, P. J., Regulation of de novo purine biosynthesis by methenyltetrahydrofolate synthetase in neuroblastoma. *J. Biol. Chem.* 2006, *281*, 4215-4221.
[44] Foster, L. J., Li, D., Randhawa, V. K., Klip, A., Insulin accelerates inter-endosomal GLUT4 traffic via phosphatidylinositol 3-kinase and protein kinase B. *J. Biol. Chem.* 2001, *276*, 44212-44221.
[45] Taniguchi, C. M., Emanuelli, B., Kahn, C. R., Critical nodes in signalling pathways: insights into insulin action. *Nat. Rev. Mol. Cell Biol.* 2006, *7*, 85-96.

[46] Carlson, C. J., Koterski, S., Sciotti, R. J., Poccard, G. B., Rondinone, C. M., Enhanced basal activation of mitogen-activated protein kinases in adipocytes from type 2 diabetes: potential role of p38 in the downregulation of GLUT4 expression. *Diabetes* 2003, *52*, 634-641.
[47] Brown, J. M., Boysen, M. S., Chung, S., Fabiyi, O.*, et al.*, Conjugated linoleic acid induces human adipocyte delipidation: autocrine/paracrine regulation of MEK/ERK signaling by adipocytokines. *J. Biol. Chem.* 2004, *279*, 26735-26747.
[48] Liu, L., Zhou, M., Lang, H., Zhou, Y., Mi, M., Dihydromyricetin enhances glucose uptake by inhibition of MEK/ERK pathway and consequent down-regulation of phosphorylation of PPARγ in 3T3-L1 cells. *J. Cell. Mol. Med.* 2018, *22*, 1247-1256.
[49] Nadeau, V., Charron, J., Essential role of the ERK/MAPK pathway in blood-placental barrier formation. *Development* 2014, dev. 107409.
[50] Hong, S.-K., Wu, P.-K., Karkhanis, M., Park, J.-I., ERK1/2 can feedback-regulate cellular MEK1/2 levels. *Cell. Signal.* 2015, *27*, 1939-1948.
[51] Fukukawa, C., Tanuma, N., Okada, T., Kikuchi, K., Shima, H., pp32/I-1PP2A negatively regulates the Raf-1/MEK/ERK pathway. *Cancer Lett.* 2005, *226*, 155-160.
[52] Kurschner, G., Zhang, Q., Clima, R., Xiao, Y.*, et al.*, Renal oncocytoma characterized by the defective complex I of the respiratory chain boosts the synthesis of the ROS scavenger glutathione. *Oncotarget* 2017, *8*, 105882-105904.
[53] Martin, J. A., Martini, A., Molinari, A., Morgan, W.*, et al.*, Mitochondrial electron transport and glycolysis are coupled in articular cartilage. *Osteoarthritis Cartilage* 2012, *20*, 323-329.
[54] Singh, R. K., van Haandel, L., Heruth, D. P., Ye, S. Q.*, et al.*, Nicotinamide Phosphoribosyltransferase Deficiency Potentiates the Antiproliferative Activity of Methotrexate through Enhanced Depletion of Intracellular ATP. *J. Pharmacol. Exp. Ther.* 2018, *365*, 96-106.
[55] Jiang, H., Ding, X., Cao, Y., Wang, H., Zeng, W., Dense intra-adipose sympathetic arborizations are essential for cold-induced beiging of mouse white adipose tissue. *Cell Metab.* 2017, *26*, 686-692. e683.
[56] Bartness, T. J., Shrestha, Y. B., Vaughan, C. H., Schwartz, G. J., Song, C. K., Sensory and sympathetic nervous system control of white adipose tissue lipolysis. *Mol. Cell. Endocrinol.* 2010, *318*, 34-43.
[57] Shi, M., Zheng, M. H., Liu, Z. R., Hu, Z. L.*, et al.*, DCC is specifically required for the survival of retinal ganglion and displaced amacrine cells in the developing mouse retina. *Dev. Biol.* 2010, *348*, 87-96.
[58] Takekoshi, T., Tada, Y., Watanabe, T., Sugaya, M.*, et al.*, Identification of a novel marker for dendritic cell maturation, mouse transmembrane protein 123. *J. Biol. Chem.* 2010, *285*, 31876-31884.
[59] Altshuller, Y., Copeland, N. G., Gilbert, D. J., Jenkins, N. A., Frohman, M. A., Gcm1, a mammalian homolog of Drosophila glial cells missing. *FEBS Lett.* 1996, *393*, 201-204.
[60] Brockschnieder, D., Sabanay, H., Riethmacher, D., Peles, E., Ermin, a myelinating oligodendrocyte-specific protein that regulates cell morphology. *J. Neurosci.* 2006, *26*, 757-762.
[61] Stich, O., Jarius, S., Kleer, B., Rasiah, C.*, et al.*, Specific antibody index in cerebrospinal fluid from patients with central and peripheral paraneoplastic neurological syndromes. *J. Neuroimmunol.* 2007, *183*, 220-224.

Supporting information methods

Body parameters and sample collection

Body weight and feed intake as well as lean and fat mass (by NMR, EchoMRI, Houston, USA) were measured weekly. Mice were provided with a limited amount of diet (with 0.8 gram of fresh experimental diet) at start of dark phase to have them fasted at end of dark phase; they were subsequently refed at start of light phase with 1.8 gram of diet for four hours and then sacrificed by decapitation. Blood glucose was measured using a Freestyle blood glucose meter (Abbott Diabetes Care, Hoofddorp, The Netherlands), after which serum was obtained by centrifugation at

3,000*g*, 4°C for 10 minutes. Serum was stored at -80°C. Right epididymal white adipose tissue (eWAT) was rapidly harvested, snap frozen and stored at -80°C. Left eWAT was weighted, divided in half and fixed for 24 hours at 4°C in PBS with 4.0% paraformaldehyde (pH=7.40) as described [1].

Oral glucose tolerance test

An oral glucose tolerance test (OGTT) was performed in week 17, as described [2]. Briefly, mice were weighed, and food was withdrawn for 6 hours, after which a small piece of the distal end of the tail was removed for blood collection. Blood glucose was measured using a Freestyle blood glucose meter (Abbott Diabetes Care, Hoofddorp, The Netherlands) as t=0 timepoint. Then the mice were orally administrated with 2 gram glucose/kg body weight. Blood glucose was measured at 15, 30, 60, 90 and 120 minutes after oral glucose gavage. At t=0, 15 and 30, 20 ul of blood was collected using Microvette CB 300 tubes (Sarstedt, Etten-Leur, The Netherlands), followed by 20-minute centrifugation at 2000*g*, 4°C to retrieve plasma for insulin determination.

Circulating parameters

Serum total cholesterol (TC), triglycerides (TG), non-esterified fatty acids (NEFA) and HDL cholesterol were measured using liquicolor enzymatic colorimetric tests (Instruchemie, Delfzijl, The Netherlands), as described [3]. LDL cholesterol concentrations were calculated according to the modified Friedewald formula (LDL cholesterol=total cholesterol - HDL cholesterol - triglycerides×0.16, for rodents) [4]. Leptin was measured with a Bio-Plex Pro Mouse Diabetes Assay using a Bio-Plex 200 system (Bio-Rad, Veenendaal, The Netherlands), as published [5]. Serum was diluted 1:10000 in assay buffer and adiponectin was measured using the mouse adiponectin ELISA kit according to instructions (Crystal Chem, Downers Grove, USA). Serum was diluted 1:32 in assay buffer and serotonin was measured using the serotonin ELISA kit according to instructions (Abcam, Boston, MA, the USA). Plasma insulin was measured using the mouse insulin ELISA kit according to instructions (Crystal Chem, Downers Grove, USA). To assess insulin sensitivity, HOMA-IR was calculated as (fasting glucose in mmol/L × fasting insulin in mU/L)/14.1 [6].

eWAT morphology

Adipocyte cell size determination and counting as well as macrophage staining and counting were performed as described,[1] with minor modifications. Briefly, tissue was fixed, washed in PBS, embedded in paraffin and sectioned at 5 µm using an automated microtome (Microm GmbH, Heidelberg, Germany). Sections after each 20 sequential cuts were used to ensure that no repetitive adipocytes were present. Tissue sections were deparaffinised, rehydrated and then stained with Mayer's haematoxylin for 75 seconds (Klinipath BV, Duiven, The Netherlands) and with 0.1% eosin for 15 seconds (Brunswig, Southborough, MA, USA). Subsequently, sections were dehydrated, mounted and then dried overnight at 37˚C. Representative pictures were photographed using a Leica DM6B microscope (Leica Microsystems, Wetzlar, Germany). Adipocyte size was measured using CellProfiler software v2.1.1 (The Carpenter Lab, Massachusetts, USA) and expressed in surface area (µm^2) per adipocyte. The frequency distribution of adipocyte size was calculated as described [5]. Briefly, adipocyte surface area were positioned in 100 µm^2 bins in Excel and

subsequently grouped in three defined fractions: small (100-1500 μm^2), medium (>1500-6000 μm^2), and large (>6000 μm^2). Values less than 100 μm^2 were excluded. Macrophages were stained using anti-MAC-2 antibody from Cedarlane (Ontario, Canada). Single macrophages and crown-like structures (CLSs) from 1000 adipocytes per animal were counted, and expressed as macrophages or CLSs per gram eWAT weight.

Immunohistochemistry

Paraffin-embedded tissue was sectioned at 5 μm using an automated microtome (Microm GmbH, Heidelberg, Germany), selected and prepared as reported [5]. Sections were blocked using 5% normal goat serum in PBS-BSAc (S-1000, Vector Laboratories, CA, USA) for 1 hour at RT, and then incubated overnight with anti-GLUT4 antibody (Abcam, Cambridge, MA, USA, 1:500 in PBS-BSAc) or rabbit IgG antibody at 4°C with gentle shaking. Sections were washed 6 times with PBS and then incubated with Alexa Fluor 488 anti-rabbit antibody (Life technologies, Carlsbad, CA, USA, 1:200 in PBS-BSAc) for 1 hour at RT. Sections were subsequently mounted and kept at 4°C overnight in the dark. Representative pictures (n=7-10 pictures per animal, 6 animals per treatment) were made using a confocal microscope (Zeiss Axiovert 100M, Munich, Germany; argon ion laser 488 nm, Sliedrecht, the Netherlands). Staining and microscopy were performed at the same time for Ctrl-NR and No-NR, with identical settings.

Westernblot

To confirm the mitochondrial downregulation on the protein level, we determined the levels of OXPHOS proteins as mitochondrial markers. We took three samples per treatment, with same mean gene expression of *Ndufb8* as the whole group (Supporting information Fig. S4).

eWAT protein was extracted from frozen tissue by homogenization in ice-cold lysis buffer [7], including complete protease inhibitor cocktail (Roche, Mannheim, Germany), followed by 18 times sonication (amplitude 40, duty cycle 40, output control 1). The lysate was centrifuged at 18,620*g*, 4°C for 15 minutes, supernatant was retrieved and the centrifugation step was repeated. The protein concentration was measured using DC protein assay (Bio-Rad).

For immunoblotting, sample was mixed with LDS loading buffer and dithiothreitol, and incubated at 37°C for 10 minutes. 15 μg protein per sample was run on a 4-12% Bis-Tris gel (Invitrogen, Carlsbad, CA, USA), after which the protein was transferred to an Immobilon PVDF membrane (Merck Millipore, Amsterdam, the Netherlands) at 300mA for 1 hour. The membrane was blocked with 3% BSA in TBS containing 0.1% Tween-20 at RT for 1 hr and then incubated overnight at 4°C with oxidative phosphorylation (OXPHOS) antibody cocktail (Abcam, Cambridge, MA, USA) in blocking buffer. After several washes, the membrane was incubated with IRDye-labelled goat anti-mouse antibody (LI-COR, Lincoln, NE, USA) at RT for 1 hour. The membrane was washed and scanned on an Odyssey scanner. For loading control, the membrane was incubated with β-actin antibody (Abcam) and then with donkey anti-rabbit antibody (LI-COR) by following the same procedure. Bands were analysed using Odyssey software V3.0 (LI-COR).

Supporting information Table S1. Composition of diets [a]

Ingredients (g·kg-1 diet)	Adaptation	Ctrl-NR	No-NR
Casein	100.0	100.0	100.0
Wheat starch	233.1	233.1	233.1
Gelatin (hydrolysed)	100.0	100.0	100.0
Maltodextrin	100.0	100.0	100.0
Sugar	100.0	100.0	100.0
Dextrose	50.0	50.0	50.0
Arbocel B800	50.0	50.0	50.0
Linseed oil	4.0	4.0	4.0
Palm oil	206.0	206.0	206.0
Mineral mixture AIN-93	35.0	35.0	35.0
Vitamin mixture AIN-93 [b]	10.0	10.0	10.0
L-cystine	3.25	3.25	3.25
L-phenylalanine	4.32	4.32	4.32
Choline chloride 50%	1.55	1.55	1.55
Nicotinamide riboside (mg·kg-1 diet)	30.0	30.0	0.0
Calculated amount of L-tryptophan (%)	1.15	1.15	1.15
Calculated energy (kcal·kg-1)	4653	4653	4653
Carbohydrate (% of total energy)	41	41	41
Fat (% of total energy)	40 [c]	40	40
Protein (% of total energy)	19	19	19

[a] Pellet diet (Research Diet Services, Wijk bij Duurstede, The Netherlands)
[b] Contains no vitamin B3 but sufficient minerals and the other vitamins, including iron, vitamin B1, B2 and B6, which are relevant to NAD^+ metabolism [8] at the recommended AIN93 levels [9], in order to exclude metabolic interference.
[c] Corresponding to the average human intake of fat in the Netherlands [10].

Supporting information Table S2. Sequences of primers for qRT-PCR [a]

Gene symbol	**Primer forward 5'-3'**	**Primer reverse 5'-3'**
Anp32a (Pp32)	CCGTGGGTTCGGGGTTTATT	CTCTTTCACATCAGAGGGCGT
B2m	CCCCACTGAGACTGATACATACGC	AGAAACTGGATTTGTAATTAAGCAGGTTC
End2	TCCCCAGATCCCTGGTGAG	CCGGTGAATGGAAAGACCCA
Map2k1 (Mek1)	TGGGCACGAGATCCTACATG	TGGCATCAGGAGGAGGAATG
Mapk1 (Erk2)	ATGACCCAAGTGATGAGCCC	AGCCCTTGTCCTGACCAATTT
Mthfs	GTCTCTCCTCCTCACGCAGA	GGTCAAGTCCACCAGTGGATAA
Mthfsl	CGGTGCTTGCCAGGAATG	GCAATCACCTTCTGCGTGAG
Qdpr	CATTGCTGTGCTCCCCGTTA	TCCTGAGTTTGGCCGTTTGT
Rps15	CGGAGATGGTGGGTAGCATGG	ACGGGTTTGTAGGTGATGGAGAAC
Slc2a4 (Glut4)	CCATTCCCTGGTTCATTGTG	GTTTTGCCCCTCAGTCATTC
Tnk2 (Ack1)	ACTTTGGGCTGATGCGAGCACT	AAGGTGCGTGTCTTCAGGCTCT

[a] All the primers were used with the optimal annealing temperature at 60°C, except for Map2k1 (at 59°C) and Tnk2 (at 62°C). Genes underlined are used as reference genes.

Supporting information Table S3. Top 30 down-and up- regulated unique genes (FDR<0.2) of eWAT.

A. Top 30 down regulated unique genes

Gene symbol	Gene name	Systematic name	Fold change	Function
Anp32a	acidic (leucine-rich) nuclear phosphoprotein 32 family, member A	NM_009672	-1.95	A tumour suppressor, regulating apoptotic processes; inhibition of protein phosphatase 2A and acetyltransferases as part of the INHAT (inhibitor of histone acetyltransferases) complex
Isoc2a	isochorismatase domain containing 2a	NM_001101598	-1.86	Interacts with p16, implicated as histone deacetylase inhibitor
Fmr1nb	fragile X mental retardation 1 neighbor	NM_174993	-1.76	ERK activation
DefB36	defensin beta 36	NM_001037247	-1.72	Innate immune response, differentially regulated by androgens
Pakap	paralemmin A kinase anchor protein	NM_001304544	-1.59	Regulation of cell shape, palm2-akap2 read through (fusion protein)
Ino80d	INO80 complex subunit D	NM_001114609	-1.52	Subunit of the INO80 complex, ATP dependent chromatin remodelling; needed for replication.
Esr1	estrogen receptor 1 (alpha)	NM_007956	-1.47	Mediates membrane-initiated estrogen signalling involving various kinase cascades
Cmtm4	CKLF-like MARVEL transmembrane domain containing 4	NM_153582	-1.46	Regulator of CD274, necessary for lymphocyte proliferation and IL-10 production
Cd151	CD151 antigen	NM_009842	-1.45	Role in cell adhesion, motility and stimulates proliferation; laminin-binding integrin receptor
Nr3c1	nuclear receptor subfamily 3, group C, member 1	NM_008173	-1.45	Glucocorticoid receptor; inhibits tryptophan hydroxylase (and stimulates tryptophan oxygenase)
Dtx1	deltex 1, E3 ubiquitin ligase	NM_008052	-1.44	Regulator of Notch signalling, which inhibits adipogenesis; downregulates mekk1 (map3k1)
Rnd1	Rho family GTPase 1	NM_172612	-1.44	Involves in semaphorin signalling and cytoskeleton organization
Chtf8	CTF8, chromosome transmission fidelity factor 8	NM_145412	-1.43	Positive regulator of replication; complexes with DCC1
Akap11	A kinase (PRKA) anchor protein 11	NM_001164503	-1.41	Encodes the AKAP220 protein; binds and regulates PKA (see pakap) and supresses GSK3B and interacts with cytoskeleton; regulates cell motility
4833439L19Rik	RIKEN cDNA 4833439L19 gene	NM_133797	-1.38	Oxidoreductase activity
Kdsr	3-ketodihydrosphingosine reductase	NM_027534	-1.36	NADPH dependent; role in cell survival
Ehd2	EH-domain containing 2	NM_153068	-1.35	Plays a role in membrane trafficking between the plasma membrane and endosomes; internalization of GLUT4; reduced upon adipocyte shrinkage (in association with CAV1)
Tnk2	tyrosine kinase, non-receptor, 2	NM_016788	-1.35	Activates AKT1 by phosphorylating it on 'Tyr-176';
Arl4d	ADP-ribosylation factor-like 4D	NM_025404	-1.34	Adipogenesis initiation, but hampers adipogenesis progression; glucocorticoid target; small GTP-binding protein; cytoskeleton remodelling
Abca2	ATP-binding cassette, sub-family A (ABC1), member 2	NM_007379	-1.34	Intracellular cholesterol transport
Pbrm1	polybromo 1	NM_001081251	-1.34	Chromatin remodelling; regulates glucose uptake and cholesterol homeostasis, PI3K signalling; cell adhesion; supresses proliferation
Rita1	RBPJ interacting and tubulin associated 1	NM_029096	-1.34	Negative regulator of Notch target genes
Arl6ip5	ADP-ribosylation factor-like 6 interacting protein 5	NM_022992	-1.33	Regulates intracellular concentrations of taurine and glutamate; activates MAPK/ERK/PEA3 cascade; Small GTP-binding protein
Chpf2	chondroitin polymerizing factor 2	NM_133913	-1.33	Golgi stack membrane
Rdx	Radixin	NM_001104617	-1.32	Binds the barbed end of actin filaments to the plasma membrane
Mta1	metastasis associated 1	NM_001346696	-1.32	As a part of the histone-deacetylase multiprotein complex; transcriptional corepressor of Esr1; regulates the stability and function of p53/TP53 by inhibiting its ubiquitination
Cxx1a	CAAX box 1A	NM_024170	-1.32	Role in differentiation from the ectoplacental cone
Cldnd1	claudin domain containing 1	NM_171826	-1.32	Direct RORα target; a survival factor in tumour cells
Jak3	Janus kinase 3	NM_001190830	-1.32	Non-receptor tyrosine kinase; JAK/STAT5 signalling regulates adipogenesis and insulin sensitivity
Hk1	hexokinase 1	NM_001146100	-1.32	Hexose metabolism as a part of carbohydrate metabolism

B. Top 30 up regulated unique genes

Gene symbol	Gene name	Systematic name	Fold change	Function
Mthfsl	5, 10-methenyltetrahydrofolate synthetase-like	NM_001128601	1.70	Possibly helps with the function of MTHFS
Rnu3b1	U3B small nuclear RNA 1	NR_004415	1.66	Possible role in control of the sequence homogenization process of U3B small nuclear RNA
Gm10115	predicted gene 10115	AK081831	1.64	Unknown function
Map2k1	mitogen-activated protein kinase kinase 1	NM_008927	1.57	Protein serine/threonine/tyrosine kinase activity, a key role in MAPK/ERK cascade; also targets PPARγ, by transporting PPARγ out of the nucleus
5330406M23Rik	RIKEN cDNA 5330406M23 gene	AK017236	1.54	Unknown function
Tmem123	transmembrane protein 123	NM_133739	1.52	Implicated in oncotic cell death, characterized by cell swelling, organelle swelling, vacuolization and increased membrane permeability
Dcc	deleted in colorectal carcinoma	NM_007831	1.47	Netrin 1 receptor for axon guidance; neuronal mifration/apoptosis; a tumour suppressor gene
Gmpr2	guanosine monophosphate reductase 2	NM_177992	1.46	Catalyzes the irreversible NADPH-dependent deamination of guanosine 5'-phosphate to inosine 5'-phosphate; modulate cellular differentiation
Mthfs	5, 10-methenyltetrahydrofolate synthetase	NM_026829	1.45	Catalyzes 5-formyltetrahydrofolate to 5,10-methenyltetrahydrofolate, the following product methenyltetrahydrofolate is essential for the yield of tetrahydrobiopterin (BH-4)
Qdpr	quinoid dihydropteridine reductase	NM_024236	1.42	Product of this enzyme, tetrahydrobiopterin (BH-4), is an essential cofactor for phenylalanine, tyrosine, and tryptophan hydroxylases
Gcm1	glial cells missing homolog 1	NM_008103	1.42	Histone deacetylase binding; master regulator of labyrinthine differentiation
Rhox8	reproductive homeobox 8	NM_001004193	1.42	DNA binding
LOC553096	uncharacterized LOC553096	AK047890	1.41	Unknown function
Ermn	ermin, ERM-like protein	NM_029972	1.41	Regulation of cell shape, actin binding, myelinogenesis
Sumo2	small ubiquitin-like modifier 2	NM_133354	1.40	Ubiquitin-like protein
Pnma2	paraneoplastic antigen MA2	NM_175498	1.40	Regulates paraneoplastic antigen MA1; positive regulation of apoptotic process
Gm33195	predicted gene, 33195	XR_382276	1.40	Unknown function
Dynlt3	dynein light chain Tctex-type 3	NM_025975	1.40	Regulates dynein function; motor for retrograde vesicle transport
Trpm1	transient receptor potential cation channel, subfamily M, member 1	NM_001039104	1.39	Calcium channel
B020031M17Rik	RIKEN cDNA B020031M17 gene	NM_001033769	1.39	Unknown function
GaB3	growth factor receptor bound protein 2-associated protein 3	NM_181584	1.39	Macrophage differentiation; role in proliferation suggested
Sumo2	small ubiquitin-like modifier 2	NM_133354	1.39	Ubiquitin-like protein
Eif2a	eukaryotic translation initiation factor 2A	NM_001005509	1.39	Binds methionyl-tRNAi (dependent on mthfs/mthfsl) in a codon dependent manner to initiate translation; regulates stress response
Meg3	maternally expressed 3	NR_027652	1.38	lncRNA as an inhibitor of adipogenesis
1700097N02Rik	RIKEN cDNA 1700097N02 gene	NR_045287	1.38	Testis preferably expressed, may be responsible for infertility in humans
Mapk1	mitogen-activated protein kinase 1	NM_011949	1.38	ERK2, a key role in MAPK/ERK cascade; targets PPARγ; translation regulation
4932431P20Rik	RIKEN cDNA 4932431P20 gene	XR_001778327	1.38	Unknown function
Slfn9	schlafen 9	NM_172796	1.38	DNA helicase; developmental regulation in immune cells
5033418A18Rik	RIKEN cDNA 5033418A18 gene	AK017178	1.37	Unknown function
D030002E05Rik	RIKEN cDNA D030002E05 gene	AK051948	1.37	Unknown function

Supporting information references

[1] Hoek-van den Hil, E. F., van Schothorst, E. M., van der Stelt, I., Swarts, H. J., *et al.*, Direct comparison of metabolic health effects of the flavonoids quercetin, hesperetin, epicatechin, apigenin and anthocyanins in high-fat-diet-fed mice. *Genes Nutr.* 2015, *10*, 469.
[2] Duivenvoorde, L. P., van Schothorst, E. M., Swarts, H. M., Kuda, O., *et al.*, A difference in fatty acid composition of isocaloric high-fat diets alters metabolic flexibility in male C57BL/6JOlaHsd mice. *PLoS One* 2015, *10*, e0128515.
[3] Hoek-van den Hil, E. F., Keijer, J., Bunschoten, A., Vervoort, J. J., *et al.*, Quercetin induces hepatic lipid omega-oxidation and lowers serum lipid levels in mice. *PLoS One* 2013, *8*, e51588.
[4] Friedewald, W. T., Levy, R. I., Fredrickson, D. S., Estimation of the concentration of low-density lipoprotein cholesterol in plasma, without use of the preparative ultracentrifuge. *Clin. Chem,* 1972, *18*, 499-502.
[5] Shi, W., Hegeman, M. A., van Dartel, D. A. M., Tang, J., *et al.*, Effects of a wide range of dietary nicotinamide riboside (NR) concentrations on metabolic flexibility and white adipose tissue (WAT) of mice fed a mildly obesogenic diet. *Mol. Nutr. Food Res.* 2017, *61*, 1600878.
[6] Van Dijk, T., Laskewitz, A., Grefhorst, A., Boer, T. S., *et al.*, A novel approach to monitor glucose metabolism using stable isotopically labelled glucose in longitudinal studies in mice. *Lab. Anim.* 2013, *47*, 79-88.
[7] Li, Y., Silva, J. C., Skinner, M. E., Lombard, D. B., Mass spectrometry-based detection of protein acetylation. *Methods Mol. Biol.* 2013, 81-104.
[8] Fukuwatari, T., Shibata, K., Nutritional aspect of tryptophan metabolism. *Int. J. Tryptophan Res.* 2013, *6*, 3-8.
[9] Fox, J. G., Barthold, S., Davisson, M., Newcomer, C. E., *et al.*, *The mouse in biomedical research: diseases*, Academic Press, Salt Lake City UT 2006.
[10] Van Rossum, C., Buurma-Rethans, E., Vennemann, F., Beukers, M., *et al.*, *The diet of the Dutch: Results of the first two years of the Dutch National Food Consumption Survey 2012-2016*, RIVM, Bilthoven, The Netherlands 2016.

Supporting information Figures

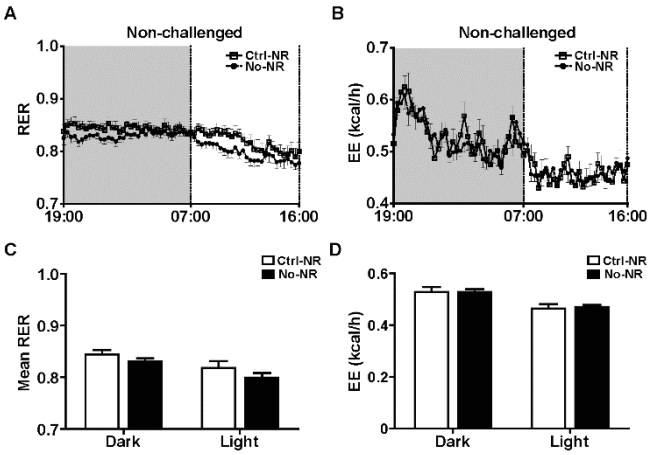

Supporting information Figure S1. Respiratory exchange ratio (RER) and energy expenditure (EE) of non-challenge conditions. RER (A) and EE (B) were measured in indirect calorimetry in week 14. Mean of RER (C) and EE (D) of the dark and the light phase were analysed. Ctrl-NR (30 mg NR/kg diet): open square with solid line or white bar, No-NR (no vitamin B3): closed circle with black dashed line or black bar. Data as mean±SEM. Analysis using two-way ANOVA. n=11-12.

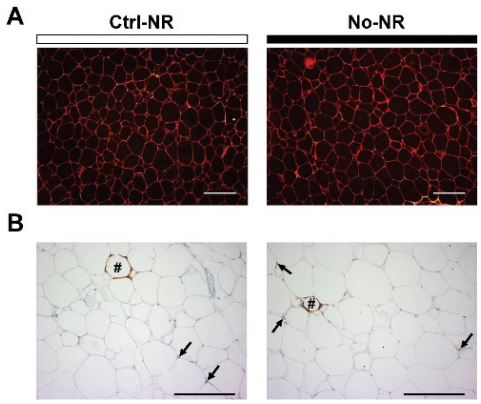

Supporting information Figure S2. Representative images of adipocyte size and crown-like structures (CLSs) and single macrophages in epididymal white adipose tissue (eWAT). Adipocyte size (A) and CLSs (indicated by octothorpes) and single macrophages (indicated by arrows) (B). Ctrl-NR: left pictures; No-NR: right pictures. Bar represents 200µm. n=8.

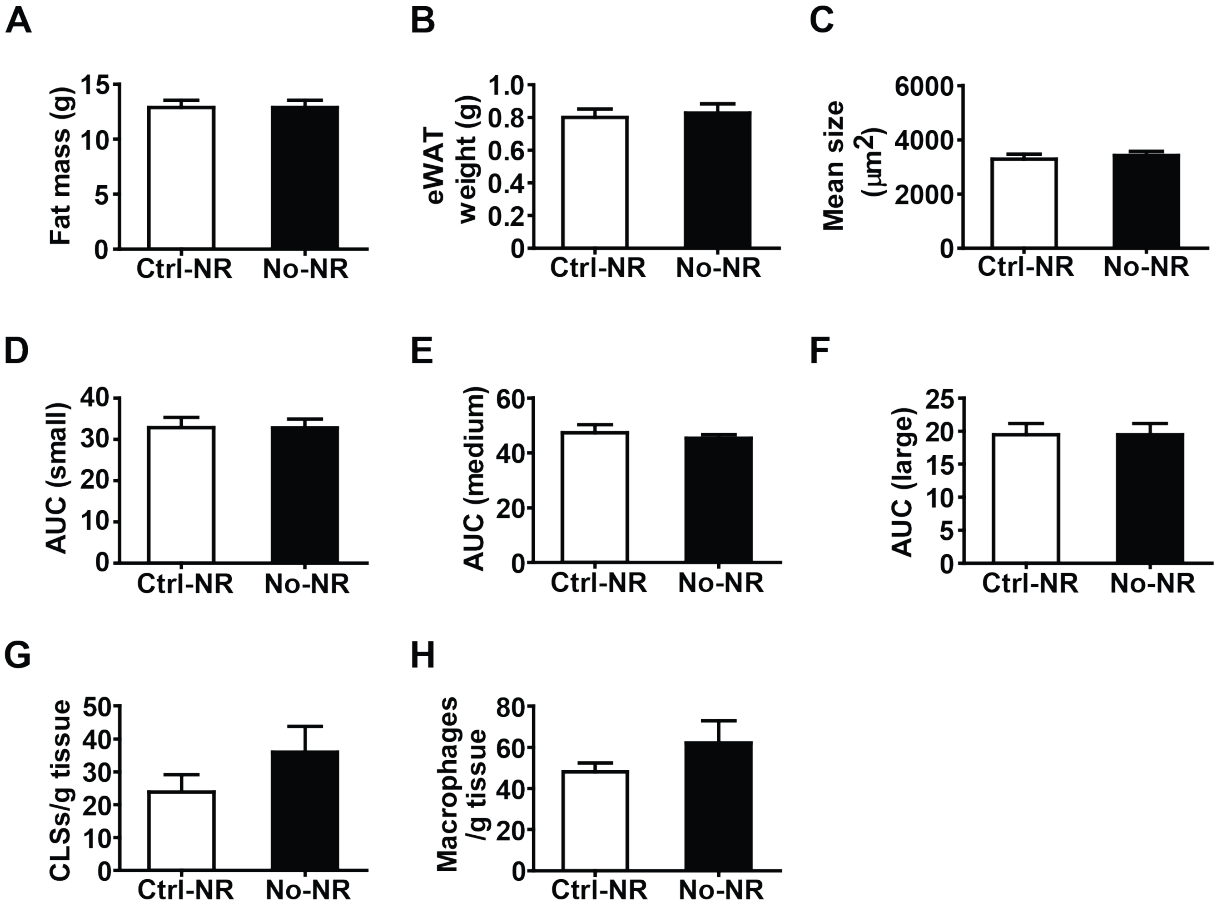

Supporting information Figure S3. Adipocyte size frequency distribution and inflammation status in eWAT. Fat mass in week 18 (A) and eWAT weight (B) (n=12 mice per treatment). Mean adipocyte size (C). Frequency distribution of adipocyte size was quantified using area under the curve (AUC) of small (100-1500μm^2, D), medium (<1500-6000μm^2, E) and large (>6000μm^2, F) fractions. Quantitation of CLSs (G) and macrophages (H) per gram tissue. Ctrl-NR: white bar. No-NR: black bar. Data as mean ± SEM. Analysis using Student's t test. n=8.

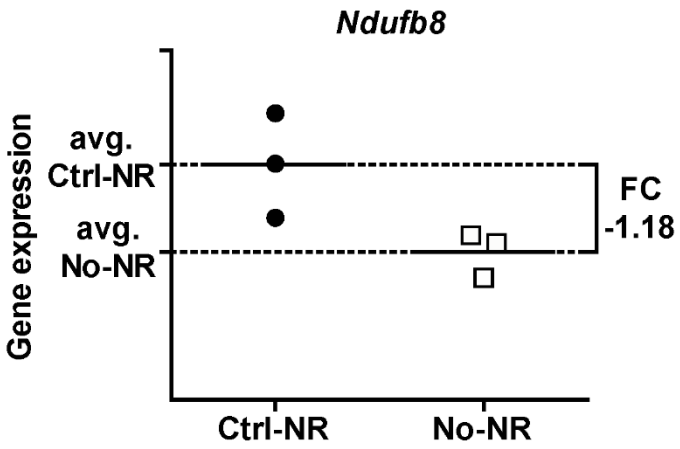

Supporting information Figure S4. Gene expression of NADH:ubiquinone oxidoreductase subunit B8 (Ndufb8) of the selected samples. Based on the gene expression of *Ndufb8* from microarray dataset, three of n=12 samples of each treatment were selected for western blot analysis. The mean gene expression of *Ndufb8* in the selected samples reflects the average expression of the respective treatment group.

Chapter 5

Dietary nicotinamide riboside affects motor function and hypothalamic gene expression in a dose-dependent manner

Maria Ibars*, Wenbiao Shi*, Dorien AM van Dartel, Hans Swarts, Maria A. Hegeman, Vincent C.J. de Boer, Jaap Keijer

Manuscript in advanced stage of preparation

Abstract

Nicotinamide ribose (NR) is a dietary vitamin B3 that is a precursor for the essential metabolic cofactor nicotinamide adenine dinucleotide (NAD^+). We previously established that among a range of concentrations, 30 mg NR per kg diet best supported metabolic health in mice. High, as well as low levels of NR had negative health effects through distinct mechanisms. Since motor performance and hypothalamic responses are important physiological read-outs for metabolic health, we now investigated this in detail. Male C57Bl/6JRccHsd mice were fed a semi-purified obesogenic diet (40% fat) containing 0.14% L-tryptophan and either 5, 30, or 900 mg NR per kg diet for 15 weeks. Compared to 30NR- fed mice, feeding a 5NR and 900NR diet lowered grip strength in mice, which was dependent on intervention time. The 900NR diet negatively affected motor coordination. Anti-oxidant defense genes *Prdx3* and *Sod1* were decreased by 900NR in the skeletal muscle. In the hypothalamus, gene expression of *Tdo2*, the first rate limiting enzyme in the *de novo* NAD^+ synthesis, was upregulated by 900NR feeding, whereas *Qdpr* was unaffected. The 5NR group displayed an upregulation of hypothalamic *Mapk1* (Erk2), a gene associated with neuronal plasticity, as well as of *Mthfs*, a key enzyme in folate metabolism. In conclusion, high dose NR reduces motor performance, which was associated with a reduction of the anti-oxidant defense in skeletal muscle. Low intake of NR implicates an interaction in the hypothalamus between the two B-vitamins folate and vitamin B3, with unknown functional consequences. Our results strengthen our previous observations that 30NR is the optimal dose to support metabolic health.

Introduction

Vitamin B3 supplies the body with the essential cofactor nicotinamide adenine dinucleotide (NAD^+). Insufficient intake of vitamin B3 in humans is associated with symptoms such as whole body weakness and fatigue [1, 2]. When vitamin B3 insufficiency is left untreated, a disease called Pellagra can develop, showing a number of rather aspecific symptoms, including skin problems, severe fatigue, depression, diarrhoea and dementia [2]. These symptoms may arise from the wide range of metabolic reactions in which NAD^+ is involved. NAD^+ is a co-factor in many oxidation-reduction reactions and acts as co-substrate for sirtuins, poly-ADP ribose polymerases (PARP) and cADP-ribose synthases [3]. Furthermore, NAD^+ is essential for energy metabolism, where it functions as an electron carrier in its reduced form. Finally, NAD^+ is a precursor of $NADP^+$, which serves as an essential co-factor in redox homeostasis and lipid metabolism [4]. Decreased levels of NAD^+ not only arise from vitamin B3 deficiency, but have also been observed in several tissues upon the consumption of high-fat diets and in obesity, conditions that can induce metabolic disease [5–8]. Several pre-clinical studies showed beneficial effects of supplementation with NAD^+ intermediates, suggesting it as a strategy to reduce metabolic disorders [9–11]. Other studies, however, dit not find beneficial effects with high dose supplementation of NAD^+ intermediates [12–16].

NAD^+ can be provided by four different dietary forms of vitamin B3, namely; nicotinic acid (NA), nicotinamide (Nam), nicotinamide riboside (NR) and nicotinamide mononucleotide (NMN). As a co-substrate, NAD^+ is degraded into Nam, from which it can be reconverted into NAD^+ via the salvage pathway [10, 11, 17]. NAD^+ can also be synthesized *de novo* from the essential amino acid tryptophan (Trp). In providing NAD^+, sixty mg of Trp is equivalent to approximately one mg of vitamin B3 [18].

To address functional effects and requirement for vitamin B3, it is thus essential to take levels of dietary Trp into account. In addition to NAD^+ biosynthesis, Trp is needed for protein synthesis and for the synthesis of the neurotransmitter serotonin [19, 20]. Serotonin has an important function in the central nervous system (CNS) [21] and can further be metabolized to melatonin. Most mouse diets contain approximately 0.23% Trp, well above the dietary requirement of 0.1%, which is needed for optimal growth [22]. 0.1% dietary Trp also suffices to mask overt symptoms of vitamin B3 deficiency [23, 24]. An interaction exists between Trp, serotonin and vitamin B3. For example, when Trp intake is below the requirement for protein synthesis, the efficiency for conversion into NAD^+ is reduced [25]. Furthermore, supplementation with a high dose of NA or Nam was shown to promote *de novo* NAD^+ biosynthesis in rodents [26, 27], a somewhat counterintuitive observation. In addition, Nam administration induced elevated plasma serotonin levels in healthy male humans [28]. These observations suggest an altered Trp metabolism upon vitamin B3 supplementation, which is poorly understood at a mechanistic level.

NR is a newly discovered vitamin B3 that is able to raise NAD^+ levels in several tissues [29, 30]. In a previous dose-response study, employing diets with 0.14% Trp and either 5, 15, 30, 180 or 900 mg NR per kg of diet, we made two key observations [14]. First, optimal metabolic flexibility was achieved at 30 mg NR per kg diet. Decreased

metabolic flexibility of mice on diets with low as well as high levels of NR were confirmed in independent studies using 0.115% Trp diets either without NR (*Shi* et al., *2018*, *submitted to MNFR*) or with 9000 mg NR per kg of diet (*Shi* et al., *2018*, *submitted to The FASEB*), compared to a reference amount of 30 mg NR per kg of diet. The second key observation was that white adipose tissue (WAT) proved the most responsive tissue amongst the tissues examined, which were liver, skeletal muscle, small intestine as well as adipose tissue. In the vitamin B3 withdrawal study (*Shi* et al., *2018*, *submitted to MNFR*), we proposed the downregulation of *Anp32a*,*Tnk2* and the upregulation of *Mapk1*, *Map2k1*, *Qdpr*, *Mthfs*, and *Mthfsl* as a WAT transcriptional signature marker for dietary vitamin B3 deficiency. The differential regulation of these genes in WAT implicated a decrease in insulin sensitivity as well as an enhanced biosynthesis of tetrahydropteridine (BH4), an essential cofactor for the production of neurotransmitters, including serotonin. In the high dose NR diet study (*Shi* et al., *2018*, *submitted to The FASEB*), we substantiated the negative effect of elevated dietary NR supplementation on glucose tolerance and insulin sensitivity (*Shi* et al., *2018*, *submitted to The FASEB*) and mechanistically delineated the associated processes in WAT.

Recently, it was demonstrated that WAT could modulate hypothalamic NAD^+ levels via secretion of nicotinamide phosphoribosyltransferase (NAMPT) [31] and NAD^+ balance has been shown to be essential for the function of the hypothalamus [32]. The hypothalamus also has a major role in regulating energy homeostasis by integrating levels of humoral signals, such as leptin and insulin. Two groups of hypothalamic neurons control food intake and energy expenditure by the release of neuropeptides. Proopiomelanocrotin (POMC) neurons produce anorexigenic responses, whereas Agrouti/related peptide (AgRP) and neuropeptide Y (NPY) neurons induce orexigenic signals [33, 34]. Since the hypothalamus supports and/or determines skeletal muscle metabolism via sympathetic nervous system [35–37], it is of interest to study how dietary NR impact the hypothalamus and motor function. Effects of various dietary levels of NR on the expression of neuropeptides, and hence on hypothalamic activation, has not been examined previously.

To better understand the effects of NR on the hypothalamus, we here tested the effects of various levels of dietary NR (5, 30 and 900 mg NR/kg diet) on the hypothalamic gene expression of enzymes involved in NAD^+ biosynthetic pathways, Trp metabolism, energy balance, as well as the transcripts that compose the proposed WAT transcriptional marker for dietary vitamin B3 deficiency and used motor performance as a functional read-out.

Material and Methods

Animals and diets

The animal experiments were approved by the Animal Welfare Committee of Wageningen University, Wageningen, The Netherlands (DEC2014029). The data reported here are new and were obtained using samples from a previously published study that reported the diet, study design, body weight, adiposity and energy expenditure, as well as gene expression in white adipose tissue, small intestine, liver and gastrocnemius [1]. Briefly, nine-week-old male C57Bl/6JRccHsd mice (Envigo,

Horst, The Netherlands) were individually housed (12h light–dark cycle, 23±1°C, 55±15% humidity) with *ad libitum* access to feed and water. After adaptation, mice were stratified into 3 experimental groups (n=12/group) and received a semi-synthetic obesogenic diet (Research Diet Services, Wijk bij Duurstede, The Netherlands) containing 40% energy from fat, 0.14% L-tryptophan and either 5, 30, or 900 mg NR per kg diet (referred to as 5NR, 30NR, and 900NR, respectively) for 15 weeks. 30NR is the reference level of vitamin B3. Mice were sacrificed by decapitation after 2 hours of fasting. Soleus muscle and brain were rapidly dissected, snap frozen in liquid nitrogen and stored at -80°C.

Grip strength test

The four-limb grip strength as well as forelimb grip strength was measured using a grip strength meter (Ugo basile SRL, Gemonio, Italy) in week 5 and week 12 following a protocol adapted from [2]. Mice were adjusted to the testing room for half an hour before testing. For the four-limb measurement, mice were placed on a grid. After the grid was grasped with all paws, the tail was gently pulled until the mice were fully released and the peak force was recorded. For the forelimb measurement, mice were positioned to grasp a rod with their forepaws and then suspended horizontally by the tail until release and the peak force was recorded. Mice were tested four times for each type of measurement with a 30-minute interval between each testing. The grid and the base were cleaned with ethanol between each test animal. The two highest measured values of peak force were averaged and normalized to the body weight in grams.

Rotarod test

Balancing capacity and motor coordination were assessed using an accelerating Rotarod system (IITC Life Science, Woodland Hills, USA) in week 6 and week 12 according to [3]. Briefly, trained mice were accustomed to the testing room for half an hour, after which mice were placed on an accelerating rod (3 to 38 rpm in 300 seconds). Latency to fall was recorded and distance on the rod was calculated. Mice were tested four times with an inter-trial rest of 30 minutes. The rods were cleaned with ethanol between each test subject. The average of two highest measured values per animal were used for analysis.

Gene expression

Hypothalamus was isolated using a brain matrix (Bio-Connect Life Sciences, Huissen, The Netherlands) and homogenized in TissueLyser II (Qiagen, Venlo, The Netherlands). Skeletal muscle were ground in liquid nitrogen. Total RNA was isolated from skeletal muscle and hypothalamus using Trizol (Invitrogen, Carlsbad, CA, USA), followed by a RNeasy Mini kit (Qiagen, Venlo, The Netherlands) according to the manufacturers' protocols. RNA purity and integrity was verified using Nanodrop (NanoDrop, Wilmington, USA) and TapeStation (Agilent, Santa Clara, CA, USA), respectively. cDNA synthesis, followed by regular qRT-PCR was performed as described [4]. Low expressed genes were pre-amplified for 12 cycles before qRT-PCR using SsoAdvanced PreAmp Supermix (Bio-Rad, Veenendaal, The Netherlands). The expression of each gene was normalized by the stably expressed reference genes using CFX Manager software (Bio-Rad). Ppia and B2m were used as reference genes in hypothalamus and

Canx in muscle. Primer sequences and PCR annealing temperatures for each gene are in Supplemental Table 1.

Results

A high dose of NR feeding affects motor performance

Grip strength and motor coordination reflect motor performance and were assessed in week 5/6 and week 12 of the dietary NR intervention. Four-limb grip strength was significantly decreased in 900NR in week 5 (Figure 1A), and tended to be reduced in week 12 (Figure 1B), compared to 30NR. A tendency for lower grip strength was seen in week 12 for 5NR compared to 30NR (Figure 1B). There was no significant difference between the groups in forelimbs grip strength, neither in week 5 nor in week 12 (Figure 1C, 2D). Motor coordination, indicated by latency to fall from the rotarod, tended to be lowered in 900NR compared to 30NR in week 6 (Figure 1E), and was significantly lower in week 12 (Figure 1F). Similarly, distance on the rod tended to be reduced in 900NR in week 6 (Figure 1G), and was significantly decreased in week 12 (Figure 1H). Altogether, our results suggest that high dose NR feeding leads to impaired motor performance in mice.

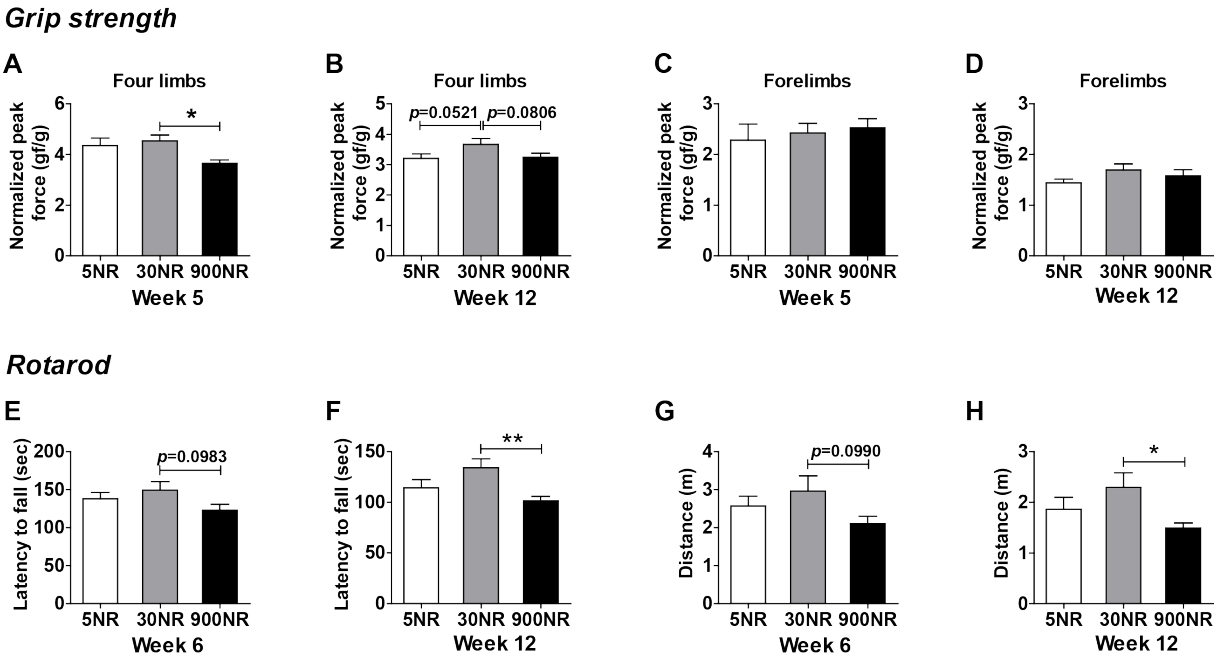

Figure 1. Grip strength test and rotarod test. These tests were performed to monitor the effects of dietary NR on muscle function and motor coordination. Four-limb grip strength of C57Bl/6JRccHSd mice in week 5 (A) and in week 12 (B), as well as strength of forelimbs in week 5 (C) and in week 12 (D) were expressed as peak force normalized by individual body weight. Duration on an accelerating rod (latency to fall) was recorded in week 6 (E) and in week 12 (F). The distance on the rod was measured in week 6 (G) and week 12 (H). White bar: 5NR; grey bar: 30NR; black bar: 900NR. NR in mg/kg diet. Data were analysed using one-way ANOVA followed by Dunnett's multiple comparison test, with 30NR as control and presented as mean±SEM (n=11-12 mice per treatment). * $p<0.05$, ** $p<0.01$.

A high dose of NR feeding induces a downregulation of genes involved in the anti-oxidant response in muscle

Very recently a pharmacological dose of NR supplementation (300 mg/kg BW/day) has been shown to compromise exercise performance in rats, potentially associated

with NR-induced systemic oxidative stress and a decrease in the activity of anti-oxidant enzymes in muscle [16]. Therefore, we examined in the soleus muscle a set of genes involved in anti-oxidant response. Because mitochondrial density and biogenesis is associated with muscle function and mitochondria are a major source of reactive oxygen species (ROS), we also examined expression of citrate synthase (*Cs*) and peroxisome proliferator-activated receptor gamma coactivator 1-alpha (*Pparga1a*), marker genes for mitochondrial density and biogenesis. The anti-oxidant defense enzymes peroxiredoxin 3 (*Prdx3*), and superoxide dismutase 1 (*Sod1*) were transcriptionally downregulated by 900NR compared to 30NR (Figure 2), while a downward trend was seen for superoxide dismutase 2 (*Sod2*) (Figure 2). The gene expression of aldehyde oxidase 1 (*Aox1*), catalase (*Cat*), and glutathione peroxidase 3 (*Gpx3*), as well as *Cs and Pparga1a* were not significantly changed by 5NR or 900NR, compared to 30NR (Figure 2). These data indicate that a high dose of NR may result in an impaired anti-oxidant response in the soleus muscle.

Figure 2. Gene expression in the soleus muscle. Genes representing anti-oxidant response and mitochondrial biogenesis were examined by qRT-PCR and their expression was normalized by the reference genes. Data were analysed using one-way ANOVA followed by Dunnett's multiple comparison test, with 30NR as control and presented as mean±SEM (n=8-12). * $p<0.05$, ** $p<0.01$.

A high dose of NR feeding leads to an upregulation of the first step of *de novo* NAD$^+$ biosynthesis

Next, we assessed whether dietary NR affects NAD$^+$ biosynthesis in the hypothalamus. Since we employed an adequate, but low Trp diet and NAD$^+$ is thus likely provided by NR, we first focused on mRNA levels of enzymes that convert NR to NAD$^+$ and on mRNA levels of enzymes of the salvage pathway (Figure 3). NR is metabolized to NMN by nicotinamide riboside kinases (NRKs). NMN is then further converted by NMN adenyl transferases (NMNATs) into NAD$^+$. NMN is also synthetized from Nam by the rate-limiting enzyme NAMPT [38]. Our results show that the expression of these enzymes at the transcriptional level was not affected by NR. Next, we examined whether the *de novo* NAD$^+$ biosynthesis pathway from Trp was modulated by the NR intervention. For this, we examined the gene expression of enzymes involved in the conversion of Trp into NAD$^+$. The gene expression of tryptophan 2,3-dioxygenase (*Tdo2*) was significantly enhanced by 900NR compared to 30NR. Over the groups, indoleamine 2,3-dioxygenase (*Ido1*) showed a similar

pattern as *Ido2*, but differences did not reach significance. Both enzymes participate in the rate-limiting step of Trp catabolism to N-formylkynurenine [10]. Gene expression from the quinolinate phosphoribosyltransferase (*Qprt*), an intermediate enzyme in the Trp-NAD⁺ pathway was not affected by NR. This may indicate that high dose NR exposure could possibly result in accumulation of kynurenines.

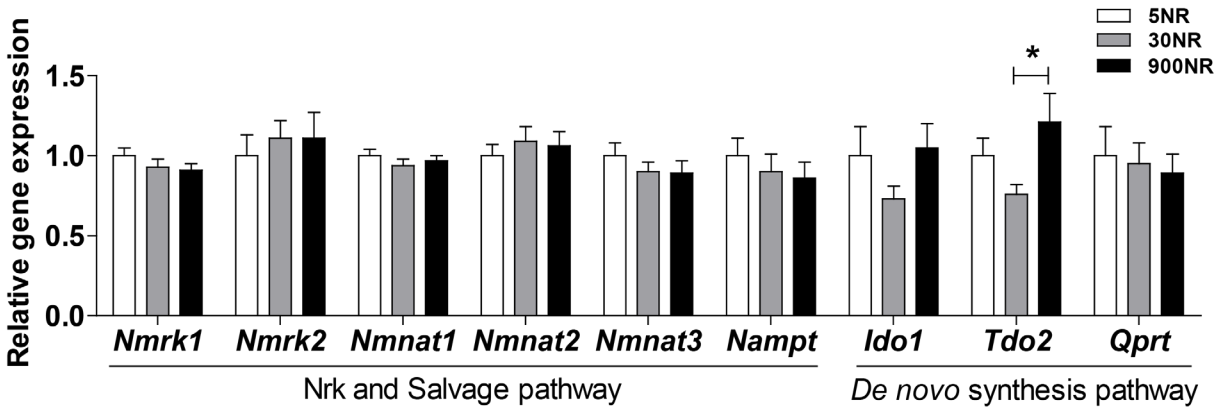

Figure 3. Gene expression of NAD⁺ biosynthesis in the hypothalamus. Gene expression was examined by qRT-PCR. Expression was normalized by the reference genes. Data was analysed using one-way ANOVA followed by Dunnett's multiple comparison test, with 30NR as control and presented as mean±SEM (n=10-12). * p<0.05.

Dietary NR does not affect hypothalamic serotonin biosynthesis, nor does it affect the hypothalamic regulation of food intake and energy expenditure.

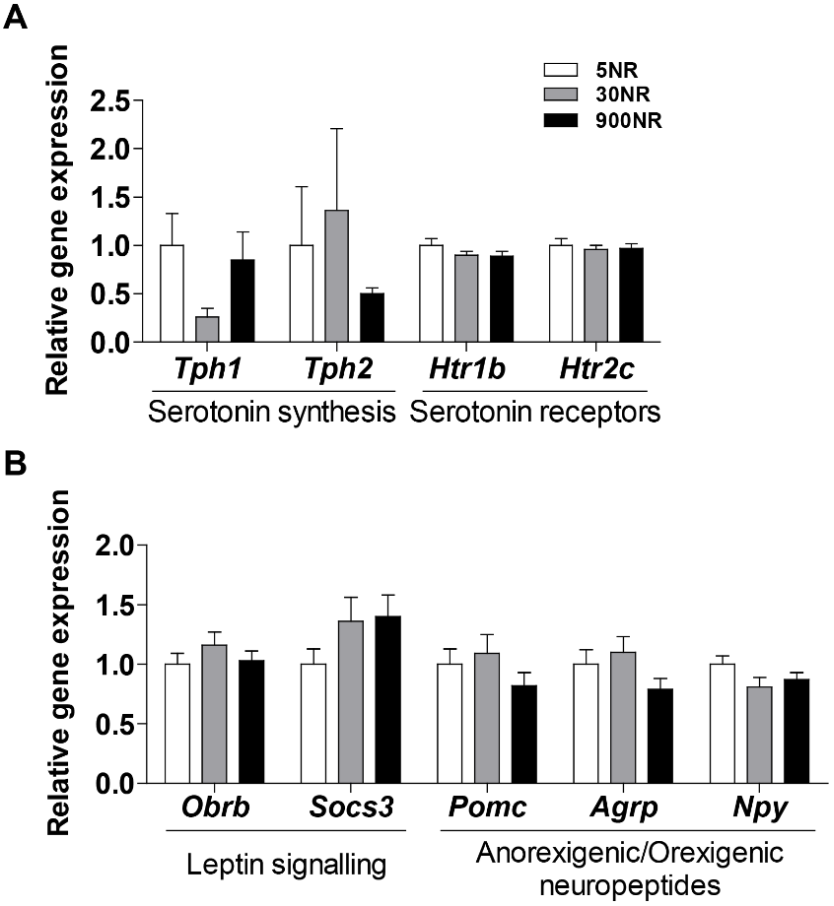

Figure 4. Gene expression serotonin pathways and leptin signalling in the hypothalamus. Gene expression was examined by qRT-PCR. Expression was normalized by the reference genes. Data were analysed using one-way ANOVA followed by Dunnett's multiple comparison test, with 30NR as control and presented as mean±SEM (n=10-12). * p<0.05.

We next examined effects of NR on different aspects of serotonin biosynthesis and signalling. Tryptophan hydroxylase 1 (*Tph1*) and tryptophan hydroxylase 2 (*Tph2*) which catalyse the first step and the rate-limiting step, respectively, in serotonin synthesis. Levels of these mRNAs did not show a change, mainly due to a high interindividual variability (Figure 4A). Similarly, the mRNA levels of the serotonin receptor isoforms 5-hydroxytryptamine receptor 1B (*Htr1b*) and 5-hydroxytryptamine receptor 2C (*Htr2c*), which have been related to the regulation of energy and food intake [20] were similar in the different experimental groups. In line with this, no differences were seen in the the gene expression of the hypothalamic neuropeptides *Pomc*, *Agrp* and *Npy*. Furthermore, the expression of the leptin receptor (*Obrb*) as well as *Socs3,* the negative regulator of leptin signalling, were not affected by dietary NR (Figure 4B). The absence of changes in these genes agrees with the absence of differences in food intake and energy expenditure in this study [14].

A low dose of NR enhances the transcription of component of the MAP Kinase pathway and an essential enzyme of folate metabolism

In an independent study, we proposed a WAT transcriptional signature for mild vitamin B3 deficiency. This signature was composed of the downregulation of Acidic leucine-rich nuclear phosphoprotein 32 family member A (*Anp32a*) and tyrosine kinase non receptor 2 (*Tnk2*), and the upregulation of mitogen-activated protein kinase 1 (*Mapk1*, also known as *Erk2*), mitogen activated protein kinase kinase 1 (*Map2k1*, also known as *Mek1*), 5,10-methenyltetrahydrofolate synthase (*Mthfs*), 5,10-methenyltetrahydrofolate synthase-like (*Mthfsl*) and quinoid dihydropteridine reductase (*Qdpr*). ANP32A, TNK2, MAPK1 and MAP2K1 have been associated with insulin signalling, while MTHFS, MTHFSL and QDPR have a role in folate metabolism. QDPR catalyses the biosynthesis of tetrabiopteridin, an essential cofactor of TPH and is thus involved in serotonin biosynthesis. Similar to what was observed in WAT, mRNA levels of *Mapk1* and *Mthfs* were significantly upregulated in the 5NR group, compared to 30NR (Figure 5). mRNA levels of *Map2k1*, *Anp32a* showed a similar pattern, but did not reach significance. *Tnk2*, and *Qdpr* were not affected by either 5NR nor 900NR, while we could not obtain reliable results for *Mthfsl*.

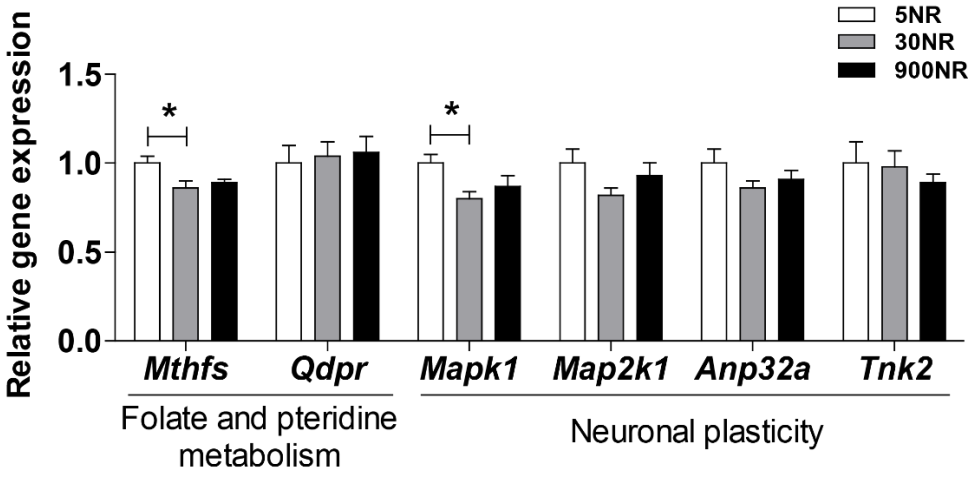

Figure 5. Gene expression of WAT vitamin B3 deficiency signature in hypothalamus. Gene expression was examined by qRT-PCR. Expression was normalized by the reference genes. Data were analysed using one-way ANOVA followed by Dunnett's multiple comparison test, with 30NR as control and presented as mean±SEM (n=10-12). * $p<0.05$.

Discussion

Here, we investigated the effects of NR on mouse motor performance and hypothalamus. We observed a decreased motor performance by a high level of dietary NR, which was associated with a downregulation of anti-oxidant defense genes in muscle and an upregulation of hypothalamic *Tdo2*. Furthermore, we showed that *Mapk1* and *Mthfs* were significantly up-regulated in the hypothalamus by low dietary vitamin B3. These two transcripts were previously identified as part of a WAT transcriptional marker profile for mild vitamin B3 deficiency (*Shi* et al., *2018*, *submitted to MNFR*).

Evidence of contrasting effects of high dose of NR on motor function has been presented across different animal models [13, 15, 16, 30, 39–42]. Our rotarod test data suggest that a high dose of dietary NR (900 mg NR /kg diet, corresponding to approximately 70 mg NR/kg BW/day) induced a worsening of motor coordination in C57Bl/6JRccHsd mice fed a mildly obesogenic diet over the intervention span (Figure 1E-H). In line, feeding with 400 mg NR/kg BW/day in a chow diet tended to reduce rotarod performance in C57Bl/6JCrl *Bcs1l* $^{p.S78G}$ mice, a mouse model with a mitochondrial complex III defect [13]. Similarly, adult rats administered with 300 mg NR/kg BW/day displayed decreased motor coordination, assessed by an incremental swimming performance test [15, 16]. In contrast, approximately 400 mg NR/kg BW daily intake was shown to ameliorate coordination disorders in old mice with Alzheimer's disease (AD) [41]. Our grip strength data showed detrimental effects especially in the four-limb grip test, rather than in the forelimb grip test (Figure 1A-D). This contrast with observations in the aged AD mice or in a mouse model for Duchene's muscular dystrophy, that showed that treatment with 400 mg NR/kg BW/day led to an improvement of forelimb grip strength [41, 42]. Collectively, the observations above suggest a modifying effect of the animal model on how high levels of NR affect motor performance. Variation in the effects of high dose NR supplementation on motor function was also seen in humans. While high dose NR supplementation, given in combination with the blueberry polyphenol pterostilbene, improved mobility in healthy middle-aged and elderly subjects [43], no improvement was seen in another high dose NR supplementation study that extensively assessed motor performance, including handgrip strength and coordinated movements [44].

The adverse effects imposed by the high dose of NR may be related to the decreased transcriptional levels of SOD1 and PRDX3 in our study, as well as a downwards trend of SOD2 in the soleus muscle following exposure to high dietary NR. Downregulation at the transcriptional level implicates a reduction in antioxidant defense capacity. While SOD1 is expressed in the nucleus and cytoplasm, PRDX3 and SOD2 reside in mitochondria. Whether the lower expression of the latter two resulted from a change in mitochondrial biogenesis or density awaits further measurements on activity or protein levels of two markers PGC-1α and CS, which showed no change on the gene expression (Figure 2). In line with our observations, a lowered activity of antioxidant enzymes has been observed in muscle of rats given a high dose of NR [16]. The downregulation of antioxidant defense in muscle may potentially aggravate oxidative stress resulted from the obesogenic diet feeding, which may, in part, be associated with the compromised motor performance [45]. Weakness and fatigue may occur due

to a long-term vitamin B3 deficiency in humans [2]. Although no signs of overt deficiency were observed, low vitamin B3 levels may explain the tendency of a reduced four-limb grip strength in mice fed a 5NR diet towards the end of the intervention period (Figure 1B).

The hypothalamus has been referred to as the central control unit of NAD^+ metabolism and is an important regulator of muscle function [37]. To date, the effects of NR on hypothalamic pathways connecting to NAD^+ metabolism have not been studied. We showed that a high dose of NR upregulated the gene expression of *Tdo2,* which is the first rate-limiting enzyme in the *de novo* NAD^+ biosynthesis pathway [17]. On the other hand, *Qprt*, the transcript encoding the more downstream enzyme responsible quinolinate catabolism, was not modulated by NR. This may suggest that quinolinate might accumulate in the brain of mice given high doses of NR. Quinolinate is a known potent endogenous neurotoxin produced preferentially in microglia, which acts as an agonist of N-methyl-D-aspartate (NMDA) receptors, a subtype of glutamate receptors [46]. Furthermore, in microglia, 3-hydroxykynurenine, the intermediate generated by IDO2, can produce high amounts of free radicals that can damage the cells and, together with its direct metabolite kynurenine, potentiates neurotoxicity which is a characteristic feature of the development of neurological diseases [47]. In fact, TDO2 inhibition was shown to improve the neurological state and to increase life span in different organisms [48–50]. The metabolic interpretation of high dose NR induced *Tdo2* downregulation awaits analysis of the various Trp metabolites.

Serotonin is a key neurotransmitter and a Trp metabolite [19]. Since 900NR feeding increased *Tdo2* expression, this could limit Trp availability for serotonin synthesis. TPH1 and TPH2 perform the rate limiting conversion of Trp into 5-hydroxytryptophan [51]. *Tph1* is mostly expressed in peripheral tissues, while *Tph2* is most abundant in brain [52]. The levels of the expression of these genes did not significantly change between groups, but we cannot completely rule out the potential modulation of these genes by NR, since the results were obscured by high interindividual variation. We previously reported that 30NR improved the HOMA-IR index and leptin/adiponectin ratio [14]. These functions can be controlled by serotonin receptors in the hypothalamus, particularly 5-HT1b and 5-HT2c, which have an important role in the regulation of energy balance, glucose homeostasis and locomotor activity [20, 53–56]. However, the levels of these genes were not different among the NR groups. This agrees with other data on energy balance regarding the orexigenic and anorexigenic neuropeptides and leptin related gene expression, which was also not affected in our study, and may suggest that serotonin signalling via these receptors is not involved in the effects of NR on glucose homeostasis and motor function.

We previously proposed a transcriptional signature as a WAT marker for mild vitamin B3 deficiency (*Shi* et al., *2018*, *submitted to MNFR*). This marker consisted of seven genes, two of these were also significantly regulated in the hypothalamus in this independent study, which was shorter (15 weeks *vs* 18 weeks) and the low dose was less extreme (5NR *vs* 0NR). Nevertheless, *Mthfs* and *Mapk1* were upregulated by exposure to the lowest dose of NR (5NR) compared to 30NR, meaning that the expression of these genes could be a robust marker for a mild vitamin B3 deficiency.

Two other genes of the WAT vitamin B3 deficiency signature, *Anp32* and *Map2k1*, showed a tendency for upregulation, which may be explained by tissues specific difference or by a lower sensitivity of these genes to vitamin B3 deficiency. MAPK1 (ERK2), MAPK2K1 (MEK1) and ANP32 all have a role in neurogenesis and cognitive function [57–59]. Future research may explore the relation between these genes, NR and cognitive function, which may shed a light on the mechanisms that are involved in vitamin B3 deficiency-associated dementia. Our observation on the upregulation of *Mthfs* is the first report that a reduced level of dietary vitamin B3 impacts on folate metabolism in the hypothalamus. Folate is essential for the synthesis of purines, thymidylate, glutathione as well as for one-carbon metabolism, which supports methylation reactions to maintain a wide range of physiological functions [60]. MTHFS is involved in the irreversible conversion of 5-formyltetrahydrofolate to 5,10-methenyltetrahydrofolate. 5-formyltetrahydrofolate is a storage form of tetrahydrofolate. Heterozygous *Mthfs*$^{+/-}$ displayed a compromised *de novo* purine synthesis, while *Mthfs* null mice were not viable, indicating the essentiality of this gene [61]. Furthermore, a biallelic loss of this gene has recently been described in two human subjects that present with a severe neuro-metabolic disorder [62]. The relevance of this enzyme in folate metabolism and the observation in two independent studies that low levels of vitamin B3 upregulate the gene expression of MTHFS, warrants further studies into the metabolic interaction effects of NR and folates.

In conclusion, a high dose of 900NR reduced motor performance and was associated with a reduction of anti-oxidant defense in the skeletal muscle. Additionally, it affected hypothalamic Trp metabolism in a way that seemed to alter the metabolic flow to NAD^+ synthesis. On the other hand, low levels of vitamin B3 induced the upregulation of *Mapk1*. It is of interest to examine whether this may be related to vitamin B3 deficiency associated dementia. Low levels of dietary NR also induced expression of *Mthfs*, encoding a central enzyme in folate metabolism, revealing an interaction between these two B-vitamins in the hypothalamus, with unknown functional consequences. The results strengthen our previous observations that 30NR is the optimal dose to support metabolic health and describe potential new targets of vitamin B3.

Acknowledgements

We thank ChromaDex for the generous and kind supply of nicotinamide riboside. We thank our colleagues at Human and Animal Physiology and the animal facility for their help. We thank Isabella Schuijf for practical contributions. Financial support by the Chinese Scholarship Council (grant# 201303250054) is gratefully acknowledged.

References

[1] Hegyi, J., Schwartz, R.A., Hegyi, V., Pellagra : Dermatitis , dementia , and diarrhea. *Int. Soc. Dermatology* 2004, *43*, 1–5.
[2] Wan, P., Moat, S., Anstey, A., Pellagra: A review with emphasis on photosensitivity. *Br. J. Dermatol.* 2011.
[3] Yang, Y., Sauve, A.A., NAD+metabolism: Bioenergetics, signaling and manipulation for therapy. *Biochim. Biophys. Acta - Proteins Proteomics* 2016.
[4] Ying, W., NAD $^+$ /NADH and NADP $^+$ /NADPH in Cellular Functions and Cell Death: Regulation and Biological Consequences. *Antioxid. Redox Signal.* 2008, *10*, 179–206.
[5] Bai, P., Cantó, C., Oudart, H., Brunyánszki, A., et al., PARP-1 Inhibition Increases Mitochondrial Metabolism through SIRT1 Activation. *Cell Metab.* 2011, *13*, 461–468.
[6] Kraus, D., Yang, Q., Kong, D., Banks, A.S., et al., Nicotinamide N-methyltransferase knockdown protects against diet-induced obesity. *Nature* 2014, *508*, 258–262.
[7] Jukarainen, S., Heinonen, S., Rämö, J.T., Rinnankoski-Tuikka, R., et al., Obesity Is Associated With Low NAD $^+$ /SIRT Pathway Expression in Adipose Tissue of BMI-Discordant Monozygotic Twins. *J. Clin. Endocrinol. Metab.* 2016, *101*, 275–283.
[8] Yoshino, J., Mills, K.F., Yoon, M.J., Imai, S., Nicotinamide Mononucleotide, a Key NAD+ Intermediate, Treats the Pathophysiology of Diet- and Age-Induced Diabetes in Mice. *Cell Metab.* 2011, *14*, 528–536.
[9] Karpe, F., Frayn, K.N., The nicotinic acid receptor–a new mechanism for an old drug. *Lancet* 2004, *363*, 1892–1894.
[10] Cantó, C., Menzies, K.J., Auwerx, J., NAD+ Metabolism and the Control of Energy Homeostasis: A Balancing Act between Mitochondria and the Nucleus. *Cell Metab.* 2015, *22*, 31–53.
[11] Yoshino, J., Baur, J.A., Imai, S., NAD+Intermediates: The Biology and Therapeutic Potential of NMN and NR. *Cell Metab.* 2017, *27*, S1550-4131.
[12] Dollerup, O.L., Christensen, B., Svart, M., Schmidt, M.S., et al., A randomized placebo-controlled clinical trial of nicotinamide riboside in obese men: safety, insulin-sensitivity, and lipid-mobilizing effects. *Am. J. Clin. Nutr.* 2018, 1–11.
[13] Purhonen, J., Rajendran, J., Tegelberg, S., Smolander, O.-P., et al., NAD $^+$ repletion produces no therapeutic effect in mice with respiratory chain complex III deficiency and chronic energy deprivation. *FASEB J.* 2018, fj.201800090R.
[14] Shi, W., Hegeman, M.A., van Dartel, D.A.M., Tang, J., et al., Effects of a wide range of dietary nicotinamide riboside (NR) concentrations on metabolic flexibility and white adipose tissue (WAT) of mice fed a mildly obesogenic diet. *Mol. Nutr. Food Res.* 2017.
[15] Kourtzidis, I.A., Stoupas, A.T., Gioris, I.S., Veskoukis, A.S., et al., The NAD+precursor nicotinamide riboside decreases exercise performance in rats. *J. Int. Soc. Sports Nutr.* 2016, *13*, 1–4.
[16] Kourtzidis, I.A., Dolopikou, C.F., Tsiftsis, A.N., Margaritelis, N. V., et al., Nicotinamide riboside supplementation dysregulates redox and energy metabolism in rats: Implications for exercise performance. *Exp. Physiol.* 2018.
[17] Bogan, K.L., Brenner, C., Nicotinic Acid, Nicotinamide, and Nicotinamide Riboside: A Molecular Evaluation of NAD + Precursor Vitamins in Human Nutrition. *Annu. Rev. Nutr* 2008, *28*, 115–30.
[18] Horwitt, M.K., Harper, A.E., Henderson, L.M., Niacin-tryptophan relationships for evaluating niacin equivalents. *Am. J. Clin. Nutr.* 1981.
[19] O'Mahony, S.M., Clarke, G., Borre, Y.E., Dinan, T.G., et al., Serotonin, tryptophan metabolism and the brain-gut-microbiome axis. *Behav. Brain Res.* 2015, *277*, 32–48.
[20] Berger, M., Gray, J.A., Roth, B.L., The Expanded Biology of Serotonin. 2008.
[21] Lv, J., Liu, F., The Role of Serotonin beyond the Central Nervous System during Embryogenesis. *Front. Cell. Neurosci.* 2017.
[22] Nutrition, S. on L.A., Nutrition, C. on A., Agriculture, B. on, Council, N.R., Formulation of diet types, 1995.
[23] Terakata, M., Fukuwatari, T., Sano, M., Nakao, N., et al., Establishment of True Niacin Deficiency in Quinolinic Acid Phosphoribosyltransferase Knockout Mice. *J. Nutr.* 2012.
[24] Terakata, M., Fukuwatari, T., Kadota, E., Sano, M., et al., The Niacin Required for Optimum Growth Can Be Synthesized from L-Tryptophan in Growing Mice Lacking

Tryptophan-2,3-Dioxygenase. *J. Nutr.* 2013.
[25] B. Kirkland, J., Niacin, in: Zempleni, J., Rucker, R.B., McCormick, D.B., John W. Suttie (Eds.), *Handbook of Vitamins*, CRC Press, New York, USA 2007, pp. 191–232.
[26] Shibata, K., Fukuwatari, T., Suzuki, C., Pharmacological Doses of Nicotinic Acid and Nicotinamide Are Independently Metabolized in Rats. *J. Nutr. Sci. Vitaminol. (Tokyo).* 2014.
[27] Mitchell, S.J., Bernier, M., Aon, M.A., Cortassa, S., et al., Nicotinamide Improves Aspects of Healthspan, but Not Lifespan, in Mice. *Cell Metab.* 2018.
[28] Yan-Jie, T., Da, L., Qiang, M., Xin-Yi, G., et al., Excess nicotinamide increases plasma serotonin and histamine levels. *Acta Physiol. Sin.* 2013.
[29] Trammell, S.A.J., Schmidt, M.S., Weidemann, B.J., Redpath, P., et al., Nicotinamide riboside is uniquely and orally bioavailable in mice and humans. *Nat. Commun.* 2016, *7*, 1–14.
[30] Cantó, C., Houtkooper, R.H., Pirinen, E., Youn, D.Y., et al., The NAD+precursor nicotinamide riboside enhances oxidative metabolism and protects against high-fat diet-induced obesity. *Cell Metab.* 2012, *15*, 838–847.
[31] Yoon, M.J., Yoshida, M., Johnson, S., Takikawa, A., et al., SIRT1-Mediated eNAMPT Secretion from Adipose Tissue Regulates Hypothalamic NAD+ and Function in Mice. *Cell Metab.* 2015, *21*, 706–717.
[32] Sasaki, T., Age-Associated Weight Gain, Leptin, and SIRT1: A Possible Role for Hypothalamic SIRT1 in the Prevention of Weight Gain and Aging through Modulation of Leptin Sensitivity. *Front. Endocrinol. (Lausanne).* 2015, *6*, 109.
[33] Sainsbury, A., Cooney, G.J., Herzog, H., Hypothalamic regulation of energy homeostasis. *Best Pract. Res. Clin. Endocrinol. Metab.* 2002, *16*, 623–37.
[34] Gareth Williams, J.A.H. and D.J.C., The hypothalamus and the regulation of energy homeostasis: lifting the lid on a black box. *Proc. Nutr. Soc.* 2000, *59*, 385–396.
[35] Braun, T.P., Marks, D.L., Hypothalamic regulation of muscle metabolism. *Curr. Opin. Clin. Nutr. Metab. Care* 2011, *14*, 237–242.
[36] Joly-Amado, A., Cansell, C., Denis, R.G.P., Delbes, A.-S., et al., The hypothalamic arcuate nucleus and the control of peripheral substrates. *Best Pract. Res. Clin. Endocrinol. Metab.* 2014, *28*, 725–737.
[37] Imai, S., The NAD World 2 . 0 : the importance of the inter-tissue communication mediated by NAMPT / NAD + / SIRT1 in mammalian aging and longevity control. *Nat. Publ. Gr.* 2016.
[38] Yoshino, J., Baur, J.A., Imai, S. ichiro, NAD+Intermediates: The Biology and Therapeutic Potential of NMN and NR. *Cell Metab.* 2017, *2*.
[39] Zhang, H., Ryu, D., Wu, Y., Gariani, K., et al., NAD repletion enhances life span in mice. *Science (80-.).* 2016, *6*.
[40] Frederick, D.W., Loro, E., Liu, L., Davila, A., et al., Loss of NAD Homeostasis Leads to Progressive and Reversible Degeneration of Skeletal Muscle. *Cell Metab.* 2016, *24*, 269–282.
[41] Hou, Y., Lautrup, S., Cordonnier, S., Wang, Y., et al., NAD $^+$ supplementation normalizes key Alzheimer's features and DNA damage responses in a new AD mouse model with introduced DNA repair deficiency. *Proc. Natl. Acad. Sci.* 2018, *115*, E1876–E1885.
[42] Ryu, D., Zhang, H., Ropelle, E.R., Sorrentino, V., et al., NAD+repletion improves muscle function in muscular dystrophy and counters global parylation. *Sci. Transl. Med.* 2016, *8*, 1–15.
[43] Dellinger, R.W., Santos, S.R., Morris, M., Evans, M., et al., Repeat dose NRPT (nicotinamide riboside and pterostilbene) increases NAD+levels in humans safely and sustainably: a randomized, double-blind, placebo-controlled study. *Npj Aging Mech. Dis.* 2017, *3*.
[44] Martens, C.R., Denman, B.A., Mazzo, M.R., Armstrong, M.L., et al., Chronic nicotinamide riboside supplementation is well-Tolerated and elevates NAD+in healthy middle-Aged and older adults. *Nat. Commun.* 2018, *9*, 1–11.
[45] Yokota, T., Kinugawa, S., Hirabayashi, K., Matsushima, S., et al., Oxidative stress in skeletal muscle impairs mitochondrial respiration and limits exercise capacity in type 2 diabetic mice. *AJP Hear. Circ. Physiol.* 2009.
[46] Bogan, K.L., Brenner, C., Nicotinic Acid, Nicotinamide, and Nicotinamide Riboside: A Molecular Evaluation of NAD $^+$ Precursor Vitamins in Human Nutrition. *Annu. Rev. Nutr.* 2008, *28*, 115–130.

[47] Guidetti, P., Schwarcz, R., 3-Hydroxykynurenine potentiates quinolinate but not NMDA toxicity in the rat striatum. *Eur. J. Neurosci.* 1999, *11*, 3857–3863.
[48] Van Der Goot, A.T., Zhu, W., Vázquez-Manrique, R.P., Seinstra, R.I., et al., Delaying aging and the aging-associated decline in protein homeostasis by inhibition of tryptophan degradation. *Proc. Natl. Acad. Sci. U. S. A.* 2012, *109*, 14912–14917.
[49] Campesan, S., Green, E.W., Breda, C., Sathyasaikumar, K.V., et al., The Kynurenine Pathway Modulates Neurodegeneration in a Drosophila Model of Huntington's Disease. *Curr. Biol.* 2011, *21*, 961–966.
[50] Breda, C., Sathyasaikumar, K. V, Sograte Idrissi, S., Notarangelo, F.M., et al., Tryptophan-2,3-dioxygenase (TDO) inhibition ameliorates neurodegeneration by modulation of kynurenine pathway metabolites. *Proc. Natl. Acad. Sci. U. S. A.* 2016, *113*, 5435–40.
[51] Invernizzi, R.W., Role of TPH-2 in brain function: News from behavioral and pharmacologic studies. *J. Neurosci. Res.* 2007, *85*, 3030–3035.
[52] Brommage, R., Liu, J., Doree, D., Yu, W., et al., Adult Tph2 knockout mice without brain serotonin have moderately elevated spine trabecular bone but moderately low cortical bone thickness. *Bonekey Rep.* 2015, *4*, 718.
[53] Xu, Y., Jones, J.E., Kohno, D., Williams, K.W., et al., 5-HT2CRs Expressed by Pro-Opiomelanocortin Neurons Regulate Energy Homeostasis. *Neuron* 2008, *60*, 582–589.
[54] Nonogaki, K., Nozue, K., Oka, Y., Hyperphagia Alters Expression of Hypothalamic 5-HT2C and 5-HT1B Receptor Genes and Plasma Des-Acyl Ghrelin Levels in A ^{y} Mice. *Endocrinology* 2006, *147*, 5893–5900.
[55] Nonogaki, K., Abdallah, L., Goulding, E.H., Bonasera, S.J., et al., Hyperactivity and reduced energy cost of physical activity in serotonin 5-HT(2C) receptor mutant mice. *Diabetes* 2003, *52*, 315–20.
[56] Zhou, L., Sutton, G.M., Rochford, J.J., Semple, R.K., et al., Cell Metabolism Serotonin 2C Receptor Agonists Improve Type 2 Diabetes via Melanocortin-4 Receptor Signaling Pathways. *Cell Metab.* n.d., *6*, 398–405.
[57] Kelleher, R.J., Govindarajan, A., Jung, H.Y., Kang, H., et al., Translational control by MAPK signaling in long-term synaptic plasticity and memory. *Cell* 2004, *116*, 467–479.
[58] Samuels, I.S., Karlo, J.C., Faruzzi, A.N., Pickering, K., et al., Development/Plasticity/ Repair Deletion of ERK2 Mitogen-Activated Protein Kinase Identifies Its Key Roles in Cortical Neurogenesis and Cognitive Function. *J. Neurosci.* 2008, *28*, 6983–6995.
[59] Chai, G.S., Feng, Q., Wang, Z.H., Hu, Y., et al., Downregulating ANP32A rescues synapse and memory loss via chromatin remodeling in Alzheimer model. *Mol. Neurodegener.* 2017, *12*, 1–12.
[60] Ducker, G.S., Rabinowitz, J.D., Cell Metabolism Review One-Carbon Metabolism in Health and Disease. *Cell Metab.* 2017, *25*, 27–42.
[61] Field, M.S., Anderson, D.D., Stover, P.J., Mthfs is an Essential Gene in Mice and a Component of the Purinosome. *Front. Genet.* 2011, *2*, 36.
[62] Rodan, L.H., Qi, W., Ducker, G.S., Demirbas, D., et al., 5,10-methenyltetrahydrofolate synthetase deficiency causes a neurometabolic disorder associated with microcephaly, epilepsy, and cerebral hypomyelination. *Mol. Genet. Metab.* 2018, *125*, 118–126.

Supplemental Table 1. Sequences of primers used for qRT-PCR [a]

Gene	Primer forward 5'-3'	Primer reverse 5'-3'
Acox1	TGCGGTGGGCACGGCTATTC	CGCTGGCTCGGCAGGTCATT
Agrp	AGTTGTGTTCTGCTGTTGGC	CTGATGCCCTTCAGTGGAG
B2m	CCCCACTGAGACTGATACATACGC	AGAAACTGGATTTGTAATTAAGCAGGTTC
Canx	GCAGCGACCTATGATTGACAACC	GCTCCAAACCAATAGCACTGAAAGG
Cat	CTCGCAGAGACCTGATGTCC	TGTGGAGAATCGAACGGCAA
Cs	ACAGTGAAAGCAACTTCGCC	GTCAATGGCTCCGATACTGC
Gpx3	CCATTCGGCCTGGTCATTCT	GGAGGGCAGGAGTTCTTCAG
Htr1b	TGCCTGCTGGTTTCACAT	GCGCACTTAAAGCGTATCA
Htr2c	CTGAGGGACGAAAGCAAAG	CACATAGCCAATCCAAACAAAC
Ido1	TCTGCTGTATGAGGGGGTCT	GGAGATTCTTTGCCAGCCTC
Ido2	ATTGCCCTCAGACTTCCTCAC	TCTTGGCAGCACCTTTTGGG
Nampt	GATTGAGACTATTCTTGTTCAGT	GTAACTTGTATTCCAGACCATC
Nmnat1	CCAAACCAACAGGTGTGCC	CCACGATTTGCGTGATGTCC
Nmnat2	GATGTTCGAGAGAGCCAGGG	AGTCATGGACCGGAGAGACA
Nmnat3	TAGCCCCACGGTCACTTTTC	GCAGTGGCCACCCTGTTTTA
Nmrk1	CTTGAAGCTTGCTCTGCGAC	CTCCGTTTGTCACACCACCA
Nmrk2	CGGGGTGGAAGTGGTCTATTT	GGACCATACAGGACGCCAG
Npy	CCCGCCACGATGCTAGGTA	TCAGCCAGAATGCCCAAACA
Mthfs	GTCTCTCCTCCTCACGCAGA	GGTCAAGTCCACCAGTGGATAA
Obrb	GGGACGATGTTCCAAACCCC	CAGGCTCCAGAAGAAGAGGAC
Pomc	CAAGGACAAGCGTTACGGTG	TCTTGTGCGCGTTCTTGATG
Ppargc1a	CCCTGCCATTGTTAAGACC	TGCTGCTGTTCCTGTTTTC
Ppia	CCAAGACTGAATGGCTGGATGG	CTCTCCTGAGCTACAGAAGGAATG
Prdx3	GTGGTTTGGGCCACATGAAC	AGAGACCTCTGAGCGCAATG
Qdpr	CATTGCTGTGCTCCCCGTTA	TCCTGAGTTTGGCCGTTTGT
Qprt	AGACAACCATGTAGTGGCGG	TGCAGCTCCTCAGGCTTAAA
Socs3	ACCAGCGCCACTTCTTCACG	GTGGAGCATCATACTGATCC
Sod1	TCGGCTTCTCGTCTTGCTCTC	GTTCACCGCTTGCCTTCTGC
Sod2	TTCTGGACAAACCTGAGCCCTAAG	GCAGCAATCTGTAAGCGACCTTG
Tdo2	ACTGTGAGCGACAGGTACAA	CTGTCACTGTACTCGGCTGT
Tph1	CAGTGGCTCTGAGGTGAGTG	GGCTCACATGATTCTCCTGGAA
Tph2	TACACCCCGGAACCAGATAC	CAAAGGATTTCACACACGCC

[a] All the primers were used with the optimal annealing temperature at 60°C, except for Htr1b (at 60.5 °C) and Htr2c (at 61.9°C).

Abbreviations: *Acox1*, Acyl-CoA Oxidase 1; *Agrp*, Agrouti-related Protein; B2m, Beta-2-Microglobulin; *Canx*, Calnexin; *Cat*, Catalase; *Cs, Citrate synthase*; *Gpx3*, Glutathione peroxidase 3; *Htr1b*, 5-Hydroxytryptamine Receptor 1B; *Htr2c,* 5-Hydroxytryptamine Receptor 2C; *Ido1,* Indoleamine 2,3-Dioxygenase; *Ido2*, Indoleamine 2,3-Dioxygenase 2; *Nampt*, Nicotinamide Phosphoribosyltransferase *Nmnat1,* Nicotinamide Nucleotide Adenylyltransferase 1; *Nmnat2,* Nicotinamide Nucleotide Adenylyltransferase 2; *Nmnat3,* Nicotinamide Nucleotide Adenylyltransferase 3; *Nmrk1,* Nicotinamide Riboside Kinase 1; *Nmrk2,* Nicotinamide Riboside Kinase 2*; Npy,* Neuropeptide Y; *Mthfs,* Methenyltetrahydrofolate Synthetase; *Obrb,* Leptin Receptor; *Pomc,* Proopiomelanocortin; *Ppargc1a*, Peroxisome proliferator-activated receptor gamma coactivator 1-alpha; *Ppia*, Peptidylprolyl Isomerase A; *Prdx3,* Peroxiredoxin 3; *Qdpr,* Quinoid Dihydropteridine Reductase; *Qprt,* Quinolinate Phosphoribosyltransferase; *Socs3*, Suppressor of cytokine signaling 3; *Sod1,* Superoxide Dismutase 1; *Sod2,* Superoxide Dismutase 2; *Tdo2,* Tryptophan 2,3-Dioxygenase; *Tph1,* Tryptophan Hydroxylase 1; *Tph2,* Tryptophan Hydroxylase 2.

Chapter 6

General discussion

Major findings

The aim of this thesis was to elucidate the effects of the dietary nicotinamide riboside (NR) on whole body metabolic health as well as its associated molecular and physiological regulation. The diets used throughout the studies in this thesis were semi-purified well-defined diets, containing a low, but adequate, level of tryptophan (Trp) and using NR as an exclusive source of vitamin B3. To understand effects on the whole body level, MRI was employed to monitor changes in body composition over time as well as a standardized indirect calorimetry based challenge tests to assess metabolic flexibility and oral glucose tolerance tests (OGTT) to assess glucose tolerance. Both indirect calorimetry and OGTT were used to determine the capacity to respond to perturbation of metabolic homeostasis. At the tissue level, the focus was mainly on morphology and molecular regulation in white adipose tissue (WAT), although transcriptional responses in skeletal muscle and brain were also examined. The major findings were:

- 30 mg NR per kg diet was most beneficial for metabolic health, based on metabolic flexibility, WAT morphology and gene expression (**Chapter 2**).
- High dose of NR (9000 mg NR per kg diet) impaired metabolic flexibility and glucose tolerance, and induced WAT dysfunction including a decreased insulin sensitivity and aggravated inflammation (**Chapter 3**).
- Vitamin B3 withdrawal resulted in a mild vitamin B3 deficiency, showing a reduced insulin sensitivity and a downward tendency of metabolic flexibility (**Chapter 4**).
- The downregulation of *Anp32a*,*Tnk2* and the upregulation of *Mapk1*, *Map2k1*, *Mthfs, Mthfsl* and *Qdpr* were proposed as a WAT transcriptional signature marker for mild vitamin B3 deficiency (**Chapter 4**).
- Vitamin B3 deficient diet (5 mg NR per kg diet) led to the upregulation of *Mapk1* and *Mthfs* in hypothalamus, while high dose of NR (900 mg NR per kg diet) induced the upregulation of hypothalamic *Tdo2*. The regulation of these genes indicated that tetrahydrofolate (THF) metabolism and Trp metabolism may be affected in the brain by dietary vitamin B3 (**Chapter 5**).

The effects of dietary NR on metabolism

Dietary NR affected metabolic flexibility in a dose-dependent manner (**Chapter 2, 3** and **4**). This altered metabolic flexibility was most likely associated with insulin-dependent glucose metabolism. Besides, dietary NR may have impacts on either Trp metabolism or THF metabolism, depending on the dose of NR. This will be discussed. The metabolic fate of dietary NR will be discussed, since understanding how dietary NR is metabolized upon entry into the body is important for the interpretation of its metabolic effects. In view of the importance of NAD^+ for sirtuin activity, I will also discuss our preliminary analysis of SIRT1 and SIRT3 activity. For convenience, the 0, 5, 15, 30, 180, 900, and 9000 mg NR per kg diet doses of NR will be referred to as 0NR, 5NR, 15NR, 30NR, 180NR, 900NR, and 9000NR, respectively, throughout this chapter. In addition, the animal study described in **Chapter 2** and **Chapter 5** will be defined as NR dose-response study, i.e. the 5-15-30-180-900NR study, and the animal studies described in **Chapter 3** and **Chapter 4** will be defined as NR extreme-dose studies, i.e. the 0-30NR and 30-9000NR study.

The metabolic fate of NR

The major site of vitamin B3 release from the diet and its absorption is the small intestine [1]. Once taken up, vitamin B3 is transported via the bloodstream and then metabolized in the liver and other organs. The vitamin B3 metabolome in circulation and liver are responsive to dietary vitamin B3 and have been used as a reflection of vitamin B3 status [2-11]. We assessed the NR metabolome in serum and liver of mice fed a wide dose range of dietary NR (**Chapter 2**), but to our surprise, there was no clear dose-response pattern. Despite NR being the exclusive source of vitamin B3 in the diet, NR was maintained at a trace amount in serum and liver. In contrast, nicotinamide (Nam) was abundant, with the levels being around 5~10 times higher than NR in all dose groups, and is likely to be the predominant form of vitamin B3. 900NR significantly elevated serum levels of Nam compared to all lower doses tested. This is in line with multiple other studies that showed that orally delivered NR at a pharmacological dose hardly elevated levels of circulating NR or liver NR, instead it boosted levels of circulating Nam or liver Nam [8-11].

In mammalian cells *in vitro*, NR can be imported and subsequently converted into NAD^+ [6, 11-17]. In this process, equilibrative nucleoside transporters (ENTs, SLC29), purine nucleoside phosphorylase (PNP) as well as NRK1 and NRK2 play a crucial role [12, 14, 15, 17]. ENTs are the putative NR transporters [14, 17]. PNP enzymatically converts NR into Nam and ribose-1-phosphate [16, 18], and nicotinamide riboside kinase (NRK) isoforms are the key enzymes in NR conversion to NAD, via phosphorylation of NR to NMN (Fig. 2 in **Chapter 1**). We found that *Nrk1* and *Nrk2* expression was not altered by dietary NR interventions in multiple tissues (**Chapter 2**). No significant changes were found in the transcript levels of ENTs, PNP and the NRK isoforms in WAT according in response to extreme doses of NR (**Chapter 3** and **4;** Fig. 1A). Since none of the NR metabolizing enzymes responded to NR dosage on the gene expression level in peripheral tissues, these findings could reflect the early intestinal conversion of NR into NAM, before it reaches the circulation. In agreement, previous studies using NR, double-labelled with stable isotopes, demonstrated that orally administrated NR was not delivered intact to the liver and peripheral tissues due to cleavage of NR into Nam [8, 11], while intravenous injection of NR could markedly enhance NR in several organs, including liver, kidney and muscle [11, 19].

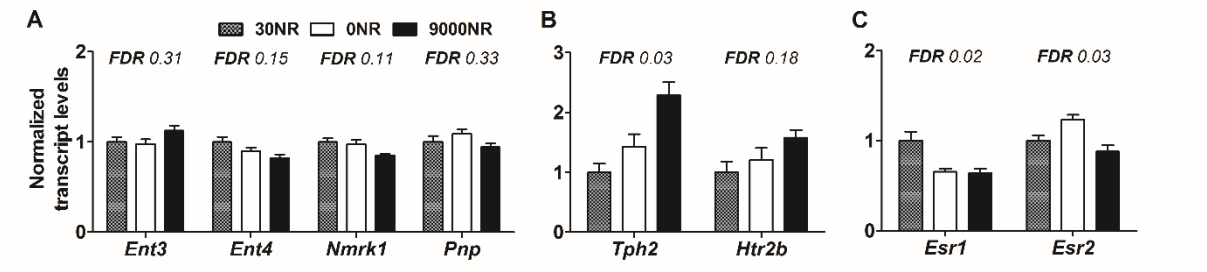

Figure 1. Transcript levels of WAT genes that are discussed in this chapter. The whole transcriptome of WAT from the refed animals in NR extreme-dose studies were analyzed. Genes involved in NR metabolism (A), serotonin synthesis (B) and estrogen receptor signaling (C) are shown. The transcript levels of each gene were normalized by mean transcript values of 30NR at 1. Data analysis was done using ANOVA test followed by Benjamini-Hochberg procedure and shown as mean±SEM. False discovery rate adjusted p-values (FDR)<0.05 is considered statistically significant.

It is conceivable that the irreversible conversion of NR into Nam may occur upon uptake in the small intestinal epithelial cells [20]. We therefore examined the expression in the mucosa of the small intestine of two other key NR metabolic genes; *Nampt* and *CD157*. Nicotinamide phosphoribosyltransferase (NAMPT) performs the first, rate-limiting step of the Nam salvage pathway. *CD157* encodes an enzyme that can convert NR into Nam on plasma membrane (Fig. 2 in **Chapter 1**). No significant differences were found in the expression of these genes in our NR dose-response study (Fig. 2A). This may be because analysis was done in the fasting condition, although differential steady-state levels could be expected. Nevertheless, under refed conditions, small intestinal mucosa *CD157* mRNA levels tended to be increased, while *Nampt* mRNA levels were significantly elevated in 9000NR compared to 0NR (Fig. 2B), indicating an activation of Nam salvage pathway in response to high dose NR. This may be due to an increased Nam influx. How intestinal cells transform NR to Nam awaits further analysis, which should involve the biochemical functions and activities of CD157, the NRK pathway and PNP.

Thus, NR is likely to be converted to Nam before entering circulation and reaching target organs. This is not the full picture of NR metabolism and other metabolites may be of functional importance as well. Very recently, nicotinic acid adenine dinucleotide (NAAD) was identified as a novel biomarker for NR administration in mice and humans [9, 19, 21, 22]. Regretfully, we did not analyze NAAD, since at that time NAAD was not expected to be involved in the NRK pathway or the salvage pathway (Fig. 2 in **Chapter 1**). How NR boosts NAAD pool is still unknown and awaits further research.

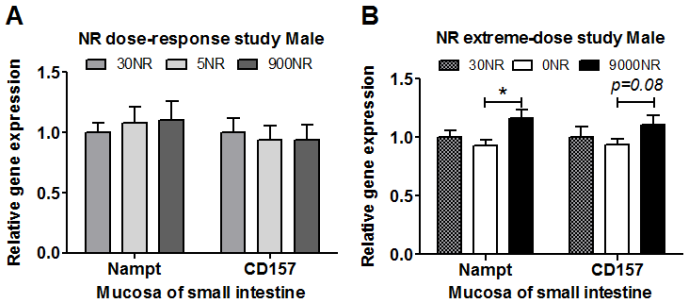

Figure 2. Gene expression of *Nampt* and *CD157*. Mucosa samples were harvested from the fasting animals in NR dose-response study (A) and from the refed animals in NR extreme-dose studies (B). Details of animal study are in **Chapter 2, 3** and **4**. Data are mean±SEM, and the analysis between 0NR and 9000NR is based on a Students' unpaired t-test. * $p<0.05$.

Changes in insulin-dependent glucose metabolism

In the NR dose-response study (**Chapter 2**), we observed a reduced metabolic flexibility in mice treated with 5NR and 900NR, compared to those treated with 30NR (control group). The reduction in metabolic flexibility has been confirmed in NR extreme-dose studies (**Chapter 3** and **Chapter 4**), in which the animals were treated with more extreme doses of NR. In these two independent animal studies, that confirm each other, the decrease in metabolic flexibility was most prominent in the first few hours during the refeeding transition from fat oxidation to carbohydrate oxidation, indicating that postprandial carbohydrate metabolism might be hampered. Further OGTT results show that mice treated with a high dose of NR as well as mice fed a vitamin B3 withdrawal diet tended to have lower glucose tolerance compared to mice fed a diet with 30NR, with both the high and the low dose treatment resulting in a decreased insulin sensitivity, as compared to their control. These results suggest

that the compromised metabolic flexibility can be attributed mainly to impaired insulin-dependent glucose metabolism in high dose NR-treated mice and in vitamin B3 deficient mice.

WAT plays an important role in the regulation of metabolic flexibility and systemic insulin sensitivity [23-25]. Therefore, we focused on WAT. In the NR dose-response study, we observed a distinct distribution of small (range), medium (range) and large (range) adipocytes between the groups. Mice on the recommended NR level (30NR) displayed more small adipocytes, compared to those on the low NR dose (5NR) and more small as well as large adipocytes compare to the high NR dose (900NR). Smaller adipocytes are thought to be more efficient in insulin-stimulated glucose uptake [26, 27]. Large adipocytes, on the other hand, are better able to buffer fatty acid flux and promote lipid mobilization [28]. This morphologic feature of WAT and its related functionality may be associated with the higher metabolic flexibility that was observed in mice on 30NR.

An impaired WAT glucose metabolism is confirmed by the reduced glucose transporter type 4 (GLUT4) levels in WAT of mice fed with high dose NR diet (9000NR, **Chapter 3**) as well as with vitamin B3 withdrawal diet (0NR, **Chapter 4**), compared to the animals on 30NR. In both cases also a down regulated in WAT insulin signalling was suggested, but the mechanisms underlying this down regulation are not the same for the 9000NR and the 0NR interventions (Fig. 2). While WAT peroxisome proliferator-activated receptor γ (PPARγ) repression is considered as a core of the molecular mechanism to explain for decreased insulin sensitivity in high dose NR-treated mice, mitogen-activated protein kinase kinase/mitogen-activated protein kinase (MEK-/ERK) activation was proposed as a key WAT response in association with a negative effect on insulin sensitivity in vitamin B3 deficient mice. This is schematically presented in Fig. 3.

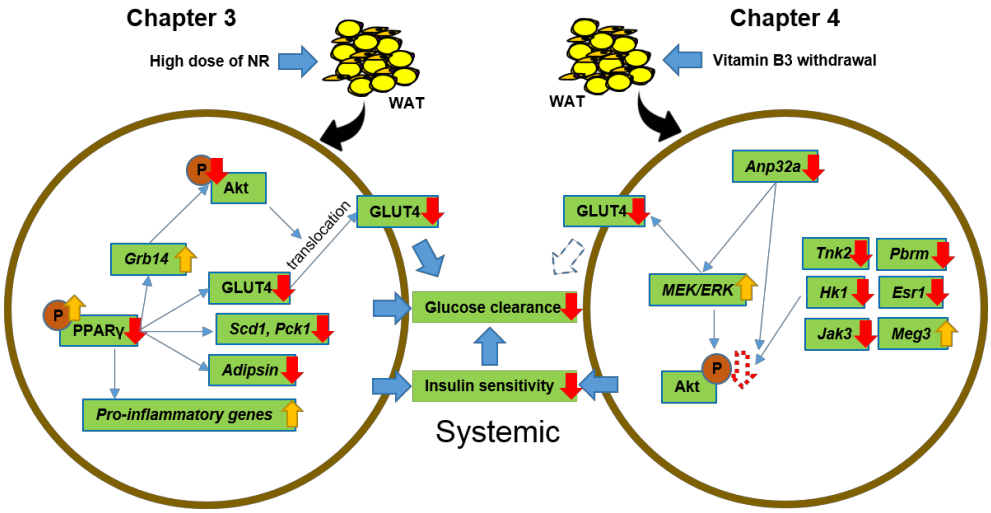

Figure 3. Schematic representation of the mechanisms of down regulated WAT insulin sensitivity in response to high dose NR (left) and vitamin B3 withdrawal (right). The genes responding to vitamin B3 withdrawal, including *Mapk1*, *Map2k1*, *Map2k2*, *Anp32a*, *Tnk2*, *Pbrm*, *Hk1*, *Jak3*, and *Meg3*, were not significantly regulated in WAT of the high dose NR feeding mice (data not shown), further supporting the mechanistic differences between high dose NR and vitamin B3 withdrawal in term of insulin sensitivity regulation.

PPARγ is best known as a master regulator of adipogenesis, but it also plays a crucial role in insulin signalling and inflammation of WAT [29-33]. PPARγ repression leads to altered regulation of a set of PPARγ-target genes. The transcriptional regulation of these genes can have impact on insulin sensitivity through distinct ways, which are discussed in more detail in **Chapter 3**. MEK/ERK activation hampers insulin-stimulated glucose utilization in adipocytes [34, 35]. This activation can also facilitate lipolysis in obese adipocytes [36], in agreement with the upregulation of lipolysis genes in vitamin B3 deficient WAT (**Chapter 4**). The molecular signature of a reduced insulin sensitivity and an increased lipolysis in WAT supports a bioenergetic shift from glucose metabolism to fatty acid metabolism in vitamin B3 deficient mice. This notion is consistent with the lower RER in mice fed *ad libitum* a vitamin B3 deficient or vitamin B3 withdrawal diet as can be seen in **Chapter 2** and **Chapter 4**.

Effects of dietary NR on Trp metabolism
Among different purposes of dietary Trp (Fig. 2 in **Chapter 1**), its use for *de novo* NAD^+ synthesis accounts for majority of overall dietary Trp disposal [37-39], linking Trp metabolism tightly to the NAD^+ pool. In advance we expected that absence or deficiency of exogenous vitamin B3 would lead to an increased influx of NAD^+ from Trp to maintain the NAD^+ pool in the normal range. However, we found no evidence for this assumption. No sign, at least on the gene expression level, of enhanced *de novo* NAD^+ synthesis was observed in liver, skeletal muscle, mucosa of small intestine, WAT and nor hypothalamus (**Chapter 2**, **Chapter 4** (data not shown) and **Chapter 5**). Furthermore, levels of the vitamin B3 metabolome and Trp in circulation and liver were similar between 5NR and 30NR (**Chapter 2**). Collectively, these results suggest that *de novo* NAD^+ synthesis pathway is not responsive to the absence or the deficiency of exogenous vitamin B3 when dietary Trp level is adequate. In full agreement, mice fed a niacin-free, 20% casein diet demonstrated an unchanged liver TDO and QPRT activity, coinciding with normal levels of plasma and liver Trp, and a normal urinary metabolome of the *de novo* pathway [7, 40].

The high dose NR intervention, on the other hand, induced the activation of the first step of the *de novo* pathway in the hypothalamus, indicated by the upregulation of *Tdo2* and *Ido1* and the absence of significant changes in expression of more downstream genes, compared to the 30NR group (**Chapter 5**). Circulating Trp is able to cross the brain blood barrier and taken up by brain. The activation of the first step of the *de novo* pathway in the hypothalamus is unlikely to be an adaptive response to augment uptake of Trp from circulation, since the serum Trp level was slightly higher and not lower in high dose NR fed mice (**Chapter 2**). On the contrary, we tend to believe that this exclusive upstream activation of the *de novo* pathway may result in increased levels of the upstream metabolites, such as kynurenine (Kyn) and quinolinic acid (QA). Furthermore, *Tph1* and *Tph2*, the genes encoding tryptophan hydroxylases, remain unchanged, possibly indicating that serotonin synthesis was not adaptively enhanced to compensate for a potential loss of the precursor Trp. This may potentially lead to serotonin deficiency [41, 42]. Kyn and QA are neurotoxic [39, 43], whereas serotonin serves to be neuroprotective [44]. Combined, the putatively altered levels of these metabolites may induce impaired hypothalamus function, which can have an impact on motor function [45-47]. This coincides with the declined

grip strength and rotarod performance in mice treated with high dose of NR (**Chapter 5**). Whether tryptophan 2,3-dioxygenase 2 (TDO2) and indoleamine 2,3-dioxygenase 1 (IDO1) are more active on the protein level and whether serotonin signaling is affected in response to high dose NR in the hypothalamus are of great interest. The animal study described in **Chapter 3** will allow us to dive deeper into these questions. Interestingly, the genes of the *de novo* pathway were not affected in the other tissues of mice treated with high dose NR that were tested. This indicates that the high dose NR-induced transcriptional regulation of the *de novo* pathway is tissue-specific and may be associated with an impaired hypothalamus function.

Effects of dietary NR on THF metabolism

One of the intriguing findings in this thesis was the strong upregulation of *Mthfs* in WAT and hypothalamus of the vitamin B3 deficient mice (**Chapter 4** and **Chapter 5**). *Mthfs* encodes methenyltetrahydrofolate synthetase (MTHFS), which catalyses the conversion of 5-formyl THF to 5,10-methenyl THF [48]. 5-formyl THF accounts for 3%-7% of total cellular folate in mammalian cells [49] and serves as a stable storage form of folate, essential for homeostasis of THF metabolism via MTHFS [48, 49]. THF is involved in a variety of metabolic processes, including purine and pyrimidine biosynthesis, amino acid metabolism and one-carbon metabolism [50, 51]. In **Chapter 4** and **Chapter 5**, the elevation of *Mthfs* gene expression in the vitamin B3 deficient mice, together with other gene expression changes, implied an enhanced *de novo* synthesis of purines. Supporting this idea, overexpression of *Mthfs* has been shown to boost the *de novo* purine synthesis via the augmented THF metabolism [48, 52]. Coincidently, levels of the THF metabolome and purines were increased in response to the *Nampt* silencing-induced NAD^+-depletion [53, 54]. In *Nrk2*-knockout skeletal muscles, the gene expression of PNP, which is also involved in purine metabolism, was induced by 2-fold [16]. Together, these observations suggest that the enhancement of compensatory THF metabolism and purine metabolism is a signature of a disturbed vitamin B3 metabolism.

Why is the enhancement of compensatory THF metabolism and purine metabolism observed in vitamin B3 deficiency? One potential explanation is given in **Chapter 4**. In brief, vitamin B3 deficiency may cause an increased NADH/NAD^+ ratio, which potentiates the activity of pteridine metabolic enzymes [55]. Another explanation may be that augmented THF metabolism can serve as a compensatory response to impaired DNA repair due to low PARP activity resulting from vitamin B3 deficiency. 5,10-methylene THF, which can be generated from 5,10-methenyl THF, is essential for the conversion of deoxyuridylate to thymidylate, which is required for incorporation of uracil into DNA [56]. Uracil misincorporation may ultimately result in DNA double-strand breakages (SBs) [57, 58]. Increased uracil misincorporation due to folate deficiency has been implicated in the loss of a capacity to repair DNA SBs in the immortalized human keratinocytes exposed to solar simulated light or H_2O_2 [59]. One the other hand, folate supplementation was shown to elevated folate status in healthy humans, concomitant with a remarkable decrease in uracil misincorporation in lymphocyte DNA [60]. In this thesis, long-term obesogenic diet feeding may have induced oxidative DNA damage [61], potentiating the demand of DNA SBs repair. DNA SBs repair requires PARP1 mediated poly(ADP-ribosyl)ation.

Rats fed a vitamin B3 deficient diet showed a markedly reduced PARP activity [62-65], in parallel with higher susceptibility to drug-induced DNA damage and with delayed DNA SBs repair [65]. In these animals, decreased tissue NAD^+ levels were found, while tissue $NADP^+$ and NADPH remain stable, indicating that $NADP^+$/NADPH pool appears more resistant to a dietary vitamin B3 deficiency. This notion is particularly relevant because THF metabolism is largely dependent of $NADP^+$/NADPH [66]. Enhanced THF metabolism may reduce the chance of uracil misincorporation, potentially preventing impaired DNA SBs repair from being further worsened. Validation of the mechanistic explanations awaits dedicated studies, that should include metabolome analysis of NAD, THF, and purines.

Sirtuin activities

Changes in sirtuin-mediated post-translational modifications serve as a measure of sirtuin activity. Sirtuin activity is NAD^+-dependent and the processes it regulates are involved in various aspects of cellular physiology [67, 68]. This explains why sirtuin activity is a target for analysis in many vitamin B3 intervention studies. Much attention has been given to the enhancement of sirtuin activities by high dose vitamin B3 supplementation. On the other hand, little attention has been given to the alterations of sirtuin activities induced by dietary vitamin B3 deficiency. In this thesis, we focused on SIRT1 and SIRT3. Mitochondrial superoxide dismutase (SOD2) is thought to be uniquely deacetylated by SIRT3 [69], and its deacetylation induces its anti-oxidant activity [6, 69, 70]. Since eWAT *Sod2* gene expression displayed a dose-dependent pattern, we assessed SOD2 acetylation using eWAT samples from 5NR, 30NR and 900NR groups, also because anti-acetylated SOD2 (Ac-SOD2) and anti-SOD2 antibodies are commercially available. The analysis based on semi-quantification showed that SOD2 acetylation was not significantly altered in response to either vitamin B3 deficiency or high dose NR (Fig. 4), suggesting that SIRT3 activity remained unchanged. One of the targets of SIRT1 is p65. p65 is a subunit of the nuclear factor NF-kappa-B complex (NFκB), a transcriptional activator of pro-inflammatory genes [71]. The acetylation (Ac-p65) and phosphorylation (p-p65) of the p65 subunit are implicated in the activity of NFκB complex [72]. We examined Ac-p65 and p-p65 in eWAT of mice fed a 9000NR, in which we found the transcriptional activation of a set of pro-inflammatory genes. Compared to 30NR, p-p65/total p65 ratio was increased in the 9000NR group while Ac-p65/p65 was reduced (Fig. 5), making it difficult to conclude on the activity of NFκB complex. The reduced ratio of Ac-p65/p65 in the 9000NR group may indicate an enhanced SIRT1 activity. However, the bands of Ac-p65 and Ac-SOD2 were in a low visibility, suggesting low affinity of antibodies used binding to target protein. Based on these trial experiments, I may conclude that the current antibodies are hardly suitable to assess sirtuin activity, at least in adipose tissue, and a need exists for alternative methods to determine sirtuin activity that are more reliable like IP, immunofluorescence, and proteomics.

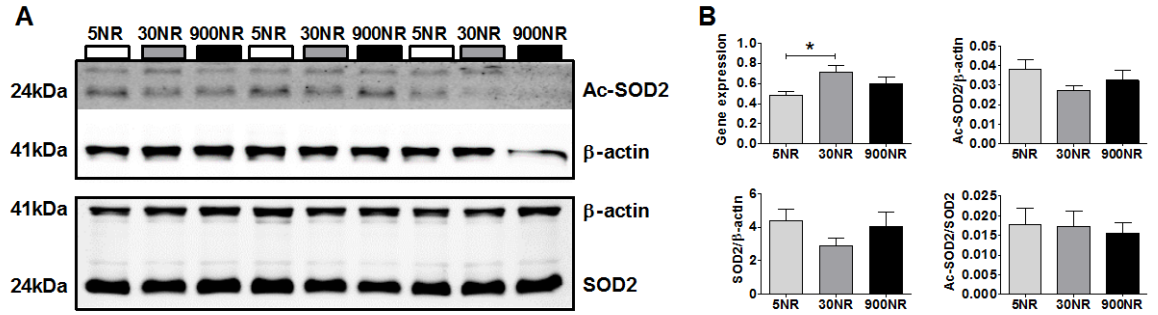

Figure 4. Immunoblot analysis for SOD2 acetylation. In NR dose-response study, SOD2 acetylation at lysine site K68 (Ac-SOD2) and total SOD2 levels in eWAT were measured by immunoblotting, using β-actin as a loading control (B). Gene expression of SOD2 was analyzed and densitometry analysis on the ratio of Ac-SOD2/β-actin, SOD2/β-actin and Ac-SOD2/SOD2 were done (B) (n=8-12 per NR group). Data are analyzed using one-way ANOVA followed by Dunnett's multiple comparison test, with 30NR as control and presented as mean±SEM. * p<0.05.

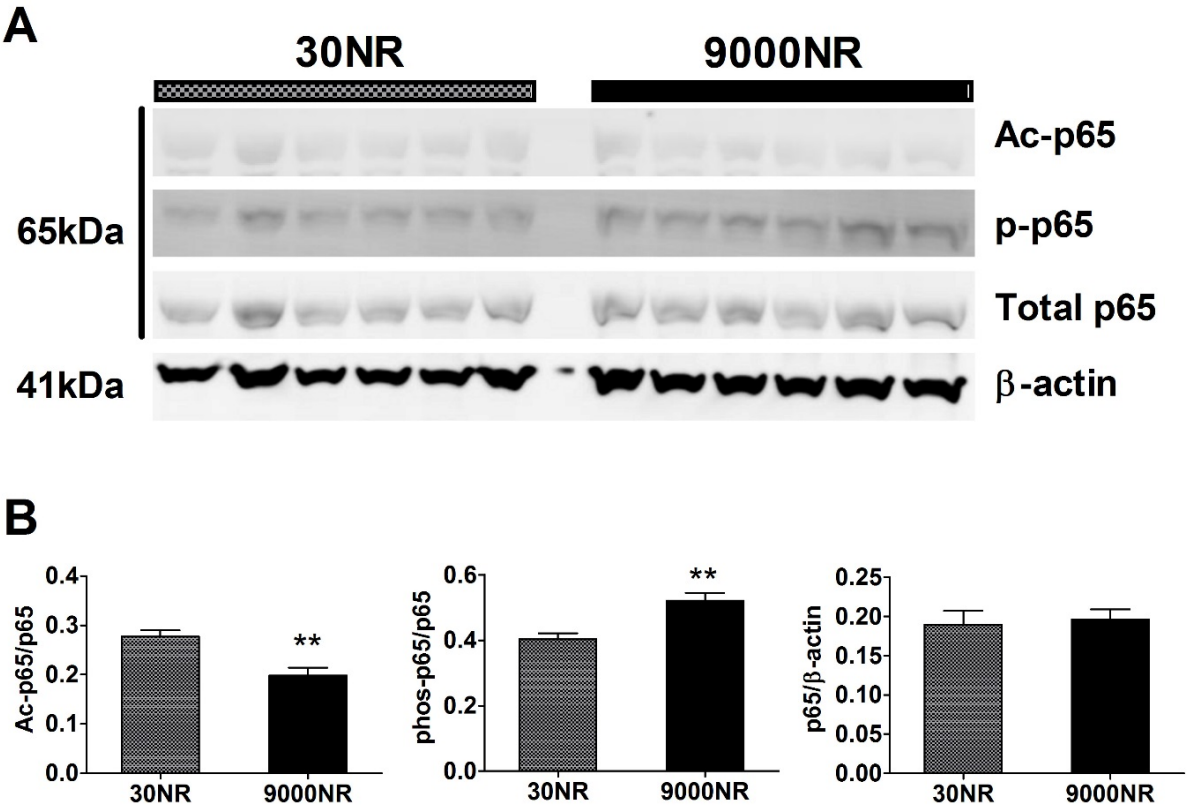

Figure 5. Immunoblot analysis for p65 activity. In NR extreme-dose studies, p65 acetylation (Ac-p65 K310) and phosphorylation (p-p65 Ser536) were measured by immunoblotting in eWAT, using β-actin as a loading control (A). Densitometry analysis on the ratio of Ac-p65/p65, p-p65/p65 and p65/β-actin were done (B) (n=6 per NR group). Data are analyzed using student's t test and presented as mean ± SEM. ** p<0.01.

The role of vitamin B3 in nervous function

The central nervous system (CSN) disorders are commonly seen in Pellagra, the classical vitamin B3 deficiency disease [73, 74]. This phenomenon is thought to be linked with the disturbed NAD^+ metabolism in the CSN [75, 76]. However, little is known about how the nervous system responds to vitamin B3 deficiency in WAT.

Recent studies have shown that the sympathetic nervous system (SNS) innervate WAT and can modulate lipid metabolism of WAT [77, 78], whereas WAT denervation of this nervous system has direct influences on adipocyte growth and cellularity [79, 80]. The **Chapter 4** elaborates molecular responses with respect to nerve regulation to a mild vitamin B3 deficiency, showing an enhanced BH4 synthesis and upregulation of neurogenesis-related genes. It can be questioned whether neurogenesis was promoted in WAT in response to a mild vitamin B3 deficiency. This could be pursued by quantification of nerve cells in WAT sections.

High dose of NR induces more than 2.5-fold upregulation of *Tph2* gene in WAT, compared to 30NR (Fig. 1B). *Tph2* encoding tryptophan hydroxylase isoform 2 (TPH2) is predominantly expressed in neurons and responsible for serotonin synthesis, thus being considered as a surrogate marker of neuronal serotonin [81-83]. The transcription of *Htr2b*, a serotonin receptor gene, tends to be increased by the high dose of NR treatment (Fig. 1B). Together, these observations may implicate an enhanced serotonin synthesis in nerve cells of WAT responding to high dose of NR, which is potentially related to the protection of nervous function. Considering that high vitamin B3 intake has been demonstrated its dual role in the regulation of nervous function, i.e. neurodegeneration and neuroprotection [84, 85], it is of interest to investigate how exactly high dose of NR affects the neurons in peripheral tissues.

Doses of vitamin B3 in health maintenance

Direct data on the requirement of vitamin B3 in mice were lacking before we started the research presented in this thesis. The requirement of vitamin B3 for rodents is 15 mg/kg diet containing a minimum of 0.1 % (w/w) Trp. Although this requirement is still widely accepted [86-88], there are several limits regarding its evaluation. First, the requirements were based on a study in rats and no studies were done in mice. Second, the diet may not have been optimal to establish deficiency. For instance, the niacin that was used can refer to NA and/or Nam, as a result of the industrial limitations in obtaining pure B3-vitamin in the 1940s. In addition, the thiamine (vitamin B1) level in the diet (2 mg/kg diet) was less than its requirement (4 mg/kg diet) for growing rats, which may have posed a risk for vitamin B1 deficiency [86]. Such a deficiency can affect the conversion of Trp to niacin [89]. Third, the animals were weanling rats, which are more susceptible to a nutrient deficiency compared to adult animals. This may hamper an evaluation of the requirement over a longer time span that has been adopted nowadays. Fourth, body weight gain was used as readout. This may miss the opportunity to measure the molecular and physiological alterations that can occur in the early stage of an intervention. In this thesis, we have taken all these factors into account.

In **Chapter 2**, among a wide range of NR doses, i.e. 5NR, 15NR, 30NR, 180NR, and 900NR, we propose 30NR as the optimal dose for male adult mice for optimal metabolic health and then continued to use this amount of NR as control in the remaining chapters. As expected, mice on 30NR show a greater metabolic flexibility, higher insulin sensitivity, better WAT function (**Chapter 3** and **Chapter 4**), as well as better motor performance, which may be linked with an optimal gene expression signature in hypothalamus (**Chapter 5**), compared to those on either less NR or high

levels of NR. Even so, there is still room left for the argument that 30NR is the most beneficial level of NR for metabolic health, since no concentrations around 30NR were examined. 30NR is equivalent to approximately 2.3 mg NR/kg BW/day for mice, based on our dose-response study. Of note, NR used in this thesis has a molecular weight of 290.7 gram per mol, which is approximately 2.37 times higher than that of NA and Nam but lower than that of NMN. In this sense, the concentration of 2.3 mg NR/kg BW/day for mice may be an overestimate for NA and Nam while an underestimate for NMN, given that these B3 vitamins may have a similar metabolic fate at the physiological level [90].

The recommended daily vitamin B3 intake for humans is based on biomarkers for niacin status, such as erythrocyte NAD^+ levels and plasma as well as urinary niacin metabolites [91]. In our study, despite a decreased metabolic flexibility in 5NR and 15NR compared to 30NR, the vitamin B3 metabolome that we measured in the serum and the liver were almost the same. This implicates that a threshold of vitamin B3 requirement based on the general biomarkers of niacin status may not represent an eligible health condition when facing a metabolic challenge. To achieve best health, we ought to investigate an optimal intake of vitamin B3 for human subjects by using homeostatic challenge strategies [92].

Clearly, our data suggest that a high dose of NR impairs metabolic health. 900NR (on average equivalent to approximately 70 mg/kg BW/day) compromises metabolic flexibility and motor performance. A more extreme dose of 9000NR (equivalent to approximately 700 mg/kg BW/day) aggravates the detrimental impacts on metabolic health. In line, NR at 300 mg/kg BW/day worsens exercise performance in rats [93, 94], potentially associated with the dysregulation in redox and energy metabolism. In a human trial, 2 g NR daily intake resulted in an elevated plasma triglycerides (TG) level after 3-month treatment [95]. Similarly, this elevation of circulating TG level was also seen in elderly individuals with daily consumption of 250 mg NR combined with 50mg pterostilbene for 2 months [96]. The other elderly cohorts who received double dosed NR showed 5-fold increase in plasma total cholesterol (TC) after treatment, as compared to those who had placebo [96]. This agrees with the elevated serum TC in mice treated with 9000NR (**Chapter 3**). Despite the observed adverse effects, these two human studies stressed on an increase in biomarkers for niacin status in the NR-treated subjects. Other human studies found an increased NAD^+ metabolome level after NR administration in healthy subjects, but did not observe remarkable improvement of health [9, 21, 97]. We question the usefulness of boosting the NAD^+ metabolome regardless of the health condition or NAD^+ insufficiency. In subjects that are still capable of maintaining homeostasis, NR has no therapeutic effect [22, 98], or can even compromise health status as discussed above. Therefore, the use of NR at high doses should be advised against, unless there is a clear medical need, as, for example, in conditions of deficiency. This notion is also appropriate for the other B3 vitamins, i.e. NA, Nam, and NMN [85].

Factors that may account for inconsistencies between results of this thesis and other studies

Since NR was discovered as a novel naturally existing vitamin B3 [13], a variety of studies have shown that high dose NR supplementation can effectively boost NAD^+ level in multiple organs of mice, including liver [6, 9-12, 99-101], skeletal muscle [6, 8, 11, 16, 100, 101], brown adipose tissue [6], and brain [102], as well as in blood cells in humans [9, 21, 96, 97]. Most of these studies have demonstrated improved metabolic profiles upon high dose of NR, which is inconsistent with our findings, presented in this thesis. To provide an explanation, we would like to highlight one key genetic difference in the mice models that were used in the various studies. The C57Bl/6JRccHsd mouse strain that was used in our studies contains a functional nicotinamide nucleotide transhydrogenase (*Nnt*) gene. However, the C57Bl/6J model that is used in the studies showing beneficial effects of high dose NR supplementation is well-known to harbour a spontaneous mutation in *Nnt,* which is responsible for an impaired glucose tolerance and decreased insulin secretion in this model [103, 104]. NNT is a mitochondrial inner membrane located protein that catalyses the reversible transfer of hydrogen between NAD^+ and $NADP^+$. It has been shown that loss of NNT decreased the NAD^+/NADH ratio whereas NNT overexpression increased this ratio [105, 106], suggesting that altered NNT expression or function can influence NAD^+ homeostasis. C57Bl/6J mice have been shown impaired glucose tolerance and insulin secretion compared to the *Nnt* knock-in transgenic model, the C3H/HeH and C57Bl/6N mice which have a complete *Nnt* gene [103, 104, 107]. Unfortunately, NAD^+ homeostasis was not examined in these studies. However, other animal models or healthy human subjects with a functional *Nnt* gene did not show a beneficial effect of high dose NR supplementation [9, 21, 93, 94, 97]. For example, NR supplementation impaired redox homeostasis in skeletal muscle of young rats using a rat model that contained the functional *Nnt* gene, leading to decreased exercise performance [93, 94]. The mechanisms underlying the significant role of NNT in high dose NR induced effects remain unknown. Nevertheless, considering the fact that NNT is generally expressed and functional in humans [108] and the increasing concerns on the validation of the C57Bl/6J model for human diabetes research [103, 104, 107], further investigation using the proper models is warranted to fully understand biological functions of NR before more human trials are being performed.

We used reduced levels of dietary Trp of 1.15 and 1.4 gram per kg diet (equivalent to 86.3 and 105 mg/kg BW/day, respectively), as compared to the level of 2.3 gram per kg diet in normal rodent diet (equivalent to 172.5 mg/kg BW/day), which is the level of dietary Trp used in those studies observing beneficial effects of NR. An argument exists that dietary Trp, rather than vitamin B3, is the most effective source for NAD^+ yield in the liver [39]. This notion is supported by the findings in several studies [11, 109-111]. Enhanced NAD^+ biosynthesis from Trp in liver has been demonstrated in mice treated with high dose of Nam [112]. As discussed above, given that Nam is the major form in circulation and tissues after NR being absorbed, high dose NR feeding is also likely to promote the *de novo* NAD^+ synthesis. It is conceivable that the *de novo* NAD^+ yield is correlated with Trp intake. Compared to the normal rodent diet, less amount of Trp is available in our diet for the *de novo* NAD^+ synthesis when feeding high dose NR, probably leading to a relatively low ratio of NAD^+/Nam, which is implicated in a reduced activity of sirtuins in the liver or kidney [113]. It is worthy to mention that an average human intake of dietary Trp in the USA was around 826 mg

/day [114], equivalent to 11.8 mg/kg BW/day for a 70kg adult, while the Estimated Average Requirement for adults is even lower, with 4 mg/kg BW/day [115]. In terms of Trp intake on a body weight basis, the levels of dietary Trp used in this thesis are more close to human intake.

Recommendations for future studies

In light of multifunctionality of NAD^+ and diversity of enzymes involved in vitamin B3 metabolism, I believe that more implications for vitamin B3 in metabolism and cell function will be discovered. For instance, recently NAD^+ has emerged as an inhibitory neurotransmitter [116-118], indicating a potential possibility of vitamin B3 to play a role in neurotransmission. More attention on neurogenesis and neurotransmission should be given to the role of vitamin B3 in multiple parts of the nervous system, at least including the CNS and the SNS. **Chapter 4** implicates an induction of WAT neurogenesis by vitamin B3 deficiency. This can potentially be validated using research in cell models, with that are able to resemble the CNS and the SNS. Ideally, primary neurons that are derived from these two system are desirable for this research, as they are representative in terms of the properties of nerve cells *in vivo* [119]. Alternatively, cell models of sympathetic neurons that are developed from human pluripotent stem cells [120] or PC12 cell line [121] and models developed from the CNS stem cells have been established [122]. The focus should be on effects of low levels of vitamin B3. It is also interesting to re-examine THF metabolism and BH4 synthesis in such an in vitro nerve cell model. **Chapter 5** leaves a question open concerning the interaction between high dose of vitamin B3 and Trp metabolism. A similar setup of cell research with a focus on high levels of vitamin B3 and analyses at the metabolite (e.g. Trp, Kyn, QA, Nam/NAD^+ and serotonin), mRNA and protein (e.g. TDO/IDO and TPH) and physiological level (e.g. neurogenesis), including enzyme activity (e.g. TDO/IDO, TPH and SIRT1), will be helpful to understand this interaction and the consequences in more detail.

We are highly interested in the role of NNT in vitamin B3 homeostasis and it modulatory effect on high dose vitamin B3 interventions in particular, because we propose that the presence of a functional NNT protein in our mouse model can explain the high dose NR-induced metabolic decline that we observed, contrasting with the improved metabolic profiles that have been shown in the work of other laboratories [6, 10, 99, 123]. Wild type C57Bl/6JRccHsd mice and *Nnt* knockout mice fully backcrossed to a C57Bl/6JRccHsd genetic background, together with C57Bl/6J mice from Jackson lab as a negative control can provide a definite answer to our hypothesis. Preferably, multiple forms of vitamin B3 should be tested and the dose should be set at 300-400 mg/kg BW/day or 3-5 g/kg diet, a dose range that has been shown beneficial in multiple studies, with 30 mg vitamin B3/kg diet being as control. Metabolic flexibility and glucose tolerance should be measured as primary systemic parameters. Since loss of NNT leads to redox dysregulation [124], *Nnt* mutant animals may be vulnerable to vitamin B3 deficiency. Therefore, it is also of great interest to investigate how these animals respond to vitamin B3 deficiency, also because this is relevant to a group of population with NNT abnormalities, including those having familial glucocorticoid deficiency or left ventricular noncompaction [108, 125].

There are many reports showing distinct responses to a vitamin B3 intervention between sex, with hardly any mechanistic explanation for these distinctions [5, 98, 126-128]. In NR extreme-dose studies, we also included female mice and have obtained some preliminary results. Intriguingly, female mice fed a vitamin B3 withdrawal diet display a slower rate of fat mass accumulation and a higher metabolic flexibility, contrasting to what we observed in male mice on this diet (Fig. 5). This observation is inconsistent with the notion that women are more sensitive to Pellagra than men, which is probably attributable to a higher level of estrone in females [126]. Estrone has been shown to disturb the *de novo* pathway [126]. This hormone interacts with estrogen receptor (ESR) [129], mediating ESR signaling, which is linked with insulin signaling [130]. More importantly, we found *Esr1* gene expression in male WAT responsive to both vitamin B3 withdrawal and high dose NR (Fig. 1C). Therefore, I suggest that to take ESR signaling as a focus to understand the mechanistic distinctions between sex in response to vitamin B3 interventions.

Additionally, we have demonstrated that challenge tests are very useful to assess the optimal intake of vitamin B3 in mice. The strategies to challenge homeostasis have been established in human studies, such as fasting-refeeding challenges, exercises challenges and hyperglycaemic/hyperinsulinemic euglycemic clamp, and etc. [92, 131, 132]. Employing such strategies and analyzing metabolic flexibility and insulin responses are promising to improve the evaluation of optimal intakes of vitamin B3 in humans.

Conclusions

Based on our studies, 30 mg NR per kg diet (or 2.3 mg NR per kg body weight per day) is the amount of dietary NR that is optimal to maintain a good health for male adult mice fed a moderate high-fat diet containing a reduced, but sufficient, Trp level. Both inadequate intake and excessive intake of vitamin B3 can affect metabolic health, by impairing metabolic flexibility and insulin sensitivity, but the underlying mechanisms are distinct for the high and the low dose of vitamin B3. More studies aiming to investigate the role of vitamin B3 in nerve cell function and to investigate sex dependent difference are strongly encouraged. Molecular biomarkers for vitamin B3 deficiency have been proposed, and await further validation in human studies.

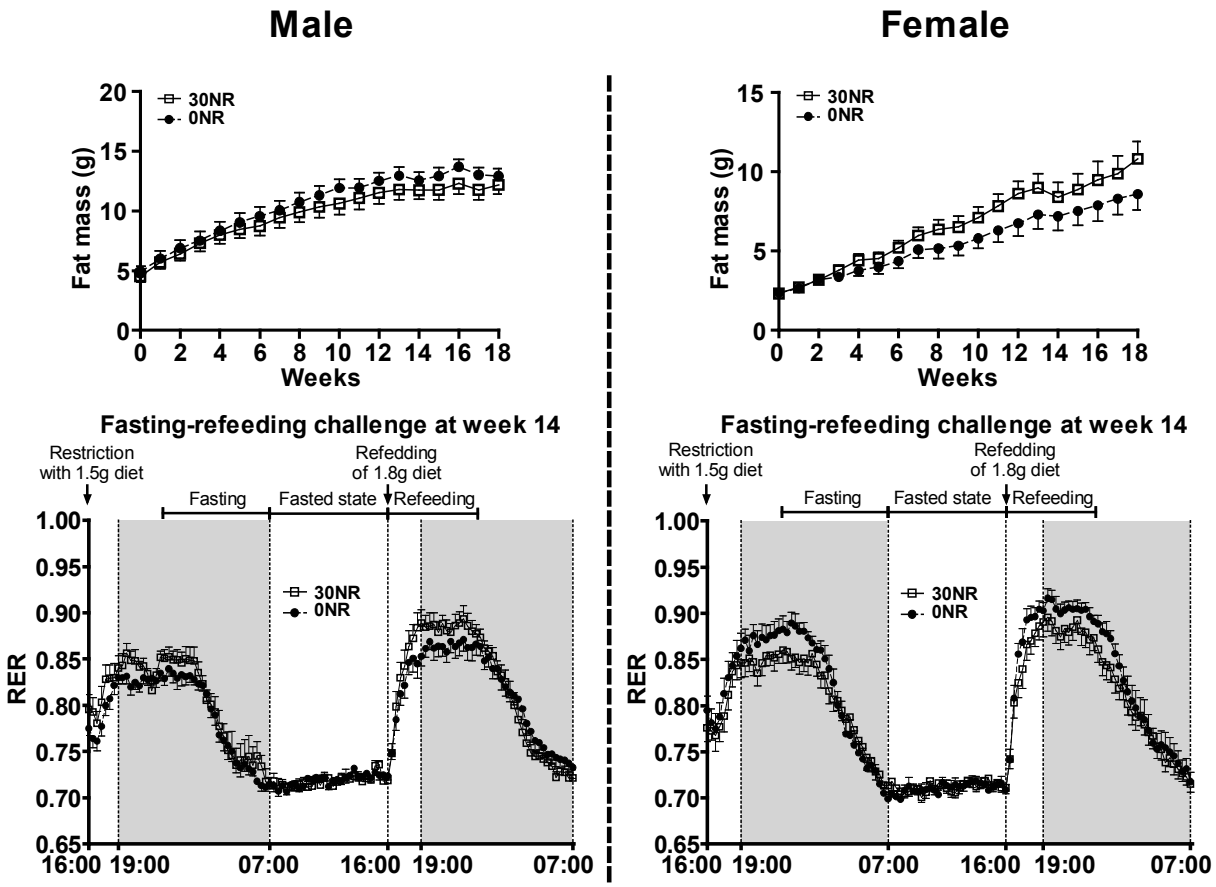

Figure 6. Different metabolic responses to vitamin B3 withdrawal between sexes. As a part of NR extreme-dose studies, adult male and female mice were fed with a vitamin B3 withdrawal diet for 18 weeks. Fat mass was monitored weekly and metabolic flexibility was assessed in week 14 using a fasting-refeeding challenge test. Contrasting patterns are seen in growth curves of fat mass and RER curves in response to the challenge between male and female mice.

References

[1] EFSA Panel on Dietetic Products, N., Allergies, Scientific opinion on dietary reference values for niacin. *EFSA Journal* 2014, *12*, 3759.
[2] Shibata, K., Blood NAD as an index of niacin nutrition. *Nutr. Int.* 1986, *2*, 177-181.
[3] Jacob, R. A., Swendseid, M. E., McKee, R. W., Fu, C. S., Clemens, R. A., Biochemical markers for assessment of niacin status in young men: urinary and blood levels of niacin metabolites. *J. Nutr.* 1989, *119*, 591-598.
[4] Jacobson, E. L., Jacobson, M. K., Tissue NAD as a biochemical measure of niacin status in humans. *Methods Enzymol.* 1997, *280*, 221-230.
[5] Yoshino, J., Mills, K. F., Yoon, M. J., Imai, S., Nicotinamide mononucleotide, a key NAD(+) intermediate, treats the pathophysiology of diet- and age-induced diabetes in mice. *Cell Metab.* 2011, *14*, 528-536.
[6] Canto, C., Houtkooper, R. H., Pirinen, E., Youn, D. Y., *et al.*, The NAD(+) precursor nicotinamide riboside enhances oxidative metabolism and protects against high-fat diet-induced obesity. *Cell Metab.* 2012, *15*, 838-847.
[7] Terakata, M., Fukuwatari, T., Sano, M., Nakao, N., *et al.*, Establishment of true niacin deficiency in quinolinic acid phosphoribosyltransferase knockout mice. *J. Nutr.* 2012, *142*, 2148-2153.
[8] Frederick, D. W., Loro, E., Liu, L., Davila, A., Jr., *et al.*, Loss of NAD homeostasis leads to progressive and reversible degeneration of skeletal muscle. *Cell Metab.* 2016, *24*, 269-282.
[9] Trammell, S. A., Schmidt, M. S., Weidemann, B. J., Redpath, P., *et al.*, Nicotinamide riboside is uniquely and orally bioavailable in mice and humans. *Nat. Commun.* 2016, *7*, 12948.
[10] Trammell, S. A., Weidemann, B. J., Chadda, A., Yorek, M. S., *et al.*, Nicotinamide riboside opposes type 2 diabetes and neuropathy in mice. *Sci. Rep.* 2016, *6*, 26933.
[11] Liu, L., Su, X., Quinn, W. J., 3rd, Hui, S., *et al.*, Quantitative analysis of NAD synthesis-breakdown fluxes. *Cell Metab.* 2018, *27*, 1067-1080 e1065.
[12] Ratajczak, J., Joffraud, M., Trammell, S. A., Ras, R., *et al.*, NRK1 controls nicotinamide mononucleotide and nicotinamide riboside metabolism in mammalian cells. *Nat. Commun.* 2016, *7*, 13103.
[13] Bieganowski, P., Brenner, C., Discoveries of nicotinamide riboside as a nutrient and conserved NRK genes establish a Preiss-Handler independent route to NAD(+) in fungi and humans. *Cell* 2004, *117*, 495-502.
[14] Nikiforov, A., Dolle, C., Niere, M., Ziegler, M., Pathways and subcellular compartmentation of NAD biosynthesis in human cells: from entry of extracellular precursors to mitochondrial NAD generation. *J. Biol. Chem.* 2011, *286*, 21767-21778.
[15] Sociali, G., Raffaghello, L., Magnone, M., Zamporlini, F., *et al.*, Antitumor effect of combined NAMPT and CD73 inhibition in an ovarian cancer model. *Oncotarget* 2016, *7*, 2968-2984.
[16] Fletcher, R. S., Ratajczak, J., Doig, C. L., Oakey, L. A., *et al.*, Nicotinamide riboside kinases display redundancy in mediating nicotinamide mononucleotide and nicotinamide riboside metabolism in skeletal muscle cells. *Mol. Metab.* 2017, *6*, 819-832.
[17] Vaur, P., Brugg, B., Mericskay, M., Li, Z., *et al.*, Nicotinamide riboside, a form of vitamin B3, protects against excitotoxicity-induced axonal degeneration. *FASEB J.* 2017, *31*, 5440-5452.
[18] Belenky, P., Christensen, K. C., Gazzaniga, F., Pletnev, A. A., Brenner, C., Nicotinamide riboside and nicotinic acid riboside salvage in fungi and mammals. Quantitative basis for Urh1 and purine nucleoside phosphorylase function in NAD+ metabolism. *J. Biol. Chem.* 2009, *284*, 158-164.
[19] Trammell, S. A., *Novel NAD+ metabolomic technologies and their applications to nicotinamide riboside interventions (thesis)*, The University of Iowa, Iowa City 2016.
[20] Gross, C. J., Henderson, L. M., Digestion and absorption of NAD by the small intestine of the rat. *J. Nutr.* 1983, *113*, 412-420.
[21] Martens, C. R., Denman, B. A., Mazzo, M. R., Armstrong, M. L., *et al.*, Chronic nicotinamide riboside supplementation is well-tolerated and elevates NAD(+) in healthy middle-aged and older adults. *Nat. Commun.* 2018, *9*, 1286.

[22] Purhonen, J., Rajendran, J., Tegelberg, S., Smolander, O.-P., *et al.*, NAD+ repletion produces no therapeutic effect in mice with respiratory chain complex III deficiency and chronic energy deprivation. *FASEB J.* 2018, fj. 201800090R.
[23] Storlien, L., Oakes, N., Kelley, D., Adipose tissue-liver-muscle interactions leading to insulin resistance. *Proc. Nutr. Soc.* 2004, *63*, 363-368.
[24] Sparks, L. M., Ukropcova, B., Smith, J., Pasarica, M., *et al.*, Relation of adipose tissue to metabolic flexibility. *Diabetes Res. Clin. Pract.* 2009, *83*, 32-43.
[25] Asterholm, I. W., Scherer, P. E., Enhanced metabolic flexibility associated with elevated adiponectin levels. *Am. J. Pathol.* 2010, *176*, 1364-1376.
[26] Franck, N., Stenkula, K. G., Öst, A., Lindström, T., *et al.*, Insulin-induced GLUT4 translocation to the plasma membrane is blunted in large compared with small primary fat cells isolated from the same individual. *Diabetologia* 2007, *50*, 1716-1722.
[27] Hammarstedt, A., Graham, T. E., Kahn, B. B., Adipose tissue dysregulation and reduced insulin sensitivity in non-obese individuals with enlarged abdominal adipose cells. *Diabetol. Metab. Syndr.* 2012, *4*, 1.
[28] Frayn, K., Adipose tissue as a buffer for daily lipid flux. *Diabetologia* 2002, *45*, 1201-1210.
[29] Wu, Z., Xie, Y., Morrison, R. F., Bucher, N. L., Farmer, S. R., PPARgamma induces the insulin-dependent glucose transporter GLUT4 in the absence of C/EBPalpha during the conversion of 3T3 fibroblasts into adipocytes. *J. Clin. Invest.* 1998, *101*, 22-32.
[30] Sharma, A. M., Staels, B., Peroxisome proliferator-activated receptor γ and adipose tissue—understanding obesity-related changes in regulation of lipid and glucose metabolism. *J. Clin. Endocrinol. Metab.* 2006, *92*, 386-395.
[31] Armoni, M., Harel, C., Karnieli, E., Transcriptional regulation of the GLUT4 gene: from PPAR-gamma and FOXO1 to FFA and inflammation. *Trends Endocrinol. Metab.* 2007, *18*, 100-107.
[32] Sugii, S., Olson, P., Sears, D. D., Saberi, M., *et al.*, PPARγ activation in adipocytes is sufficient for systemic insulin sensitization. *Proc. Natl. Acad. Sci. U. S. A.* 2009, pnas. 0912487106.
[33] Ahmadian, M., Suh, J. M., Hah, N., Liddle, C., *et al.*, PPARγ signaling and metabolism: the good, the bad and the future. *Nat. Med.* 2013, *19*, 557.
[34] Brown, J. M., Boysen, M. S., Chung, S., Fabiyi, O., *et al.*, Conjugated linoleic acid induces human adipocyte delipidation: autocrine/paracrine regulation of MEK/ERK signaling by adipocytokines. *J. Biol. Chem.* 2004, *279*, 26735-26747.
[35] Liu, L., Zhou, M., Lang, H., Zhou, Y., Mi, M., Dihydromyricetin enhances glucose uptake by inhibition of MEK/ERK pathway and consequent down-regulation of phosphorylation of PPARγ in 3T3-L1 cells. *J. Cell. Mol. Med.* 2018, *22*, 1247-1256.
[36] Hong, S., Song, W., Zushin, P.-J. H., Liu, B., *et al.*, Phosphorylation of Beta-3 adrenergic receptor at serine 247 by ERK MAP kinase drives lipolysis in obese adipocytes. *Mol. Metab.* 2018, *12*, 25-38.
[37] Bender, D. A., Biochemistry of tryptophan in health and disease. *Mol. Aspects Med.* 1983, *6*, 101-197.
[38] Badawy, A. A., Tryptophan metabolism in alcoholism. *Nutr. Res. Rev.* 2002, *15*, 123-152.
[39] Badawy, A. A., Kynurenine Pathway of Tryptophan Metabolism: Regulatory and Functional Aspects. *Int. J. Tryptophan Res.* 2017, *10*, 1178646917691938.
[40] Terakata, M., Fukuwatari, T., Kadota, E., Sano, M., *et al.*, The niacin required for optimum growth can be synthesized from L-tryptophan in growing mice lacking tryptophan-2,3-dioxygenase. *J. Nutr.* 2013, *143*, 1046-1051.
[41] Baranyi, A., Amouzadeh-Ghadikolai, O., von Lewinski, D., Breitenecker, R. J., *et al.*, Revisiting the tryptophan-serotonin deficiency and the inflammatory hypotheses of major depression in a biopsychosocial approach. *PeerJ.* 2017, *5*, e3968.
[42] Badawy, A. A., Modulation of tryptophan and serotonin metabolism as a biochemical basis of the behavioral effects of use and withdrawal of androgenic-anabolic steroids and other image- and performance-enhancing agents. *Int. J. Tryptophan Res.* 2018, *11*, 1178646917753422.
[43] Parrott, J. M., Redus, L., Santana-Coelho, D., Morales, J., *et al.*, Neurotoxic kynurenine metabolism is increased in the dorsal hippocampus and drives distinct depressive behaviors during inflammation. *Transl. Psychiat.* 2016, *6*, e918.
[44] Mawe, G. M., Hoffman, J. M., Serotonin signalling in the gut—functions, dysfunctions and therapeutic targets. *Nat. Rev. Gastroenterol. Hepatol.* 2013, *10*, 473.

[45] Lam, T. f., *Regulatory role of orexin on postnatal maturation of the central vestibular system in rats-HKU Theses Online (HKUTO)*, The University of Hong Kong Hong kong 2017.
[46] Pereira, B., Da Rocha, A., Pauli, J., Ropelle, E., *et al.*, Excessive eccentric exercise leads to transitory hypothalamic inflammation, which may contribute to the low body weight gain and food intake in overtrained mice. *Neuroscience* 2015, *311*, 231-242.
[47] Scholz, J., Niibori, Y., Frankland, P. W., Lerch, J. P., Rotarod training in mice is associated with changes in brain structure observable with multimodal MRI. *Neuroimage* 2015, *107*, 182-189.
[48] Field, M. S., Szebenyi, D. M., Stover, P. J., Regulation of de novo purine biosynthesis by methenyltetrahydrofolate synthetase in neuroblastoma. *J. Biol. Chem.* 2006, *281*, 4215-4221.
[49] Girgis, S., Suh, J. R., Jolivet, J., Stover, P. J., 5-Formyltetrahydrofolate regulates homocysteine remethylation in human neuroblastoma. *J. Biol. Chem.* 1997, *272*, 4729-4734.
[50] Nijhout, H. F., Reed, M. C., Ulrich, C. M., Mathematical models of folate-mediated one-carbon metabolism. *Vitam. Horm.* 2008, *79*, 45-82.
[51] Mc Auley, M. T., Mooney, K. M., Salcedo-Sora, J. E., Computational modelling folate metabolism and DNA methylation: implications for understanding health and ageing. *Brief. Bioinform.* 2016, *19*, 303-317.
[52] Field, M. S., Anderson, D. D., Stover, P. J., Mthfs is an essential gene in mice and a component of the purinosome. *Front Genet.* 2011, *2*, 36.
[53] Tolstikov, V., Nikolayev, A., Dong, S., Zhao, G., Kuo, M. S., Metabolomics analysis of metabolic effects of nicotinamide phosphoribosyltransferase (NAMPT) inhibition on human cancer cells. *PLoS One* 2014, *9*, e114019.
[54] Singh, R. K., van Haandel, L., Heruth, D. P., Ye, S. Q., *et al.*, Nicotinamide phosphoribosyltransferase deficiency potentiates the antiproliferative activity of methotrexate through enhanced depletion of intracellular ATP. *J. Pharmacol. Exp. Ther.* 2018, *365*, 96-106.
[55] Kaufman, S., Some metabolic relationships between biopterin and folate: implications for the "methyl trap hypothesis". *Neurochem. Res.* 1991, *16*, 1031-1036.
[56] Moffatt, B. A., Ashihara, H., Purine and pyrimidine nucleotide synthesis and metabolism. *The Arabidopsis Book/American Society of Plant Biologists* 2002, *1*.
[57] Reidy, J. A., Role of deoxyridine incorporation and DNA repair in the expression of human chromosomal fragile sites. *Mutat. Res.* 1988, *200*, 215-220.
[58] Blount, B. C., Ames, B. N., Analysis of uracil in DNA by gas chromatography-mass spectrometry. *Anal. Biochem.* 1994, *219*, 195-200.
[59] Williams, J. D., Jacobson, M. K., Photobiological implications of folate depletion and repletion in cultured human keratinocytes. *J. Photochem. Photobiol. B: Biol.* 2010, *99*, 49-61.
[60] Basten, G., Duthie, S. J., Pirie, L., Vaughan, N., *et al.*, Sensitivity of markers of DNA stability and DNA repair activity to folate supplementation in healthy volunteers. *Br. J. Cancer* 2006, *94*, 1942.
[61] Loft, S., Thorling, E. B., Poulsen, H. E., High fat diet induced oxidative DNA damage estimated by 8-oxo-7,8-dihydro-2-deoxyguanosine excretion in rats. *Free Radic. Res.* 1998, *29*, 595-600.
[62] Rawling, J. M., Jackson, T. M., Driscoll, E. R., Kirkland, J. B., Dietary niacin deficiency lowers tissue poly(ADP-ribose) and NAD+ concentrations in Fischer-344 rats. *J. Nutr.* 1994, *124*, 1597-1603.
[63] Boyonoski, A. C., Spronck, J. C., Gallacher, L. M., Jacobs, R. M., *et al.*, Niacin deficiency decreases bone marrow poly(ADP-ribose) and the latency of ethylnitrosourea-induced carcinogenesis in rats. *J. Nutr.* 2002, *132*, 108-114.
[64] Spronck, J. C., Kirkland, J. B., Niacin deficiency increases spontaneous and etoposide-induced chromosomal instability in rat bone marrow cells in vivo. *Mutat. Res.* 2002, *508*, 83-97.
[65] Kostecki, L. M., Thomas, M., Linford, G., Lizotte, M., *et al.*, Niacin deficiency delays DNA excision repair and increases spontaneous and nitrosourea-induced chromosomal instability in rat bone marrow. *Mutat. Res.* 2007, *625*, 50-61.
[66] Brosnan, M. E., MacMillan, L., Stevens, J. R., Brosnan, J. T., Division of labour: how does folate metabolism partition between one-carbon metabolism and amino acid oxidation? *Biochem. J.* 2015, *472*, 135-146.
[67] Michan, S., Sinclair, D., Sirtuins in mammals: insights into their biological function. *Biochem. J.* 2007, *404*, 1-13.

[68] Verdin, E., Hirschey, M. D., Finley, L. W., Haigis, M. C., Sirtuin regulation of mitochondria: energy production, apoptosis, and signaling. *Trends Biochem. Sci.* 2010, *35*, 669-675.
[69] Chen, Y., Zhang, J., Lin, Y., Lei, Q., *et al.*, Tumour suppressor SIRT3 deacetylates and activates manganese superoxide dismutase to scavenge ROS. *EMBO Rep.* 2011, *12*, 534-541.
[70] Giralt, A., Villarroya, F., SIRT3, a pivotal actor in mitochondrial functions: metabolism, cell death and aging. *Biochem. J.* 2012, *444*, 1-10.
[71] Kempe, S., Kestler, H., Lasar, A., Wirth, T., NF-κB controls the global pro-inflammatory response in endothelial cells: evidence for the regulation of a pro-atherogenic program. *Nucleic Acids Res.* 2005, *33*, 5308-5319.
[72] Zhong, H. H., May, M. J., Jimi, E., Ghosh, S., The phosphorylation status of nuclear NF-kappa B determines its association with CBP/p300 or HDAC-1. *Mol. Cell* 2002, *9*, 625-636.
[73] Hegyi, J., Schwartz, R. A., Hegyi, V., Pellagra: dermatitis, dementia, and diarrhea. *Int. J. Dermatol.* 2004, *43*, 1-5.
[74] Wan, P., Moat, S., Anstey, A., Pellagra: a review with emphasis on photosensitivity. *Br. J. Dermatol.* 2011, *164*, 1188-1200.
[75] Conforti, L., Gilley, J., Coleman, M. P., Wallerian degeneration: an emerging axon death pathway linking injury and disease. *Nat. Rev. Neurosci.* 2014, *15*, 394-409.
[76] Verdin, E., NAD(+) in aging, metabolism, and neurodegeneration. *Science* 2015, *350*, 1208-1213.
[77] Bartness, T. J., Shrestha, Y. B., Vaughan, C. H., Schwartz, G. J., Song, C. K., Sensory and sympathetic nervous system control of white adipose tissue lipolysis. *Mol. Cell. Endocrinol.* 2010, *318*, 34-43.
[78] Bartness, T. J., Song, C. K., Thematic review series: adipocyte biology. Sympathetic and sensory innervation of white adipose tissue. *J. Lipid Res.* 2007, *48*, 1655-1672.
[79] Shi, H., Song, C. K., Giordano, A., Cinti, S., Bartness, T. J., Sensory or sympathetic white adipose tissue denervation differentially affects depot growth and cellularity. *Am. J. Physiol. Regul. Integr. Comp. Physiol.* 2005, *288*, R1028-1037.
[80] Youngstrom, T. G., Bartness, T. J., White adipose tissue sympathetic nervous system denervation increases fat pad mass and fat cell number. *Am. J. Physiol.* 1998, *275*, R1488-1493.
[81] Invernizzi, R. W., Role of TPH-2 in brain function: news from behavioral and pharmacologic studies. *J. Neurosci. Res.* 2007, *85*, 3030-3035.
[82] Hong, K. W., Weiss, A., Morimura, N., Udono, T., *et al.*, Polymorphism of the tryptophan hydroxylase 2 (TPH2) gene is associated with chimpanzee neuroticism. *PLoS One* 2011, *6*, e22144.
[83] Welford, R. W., Vercauteren, M., Trebaul, A., Cattaneo, C., *et al.*, Serotonin biosynthesis as a predictive marker of serotonin pharmacodynamics and disease-induced dysregulation. *Sci. Rep.* 2016, *6*, 30059.
[84] Fricker, R. A., Green, E. L., Jenkins, S. I., Griffin, S. M., The influence of nicotinamide on health and disease in the central nervous system. *Int. J. Tryptophan Res.* 2018, *11*, 1178646918776658.
[85] Hill, L. J., Williams, A. C., Meat Intake and the Dose of Vitamin B3–Nicotinamide: Cause of the Causes of Disease Transitions, Health Divides, and Health Futures? *Int. J. Tryptophan Res.* 2017, *10*, 1178646917704662.
[86] National Academy of Sciences (NRC), *Nutrient Requirements of Laboratory Animals, Fourth Revised Edition*, National Academies Press, Washington DC 1995, pp. 92-95.
[87] Suckow, M. A., Weisbroth, S. H., Franklin, C. L., *The laboratory rat*, Elsevier Academic Press, Burlington, MA 2005.
[88] Fox, J. G., Barthold, S., Davisson, M., Newcomer, C. E., *et al.*, *The mouse in biomedical research: diseases*, Academic Press, Salt Lake City UT 2006.
[89] Shibata, K., Kondo, T., Yonezima, M., Conversion ratio of tryptophan to niacin in rats fed a vitamin B1-free diet. *J. Nutr. Sci. Vitaminol. (Tokyo)* 1997, *43*, 479-483.
[90] Shibata, K., Matsuo, H., Comparison between the metabolic-fate of physiological amount of dietary nicotinic-acid and nicotinamide in rats. *Agric. Biol. Chem.* 1990, *54*, 223-224.
[91] National Academy of Sciences (NRC), *Dietary Reference Intakes for Thiamin, Riboflavin, Niacin, Vitamin B6, Folate, Vitamin B12, Panothenic Acid, Biotin, and Choline*, The National Academies Press, Washington DC 1988, pp. 123-145.
[92] van Ommen, B., Keijer, J., Heil, S. G., Kaput, J., Challenging homeostasis to define biomarkers for nutrition related health. *Mol. Nutr. Food Res.* 2009, *53*, 795-804.

[93] Kourtzidis, I. A., Stoupas, A. T., Gioris, I. S., Veskoukis, A. S., *et al.*, The NAD(+) precursor nicotinamide riboside decreases exercise performance in rats. *J. Int. Soc. Sports Nutr.* 2016, *13*, 32.
[94] Kourtzidis, I. A., Dolopikou, C. F., Tsiftsis, A. N., Margaritelis, N. V., *et al.*, Nicotinamide riboside supplementation dysregulates redox and energy metabolism in rats: Implications for exercise performance. *Exp. Physiol.* 2018, *103*, 1357-1366.
[95] Dollerup, O. L., Christensen, B., Svart, M., Schmidt, M. S., *et al.*, A randomized placebo-controlled clinical trial of nicotinamide riboside in obese men: safety, insulin-sensitivity, and lipid-mobilizing effects. *Am. J. Clin. Nutr.* 2018, *108*, 343-353.
[96] Dellinger, R. W., Santos, S. R., Morris, M., Evans, M., *et al.*, Repeat dose NRPT (nicotinamide riboside and pterostilbene) increases NAD(+) levels in humans safely and sustainably: a randomized, double-blind, placebo-controlled study. *NPJ Aging Mech. Dis.* 2017, *3*, 17.
[97] Airhart, S. E., Shireman, L. M., Risler, L. J., Anderson, G. D., *et al.*, An open-label, non-randomized study of the pharmacokinetics of the nutritional supplement nicotinamide riboside (NR) and its effects on blood NAD+ levels in healthy volunteers. *PLoS One* 2017, *12*, e0186459.
[98] Serrano, A., Asnani-Kishnani, M., Rodriguez, A. M., Palou, A., *et al.*, Programming of the beige phenotype in white adipose tissue of adult mice by mild resveratrol and nicotinamide riboside supplementations in early postnatal life. *Mol. Nutr. Food Res.* 2018, e1800463.
[99] Gariani, K., Menzies, K. J., Ryu, D., Wegner, C. J., *et al.*, Eliciting the mitochondrial unfolded protein response by nicotinamide adenine dinucleotide repletion reverses fatty liver disease in mice. *Hepatology* 2016, *63*, 1190-1204.
[100] Cerutti, R., Pirinen, E., Lamperti, C., Marchet, S., *et al.*, NAD(+)-dependent activation of Sirt1 corrects the phenotype in a mouse model of mitochondrial disease. *Cell Metab.* 2014, *19*, 1042-1049.
[101] Ryu, D., Zhang, H., Ropelle, E. R., Sorrentino, V., *et al.*, NAD+ repletion improves muscle function in muscular dystrophy and counters global PARylation. *Sci. Transl. Med.* 2016, *8*, 361ra139.
[102] Gong, B., Pan, Y., Vempati, P., Zhao, W., *et al.*, Nicotinamide riboside restores cognition through an upregulation of proliferator-activated receptor-γ coactivator 1α regulated β-secretase 1 degradation and mitochondrial gene expression in Alzheimer's mouse models. *Neurobiol. Aging* 2013, *34*, 1581-1588.
[103] Toye, A. A., Lippiat, J. D., Proks, P., Shimomura, K., *et al.*, A genetic and physiological study of impaired glucose homeostasis control in C57BL/6J mice. *Diabetologia* 2005, *48*, 675-686.
[104] Freeman, H. C., Hugill, A., Dear, N. T., Ashcroft, F. M., Cox, R. D., Deletion of nicotinamide nucleotide transhydrogenase: a new quantitive trait locus accounting for glucose intolerance in C57BL/6J mice. *Diabetes* 2006, *55*, 2153-2156.
[105] Son, M. J., Kwon, Y., Son, T., Cho, Y. S., Restoration of mitochondrial NAD(+) levels delays stem cell senescence and facilitates reprogramming of aged somatic cells. *Stem Cells* 2016, *34*, 2840-2851.
[106] Ho, H. Y., Lin, Y. T., Lin, G., Wu, P. R., Cheng, M. L., Nicotinamide nucleotide transhydrogenase (NNT) deficiency dysregulates mitochondrial retrograde signaling and impedes proliferation. *Redox Biol.* 2017, *12*, 916-928.
[107] Santos, L. R. B., Muller, C., de Souza, A. H., Takahashi, H. K., *et al.*, NNT reverse mode of operation mediates glucose control of mitochondrial NADPH and glutathione redox state in mouse pancreatic beta-cells. *Mol. Metab.* 2017, *6*, 535-547.
[108] Meimaridou, E., Kowalczyk, J., Guasti, L., Hughes, C. R., *et al.*, Mutations in NNT encoding nicotinamide nucleotide transhydrogenase cause familial glucocorticoid deficiency. *Nat. Genet.* 2012, *44*, 740-742.
[109] Bender, D. A., Olufunwa, R., Utilization of tryptophan, nicotinamide and nicotinic acid as precursors for nicotinamide nucleotide synthesis in isolated rat liver cells. *Br. J. Nutr.* 1988, *59*, 279-287.
[110] Bender, D. A., Magboul, B. I., Wynick, D., Probable mechanisms of regulation of the utilization of dietary tryptophan, nicotinamide and nicotinic acid as precursors of nicotinamide nucleotides in the rat. *Br. J. Nutr.* 1982, *48*, 119-127.
[111] McCreanor, G. M., Bender, D. A., The metabolism of high intakes of tryptophan, nicotinamide and nicotinic acid in the rat. *Br. J. Nutr.* 1986, *56*, 577-586.

[112] Mitchell, S. J., Bernier, M., Aon, M. A., Cortassa, S., *et al.*, Nicotinamide improves aspects of healthspan, but not lifespan, in mice. *Cell Metab.* 2018, *27*, 667-676. e664.
[113] Canto, C., Menzies, K. J., Auwerx, J., NAD(+) metabolism and the control of energy homeostasis: a balancing act between mitochondria and the nucleus. *Cell Metab.* 2015, *22*, 31-53.
[114] Lieberman, H. R., Agarwal, S., Fulgoni III, V. L., Tryptophan intake in the us adult population is not related to liver or kidney function but is associated with depression and sleep outcomes. *J. Nutr.* 2016, *146*, 2609S-2615S.
[115] National Academy of Sciences, Institute of Medicine, Food and Nutrition Board, *Dietary reference intakes for energy, carbohydrate, fiber, fat, fatty acids, cholesterol, protein, and amino acids (macronutrients)*, National Academics Press, Washington DC 2002.
[116] Hwang, S. J., Durnin, L., Dwyer, L., Rhee, P. L., *et al.*, β-Nicotinamide adenine dinucleotide is an enteric inhibitory neurotransmitter in human and nonhuman primate colons. *Gastroenterology* 2011, *140*, 608-617. e606.
[117] Mutafova-Yambolieva, V. N., Hwang, S. J., Hao, X., Chen, H., *et al.*, β-Nicotinamide adenine dinucleotide is an inhibitory neurotransmitter in visceral smooth muscle. *Proc. Natl. Acad. Sci. U.S.A.* 2007, *104*, 16359-16364.
[118] Mutafova-Yambolieva, V. N., Neuronal and extraneuronal release of ATP and NAD(+) in smooth muscle. *IUBMB Life* 2012, *64*, 817-824.
[119] Gordon, J., Amini, S., White, M. K., *Neuronal Cell Culture*, Springer 2013, pp. 1-8.
[120] Kirino, K., Nakahata, T., Taguchi, T., Saito, M. K., Efficient derivation of sympathetic neurons from human pluripotent stem cells with a defined condition. *Sci. Rep.* 2018, *8*, 12865.
[121] Mesner, P. W., Winters, T. R., Green, S. H., Nerve growth-factor withdrawal-induced cell-death in neuronal PC12 cells resembles that in sympathetic neurons. *J. Cell Biol.* 1992, *119*, 1669-1680.
[122] McKay, R., Stem cells in the central nervous system. *Science* 1997, *276*, 66-71.
[123] Khan, N. A., Auranen, M., Paetau, I., Pirinen, E., *et al.*, Effective treatment of mitochondrial myopathy by nicotinamide riboside, a vitamin B3. *EMBO Mol. Med.* 2014, *6*, 721-731.
[124] Ronchi, J. A., Figueira, T. R., Ravagnani, F. G., Oliveira, H. C., *et al.*, A spontaneous mutation in the nicotinamide nucleotide transhydrogenase gene of C57BL/6J mice results in mitochondrial redox abnormalities. *Free Radic. Biol. Med.* 2013, *63*, 446-456.
[125] Bainbridge, M. N., Davis, E. E., Choi, W. Y., Dickson, A., *et al.*, Loss of function mutations in NNT are associated with left ventricular noncompaction. *Circ. Cardiovasc. Genet.* 2015, *8*, 544-552.
[126] Shibata, K., Toda, S., Effects of sex hormones on the metabolism of tryptophan to niacin and to serotonin in male rats. *Biosci. Biotechnol. Biochem.* 1997, *61*, 1200-1202.
[127] Stromsdorfer, K. L., Yamaguchi, S., Yoon, M. J., Moseley, A. C., *et al.*, NAMPT-mediated NAD(+) biosynthesis in adipocytes regulates adipose tissue function and multi-organ insulin sensitivity in mice. *Cell Rep.* 2016, *16*, 1851-1860.
[128] Conze, D. B., Crespo-Barreto, J., Kruger, C. L., Safety assessment of nicotinamide riboside, a form of vitamin B3. *Hum. Exp. Toxicol.* 2016, *35*, 1149-1160.
[129] Sasson, S., Notides, A. C., Estriol and estrone interaction with the estrogen receptor. I. Temperature-induced modulation of the cooperative binding of [3H]estriol and [3H]estrone to the estrogen receptor. *J. Biol. Chem.* 1983, *258*, 8113-8117.
[130] Ribas, V., Nguyen, M. A., Henstridge, D. C., Nguyen, A.-K., *et al.*, Impaired oxidative metabolism and inflammation are associated with insulin resistance in ERα-deficient mice. *Am. J. Physiol. Endocrinol. Metabol.* 2009, *298*, E304-E319.
[131] Galgani, J. E., Heilbronn, L. K., Azuma, K., Kelley, D. E., *et al.*, Metabolic flexibility in response to glucose is not impaired in people with type 2 diabetes after controlling for glucose disposal rate. *Diabetes* 2008.
[132] Galgani, J. E., Moro, C., Ravussin, E., Metabolic flexibility and insulin resistance. *Am. J. Physiol. Endocrinol. Metab.* 2008, *295*, E1009-1017.

Appendices

Summary of main findings

Vitamin B3 serves as a precursor of NAD^+, a multifunctional molecule that is involved in various cellular processes, such as energy metabolism, inflammation and insulin signalling. Adequate intake of vitamin B3 is essential to maintain health, especially in aging and obese subjects. In addition, vitamin B3 supplementation in certain high doses have been considered as a therapeutic strategy to counteract the decline of metabolic health that occurs in some diseases, such as type II diabetes. Nicotinamide riboside (NR) is a novel dietary vitamin B3, thus having large potential as dietary component, in fortification or as supplement. However, it is not known how NR as an exclusive source of vitamin B3 affects metabolic health. A better understanding of these effects and the relevant underlying molecular mechanisms will contribute to the proper use of this vitamin B3 in dietary and clinical approaches for health improvement and disease prevention.

The aim of this thesis is to elucidate the effects of the dietary NR on whole body metabolic health and to obtain insight in the associated molecular and physiological mechanisms.

The mouse is widely used as a model in pre-clinical and nutritional studies. In particular, the C57Bl/6J stain is most widely used. This strain is, like humans, susceptible to diet induced obesity. In this thesis, a specific C57Bl/6J strain is used with an intact nicotinamide nucleotide transhydrogenase (NNT) gene as is present in humans. Despite the wide use of mice in in nutritional research and the key role of vitamin B3 in metabolic health, surprisingly, the optimal dose of this vitamin in mice has not been established. In **chapter 2**, we investigated the effects of a wide range of dietary NR doses (5, 15, 30, 180 and 900 mg NR/kg diet) on metabolic health. We employed a semi-synthetic diet containing 40% energy from fat. This diet was designed to contain a reduced but still sufficient level of Tryptophan (Trp, 0.14%), to minimize the contribution of Trp to the NAD^+ pool. Animals grew normally over the 15 weeks of the experimental intervention and the phenotypical parameters, such as body weight, lean mass and fat mass, were similar between treatments. By using a fasting-refeeding challenge to perturb the homeostasis, we found that NR influences metabolic flexibility dose-dependently, with mice on 30 mg NR/kg diet being most metabolically flexible. Epididymal white adipose tissue (eWAT) morphology showed a different adipocyte size profile in mice on the 30 mg NR/kg diet. The genes, *Pparγ*, *Sod2* and *Prdx3*, were transcriptionally upregulated in the treatment of 30 mg NR/kg diet compared to 5 mg NR/kg diet, whereas their expression were not significantly altered by the 900 mg NR/kg diet any further. These data suggest that adipogenesis and antioxidant response in eWAT are sensitive to low dietary NR, but not to supplemental NR. Altogether, these findings suggest that 30 mg NR/kg diet is most beneficial for metabolic health, in terms of metabolic flexibility and eWAT gene expression, of mice on an obesogenic diet. On a molar basis the 30 mg NR/kg diet is slightly below the current recommendation vitamin B3 for mice (which was based on studies in rats).

In **chapter 3**, we examined the effects of high dose of NR (9000 mg NR/kg diet) on metabolic health, in the context of a moderate high-fat diet (40%en from fat). The 30

mg NR/kg diet was used as control. We did not observe significant differences in the phenotypical parameters throughout the18-week experiment between two dietary groups. The high-dose NR feeding, however, decreased metabolic flexibility, in agreement with the finding of the 900 mg NR/kg diet treatment in **chapter 2**. An oral glucose tolerance test (OGTT) showed that the high-dose NR treated mice were less glucose tolerant and less insulin sensitive compared to control. Despite similar fat mass, the high-dose NR feeding decreased eWAT weight, concurrent with the increased liver triglycerides content. We then focused on eWAT and demonstrated a PPARγ repression in eWAT. The amount of single macrophages and crown-like structures (CLSs) was increased in high dose NR, in line with the overt upregulation of pro-inflammatory genes, suggesting increased WAT inflammation. We concluded that high dose of dietary NR induces glucose intolerance and the impaired WAT function in mice fed a mildly obesogenic diet. In light of these adverse effects of high dose NR, we suggested that the use of high dose NR supplementation should be discouraged.

In **chapter 4**, we aimed to identify potential molecular markers for mild vitamin B3 deficiency. The components of the diet used were identical to that of the diet used in **chapter 2**, but the composition was slightly altered to obtain slightly further reduced Trp level (0.115%), which still meets the requirement of Trp in mice (0.1%). Mice were on a diet without vitamin B3 or with 30 mg NR/kg diet, which was used as control. The intervention lasted 18 weeks. A the end of this period, no overt sign of vitamin B3 deficiency was observed in mice on the diet without vitamin B3 and no differences in feed intake, body weight, fat mass or lean mass were found between the diets. Metabolic flexibility trended to be lower in mice in the group without vitamin B3 in the diet, which is consistent with the reduced metabolic flexibility that was observed using 5 mg NR/kg diet in **chapter 2**. By applying an OGTT we further demonstrated that mice having no intake of vitamin B3 were less insulin sensitive. Through global transcriptome analysis , immunohistochemistry and Western blotting, we found MEK/ERK activation, a lowering of markers for glucose utilization , an increase in makers of fatty acid catabolism and a downregulation of mitochondrial Complex I in eWAT of the vitamin B3 deficient mice. together, these results indicate a shift from carbohydrate to fatty acid oxidation in mice fed the vitamin B3 withdrawal diet. Interestingly, in these mice we also observed an upregulation of genes involving the synthesis pathway of tetrahydropteridine (BH4), an essential cofactor for neurotransmitter synthesis. Based on the results, validated by qRT-PCR, we proposed the downregulation of *Anp32a*,*Tnk2* and the upregulation of *Mapk1*, *Map2k1*, *Mthfs*, *Mthfsl* and *Qdpr* as a WAT transcriptional signature marker for mild vitamin B3 deficiency.

The study described in **chapter 5** uses the animal experiment described in **chapter 2**. We assessed the motor performance of mice fed either 5, 30, or 900 mg NR/kg diet and analysed the gene expression in skeletal muscle (soleus) and hypothalamus. Results showed that there was a dose-dependent pattern in motor performance, with 30 mg NR/kg diet being best. Mice fed a 900 mg NR/kg diet displayed reduced rotarod performance, and a downward tendency in grip strength in week 12, compared to 30 mg NR/kg diet. In line, 900 mg NR/kg diet feeding decreased the expression of three

antioxidant genes (*Prdx3*, *Sod1* and a trend for *Sod2)* in muscle. In the hypothalamus the 900 mg NR/kg diet feeding induced the upregulation of *Tdo2*, indicating activation of the upstream part of the de novo NAD^+ metabolism from Trp. The 5 mg NR/kg diet increased the gene expression of *Mthfs* and *Mapk1*. This results validates the two most prominent biomarkers for mild vitamin B3 deficiency that were proposed in **Chapter 4**, in another tissue.

To conclude, the results of this thesis show that 30 mg NR per kg diet, or 2.3 mg NR per kg body weight per day, to be optimal for health of male adult mice fed a moderate high-fat diet containing a reduced, but sufficient, Trp level. Both inadequate intake and excessive intake of vitamin B3 can affect metabolic health. In both conditions metabolic flexibility and insulin sensitivity were impaired, but the underlying mechanisms were distinct. This thesis also proposes molecular biomarkers for mild vitamin B3 deficiency. When validated in humans it can be used to establish the prevalence of subclinical vitamin B3 deficiency in humans. Overall, this thesis underlines the importance of an optimal vitamin B3 intake to support health.

Acknowledgement

The long journey of my PhD study ends, and I see this end with inner peace. Before the next adventure starts, I must express my sincere gratitude for all support that I have got during my PhD journey.

I would like to give my greatest thanks to my promoter Prof. Dr. Jaap Keijer. Jaap, it is your admittance letter being the key to my successful application for a grant from the Chinese Scholarship Council (CSC), making the very first step of my PhD journey. I would like to greatly thank you for every efforts you spent on the training of my critical thinking and independence of studying. Your structural suggestions and novel ideas gave me inspirations, encouraging me to get into my PhD project with increasing interest. Your supervision with patience and enthusiasm helped me get through when I was too stubborn to move a step further, and thus are especially appreciated.

I am highly grateful for the financial support from CSC, which allows me to focus on my PhD study without living concern in the Netherlands.

Recounting the contributions of all members of the HAP group is impossible due to my inability to properly measure the warm aid and friendship each person provided. However, I would like to specially thank my co-promoter Dr. Vincent de Boer, and my former daily supervisors Dr. Jessica Hegeman and Dr. Dorien van Dartel. Vincent, thank you for your critical comments, which inspired me to dive into deeper levels in science field. Jessica, I could never properly thank you for your supervision in the first three years of my PhD study. I have gained a lot from your supervision, especially a significant improvement of my English writing. Dorien, your supervision in the beginning of my PhD study was very helpful and impressive and a lot of thanks for that. I would like to highly thank Hans and Melissa for your help with my animal experiments and highly thank Annelies and Inge for your technical supports in the lab. All of you were really helpful! Because of your support, I can do animal experiments smoothly and work in a well-organised lab. Corine and Irene, and former secretaries Annika and Annet, thank you for all practical help and organising wonderful HAP events which I really enjoyed. Evert, thank you for your scientific input on bioinformatics and my papers. Now, HAPpiers, it is time to give my thanking words and a huge hug to all of you, Lianne, José, Jeske, Bart, Anna, Taolin, Marjanne, Natasja, Joëlle, Maria, Miranda, Li, Lonneke, Jing, Yu, and Iyabo. It is a great luck for me to have your company during my PhD journey. I will remember every delightful moment in our HAPpy reunions. José and Taolin, thank you with a big hug for agreeing to be my paranymphs during the PhD ceremony. Of course, many thanks for kind cooperation, help and fun from all the other (former) colleagues at HAP: Sander, Arie, Katja, Silvie, Marcel, Loes, Elisa, Shujin, and Femke.

I would also like to thank all the students who have worked on my projects: Wessel, Anouk, Jasmijn, Isabella, Jasper and Liza, and special thanks giving to Atanaska, Bart, and Ruth. It is always nice to share the funny experience and outlook of life with you. Besides, I would like to thank the staff of the CKP for technical assistance in my animal experiments.

I would never forget to thank Prof. Dr. Shuisheng Hou, my supervisor during my MSc study in China. Thank you very much for your encouragement and support on the application for the CSC and my PhD program.

Friendship is a need for a wonderful PhD journey. Here I would like to highlight my thanks for all help and supports from my friends. Yongfu family- Yongfu (老唐), Jiacui (翠姐), Xinzhi (糖糖); Jing family- Jing (唐仔), Guanghui (小荣), Xintong (果果); Fahui family- Fahui (刘师兄), Wen (多宝妈), Jinmu (多宝), Moyi (多米); Tieshan family- Tieshan (徐师兄), Lihong (嫂子); Qi family- Qi (刘奇), Jing (李静); Roy (张海璘), Yang (阿日) and other previous housemates in House 84; My CSC fellows- Tao (涛儿), Mandy (包小妹儿), Xiaoning (小米兰), Tian (添儿), Fubiao (老牛), Jinling (老湿), Huicui (卢慧萃), Xiao (林啸), Fengjiao (卜凤娇), Yujie (何玉洁), Defeng (申德峰), Dandan (刘丹丹), Wenbo (刘文博); My Zodiac fellows- Yuan (何源儿), Juncai (陈师兄), Wenjuan (牟师姐) and Xuezhen (郭师兄), Lei (毛磊), Wei (徐蔚), Lu (罗露), Haibo (陆海博), Qiuyu (王秋宇), Fang (吕芳), Yixin (胡义信), Xiaofei (于小飞); My friends- Xu (旭哥), Yin (宋师兄), Huchen (虎臣师兄), Lingmin (田师兄), Minggang (明刚师兄), Caifang (芳芳), Shuo (杨硕), Xixi (闽钱希曦), Ya (王娅师姐), Jiao (龙姣); My Champion football team players including Zhichun (小严) and my basketball team players including Li (谢哥) and Bing (白冰). Your company was, is and will always be the wonderful moments in my memory.

I would like to express my best sincere gratitude to my family. Mom and dad, thank you so much for everything you've done for me. Every support, encouragement and care from you are always the most precious, selfless gift for me. Luluwa, maybe it is a bit too formal to say thank you for your close company, but I wish that we can hold this close company till the end of time.

Curriculum Vitae

Wenbiao Shi (石文标) was born on January 14th, 1988 in Shandong province, China. He completed his pre-university education in No.1 high school of Jining in 2006, after which he started his BSc in Animal Science at Southwest University For Nationalities in Chengdu, China. Following the accomplishment of his BSc study in 2010, he started his MSc study in Animal Nutrition and Feed Science at the Institute of Animal Sciences of Chinese Academy of Agricultural Sciences (CAAS). During the MSc period, he focused on the comparison of bioavailability of vitamin D3 and 25-hydroxy vitamin D3 in Pekin ducks. He obtained his MSc diploma in July, 2013. On May of 2013, he was granted a scholarship from the Chinese Scholarship Council, which contributed to the successful application for a PhD position in Human and Animal Physiology (HAP) Group at Wageningen University. In HAP, he has performed all the experiments described in this thesis from September 2013 till April 2019.

List of publications

- **Shi W**, Hegeman MA, van Dartel DAM, Tang J, Suarez M, Swarts H, van der Hee B, Arola L, Keijer J. Effects of a wide range of dietary nicotinamide riboside (NR) concentrations on metabolic flexibility and white adipose tissue (WAT) of mice fed a mildly obesogenic diet. *Molecular Nutrition & Food Research.* 2017 Aug; 61(8). doi: 10.1002/mnfr.201600878.
- **Shi W**, Hegeman MA, Doncheva A, Grovenstein MB, de Boer VCJ, Keijer J. High dose of dietary nicotinamide riboside (NR) induces glucose intolerance and white adipose tissue (WAT) dysfunction of mice fed a mildly obesogenic diet. *Submitted.*
- **Shi W**, Hegeman MA, Doncheva A, van der Stelt I, Grovenstein MB, van Schothorst EM, de Boer VCJ, Keijer J. Transcriptional response of white adipose tissue to vitamin B3 withdrawal. *Submitted.*
- Maria Ibars Serra*, **Wenbiao Shi***, Hegeman Maria, Vincent de Boer, Jaap Keijer. Dietary vitamin B_3 nicotinamide riboside dose-dependently affects motor performance and hypothalamic gene expression. *In advanced stage of preparation.* *equal contribution.
- Tang J, Hegeman MA, Hu J, Xie M, **Shi W**, Jiang Y, de Boer V, Guo Y, Hou S, Keijer J. Severe riboflavin deficiency induces alterations in the hepatic proteome of starter Pekin ducks. *British Journal of Nutrition.* 2017 Nov; 118(9):641-650. doi: 10.1017/S0007114517002641.

Authorship statements

Wenbiao Shi, Jessica Hegeman, Dorien van Dartel and Jaap Keijer were responsible for the study concept and design of **Chapter 2** and **Chapter 5**; Wenbiao Shi, Jessica Hegeman, Vincent CJ de Boer and Jaap Keijer were responsible for the study concept and design of **Chapter 3** and **Chapter 4**.

Wenbiao Shi conducted the animal experiments mentioned in this thesis, and was technically supported by Hans Swarts in the animal experiments described in **Chapter 2** and **Chapter 5** and by Melissa Bekkenkamp-Grovenstein in **Chapter 3** and **Chapter 4**. In **Chapter 2**, Wenbiao Shi performed biochemical and statistical analysis; Wenbiao Shi and Jing Tang performed molecular analysis; Manuel Suarez and Lluis Arola performed NAD metabolome analysis; Bart van der Hee performed histological analysis. In **Chapter 3**, Wenbiao Shi performed biochemical, molecular and statistical analysis; Atanaska Doncheva performed histological analysis. In **Chapter 4**, Wenbiao Shi performed biochemical, molecular and statistical analysis; Inge van der Stelt and Evert M. van Schothorst assisted in microarray assay and data processing; Atanaska Doncheva performed histological analysis. In **Chapter 5**, Maria Ibars and Wenbiao Shi performed molecular and statistical analysis; Wenbiao Shi performed motor function analysis.

Wenbiao Shi wrote the manuscripts of **Chapter 1**, **Chapter 3**, **Chapter 4** and **Chapter 6**, which were finalized by Wenbiao Shi, Vincent CJ de Boer and Jaap Keijer; Wenbiao Shi, Jessica Hegeman and Jaap Keijer wrote and finalize the manuscript of **Chapter 2**; Maria Ibars and Wenbiao Shi wrote the manuscripts of **Chapter 5**, which were finalized by Maria Ibars, Wenbiao Shi, Vincent CJ de Boer and Jaap Keijer.

All authors revised and approved the final version of the paper and agree to be accountable for all aspects of the work in ensuring that questions related to the accuracy or integrity of any part of the work are appropriately investigated and resolved. All persons designated as authors qualify for authorship, and all those who qualify for authorship are listed.

Overview of completed training activities

Discipline specific activities

Name	Organizer	Year	Remark
Courses			
Use of Laboratory Animals (Article 9)	WGS	2014	
5th International Symposium on Energy and Protein Metabolism and Nutrition	WGS/ INRA	2016	
Conferences / Seminars			
NuGo week	VLAG	2015	Poster
Dutch Nutritional Science Days (NSD)	NWO	2016	Presentation
10th MiPschool 2017 MITOEAGLE and MITOEAGLE Workshop WG1-4	MiPschool	2017	
Dutch Nutritional Science Days (NSD)	NWO	2017	
LC/LCMS GC/GCMS Lab Informatics Seminar	Agilent	2017	
WIAS science day	WIAS	2018	Poster

General courses

Name	Organizer	Year
VLAG PhD week	VLAG	2013
Practical English Plus	Radboud in'to Languages	2014
Project and Time management	WGS	2015
Techniques for Writing and Presenting a Scientific Paper	WGS	2015
Teaching and Supervising Thesis Students	WGS	2015
Big Data in the Life Sciences	VLAG	2017
PhD Workshop Carousel	WSG	2017

Optionals

Name	Organizer	Year(s)
Preparation of Research Proposal	HAP	2013
Attending Scientific Presentations	HAP	2017-2018
Weekly Group Meetings	HAP	2013-2018
MSc Thesis Rings	HAP	2017-2018

Colophon
The research described in this thesis was financially supported by China Scholarshop Council, China and Human and Animal Physiology Group of Wageningen University, the Netherlands.

Financial support from the Human and Animal Physiology Group of Wageningen University and TSE Systems GmbH for printing this thesis is gratefully acknowledged.

Layout: Wenbiao Shi
Cover design: Wenbiao Shi & Zhijian Shi
Printing: GVO drukkers & vormgevers B.V. Ede (NL)|gvo.nl

Molecular physiological studies on health effects of dietary nicotinamide riboside, a vitamin B3

Molecular physiological studies on health effects of

dietary nicotinamide riboside

a vitamin B3

Wenbiao Shi